

## **General Disclaimer**

### **One or more of the Following Statements may affect this Document**

- This document has been reproduced from the best copy furnished by the organizational source. It is being released in the interest of making available as much information as possible.
- This document may contain data, which exceeds the sheet parameters. It was furnished in this condition by the organizational source and is the best copy available.
- This document may contain tone-on-tone or color graphs, charts and/or pictures, which have been reproduced in black and white.
- This document is paginated as submitted by the original source.
- Portions of this document are not fully legible due to the historical nature of some of the material. However, it is the best reproduction available from the original submission.



# THE CONCEPTUAL DESIGN OF AN INTEGRATED NUCLEAR-HYDROGEN PRODUCTION PLANT USING THE SULFUR CYCLE WATER DECOMPOSITION SYSTEM

(NASA-CR-134976) THE CONCEPTUAL DESIGN OF AN INTEGRATED NUCLEARHYDROGEN PRODUCTION PLANT USING THE SULFUR CYCLE WATER DECOMPOSITION SYSTEM (Westinghouse Astronuclear Lab., Pittsburgh) 208 p HC	N76-23689 HC \$7.75
	Unclas G3/44 26952

WESTINGHOUSE ELECTRIC CORPORATION  
ASTRONUCLEAR LABORATORY

prepared for  
NATIONAL AERONAUTICS AND SPACE ADMINISTRATION

NASA Lewis Research Center  
Contract NAS 3-18934



1. Report No. NASA-CR-134976		2. Government Accession No.		3. Recipient's Catalog No.	
4. Title and Subtitle THE CONCEPTUAL DESIGN OF AN INTEGRATED NUCLEAR - HYDROGEN PRODUCTION PLANT USING THE SULFUR CYCLE WATER DECOMPOSITION SYSTEM				5. Report Date April, 1976	
				6. Performing Organization Code	
7. Author(s) G. H. Farberman, Project Manager				8. Performing Organization Report No.	
				10. Work Unit No.	
9. Performing Organization Name and Address Westinghouse Electric Corporation Astronuclear Laboratory P. O. Box 10864 Pittsburgh, Pennsylvania 15236				11. Contract or Grant No. NAS 3-18934	
				13. Type of Report and Period Covered Contractor Report	
12. Sponsoring Agency Name and Address National Aeronautics and Space Administration Washington, D. C. 20546				14. Sponsoring Agency Code	
15. Supplementary Notes Project Manager, Donald Bogart, NASA Lewis Research Center, Cleveland, Ohio 44135					
16. Abstract A conceptual design of a hydrogen production plant has been prepared based on a hybrid electrolytic-thermo-chemical process for decomposing water. The process, called the Sulfur Cycle Water Decomposition System, is driven by a Very High Temperature Nuclear Reactor (VHTR) that provides 1283K (1850°F) helium working gas for electric power and process heat. The plant is sized to produce approximately ten million standard cubic meters per day [or 380 million standard cubic feet per day (SCFD)] of electrolytically pure hydrogen and has an overall thermal efficiency of 45.2 percent.  The economics of the plant have been evaluated, predicated on a set of ground rules which include a 1974 cost basis without escalation, financing structure (utility and industrial), and other economic factors. Taking into account capital, operation, maintenance and nuclear fuel cycle costs, the cost of product hydrogen has been calculated at 5.96¢/std m <sup>3</sup> (\$1.59/MSCF) for utility financing with no credit taken for by-product oxygen production. These values are significantly lower than hydrogen costs from conventional water electrolysis plants. Furthermore, they are competitive with hydrogen from coal gasification plants when coal costs are in the order of \$1.35 per GJ (\$1.42 per million Btu).  A development plan to take the Sulfur Cycle Water Decomposition System to commercial viability has been defined. The plan involves several phases and can lead to an operating pilot plant in seven to eight years.					
17. Key Words (Suggested by Author(s)) Hydrogen Nuclear Power Sulfur Chemistry Thermochemical Hydrogen Production Electrochemical Hydrogen Production Very High Temperature Reactor (VHTR)			18. Distribution Statement  Unclassified - Unlimited		
19. Security Classif. (of this report) Unclassified		20. Security Classif. (of this page) Unclassified		21. No. of Pages 209	22. Price* \$3.00

FOREWARD

Acknowledgment is gratefully given to those organizations who substantially contributed to the work reported herein. These include United Engineers and Constructors, Inc., the University of Kentucky Research Foundation, Westinghouse Environmental Systems Department, and the Westinghouse Research Laboratories.

## TABLE OF CONTENTS

	<u>Page</u>
FORWARD	
SUMMARY	
1.0 INTRODUCTION	1
2.0 CONCEPTUAL DESIGN	2
2.1 GENERAL	2
2.2 PLANT LAYOUT	6
2.2.1 Site Description	6
2.2.2 Plot Plan	6
2.2.3 Plant Buildings	8
2.2.3.1 Major VHTR Buildings	8
2.2.3.2 Major Water Decomposition Plant Buildings	13
2.3 BATTERY A - NUCLEAR HEAT SOURCE AND HEAT TRANSPORT SYSTEMS	14
2.3.1 General	14
2.3.2 Major Features	17
2.4 BATTERY G - ELECTROLYZER SYSTEM AND AUXILIARIES	22
2.4.1 General	22
2.4.2 Electrolyzer Module Design	22
2.4.2.1 Introduction	22
2.4.2.2 Electrolyzer Design	26
2.4.3 Electrolyzer Bay Arrangement	31
2.4.4 Electrolyzer Power Supply	34
2.4.5 Electrolyzer Auxiliaries	34
2.4.5.1 Surge Tank	34
2.4.5.2 Heat Exchangers	34
2.4.5.3 Pumps	34
2.4.5.4 Vessels	38

## TABLE OF CONTENTS (Continued)

		<u>Page</u>
2.5	BATTERY H - SULFURIC ACID DECOMPOSITION	38
2.5.1	General	38
2.5.2	Acid Vaporizer (AV-1)	41
2.5.3	Decomposition Reactor (DR-1)	41
2.5.4	Balance of Battery H Equipment	52
2.6	BATTERY I - SULFUR DIOXIDE - OXYGEN SEPARATION	56
2.6.1	General	56
2.6.2	Components	60
	2.6.2.1 Heat Exchangers	60
	2.6.2.2 Knock-Out Drums	60
	2.6.2.3 Surge Tanks	60
	2.6.2.4 Ammonia Chiller	60
	2.6.2.5 Compressors	63
	2.6.2.6 Turbo-Expanders	63
	2.6.2.7 Pumps	63
2.7	BATTERY J - STEAM TURBINES AND GENERATORS	66
2.7.1	Battery J/Battery A Interface	66
2.7.2	Battery J Equipment	66
2.8	COOLING WATER SYSTEM	70
2.9	WATER MAKE-UP AND WASTE TREATMENT SYSTEM	70
2.10	ELECTRICAL AUXILIARY POWER SYSTEM	75
2.11	GENERAL FACILITIES	77
2.12	OVERALL PLANT PERFORMANCE AND AREAS FOR IMPROVEMENT	78
2.12.1	Plant Thermal Efficiency	78
2.12.2	Areas for Performance Improvement	78

TABLE OF CONTENTS (Continued)

	<u>Page</u>	
3.0	PLANT ECONOMICS	82
3.1	GENERAL AND GROUND RULES	82
3.2	CAPITAL COSTS	84
3.3	OPERATION AND MAINTENANCE COSTS	90
3.4	FUEL COSTS	92
3.5	HYDROGEN PRODUCTION COSTS	92
3.6	SENSITIVITY ANALYSIS	94
3.7	COMPARATIVE HYDROGEN PRODUCTION COST	94
4.0	DEVELOPMENT PLAN FOR COMMERCIAL PLANT	100
4.1	GENERAL	100
4.2	DEVELOPMENT OF THE VHTR	100
4.3	DEVELOPMENT OF THE SULFUR CYCLE WATER DECOMPOSITION SYSTEM	103
4.3.1	Phase 1.0 - Supporting Research	103
4.3.2	Phase 2.0 - Laboratory Demonstration	107
4.3.3	Phase 3.0 - Process Evaluation	108
4.3.4	Phase 4.0 - Pilot Scale Development	109
4.3.5	Phase 5.0 - Pilot Plant	109
4.3.6	Phase 6.0 - Demonstration or Commercial Plant	109
4.3.7	Development Cost	109
5.0	SUPPORTING ENGINEERING STUDIES AND CONSIDERATIONS	112
5.1	GENERAL	112
5.2	ENVIRONMENTAL IMPACTS	112
5.2.1	Resource Consumption	112
5.2.2	Non-Radiological Air Impacts	113
5.2.3	Water Impacts	114
5.2.4	Solid Wastes	114

## TABLE OF CONTENTS (Continued)

		<u>Page</u>
5.2.5	Radiological Impact on Humans	115
5.2.5.1	Exposure Pathways	115
5.2.5.2	Evaluation Methods	115
5.2.5.3	Results of the Dose Evaluations	116
5.2.6	Land Use, Terrestrial Effects and Aesthetics	118
5.2.7	Social and Economic Impacts	119
5.2.8	Summary Benefit - Cost Analysis	120
5.2.8.1	Benefits	120
5.2.8.2	Costs	120
5.2.8.3	Balance of Benefits and Costs	121
5.3	TECHNOLOGY OF THE SULFUR CYCLE WATER DECOMPOSITION SYSTEM	122
5.3.1	General	122
5.3.2	Water Splitting Processes as a Class of Hydrogen Generation Methods	123
5.3.3	The Westinghouse Sulfur Cycle Water Decomposition Process	130
5.3.4	Process Performance Sensitivity Analysis	133
5.3.5	Energy Sources for the Westinghouse Sulfur Cycle Water Decomposition System	144
5.3.6	Status of Electrochemical Hydrogen Generation Technology	156
5.3.7	Status of Sulfur Trioxide Reduction Technology	166
5.3.8	Status of Materials Technology	174
6.0	SUMMARY OF RESULTS	184
6.1	CONCEPTUAL DESIGN OF THE NUCLEAR DRIVEN WATER DECOMPOSITION PLANT	184
6.2	PLANT ECONOMICS	186
6.2.1	Capital Costs	186
6.2.2	Operation and Maintenance Costs	186

TABLE OF CONTENTS (Continued)

	<u>Page</u>
6.2.3 Fuel Costs	186
6.2.4 Hydrogen Production Costs	187
6.2.5 Sensitivity Analysis	187
6.2.6 Comparative Hydrogen Production Cost	188
6.3 ENVIRONMENTAL IMPACT	190
6.4 DEVELOPMENT PLAN FOR COMMERCIAL PLANT	191
6.4.1 Development of the VHTR	191
6.4.2 Development of the Sulfur Cycle Water Decomposition System	192
6.5 CONCLUSIONS	195
7.0 REFERENCES	196

## SUMMARY

A conceptual design of a hydrogen production plant has been prepared based on a hybrid electrolytic-thermochemical process for decomposing water. The process, called the Sulfur Cycle Water Decomposition System, is driven by a Very High Temperature Nuclear Reactor (VHTR) that provides 1283K (1850°F) helium working gas for electric power and process heat. The plant is sized to produce approximately ten million standard cubic meters per day [or 380 million standard cubic feet per day (SCFD)] of electrolytically pure hydrogen and has an overall thermal efficiency of 45.2 percent.

The economics of the plant have been evaluated, predicated on a set of ground rules which include a 1974 cost basis without escalation, financing structure (utility and industrial), and other economic factors. The ultimate economic competitiveness of the water decomposition system would depend, of course, on the economic ground rules that eventually pertain to the venture. The capital investment for the nuclear water decomposition plant has been estimated at \$994,795,000. Taking into account operation, maintenance and nuclear fuel cycle costs, the cost of product hydrogen has been calculated at 5.96¢/std m<sup>3</sup> (\$1.59/MSCF) for utility financing with no credit taken for by-product oxygen production. These values are significantly lower than hydrogen costs from conventional water electrolysis plants. Furthermore, they are competitive with hydrogen from coal gasification plants when coal costs are in the order of \$1.35 per GJ (\$1.42 per million Btu).

Supporting analyses of the plant design have included a preliminary evaluation of environmental impacts based on a standard plant site definition. Areas of impact assessment include resource consumption; air, water and radiological impacts; waste products, land use and aesthetics; socio economic impacts and environmental cost/benefit factors.

A development plan to take the Sulfur Cycle Water Decomposition System to commercial viability has been defined. The plan involves several phases and can lead to an operating pilot plant in seven to eight years. The development plan builds on previous laboratory scale programs that have verified the scientific feasibility of two major steps in the Sulfur Cycle; electrochemical hydrogen generation and the sulfur trioxide reduction step.

## 1.0 INTRODUCTION

The objectives of the work performed under Contract NAS 3-18934, "Studies of the Use of Heat from High Temperature Nuclear Sources for Hydrogen Production Processes", are:

- To survey existing and advanced processes for the production of hydrogen by use of fossil, nuclear, and other energy sources or appropriate combinations thereof.
- To analyze and evaluate these various processes in terms of cost, energy supply, environmental impact, critical materials, and other factors; to assess the status of technology for the promising processes; and to specify the R&D needed to make the promising processes practical.
- To prepare a conceptual design of a hydrogen-production plant based on one of the most promising processes; and for this process, to prepare program plans for the needed R&D and demonstration at the pilot-plant scale.

To achieve these objectives, a scope of effort has been undertaken which is divided into three major technical tasks. These tasks are summarized below:

- TASK I - Identification of Candidate Processes for Production and Market Surveys for Uses of Hydrogen

The results of this task are a comparative evaluation of various hydrogen generation processes supporting the selection of the electrolysis, coal gasification, and water decomposition processes studied in more detail; preliminary technical, environmental, and sociological information pertinent to the selected hydrogen generation processes; and projections, to the year 2000, of the market demand for hydrogen as a fuel, feedstock, or reagent.

- TASK II - Technical Analyses and Economic Evaluation of Hydrogen Process Systems

This task results in a more detailed evaluation of the four hydrogen production processes selected in Task I, i.e., electrolysis using the Teledyne HP modules, coal gasification using the Koppers-Totzek atmospheric gasifier, coal gasification using the Bi-Gas pressurized gasifier, and a combined electrolytic-thermochemical process using the Westinghouse Sulfur Cycle Water Decomposition System. The evaluation considers the economics, technical status, R&D requirements, resource requirements, environmental impacts, and other factors that bear on a recommendation of a hydrogen production process that can best meet the requirements of the market identified in Task I.

- TASK III - Conceptual Design of a Plant for Hydrogen Production

The results of this task are a conceptual design of an integrated nuclear-hydrogen production plant, using the Westinghouse Sulfur Cycle hydrogen production process, including an evaluation of the economics, environmental effects, benefits, and the program, in respect to technical areas, costs, and schedules, needed to develop the hydrogen production system to the demonstration stage.

This report documents the results of Task III. The results of Tasks I and II are reported in NASA-CR-134918, "Studies of the Use of Heat from High Temperature Nuclear Sources for Hydrogen Production Processes (Reference 1)."

In performing this work, it was recognized that ERDA-Nuclear Energy is conducting studies to assess the potential for development of nuclear systems to provide process heat at temperatures in the range of 922 to 1366K (1200 to 2000°F). These ERDA studies are also concerned with identifying and evaluating present and projected industrial processes that can utilize high temperature nuclear heat. NASA is participating in the ERDA evaluation through the assessment of processes for hydrogen production using nuclear, as well as fossil, heat sources.

In order to make the results of this work most useful to ERDA, the hydrogen production capacity of the systems investigated was established consistent with the size of nuclear heat sources being considered in the ERDA evaluation. This results for the system investigated and reported herein, in a nominal hydrogen generation rate of  $10.1 \times 10^6$  standard cubic meters per day ( $380 \times 10^6$  SCFD) (1). Moreover, the methodology and format for estimating capital, operating, and production costs are consistent with those used by ERDA-Nuclear Energy in their studies of the very high temperature nuclear heat sources.

---

(1) Throughout this report, the standard cubic meter is defined as a gas volume at normal atmospheric pressure and a temperature of 273K (32°F). The standard cubic foot is defined as a gas volume at normal atmospheric pressure and a temperature of 289K (60°F).

## 2.0 CONCEPTUAL DESIGN

### 2.1 GENERAL

The water decomposition system used for hydrogen production is the Westinghouse Sulfur Cycle two-step process. In this process, hydrogen and sulfuric acid are produced electrolytically by the reaction of sulfur dioxide and water. The process is completed by vaporizing the sulfuric acid and thermally reducing, at higher temperatures, the resultant sulfur trioxide into sulfur dioxide and oxygen. Following separation, sulfur dioxide is recycled to the electrolyzer and oxygen is either utilized, sold, or vented.

As in conventional water electrolysis, hydrogen is produced at the electrolyzer cathode. Unlike conventional electrolysis, sulfuric acid rather than oxygen, is produced at the anode. Operation in this fashion reduces the theoretical power required per unit of hydrogen production by more than 85 percent over that required in water electrolysis. This is partially offset, however, by the need to add thermal energy to the process in the acid vaporizer and the sulfur trioxide reduction reactor. Even so, by avoiding the high overvoltages at the oxygen electrode of a conventional electrolyzer, as well as the inefficiencies associated with power generation, this hydrogen generation process provides overall thermal efficiencies approximately double those attainable by conventional electrolytic hydrogen and oxygen production technology.

The characteristics and technology of the hydrogen production process are discussed in more detail in Section 5.3, "Technology Status of the Sulfur Cycle Water Decomposition System."

The overall process flowsheet for the water decomposition system is shown in Figure 2.1.1. The energy source for the water decomposition system is a very high temperature nuclear reactor (VHTR) producing both electric power and a high temperature helium stream to the process. Within Battery G, electrical power, water, and recycled sulfur dioxide are consumed to produce hydrogen and sulfuric acid. The hydrogen, of electrolytic purity, is withdrawn as product while the sulfuric acid is sent to Battery H. Using thermal energy from the VHTR, the acid in Battery H is vaporized to produce a mixture of steam and sulfur trioxide. The sulfur trioxide is thermal-catalytically reduced at higher temperatures to produce sulfur dioxide and oxygen. These gases are separated within Battery I. The sulfur dioxide is recycled to Battery G and the oxygen is available as a by-product for sale. The only major consumable for the process is water. Small quantities of make-up are naturally required to compensate for sulfur leakage and losses, catalyst deactivation, and similar things. The sulfur oxides are recycled and all process and plant energy needs are provided by the VHTR.

The conceptual design presented is not intended to represent an optimized process configuration nor a final design of major process components. Rather, design decisions were made, based on engineering judgment, to reflect workable solutions that could result in a conservative evaluation of the process potential. Section 2.12 of this report discusses many of

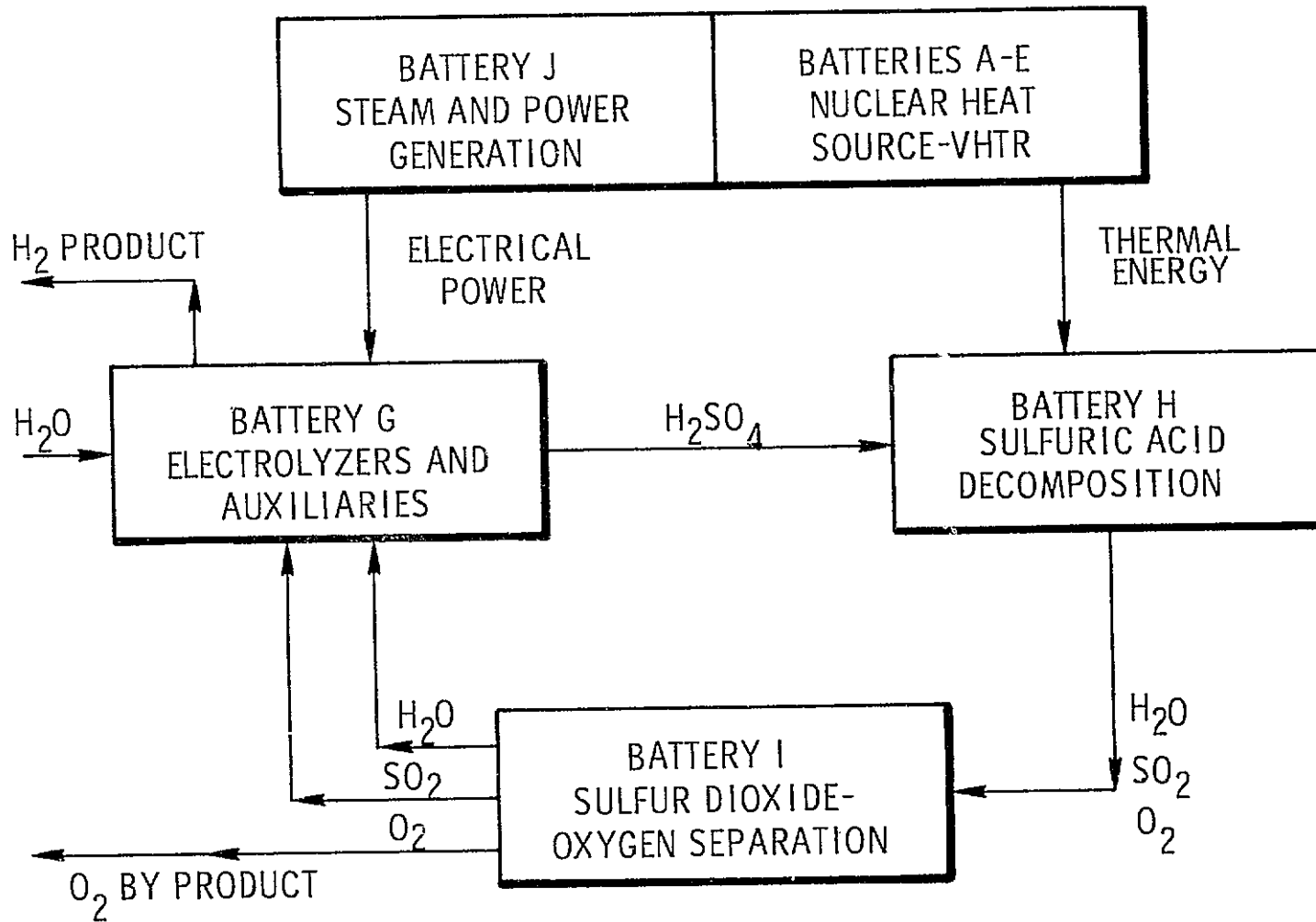


Figure 2.1.1 Overall Process Schematic

the areas which have currently been identified where significant improvements in efficiency and/or economics can be achieved. Similarly, the component designs presented, particularly for the electrolyzers, sulfur trioxide reduction reactors, and acid vaporizers, are subject to change as additional effort is applied in design development and evaluation of alternate configurations.

The principal operating and performance characteristics of the water decomposition system are given in Table 2-1.

TABLE 2.1  
PRINCIPAL OPERATING AND PERFORMANCE CHARACTERISTICS  
OF THE SULFUR CYCLE WATER DECOMPOSITION SYSTEM

<u>General</u>		
Hydrogen Production Rate	$10.12 \times 10^6$ standard $m^3$ /day	$(380 \times 10^6$ SCFD)
Hydrogen Purity	99.9 volume percent	
Oxygen Production Rate	306, 100 kg/hr	(675, 000 lb/hr)
Nuclear Heat Source Rating	3345 MWt	
Net Process Thermal Efficiency	45.2 percent	
<u>Electrolysis</u>		
Acid Concentration	75 wt percent	
Pressure	2586 kPa	(375 psia)
Temperature	361 K	(190°F)
Electrolyzer Power Requirement	458 MWe	
Cell Voltage, Nominal	0.45 volts	
Cell Current Density, Nominal	2000 A/ $m^2$	(186 A/ $ft^2$ )
<u>Sulfur Trioxide Reduction System</u>		
Peak Temperature	1144 K	(1600°F)
Operating Pressure	310 kPa	(45 psia)
<u>Sulfur Dioxide - Oxygen Separation System</u>		
SO <sub>2</sub> Liquefaction Pressure	5171 kPa	(750 psia)
Oxygen Discharge Pressure	103 kPa	(15 psia)

## 2.2 PLANT LAYOUT

### 2.2.1 Site Description

The plant is presumed to be located at the hypothetical Middletown site described in NUS-531 (Reference 2). The site is located on the east bank of the North River at a distance of 40 km (25 miles) south of Middletown, the nearest large city. The North River flows from north to south and is 0.8 km (2600 feet) wide adjacent to the plant site. A flood plain extends from both river banks an average distance of 0.8 km (2600 feet), ending with hilltops generally 45 to 75 m (150 to 250 feet) above the river level. Beyond this area, the topography is gently rolling, with no major critical topographical features. The plant site itself extends from river level to elevations of 15 m (50 feet) above river level. The containment building and other Class I structures are located on level ground at an elevation of 5.5 m (18 feet) above the mean river level. This elevation is 3 m (10 feet) above the 100-year maximum river level, according to U. S. Army Corps of Engineers studies of the area.

Highway access is provided to the Hypothetical Site by 8 km (5 miles) of secondary road connecting to a state highway; this road is in good condition and needs no additional improvements. Railroad access will be provided by constructing a spur which intersects the B&M Railroad. The length of the required spur from the main line to the plant site is assumed to be 8 km (5 miles) in length. The North River is navigable throughout the year with a 12 m (40 feet) wide channel, 3.66 m (12 feet) deep. The distance from the shoreline to the center of the ship channel is 61 m (2000 feet). All plant shipments will be made overland except that heavy equipment may be transported by barge. The Middletown Municipal Airport is located 4.8 km (3 miles) west of the State Highway, 24 km (15 miles) south of Middletown, and 16 km (10 miles) north of the site.

Other site related parameters affecting the plant design, e.g., population density and land use, cooling water and public utility services, meteorology, climatology, geology, seismology, and the like, are specified in Reference 2.

### 2.2.2 Plot Plan

A preliminary plot plan was prepared, showing the general location and space requirements for the plant facilities, including the nuclear heat source. This is shown in Figure 2.2.1. The facilities associated with the plant are grouped in the categories of the VHTR (nuclear heat source), the hydrogen plant on-sites, and the support facilities, or off-sites. Within each category, "batteries", identified by an alphabetic or alpha-numeric designation, are defined. These batteries are used to describe related groups of equipment for both design and cost estimating purposes.

The plot plan shows the VHTR and its supporting facilities located at the southern end of the plant. The hydrogen production facilities are arranged so that piping and other interconnections are kept to a minimum while sufficient space is provided to allow for constructability and maintainability of the unit. Fronting on the river is the plant's water make-up and non-radioactive waste treatment systems. Heat rejection from the plant is accomplished through the cooling tower L-2 and the Class I VHTR cooling tower L-1. Not shown on the plot plan are the switchyards for electric power supply to the VHTR and water decomposition plant.

# Ⓜ H<sub>2</sub> PROCESS PLOT PLAN

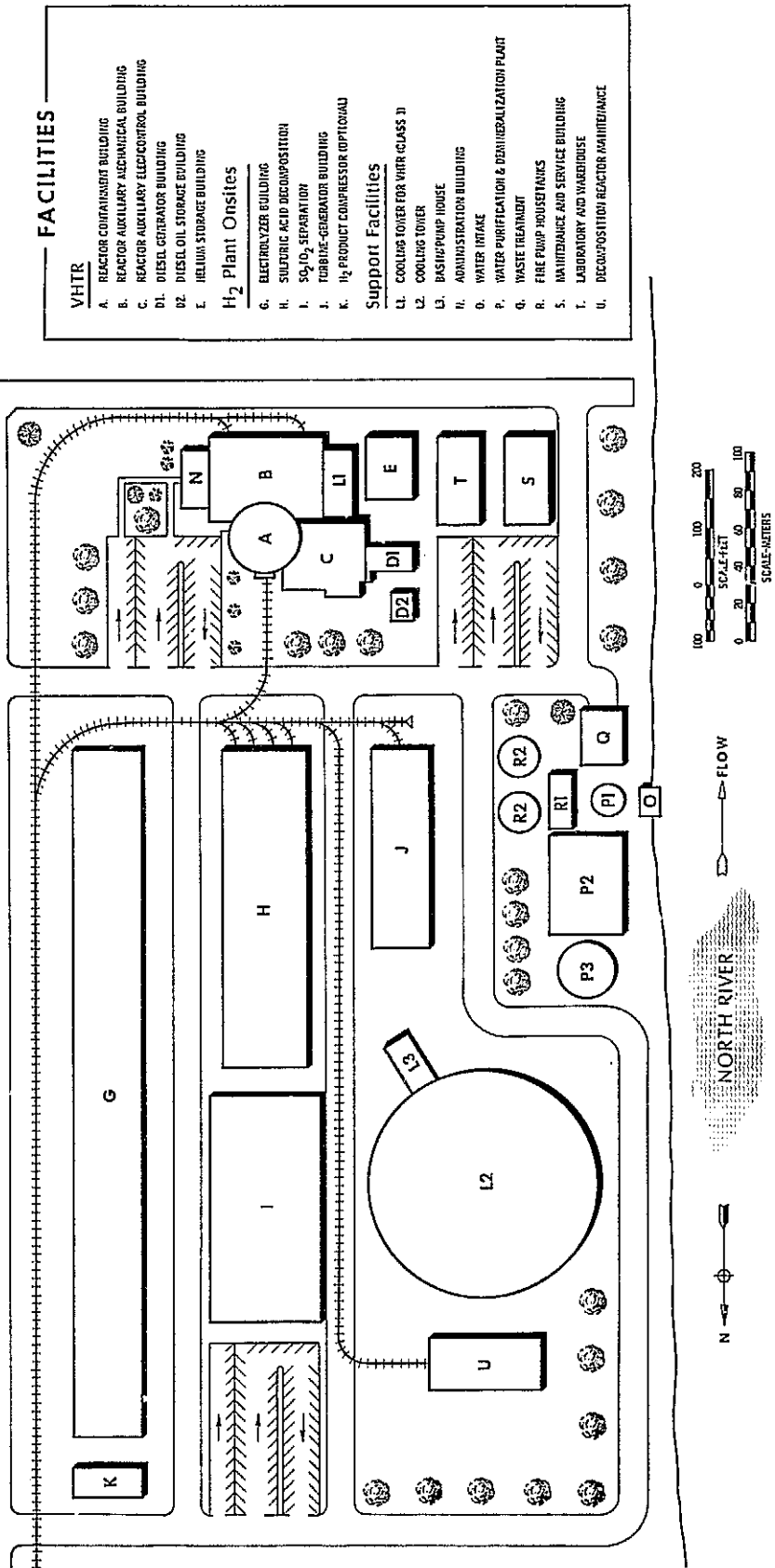


Figure 2.2.1 Plant Plot Plan

### 2.2.3 Plant Buildings

The buildings and structures in the plant are shown on the plot plan. Brief descriptions of the major buildings are given below. The VHTR building arrangements are taken from Reference 3.

#### 2.2.3.1 Major VHTR Buildings

##### Reactor Containment

The reactor containment, shown in Figures 2.2.2 and 2.2.3, is a right circular steel-lined prestressed concrete structure in which is located the integrated reactor vessel and reactor coolant system. It has an inside diameter of 33.5 m (110 feet) and measures 76.2 m (250 feet) from the base mat to the top of the dome.

The major structures located within the containment consist of the nuclear reactor and its supports, the refueling floor located just above the top of the reactor, the intermediate platforms for heating, ventilating, and air conditioning (HVAC) equipment and certain control and instrumentation racks, and the 200/15 ton capacity polar crane supported just below the dome spring line.

The crane is capable of lifting the intermediate heat exchangers, the fuel handling machines, the fuel transfer cask, and construction and maintenance loads.

##### Reactor Auxiliary Building

The reactor auxiliary building, Figures 2.2.2, 2.2.3, and 2.2.4, is located adjacent to the containment and is structurally independent of it. The building is a reinforced concrete structure, approximately 39.6 m (130 feet) wide, 57.9 m (190 feet) long, and 48.8 m (160 feet) high. At the east end of the building is a crane hall for handling the heavy components and the fuel transfer equipment from the containment. This crane hall is 27.4 m (90 feet) wide, 39.6 m (130 feet) long, and increases the height of the auxiliary building by 27.1 m (89 feet).

Located in the building are the fuel storage facilities, fuel shipping and receiving facilities, equipment service and decontamination areas, various reactor auxiliary systems, radioactive waste processing systems, and other service facilities for the plant.

##### Control and Electrical Building

The Control and Electrical Building, Figure 2.2.5, is located west of the containment and reactor auxiliary building. The building houses the total plant centralized control as well as the nuclear reactor control and auxiliary electrical equipment and supporting building services. These facilities are located in various roomed areas containing controls, a computer, switchgear, relays, instruments, batteries, and HVAC equipment.



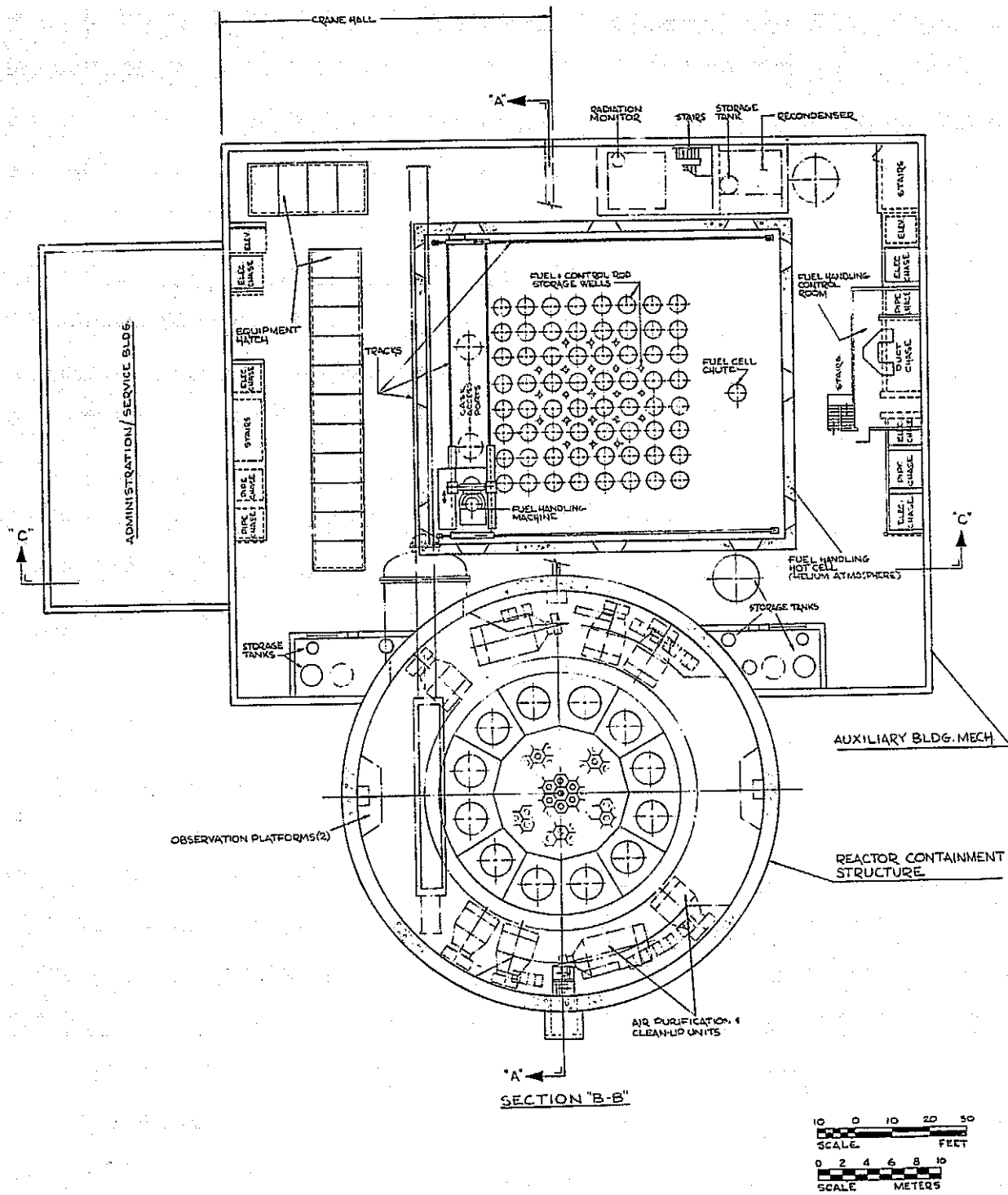


Figure 2.2.3 Reactor Containment and Auxiliary Building - Plan





### Diesel-Generator Building

The diesel-generator building adjoins the west end of the Control and Electrical Building and is structurally independent of it. The structure is of reinforced concrete construction. Housed in the building are the two diesel generators, fuel oil day tanks, combustion air intake louvers and filters, exhaust air silencers, air-starting compressors, emergency cooling water supply, and all the instrumentation necessary for proper operation of the diesel-generator emergency power supply units for the nuclear systems.

### Administration/Service Building

The administration facilities, consisting of general offices, engineering offices, conference rooms, and cafeteria, serves the entire plant. The VHTR service facilities located in this building are lockers and showers, health physics control facilities and radiolytic laboratories.

### Helium Storage Building

The helium storage building is a prefabricated rigid steel frame building housing the helium storage system.

## 2.2.3.2 Major Water Decomposition Plant Buildings

### Electrolyzer Building

The electrolyzer building is constructed of steel siding and roofing on a concrete slab. The building is 366 m (1200 feet) long by 36.6 m (120 feet) wide by 8.5 m (28 feet) from the top of the floor slab to the roof siding eave line. A double ridge roof is provided with gravity ventilators running the length of the building in each ridge to assure free and rapid escape of buoyant hydrogen from the building in the unexpected event of a hydrogen line rupture.

### Sulfuric Acid Decomposition Building

The Sulfuric Acid Decomposition Building houses all of the equipment in Battery H. The building, located just west of the Electrolyzer Building, is 171 m (560 feet) long and 53 m (175 feet) wide.

### SO<sub>2</sub>/O<sub>2</sub> Separation Building

The Battery I equipment for separating oxygen from sulfur dioxide is located in a building located north of the Sulfuric Acid Decomposition Building and west of the Electrolyzer Building. This building is 122 m (400 feet) long and 61 m (200 feet) wide.

## Turbine-Generator Building

The Turbine Generator Building, Battery J, houses the steam generators, turbine generator, and condenser used to produce electrical power from various heat sources within the process plant. The building, located close to the cooling tower, measures 106.7 m (350 feet) by 30.5 m (100 feet) by 30.5 m (100 feet) high.

### 2.3 BATTERY A - NUCLEAR HEAT SOURCE AND HEAT TRANSPORT SYSTEMS

#### 2.3.1 General

The very high temperature nuclear reactor (VHTR), suitable for use with the water decomposition system, is predicated on the integration of the technologies from the NERVA nuclear rocket engine program and land-based gas cooled reactor programs into an advanced graphite moderated, helium cooled reactor. The VHTR conceptual design, costs, and R&D program required for demonstration are more fully described in Reference 3. The plant consists of a Nuclear Island producing both very high temperature heat and electric power for the chemical water decomposition process. The heat is transported to the process via an intermediate heat transfer loop at temperatures sufficiently high to permit peak process temperatures of 1144K (1600°F). Principal parameters of the reactor are shown in Table 2.3.1.

The reactor and its coolant loops are contained within a multi-cavity prestressed cast iron reactor vessel (PCIV), as shown in Figure 2.3.1. The vessel walls contain smaller vertical cavities, or pods, in which are located very high temperature intermediate heat exchangers, circulators, turbogenerators and high temperature intermediate heat exchangers and auxiliary cooling systems for shutdown and emergency cooling of the reactor. Reactor helium coolant enters and discharges from the pods through coaxial piping at the upper end of the cavity, while the intermediate loop, or secondary, helium coolant is introduced and leaves through the bottom of the pod. The PCIV has a continuous internal steel liner to act as a primary coolant boundary and leak-tight membrane. A thermal barrier and insulation system is used to limit the temperature of the liner and minimize the heat loss to the PCIV. A cooling system circulates water through the walls of the PCIV to remove the heat deposited in the vessel. The PCIV is fabricated as a series of foundry cast iron blocks field assembled around the welded steel liner. Prestress cables are wound around the external cylindrical surface imposing the radial and tangential forces required to prevent the castings from separating under the internal gas pressure. Similarly, axial cables running longitudinally, through ports provided in the castings, maintain a compressive stress in the axial direction and carry the axial pressure loads.

The reference reactor core is designed to operate on the uranium-233/thorium-232 cycle, although it could operate equally well on other fuel cycles. The basic concept of fuel moderator blocks for the reactor is similar to that used in other gas cooled reactors. The extruded fuel elements are directly cooled by the helium. An objective in the core thermal design is to use an existing fuel particle; i.e., the TRISO bead, in the fissile fuel element and to achieve a high exit gas temperature without exceeding the fuel particle limitations.

TABLE 2.3.1

## PRINCIPAL PARAMETERS OF THE VHTR

<u>Reactor Thermal Power, MWt</u>	3345
<u>Reactor Vessel</u>	
Type	Prestressed Cast Iron
Overall Height, meters (ft)	33.5 (110)
Overall Diameter, meters (ft)	20.5 (67)
Material	Gray Iron (Class 40)
<u>Reactor Core</u>	
Nominal System Pressure, kPa (psia)	6895 (1000)
Coolant Mixed Mean Outlet Temperature, K (°F)	1283 (1850)
Reactor Power Density, W/cm <sup>3</sup>	10
<u>Very High Temperature Intermediate Heat Exchangers</u>	
Coolant, Tube Side/Shell Side	Helium/Helium
Pressure, Tube Side/Shell Side, kPa	6895/6895
Intermediate Coolant Outlet Temperature, K (°F)	1200 (1700)
<u>Circulators</u>	
Type	Axial Flow
Inlet Pressure, kPa (psia)	6688 (970)
Discharge Pressure, kPa (psia)	6895 (1000)
<u>Turbogenerators</u>	
Turbine Inlet Temperature, K (°F)	1283 (1850)
Electric Power Output, MW	150
<u>High Temperature Intermediate Heat Exchangers</u>	
Coolant, Tube Side/Shell Side	Helium/Helium
Intermediate Coolant Outlet Temperature, K (°F)	1033 (1400)

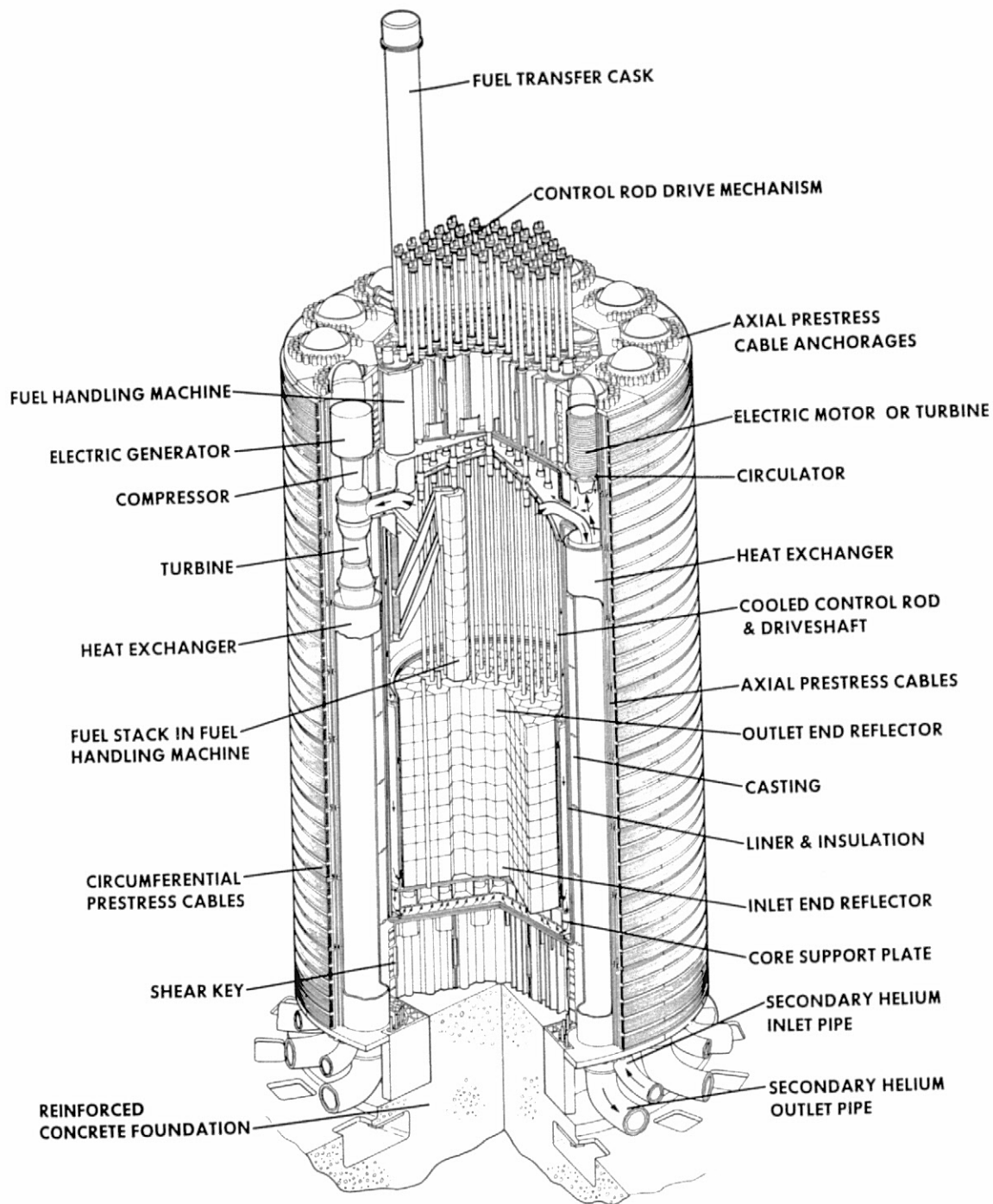


Figure 2.3.1 Very High Temperature Reactor (VHTR)

REPRODUCIBILITY OF THE  
ORIGINAL DRAWING IS POOR

When considering the use of nuclear heat in a process plant; the question of how that heat is to be applied must be answered. There are two alternatives; i.e., the direct cycle, where the reactor coolant is used in the process heat exchanger, and the indirect or intermediate loop cycle, where the reactor coolant transfers its heat to an intermediate buffer coolant system which in turn gives up its heat in the process heat exchanger.

The choice of the intermediate heat transfer loop approach for the process heat reactor was made after considering the advantages and disadvantages of the two alternatives in light of the all-important criteria of operability, maintainability, licensability, and economics. The cost of additional equipment and higher reactor coolant temperatures must be balanced against the other factors of operation and maintenance procedures and costs, licensing requirements, and public acceptance.

The reactor coolant system consists of the parallel power and heat exchanger loops located in the PCIV cavities. The function of the very high temperature intermediate heat exchangers is to transfer heat from the reactor core to the intermediate helium loops, which in turn transfer this heat to the high temperature  $\text{SO}_3$  reduction reactor, steam generators, and steam superheaters (Figure 2.3.2). Approximately 45 percent of the reactor thermal power is transferred through these loops, producing an intermediate helium coolant flow at a temperature of 1200K (1700°F) for use in the process plant. Each loop contains a very high temperature heat exchanger, valve, and helium circulator.

The turbogenerator loops produce electric power and supply high temperature heat, via high temperature intermediate heat exchangers, to the acid vaporizer and to steam generators in Battery J for the production of additional electric power in a Rankine cycle. Fifty-five percent of the reactor heat is transported by primary helium to the gas turbine generators which provide about 150 MWe of electrical power and compressor work. Exiting from the turbine at 4537 kPa (658 psia), the primary helium delivers heat to high temperature intermediate heat exchangers. The secondary side of these heat exchangers provides 1033K (1400°F) helium to meet the other thermal needs of the process.

Associated with the reactor are all the ancillary structures, services, systems and facilities to make a self-sufficient, operable Nuclear Island. These include reactor auxiliary systems, waste processing systems, instrumentation and control, fuel handling facilities, containment systems, electrical systems, and plant service systems.

### 2.3.2 Major Features

A number of significant features have been incorporated into the conceptual design of the very high temperature reactor (VHTR) to make it particularly attractive as a heat source for the water decomposition system.

Fuel. The ability to achieve the very high temperatures needed for the application, without exceeding the fuel bead temperatures currently considered as a maximum allowable, is achieved with extruded direct cooled fuel elements. Fuel elements using this technology have successfully operated, in the NERVA program, with coolant outlet temperatures up to 2475K (4000°F).

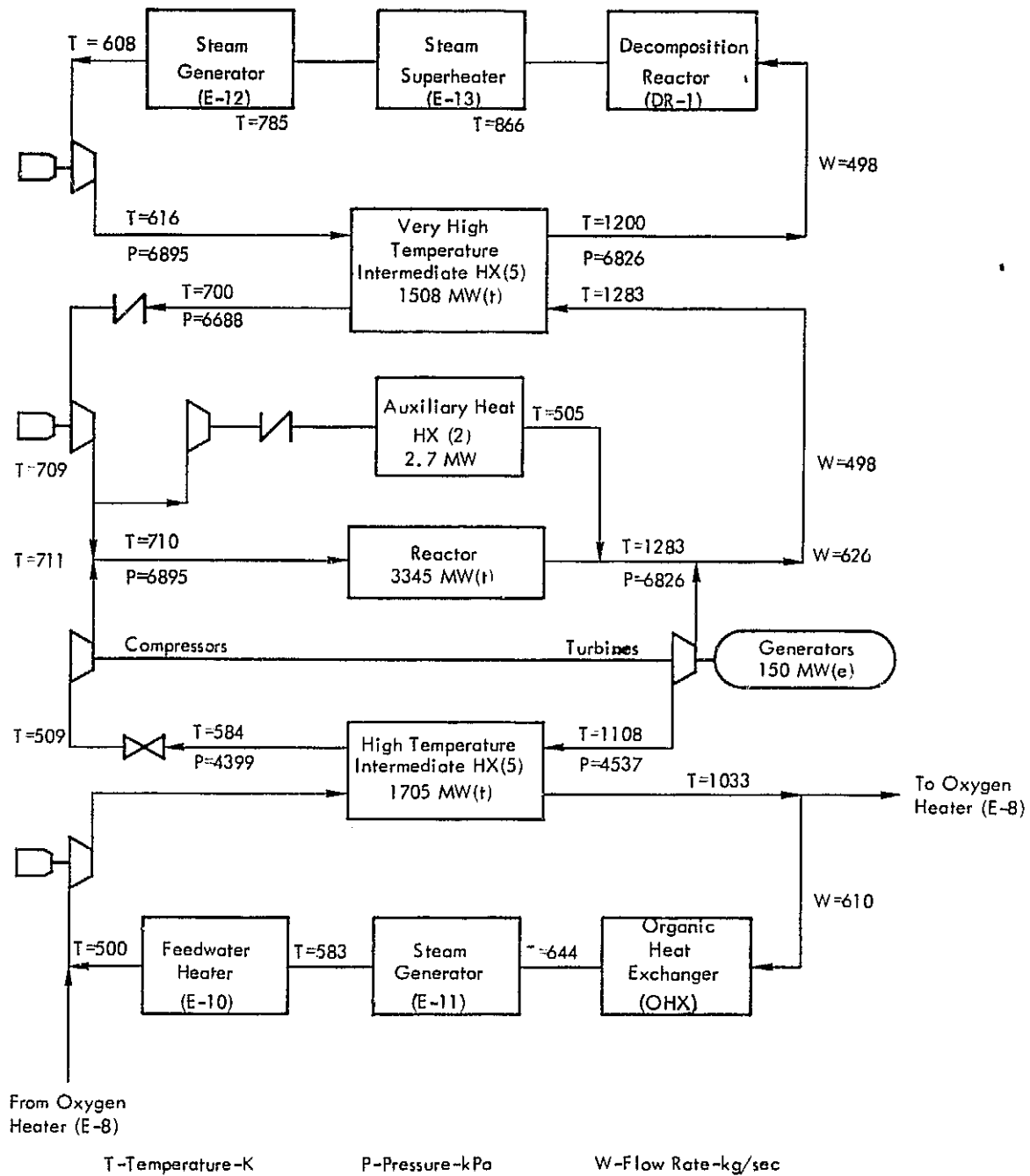


Figure 2.3.2 Reactor Coolant and Secondary Helium Flow Schematic

Reactor Vessel. Three different reactor vessel types had been considered. These were a welded steel vessel, a prestressed concrete vessel (PCRV) and a prestressed cast iron vessel (PCIV).

The steel vessel was discarded on the basis of the problems foreseen in the manufacture and transportation of vessels of the size required for large gas cooled reactors. The alternate of a field assembled welded steel vessel would require a very complex "one-time" fabrication facility and quality assurance program. The prestressed concrete reactor vessel (PCRV) technology has been used in European gas cooled reactors and is currently being applied in the United States. There does not appear to be any reason why the reactor could not be accommodated in a PCRV.

The prestressed cast iron reactor vessel (PCIV) design is based on analytical and experimental work by the German firm, Stempelkamp Giesserei KG, Krefeld, FRG. The concept is generally similar to that of the PCRV, with the exception that the concrete is replaced by cast iron. Cast iron compressive strength is twenty times that of concrete while its density and Young's Modulus are three times that of concrete. In addition, it has predictable physical properties and little or no in-situ creep or shrinkage. It has reduced weight and size, as shown in Table 2.3.2, with reduced sensitivity to overtemperature incidents. The cast iron blocks are poured and machined under factory, rather than field, conditions, resulting in a greater capability for the control of quality. Other foreseeable advantages include reduced construction time, reduced reactor containment building size, and reduced cost.

Reactor Flowpath. It is especially desirable, as coolant temperature is increased, to devise design solutions which minimize the problems of materials, insulation and fabrication. The proper choice of coolant flowpath is important to the design of the reactor vessel, liner, control rods, and drive mechanisms. The selected approach is to use the low temperature helium, returning to the reactor, to cool those components that would otherwise be exposed at or near the reactor exit gas temperatures of 1283K (1850°F)

Reactor Core. The reactor core is characterized by a large volume, large inventory of the fertile material with its attendant prompt negative coefficient of reactivity and low power density. The reactor fuel takes advantage of the unique capability of ceramic fuel microspheres to achieve very high burnups. Low temperature gradients in the extruded fuel elements are expected to minimize the adverse effects of temperature gradients on the integrity of fuel beads (the amoeba effect). The flexibility of the core design facilitates the consideration of alternative fuel configurations, coolant control schemes and refueling cycles.

The reactor core consists of sixty-one columns, each composed of eight hexagonal moderator blocks and one reflector block at each end of the core. Each moderator block has two types of fuel - fissile (highly enriched U-235) and fertile (natural thorium) on a one-to-two ratio, respectively. A central hole is incorporated in each moderator block to allow for the passage of the control rod and fuel handling tools.

TABLE 2.3.2

## REACTOR VESSEL COMPARISON

	Prestressed Cast Iron (PCIV)	Prestressed Concrete (PCRV)
Overall Height, meters	33.5	39.6
Overall Diameter, meters	20.5	33.4
Wall Thickness, meters	4.3	10.7
Head Thickness, meters	4.0	7.3

CONFIDENTIAL

Reactor Coolant System. The reactor coolant system consists of the very high temperature heat exchanger loops, the turbocompressor generator loops, the auxiliary cooling loops and the structures and ducting required to direct the cooling flow through the reactor and loops.

The reactor coolant is helium, which is chemically inert, is stable, is not subject to phase change and has good heat transfer characteristics. Helium has essentially zero neutron capture cross section, except for the fraction of helium-3 present in the gas. Some impurities will be present in the primary coolant due to desorption of impurities from material in the primary system, due to residual air during initial plant startup and release of gaseous fission products. The release of gaseous fission products is the only significant source that affects the steady state impurity level, and this concentration will be small due to the small mass of gaseous products produced by the fission process and the ability of the coated fuel particles to retain fission products.

The function of the turbocompressor loops is to generate electrical power and supply high temperature heat energy. These loops contain gas turbines, high temperature heat exchangers, valves and compressors.

There are two auxiliary cooling loops to provide independent means of cooling the reactor system when the reactor is shut down. The major components included in the auxiliary cooling loops are heat exchangers, shutoff valves, and circulators.

Gas Circulators. Each of the intermediate heat exchanger loops is provided with its own gas circulator. To permit the necessary independence and capability to handle each IHX pod as a separate unit, these circulators are powered by individual electric motor drives.

Intermediate Heat Exchangers. The principal requirements for heat exchangers, in this application, are the very high temperature intermediate heat exchanger, the high-temperature intermediate heat exchanger, and the process heat exchanger (SO<sub>3</sub> reduction reactor). These heat exchangers must operate for long periods of time under high temperature conditions, while maintaining a high degree of leak-tightness. The intermediate heat exchangers also have to meet the requirements of the nuclear codes. The process heat exchanger (DR-1), must handle similar temperatures while operating in the chemical environment of the water decomposition process.

## 2.4 BATTERY G - ELECTROLYZER SYSTEM AND AUXILIARIES

### 2.4.1 General

Battery G comprises the electrolyzers and auxiliary equipment necessary to produce hydrogen and sulfuric acid from sulfur dioxide and water. As shown in Figure 2.4.1 make-up and recycle water, streams (1) and (19), are mixed with sulfur dioxide, stream (45), and recirculating anolyte, stream (50), in an anolyte mixing drum (MD-1). This solution is then pumped into the electrolyzer where about one-half of the incoming sulfur dioxide is oxidized. Upon leaving the electrolyzer, the anolyte acid stream is split. A portion returns to MD-1 after being cooled in the electrolyte cooler, E-2G. The remainder flows to a flash drum, FD-1, where a pressure let-down out-gases about one-half of the dissolved sulfur dioxide. This gas is condensed in a sulfur dioxide condenser, E-1G, and pumped to the sulfur dioxide surge tank, stream (44). The acid stream leaving FD-1 is split; the product acid pumped to surge tank ST-1 and flows subsequently, stream (4), to Battery H for acid decomposition, the remainder flows to stripping tower T-1G where oxygen, stream (47), strips it of its dissolved sulfur dioxide. The resultant sulfur dioxide-oxygen mixture, stream (12), goes to Battery I for separation while the stripped acid flows to surge tank ST-1G. Stripped acid is held in ST-1G and pumped into the catholyte recirculation system, as required, to make up the sulfuric acid losses resulting from the flow of catholyte to the electrolyzer anode. Table 2.4.1 itemizes the mass rates, pressures and temperatures for each of twelve parallel circuits that make up Battery G.

### 2.4.2 Electrolyzer Module Design

#### 2.4.2.1 Introduction

The electrolyzer design is based largely on experimental data, described in Section 5.3.6, and on conventional practice in the design of conventional pressurized water electrolyzers. An acceptable design for the electrolyzer will involve maximization of the current efficiency for hydrogen generation and a minimization of the voltage losses in individual cells. The following system parameters will be influential:

- Diaphragm Properties

If the sulfurous acid component of the anolyte penetrates to the cathode, preferential deposition of sulfur will occur with a consequent reduction in the current efficiency for hydrogen evolution. It has been demonstrated experimentally that use of a certain type of diaphragm, coupled with a certain minimum of catholyte overpressure, will prevent sulfurous acid migration into the catholyte. For this design study, a membrane thickness of 0.76 mm (0.030 inch), a catholyte overpressure of 1.7 kPa (0.25 psi), and a membrane porosity, consistent with the achievement of a total cell voltage of 0.45 V, have been selected.

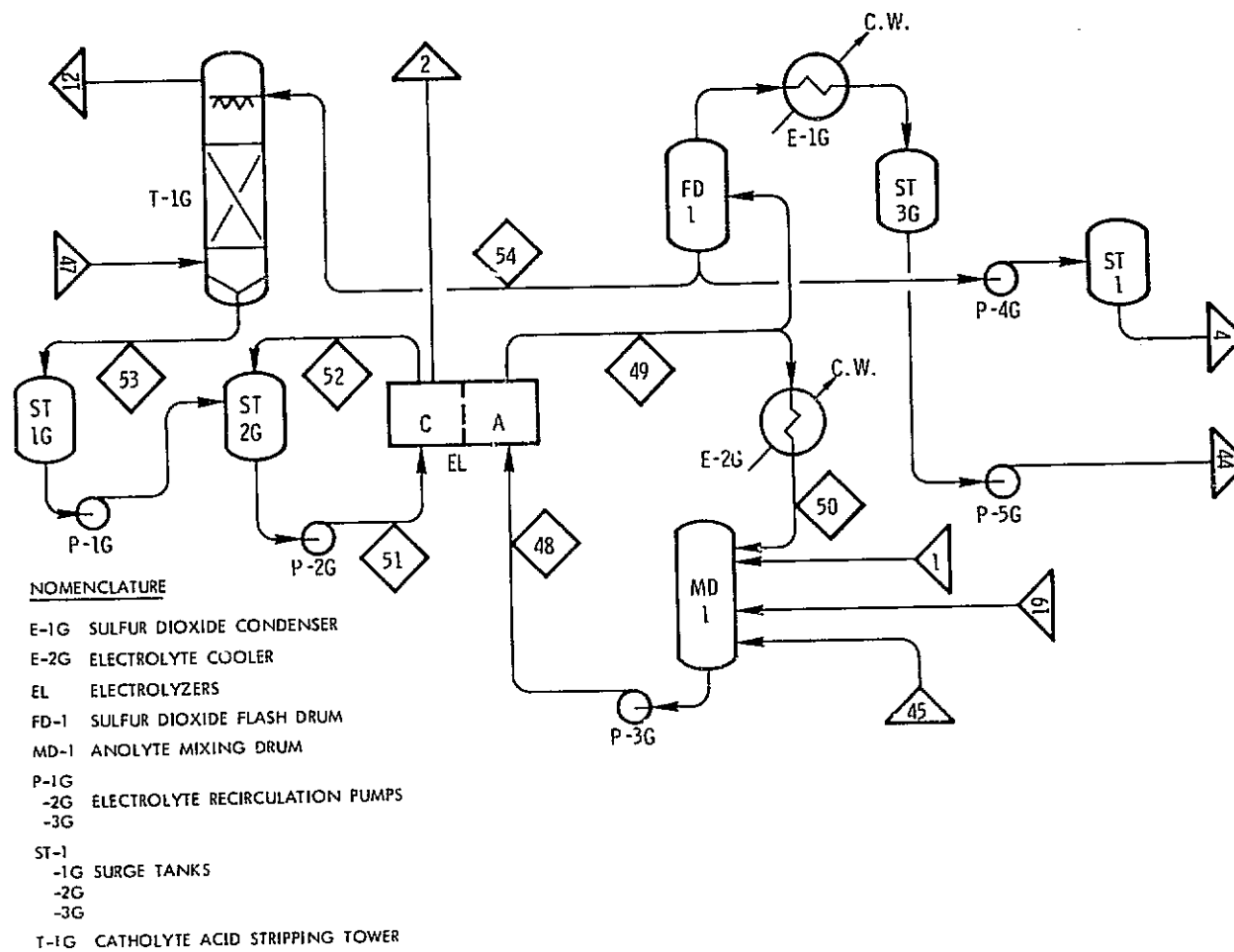


Figure 2.4.1 Battery G: Electrolyzers and Auxiliaries

TABLE 2.4.1

## BATTERY G MASS RATES

(Mass Rates Shown Are For Each Of Twelve Parallel Circuits)

Stream Number Temperature, K (°F) Pressure, kPa (psia) Mass Rate, kg/hr (lbs/hr) Composition, Weight Percent	1	2	4	12	19	44
	294 (70)	361 (190)	361 (190)	366 (200)	311 (100)	311 (100)
	2,586 (375)	2,586 (375)	579 (84)	517 (75)	2,930 (425)	2,758 (400)
	28,700 (63,300)	3,190 (7,030)	213,000 (470,000)	2,870 (6,320)	82,700 (182,000)	5,630 (12,400)
		100.0		19.9		
	H <sub>2</sub>					
	O <sub>2</sub>					
H <sub>2</sub> O	100.0		24.5		95.6	
SO <sub>2</sub>			2.2	80.1	4.4	100.0
SO <sub>3</sub>						
H <sub>2</sub> SO <sub>4</sub>			73.3			
Stream Number Temperature, K (°F) Pressure, kPa (psia) Mass Rate, kg/hr (lbs/hr) Composition, Weight Percent	45	47	48	49	50	51
	305 (90)	430 (315)	347 (165)	363 (194)	352 (174)	366 (200)
	2,689 (390)	2,413 (350)	2,620 (380)	2,586 (375)	2,517 (365)	2,620 (380)
	112,600 (248,300)	572 (1,260)	2,326,000 (5,124,000)	2,425,000 (5,347,000)	2,100,000 (4,630,000)	2,072,000 (4,568,000)
	H <sub>2</sub>					
	O <sub>2</sub>		100.0			
H <sub>2</sub> O	1.5		26.0	24.0	24.0	25.0
SO <sub>2</sub>	98.5		7.7	3.9	3.9	
SO <sub>3</sub>						
H <sub>2</sub> SO <sub>4</sub>			66.3	72.1	72.1	75.0
Stream Number Temperature, K (°F) Pressure, kPa (psia) Mass Rate, kg/hr (lbs/hr) Composition, Weight Percent	52	53	54			
	366 (200)	363 (194)	363 (194)			
	2,586 (375)	517 (75)	579 (84)			
	1,968,000 (4,338,000)	104,000 (230,000)	106,600 (235,000)			
	H <sub>2</sub>					
	O <sub>2</sub>					
H <sub>2</sub> O	25.0	25.0	24.5			
SO <sub>2</sub>			2.1			
SO <sub>3</sub>						
H <sub>2</sub> SO <sub>4</sub>	75.0	75.0	73.4			

- Cell Design

A bipolar configuration has been selected for this design study. This design is also preferred for the similar phosphoric acid fuel cell stack from the standpoints of cost and efficiency. The bipolar element typically consists of an embossed reinforced graphite plate. It was assumed also that the plate surfaces are activated electrochemically with electrocatalysts. Experimented demonstration of this concept remains to be performed.

- Anolyte Recirculation

Recirculation of the anolyte was found to offer the simplest methods for the addition of make-up sulfur trioxide and water. Extrapolation of data for 74 W/O H<sub>2</sub>SO<sub>4</sub> at 90°C (194°F) to 2586 kPa (375 psi) indicated that the solubility of sulfur dioxide is 0.08 g/g or 0.1 g/ml under the expected conditions. Thus the concentration of sulfur dioxide at anolyte inlet is assumed to be at this level. To minimize concentration polarization phenomena at the anode, an exit concentration corresponding to 0.04 g/g has been selected.

- Catholyte Recirculation

Recirculation of the catholyte was included in this design because of three considerations: (a) the need for continuous catholyte make-up; (b) to minimize ohmic losses in the electrolyte due to the hydrogen volume; and (c) cell cooling. Because of the catholyte overpressure, there is a net loss of electrolyte to the anolyte through the porous diaphragm. A recirculating catholyte stream ensures that catholyte will always be available for make-up.

- Dimensions of Manifolding and Ports

For this design, care has been taken to ensure that the parasitic current inefficiency, due to leakage paths through cell inlets and outlets and along the catholyte and anolyte manifolds, represents only a small percentage of the total. These considerations involve keeping the cross-sectional area of given lengths of exit ports, which are larger than the inlet ports because of the need to maintain a pressure differential across the diaphragm, below a certain minimum. The pressure drops from cell inlet to outlet, required for adequate flow, are thus a source of process inefficiency.

It is recognized that the ultimate electrolyzer design will be based on trade-off studies which will involve simultaneous optimization of anolyte and catholyte recirculation rates, cell voltages, current densities, inlet and outlet port dimensions and placement, and manifold dimensions.

### 2.4.2.2 Electrolyzer Design

The basic building block of Battery G is the electrolyzer module. The module consists of a stack of 400 cells, each approximately 2.4 m (8 feet) in diameter and 7.5 mm (0.3-inch) thick, supported, together with the electrolyte distribution piping and tanks, inside a pressure vessel. The vessel, pressurized by hydrogen produced in the electrolyzer, allows the use of low pressure plastic piping and tanks within the vessel, thus minimizing current leakage problems. Piping and valves external to the pressure vessel are made of corrosion resistant alloy. Figures 2.4.2 through 2.4.5 illustrate the conceptual design of the electrolyzer module.

Figure 2.4.2 shows a side view of the electrolyzer with the pressure vessel cut away to reveal the cell support structure, piping, and electrolyte tanks. The pressure vessel is made of carbon or low alloy steel and is approximately 3.8 cm (1.5 inch) thick. The vessel is a circular cylinder, approximately 3.8 m (12.5 feet) in diameter with elipsoidal ends. The overall length is approximately 6.25 m (20.5 feet). The vessel is split horizontally across its diameter. The split line flange is bolted and sealed to permit assembly and disassembly. Penetration nozzles are provided for the electrical conductors and fluid and gas piping connections. Provision is made for purging the vessel with nitrogen prior to disassembly. All the external lines are provided with valves to permit the isolation of the electrolyzer from the system.

The cells consist of fiber reinforced phenolic plates separated by microporous membranes, as shown schematically in Figure 2.4.3. One of the surfaces of a plate functions as an anode while the other surface acts as the cathode of the adjacent cell. A single cell consists of an anode surface, a microporous membrane, and a cathode surface. Electric current flows axially through the cell stack with a voltage drop of 0.45 V per cell (180 V per electrolyzer module). The cathode and anode surfaces of the plates are activated electrochemically by bonding small quantities of active elements to them.

The fiber reinforced cell plates are approximately 2.4 m (8 feet) in diameter and 6.4 mm (0.25 inch) thick at the rim. The rim is reinforced with glass fiber and extends radially inward for approximately 8.9 cm (3.5 inch). Holes are distributed around the rim to provide axial passages which distribute electrolyte to the cells and collect the electrolyte and hydrogen gas returning from the cells.

The region of the cell plate inside the rim is reinforced with graphite fibers and is therefore, electrically conductive. This area of the plate is approximately half as thick as the rim and is embossed in both surfaces so that the total thickness through the embossing is equal to that of the rim. The embossing thus locates and supports the microporous membrane, providing flow passages along the plate surfaces approximately 1.5 mm (0.060 inch) wide.

The microporous membrane is approximately 0.76 mm (0.030 inch) thick and extends to the outer diameter of the plate rim. The rim area of the membrane is treated with sealant to eliminate the porosity in this area and so provide sealing between the plates. Holes are provided in the membrane rim to match the electrolyte distribution holes in the plates.

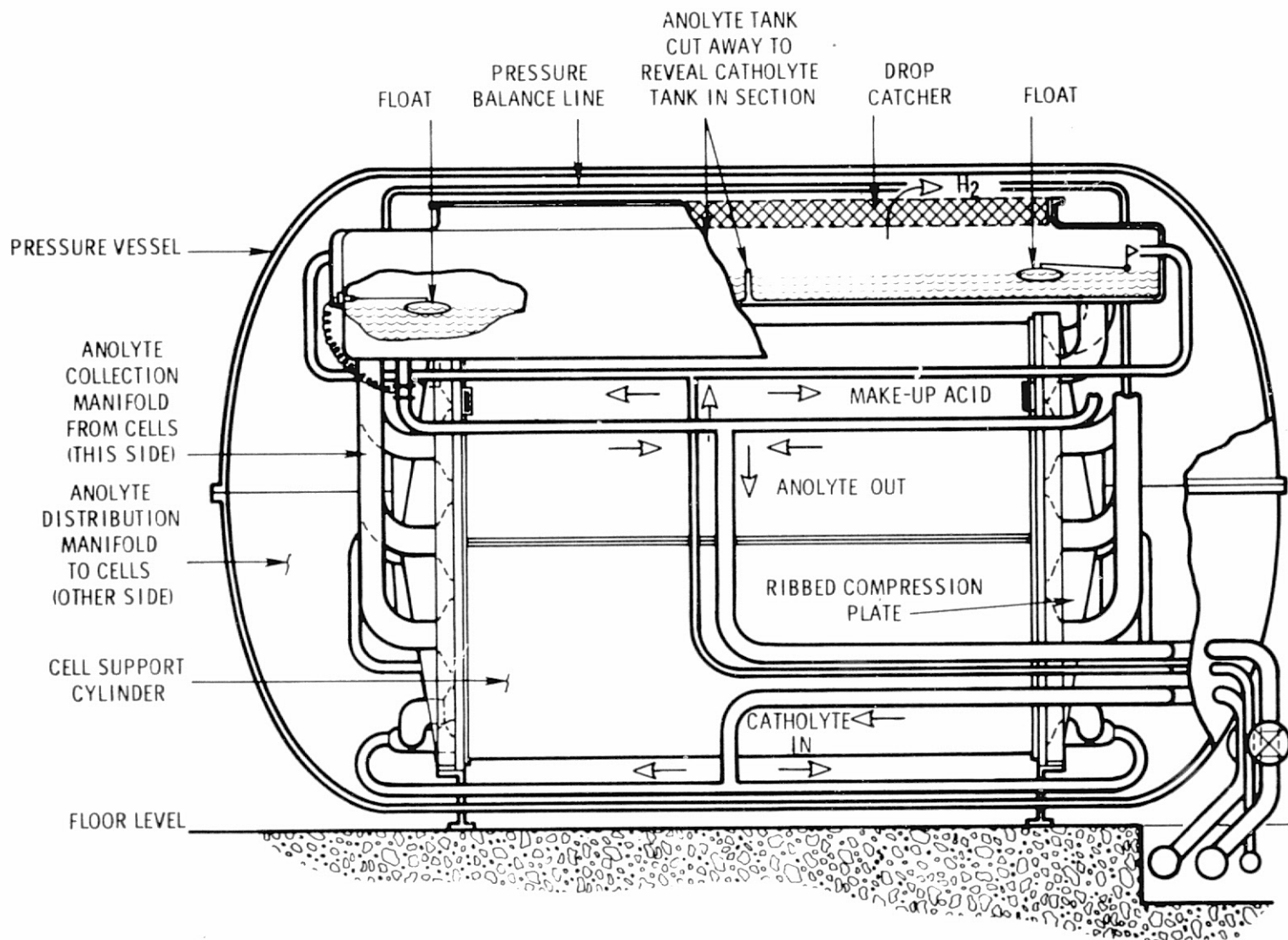


Figure 2.4.2 Side View with Pressure Vessel Cut Away to Reveal Cell Support Structure and Piping

EMBOSSSED GRAPHITE FIBER REINFORCED  
PHENOLIC PLATES WITH FIBERGLASS RIM  
(EMBOSSING OMITTED FOR CLARITY)

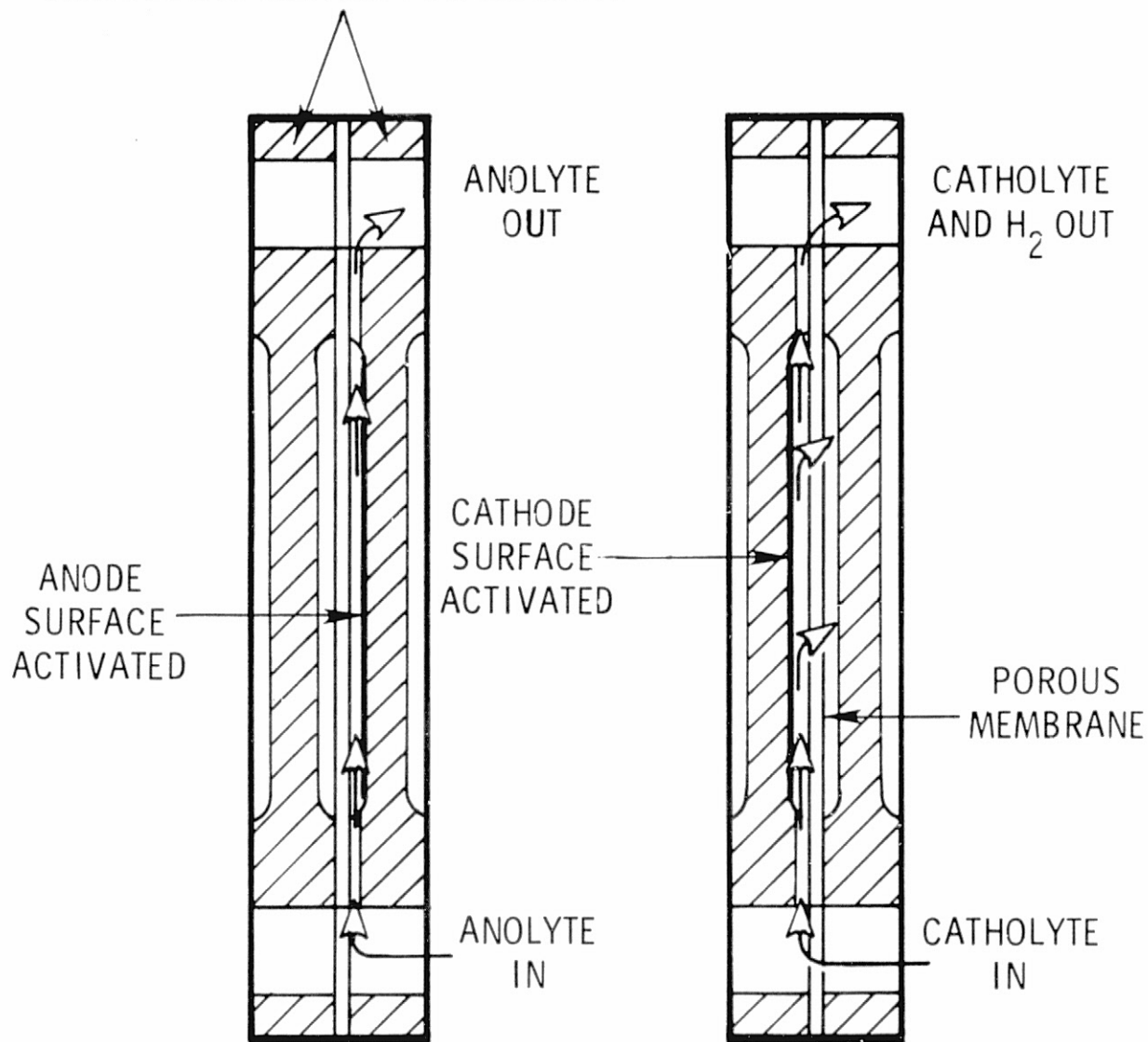


Figure 2.4.3 Electrolyzer Cell

Metering slots in the surfaces of the plates control the flow of electrolyte from the axial distribution holes in the rim to the flow gaps in the cell spaces. Figure 2.4.4 shows how the cells are stacked in the electrolyzer and electrolyte distributed to the cells. The arrangement of catholyte and anolyte delivery and withdrawal manifolds is shown in Figure 2.4.5.

The slots connecting the cell spaces to the axial distribution holes are much greater in flow area at cell outlet than at cell inlet in order to minimize the difference in pressure from the cells to the collector tanks and thus ensure that the fluid levels controlled in the tanks properly influence the cell pressures. The slots at cell inlet are much more restricted in area to properly meter the flow and control the distribution of electrolyte across the 1.5 mm (0.06 inch) gaps in the cells. The axial holes in the plate rims are provided with sufficiently large flow area to minimize the pressure drop along them in relation to the metering pressure drop and thus ensure that the cells near the center of the stack are not starved.

The pressure in the catholyte cell space is maintained at a pressure of approximately 1.7 kPa (0.25 psi) above that of the anolyte causing a small portion of the catholyte to diffuse through the membrane into the anolyte space. The pressure difference is maintained by float control of the liquid levels in the anolyte and catholyte collector tanks which are supported above the electrolyzer cells and which receive the electrolyte leaving the cells. A pressure balance line from the anolyte tank vents any  $\text{SO}_2$  released in the tank to the main dissolution tank at the same pressure as the hydrogen in the electrolyzer pressure vessel. The hydrogen pressure is maintained 2.6 kPa (375 psi) by a pressure control valve in the main hydrogen delivery line. The catholyte collector tank, supported above the electrolyzer cells, is vented to the hydrogen in the pressure vessel through a drop catcher which ensures that the hydrogen produced on the cells is free of liquid as it enters the pressure vessel. The hydrogen product gas passes from the pressure vessel through a short pipe and shut-off valve into the main hydrogen delivery line.

The anolyte and catholyte collector tanks are both divided into two halves, one for each end of the electrolyzer. The float level controls are duplicated in each half and the electrolyte is piped to and from each end of the cell stack to minimize the pressure drop in the axial distribution holes. A central wall in each tank insulates each end of the tank from the other, eliminating current leakage. All pipes inside the pressure vessel, as well as the electrolyte collector tanks, are made of plastic. The pipes which carry make-up acid to the catholyte tank float control and which carry anolyte released from the anolyte tank float controlled valve are of relatively small diameter, resulting in an acceptably small leakage current. Similarly, small pipes are used to convey the anolyte and catholyte streams from the vessel wall to the inlet manifolds, to minimize current leakage at these locations.

Both catholyte and anolyte are recirculated. Catholyte is recirculated to ensure a minimum ratio of liquid/liquid + gas at the cell outlet to prevent drying out of the upper portion of the cathode surface. Anolyte is recirculated to provide the necessary  $\text{SO}_2$  transport to the cells recognizing the  $\text{SO}_2$  solubility limit and minimum concentration desirable at the cell exit.

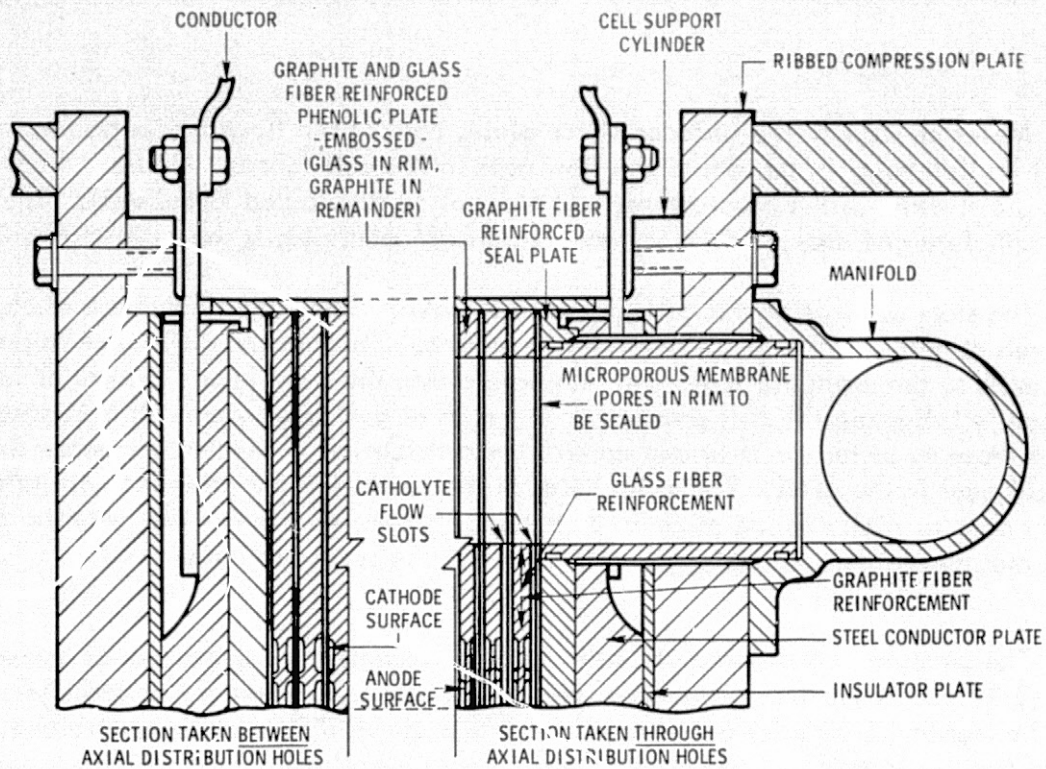


Figure 2.4.4 Detail Section through Cells and Manifold

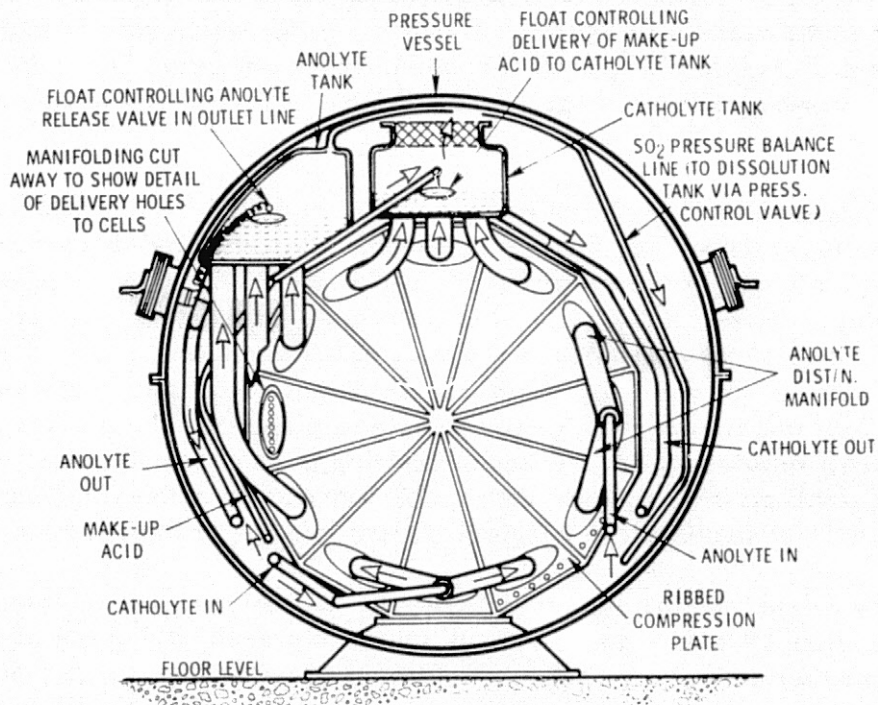


Figure 2.4.5 Front View on Cell Structure with Vessel Cut Away

REPRODUCIBILITY OF THE ORIGINAL PAGE IS POOR

The cell support cylinder is split axially to facilitate its placement around the cells after completion of the stacking operation. Flanges at the ends of the cylinder are bolted to the ribbed compression plates inducing an axial tension load in the cylinder and a corresponding compressive force in the cell stack. The force will provide a tensile strain in the cylinder and compressive strain in the stack sufficient to accommodate the differential thermal growth of the cylinder and stack while ensuring enough residual compression in the stack to provide a leak proof assembly. Since the liquid pressure to be sealed is in the order of 34.5 kPa (5 psi), a nominal compression of the membrane rims should provide sufficient sealing. In providing the appropriate degree of prestress, some shimming of the support cylinder may be required. This would be easily provided at the end flanges, the shims being fitted in accordance with the measured cell stack-up dimension.

At the ends of the cell stack, a graphite fiber reinforced seal plate is provided to protect the steel conduction plate from acidic attack. Bobbin and O-ring connections convey the electrolyte from the axial holes to the plastic distribution manifolds. The steel conductor plates carry the electrical conductors which are attached by setscrews to milled recesses in the plates. Insulating plates, made of fiberglass or rubber, separate the conduction plates from the ribbed compression plates.

The ribbed compression plates are designed to possess the necessary bending stiffness to ensure a reasonably uniform compressive strain across the cell stack.

The structure provided by the ribbed compression plates and the cell support cylinder allows the cell stack to be lifted as an assembly and turned on its side, the cell support cylinder providing sufficient shear strength and stiffness to allow the assembly to be supported at the ends on the lower flanges of the ribbed compression plates. An additional function of the cell support cylinder is to protect the cell plates from handling damage while the cell structure is lifted into position in the lower half of the pressure vessel.

The electrolyte tanks and manifold piping can be attached to the electrolyzer either before or after it is lifted into the vessel lower half. All piping connections inside the pressure vessel can be made and leak tested prior to closing the vessel.

#### 2.4.3 Electrolyzer Bay Arrangement

The electrolyzer modules are arranged in the electrolyzer building so that a group of five modules is wired in series and supplied with power from a 900 volt, 10,600 amp rectifier. Vessels and external piping are grounded electrically. Four sets of five modules are arranged so that 20 modules occupy most of the floor space in a 30 x 36 m (100 x 120 feet) bay of the electrolyzer building. The remaining space in the bay contains the auxiliary cooling and dissolution equipment required to process the electrolyte for the electrolyzers within the bay. Figure 2.4.6 illustrates the general layout of the 20 modules and auxiliary equipment into a bay. Table 2.4.2 summarizes the major parameters of the electrolyzer system.

NOTE: TWELVE PARALLEL CIRCUITS, AS SHOWN, REQUIRED

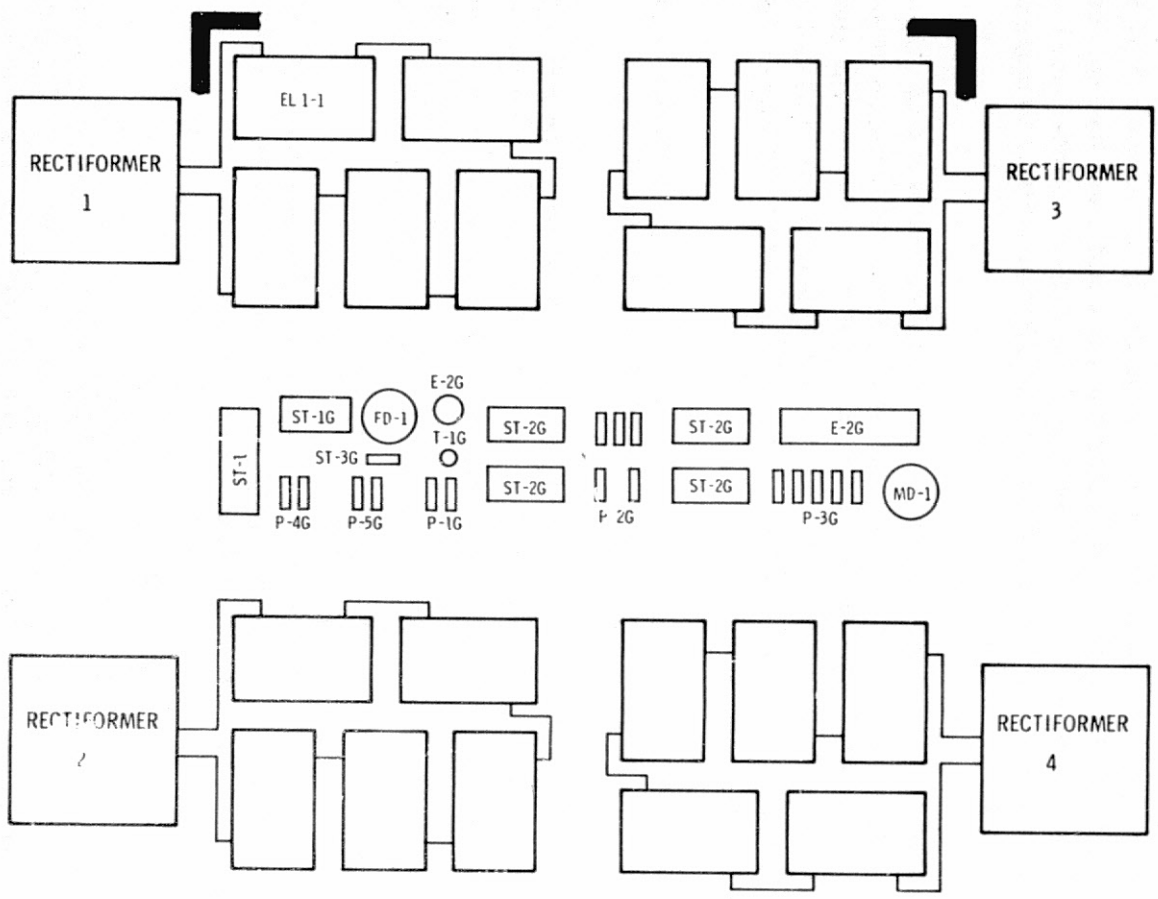


Figure 2.4.6 Battery G: Electrolyzer Circuit and Auxiliary Equipment Layout

TABLE 2.4.2  
 MAJOR PARAMETERS - ELECTROLYZER SYSTEM

Total Number Modules	240
Modules Per Bay	20
Total Number of Bays	12
Modules in Electrical Series	5
Power Supply:	9.54 MW(e) Rectifiers
Voltage	900 VDC per Rectifiers
Current	10,600 amp per Rectifiers
Rectifiers Per Bay	4
Total Number of Rectifiers	48

The electrolyzer modules are located in a separate building, identified as G on the plot plan, along with their associated equipment and service facilities. These are a total of 12 bays arranged within the building.

#### 2.4.4 Electrolyzer Power Supply

Rectifiers are employed to supply the dc power to the electrolyzers. Each Rectifier, rated at 9.54 MWe, 900 V-dc, 10,600 amperes feeds five electrolyzer modules in series. The Rectifier consists of an a-c connection (3 phase, 60 Hz), regulating transformer, stepdown transformer, diodes (rectifiers), and a d-c connection. Controls are supplied to vary the a-c voltage to adjust the d-c voltage for changes in the electrolyzer module circuits, such as a module taken out of service. The Rectifiers are located outside the electrolyzer building as shown on the bay arrangement Figure 2.4.6.

#### 2.4.5 Electrolyzer Auxiliaries

Several pieces of equipment, as shown in Figure 2.4.1, are required to handle the anolyte and catholyte for the electrolyzer and are therefore included in Battery G. The electrolyzer auxiliary system is replicated for each of the twelve bays of twenty electrolyzers. The equipment is described in the paragraphs below.

##### 2.4.5.1 Surge Tanks

There are four surge tank applications in the electrolyzer system. ST-1 provides storage for the sulfuric acid stream from the electrolyzers prior to its flow to Battery H, the Sulfuric Acid Decomposition System. ST-1G provides storage capacity and NPSH requirements for pump P-1G. It handles sulfuric acid to be used as catholyte make-up. ST-2G provide capacity for recirculating sulfuric acid in the catholyte system. ST-3G provides storage for SO<sub>2</sub> recovered from the flash drum prior to its flow to the SO<sub>2</sub> surge tank in Battery I, the SO<sub>2</sub>/O<sub>2</sub> Separation System. Principal characteristics of these surge tanks is given in Table 2.4.3.

##### 2.4.5.2 Heat Exchangers

There are two heat exchangers in the system. They are E-1G, a sulfur dioxide condenser, and E-2G, the electrolyte cooler. Their principal parameters are given in Table 2.4.4.

##### 2.4.5.3 Pumps

Pumps are used to circulate fluids within the system and transfer fluids to other batteries. The pumps in Battery G are characterized in Table 2.4.5.

TABLE 2.4.3  
SURGE TANKS

Component	ST-1	ST-1G	ST-2G	ST-3G
Number Per Bay	1	1	4	1
Contained Fluid	Sulfuric Acid	Sulfuric Acid	Sulfuric Acid	Sulfur Dioxide
Diameter, m (ft)	1.8 (6)	1.8 (6)	1.8 (6)	0.9 (3)
Length, m (ft)	4.9 (16)	3.0 (10)	3.0 (10)	1.5 (5)
Pressure, kPa (psia)	579 (84)	517 (75)	2586 (375)	517 (75)
Temperature, K (°F)	361 (190)	363 (194)	366 (200)	311 (100)
Material of Construction	Hastelloy	Hastelloy	Hastelloy	Carbon Steel

TABLE 2.4.4  
HEAT EXCHANGERS

Component	E-1G	E-2G
Service	SO <sub>2</sub> Condenser	Electrolyte Cooler
Type of Design	Shell & Tube	Shell & Tube
Number Per Bay	1	1
Characteristics Per Unit		
Heat Duty, MWt (Btu/hr)	0.55 (1.88 x 10 <sup>6</sup> )	13.3 (45.4 x 10 <sup>6</sup> )
Shell Diameter, m (ft)	1.5 (5)	1.8 (6)
Length, m (ft)	3.0 (10)	6.1 (20)
Shell Side		
Fluid	Water	Water
Flow Rate, kg/hr (lb/hr)	28,000 (63,000)	690,000 (1.5 x 10 <sup>6</sup> )
Inlet Temperature, K (°F)	305 (90)	305 (90)
Outlet Temperature, K (°F)	322 (120)	322 (120)
Nominal Operating Pressure, kPa (psia)	345 (50)	345 (50)
Tube Side		
Fluid	SO <sub>2</sub>	H <sub>2</sub> O, SO <sub>2</sub> , H <sub>2</sub> SO <sub>4</sub>
Flow Rate, kg/hr (lb/hr)	5,630 (12,400)	2.1 x 10 <sup>6</sup> (4.63 x 10 <sup>6</sup> )
Inlet Temperature, K (°F)	363 (194)	363 (194)
Outlet Temperature, K (°F)	311 (100)	352 (174)
Nominal Operating Pressure, kPa (°F)	579 (84)	2,550 (370)

TABLE 2.4.5

## PUMPS

Component	P-1G	P-2G	P-3G	P-4G	P-5G
Number Per Bay	2	5	5	2	2
Fluid	Sulfuric Acid	Sulfuric Acid	Anolyte Make-Up	Sulfuric Acid	Sulfur Dioxide
Characteristics Per Unit					
Rating, percent	50	25	25	50	50
Flow Rate, kg/hr (lb/hr)	52,000 (115,000)	518,000 (1,142,000)	581,000 (1,281,000)	107,000 (235,000)	2,800 (6,200)
Inlet Pressure, kPa (psia)	517 (75)	2,586 (375)	2,517 (365)	579 (84)	517 (75)
Outlet Pressure, kPa (psia)	2,586 (375)	2,620 (380)	2,620 (380)	613 (89)	2,758 (400)
Temperature, K (°F)	363 (194)	366 (200)	347 (165)	361 (190)	311 (100)
Motor Rating, horsepower	35	7.5	20	1.5	2.5

#### 2.4.5.4 Vessels

In addition to the electrolyzer modules, Battery G includes, for each bay, one sulfur dioxide flash drum (FD-1), one anolyte mixing drum (MD-1), and one catholyte acid stripping tower (T-1G). These components are located as shown in Figure 2.4.6.

### 2.5 BATTERY H - SULFURIC ACID DECOMPOSITION

#### 2.5.1 General

The sulfuric acid decomposition battery consists of that equipment required to take the sulfuric acid from the electrolyzer, vaporize it, decompose it to water and sulfur trioxide, and reduce the sulfur trioxide to sulfur dioxide and oxygen. The equipment required for these functions is located in the area identified by the letter "H" on the plot plan.

The operating pressures and temperatures utilized in the process were selected on the basis of minimizing the technical risks associated with the applicability of materials for the acid vaporization step. The use of a pressure of 380 to 450 kPa (55 to 65 psi) and a peak acid temperature of 700K (800°F) permits the use of high silicon irons, such as Duriron, as the material of construction for the acid vaporizer (AV-1). Since Duriron is a cast material, considerations of manufacture dictate that plate type heat exchangers be utilized for the vaporizers and that differential pressures across the plates be kept low. This led to the selection of a low pressure organic, rather than helium, heat transfer fluid as the heat source in the vaporizer to avoid the excessively high pumping powers that would otherwise be required in a low pressure helium system. Similarly, the desire to keep the total pressure drop in the acid vaporization/decomposition loop low results in the need for low velocity in the catalyst beds of the decomposition reactors (DR-1), with the result that large volumes of catalyst, which must therefore operate at very low space velocities, are required. These design considerations, adopted to assure that the concerns with structural material performance in high temperature boiling sulfuric acid are minimized within the limits of today's technology, produce a design which has a higher capital cost and pumping power (i.e., lower efficiency) than is believed to be representative of a developed system. It is expected that the development program will identify materials that can successfully operate in a boiling sulfuric acid environment at higher pressures and temperatures and can be fabricated into tubular heat exchangers, or will identify an economically attractive alternate chemical, rather than evaporative, concentration system. Either of these developments should result in improvements in both the process economics and thermal efficiency.

The process flow sheet for the sulfuric acid decomposition battery is shown in Figure 2.5.1 and the mass balance in Table 2.5.1. Sulfuric acid produced in Battery G, (4), is sent to Battery H. A portion of this acid is withdrawn, (5), and injected into the 1144K (1600°F) effluent leaving the decomposition reactor (DR-1), (9). Vaporization of this acid absorbs a major portion of the gas sensible heat, lowering its temperature, (10), to 700K (800°F). This cooler enters T-1, a packed tower irrigated with the balance of the electrolyzer product acid. Within the tower, the incoming acid is stripped of its sulfur dioxide, concentrated

NOMENCLATURE

- AV-1 SULFURIC ACID VAPORIZER
- DR-1 SULFUR TRIOXIDE REDUCTION REACTOR
- E-1 BOILER FEEDWATER HEATER
- MV-1 MIXING VESSEL
- OHX ORGANIC HEAT EXCHANGER
- P-1,2 PUMPS
- ST-1H  
-2H SURGE TANKS
- T-1 ACID CONTACTING PACKED TOWER

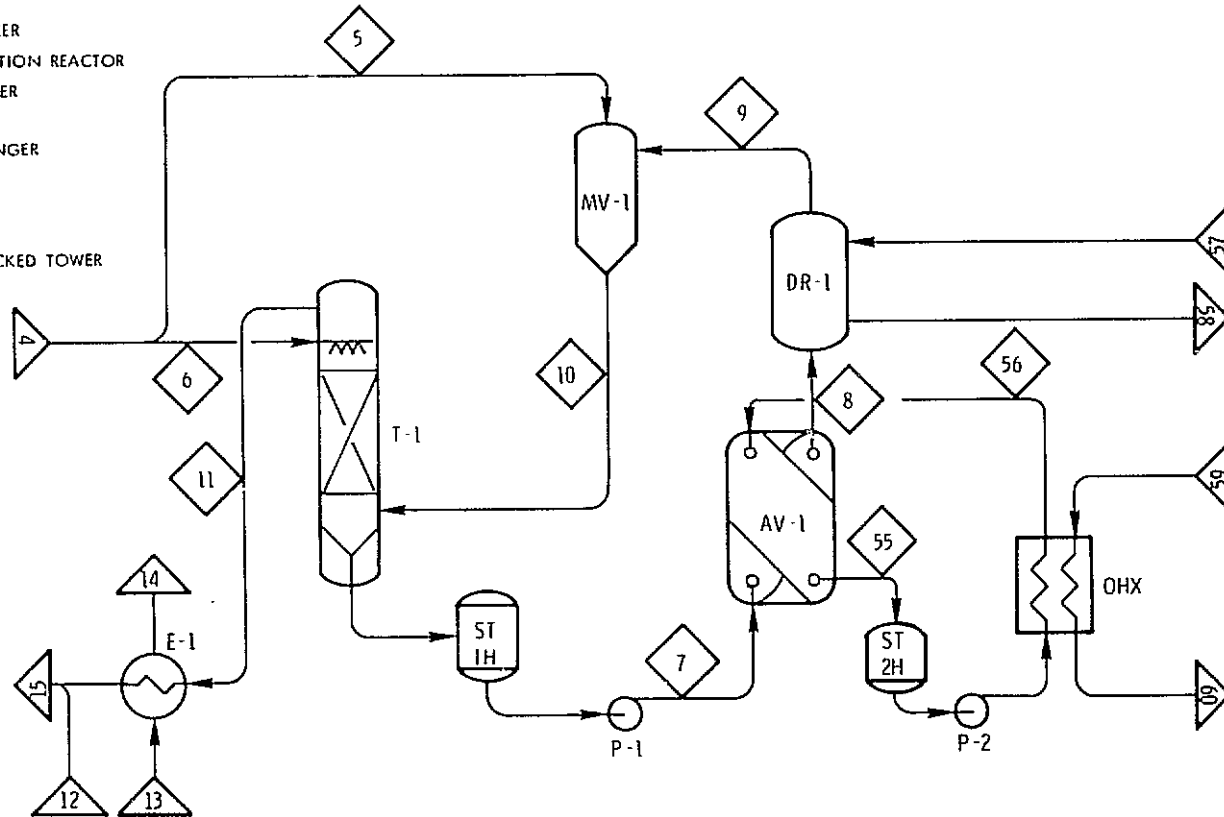


Figure 2.5.1 Battery H: Sulfuric Acid Decomposition

TABLE 2.5.1  
BATTERY H MASS BALANCE

Stream Number	4	5	6	7	8	9
Temperature, K (°F)	361 (190)	361 (190)	361 (190)	576 (577)	700 (800)	1,144 (1,600)
Pressure, kPa (psia)	517 (75)	517 (75)	517 (75)	448 (85)	379 (55)	310 (45)
Mass Rate, kg/Hr (Lbs/Hr)	2,556,000 (5,634,000)	446,500 (984,400)	2,109,000 (4,650,000)	2,551,000 (5,623,000)	2,551,000 (5,623,000)	2,551,000 (5,623,000)
Composition, Weight Percent						
H <sub>2</sub>						
O <sub>2</sub>						12.0
H <sub>2</sub> O	24.5	24.5	24.5		18.4	18.4
SO <sub>2</sub>	2.1	2.1	2.1			48.0
SO <sub>3</sub>					81.6	21.6
H <sub>2</sub> SO <sub>4</sub>	73.4	73.4	73.4	100.0		
Stream Number	10	11	12	13	14	15
Temperature, K (°F)	700 (800)	470 (387)	366 (200)	322 (120)	435 (323)	380 (225)
Pressure, kPa (psia)	310 (45)	241 (35)	517 (75)	8,690 (1,260)	8,620 (1,250)	207 (30)
Mass Rate, kg/Hr (Lbs/Hr)	2,997,000 (6,607,000)	2,556,000 (5,634,000)	34,410 (75,850)	1,054,000 (2,323,000)	1,054,000 (2,323,000)	2,590,000 (5,710,000)
Composition, Weight Percent				B. F. W.	B. F. W.	
H <sub>2</sub>						
O <sub>2</sub>	10.2	12.0	19.9			12.1
H <sub>2</sub> O	21.3	37.9				37.4
SO <sub>2</sub>	41.2	50.1	80.1			50.5
SO <sub>3</sub>	27.3					
H <sub>2</sub> SO <sub>4</sub>						
Stream Number	55	56	57	58	59	60
Temperature, K (°F)	617 (650)	755 (900)	1,200 (1,700)	866 (1,100)	1,033 (1,400)	644 (700)
Pressure, kPa (psia)	345 (50)	448 (65)	6,895 (1,000)	6,760 (980)	4,520 (655)	4,480 (650)
Mass Rate, kg/Hr (Lbs/Hr)	8,733,000 (19,250,000)	8,733,000 (19,250,000)	1,793,000 (3,953,000)	1,793,000 (3,953,000)	2,195,000 (4,838,000)	2,195,000 (4,838,000)
Composition, Weight Percent	Organic*	Organic*	H <sub>2</sub>	H <sub>2</sub>	H <sub>2</sub>	H <sub>2</sub>
H <sub>2</sub>						
O <sub>2</sub>						
H <sub>2</sub> O						
SO <sub>2</sub>						
SO <sub>3</sub>						
H <sub>2</sub> SO <sub>4</sub>						

\* MIPA, Therminol 88, or Similar

from 75 weight percent to greater than 98 weight percent and preheated. A mixture of steam, sulfur dioxide, and oxygen leaves the tower, (11), and after being joined by the  $\text{SO}_2/\text{O}_2$  mixture leaving the electrolyzer stripping tower (12), flows to Battery 1, (15). Hot, concentrated acid (7) leaving the tower is pumped to the acid vaporizer (AV-1), where it is decomposed into a mixture of steam and sulfur trioxide (8). These gases enter DR-1, a convectively heated catalytic reactor, where the sulfur trioxide is decomposed into sulfur dioxide and oxygen. Unreacted sulfur trioxide is condensed in T-1 as sulfuric acid and recycled. Thermal energy is provided by hot secondary helium from the VHTR, (57) and (59). To minimize helium recirculation power while not exceeding the 450 kPa (65 psia) limitation on the Duriron plate heat exchangers employed in AV-1, a recirculating organic loop is provided.

### 2.5.2 Acid Vaporizer (AV-1)

The acid vaporizers are plate heat exchangers using Duriron as the material of construction. This selection was made based upon an evaluation of currently available materials that could be expected to perform in the high temperature concentrated sulfuric acid environment of the vaporizer. Duriron, a casting alloy of iron containing 14.5 percent silicon, 0.85 percent carbon, and 0.65 percent manganese, is highly resistance to corrosion for all concentrations of sulfuric acid to the boiling point at the pressures selected for the design. The use of Duriron in a tubular heat exchanger has not been considered, since current casting technologies would limit tubes to roughly 2.54 cm (1 inch) in diameter and 0.9 meters (3 feet) long, and the development required to produce longer tube and shell heat exchangers is not warranted. Duriron can be cast, however, into plates which permit the proposed configuration of heat exchanger to be used.

A reference configuration of the Duriron Plate Heat Exchanger is shown in Figure 2.5.2. It uses plates measuring 1524 mm (5 feet) by 1067 mm (3.5 feet) by 19 mm (0.75 inch) thick, with 3.175 mm (1/8 inch) ridges to achieve approximately  $1.11 \text{ m}^2$  (12 feet<sup>2</sup>) of heat transfer surface per plate. The plate weighs approximately 215 Kg (475 lbs.). Fifty plates are assembled into each heat exchanger, with leakage between plates prevented by a gasket plated with gold for corrosion resistance. The gold plating should be largely recoverable and reuseable from used gaskets. A total of 780 heat exchangers are required to meet the total duty of the process. The characteristics of the heat exchangers are given in Table 2.5.2.

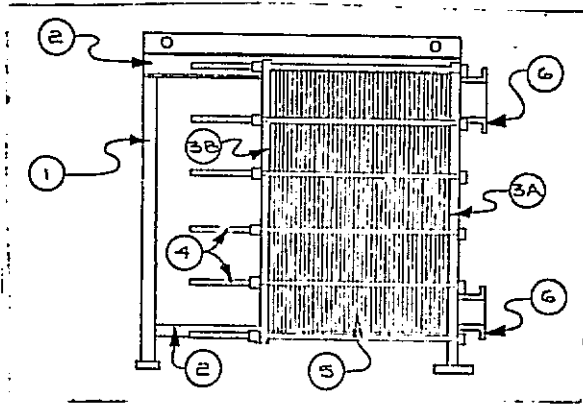
The heat exchangers are arranged in a basic module of twelve units, with six on the ground and six above them, elevated about 2.44 meters (8 feet) above ground on grates, as shown in Figure 2.5.3. The heat exchangers are arranged three on each side of a module main, with approximately 0.9 meters (3 feet) spacing between heat exchangers for maintenance access. The basic module is approximately 8.53 by 8.53 meters (28 x 28 feet). There are five rows of 13 modules each requiring a plot plan area of 42.7 meters (140 feet) by 111 meters (364 feet).

### 2.5.3 Decomposition Reactor (DR-1)

The decomposition reactor is a shell and tube heat exchanger in which high temperature helium, from the intermediate heat transport loop of the nuclear heat source, flow through

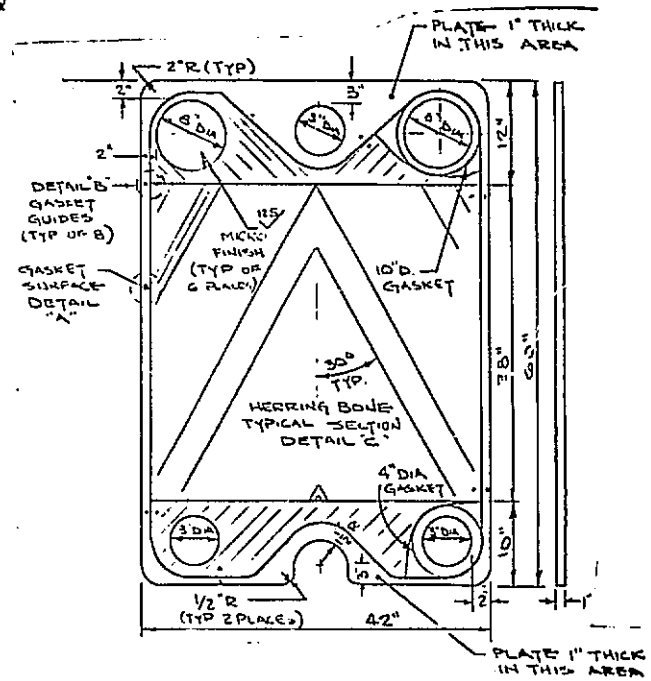
# H<sub>2</sub>SO<sub>4</sub> ACID VAPORIZER (AV)

## PLATE HX CONFIGURATION



- ① FRAME
- ② SUPPORT BARS
- ③A END PLATE WITH NOZZLES
- ③B PRESSURE PLATE
- ④ TIE RODS WITH END BOLTS
- ⑤ HEAT EXCHANGER PLATES
- ⑥ INLET AND OUTLET NOZZLES

## PLATE DETAIL



HtTr AREA ~ 12 ft<sup>2</sup>/PLATE  
 WEIGHT ~ 475 lbs DURIRON  
 COST ~ \$400/PLATE IN QUANTITY


**united engineers**

11/5/75

Figure 2.5.2 Duriron Plate Heat Exchanger

TABLE 2.5.2  
ACID VAPORIZERS (AV-1)

Type of Heat Exchanger	Plate
Number of Units	780
Material of Construction	Duriron
Characteristics Per Unit	
Heat Duty, MW (Btu/Hr)	1.58 (5.38 × 10 <sup>6</sup> )
Surface Area, m <sup>2</sup> (ft <sup>2</sup> )	1.11 (12)
Overall Length, m (ft)	2.44 (8)
Overall Width, m (ft)	1.22 (4)
Overall Height, m (ft)	1.98 (6.5)
Primary Side	
Fluid	Sulfuric Acid
Flow Rate, kg/hr (lb/hr)	3270 (7209)
Inlet Temperature, K (°F)	576 (577)
Outlet Temperature, K (°F)	700 (800)
Inlet Pressure, kPa (psia)	448 ( 65)
Outlet Pressure, kPa (psia)	379 ( 55)
Secondary Side	
Fluid	Organic (MIPB, Therminol VP-1, or Therminol 88)
Flow Rate, kg/hr (lb/hr)	11,196 (24,680)
Inlet Temperature, K (°F)	755 (900)
Outlet Temperature, K (°F)	617 (650)
Inlet Pressure, kPa (psia)	448 ( 65)
Outlet Pressure, kPa (psia)	345 ( 50)

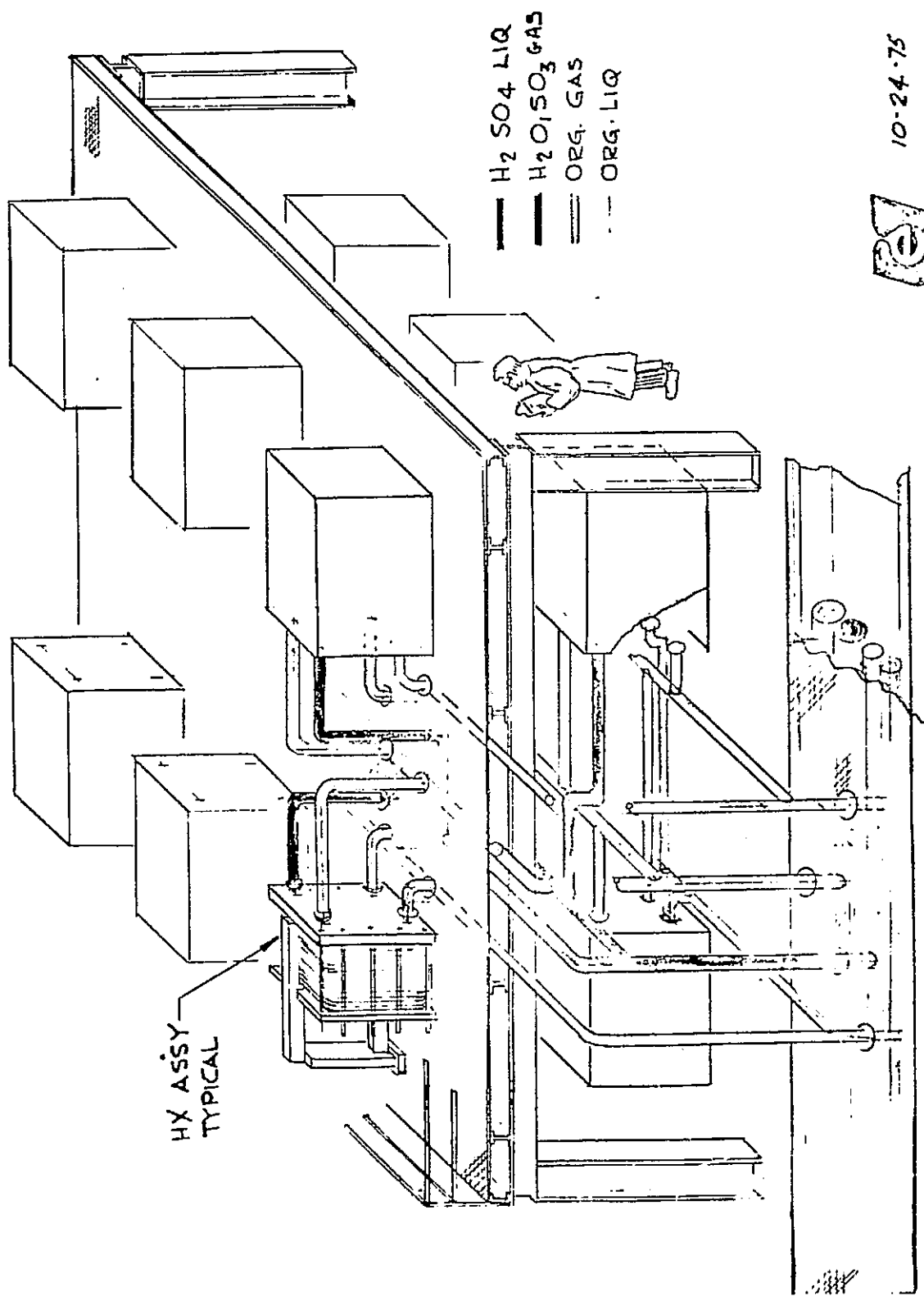


Figure 2.5.3 Westinghouse H<sub>2</sub> Process Duriron Plate HX Arrangement Concept

the tubes and supplies the energy for the catalytically assisted thermal reduction of sulfur trioxide and oxygen.

The decomposition reactor consists of a cylindrical vessel, approximately 3.66 meters (12 feet) in diameter and 10.7 meters (35 feet) high supported inside an external pressure vessel, as shown in Figure 2.5.4. Sulfuric acid vapor at 700K (800°F) is supplied to a plenum inside the external pressure vessel immediately below the catalyst vessel. The acid vapor travels upward along the annular passage formed between the catalyst vessel and the external pressure vessel and enters the catalyst vessel at its upper end. 1840 heat exchange tubes 25.4 mm (1 inch) outside diameter by 4mm (0.156 inch) wall thickness pass through the bed in the axial direction. The tubes are uniformly spaced throughout the catalyst bed on an approximately 76 mm (3 inch) triangular pitch and convey helium gas at approximately 6895 kPa (1000 psi) from a tubular header vessel below the catalyst vessel to a similar header at the upper end. The helium gas enters the lower header at 1200K (1700°F) and leaves the upper header at 866K (1100°F).

The heat extracted from the helium passes into the catalyst bed and raises the temperature of the acid vapor to 1144K (1600°F) in its passage through the bed. The acid vapor is decomposed and leaves the bed at the lower end through a supporting screen or grating. The decomposition products are then piped away from the reactor to the packed tower (T-1).

The major characteristics of the decomposition reactors are indicated in Table 2.5.3. Noteworthy among these characteristics is the low pressure drop experienced by the process gas through the catalyst bed. This pressure drop is required to maintain a reasonable total pressure throughout the entire acid vaporization/decomposition loop, consistent with the low pressure requirements of the Duriron plate heat exchanger used for acid vaporization, and a total pressure drop consistent with reasonable pumping powers. These considerations call for a low process gas velocity through the beds, resulting in large flow areas, low catalyst space velocities, large catalyst volumes, and, in order to allow shop fabrication and shipping to the plant site, a large number of units. The successful development of alternate acid concentration methods, or materials that would permit the selection of high pressure, high temperature tubular acid vaporizers, would significantly reduce the limitations on pressure drop and result in fewer, smaller, decomposition reactors.

The lower header, carrying the 1200K (1700°F) helium gas, is designed in such a way that its structural material is cooled by the 700K (800°F) acid vapor. This is shown in Figure 2.5.5. Excessive loss of heat from the helium to the acid vapor is prevented by a stagnant layer of helium gas. A hot gas liner inside the header structural cylinder carries the 1200K (1700°F) helium and delivers it to the heat exchanger tubes through 1840 short delivery tubes. Thus, 1200K (1700°F) helium is isolated from the header structural material by a layer of stagnant helium gas which is trapped between the liner and the header. The lower header arrangement, as seen from below, is shown in Figure 2.5.6.

An alternative cooled header concept which augments the cooling of the header structural material by recirculating the 866K (1100°F) return helium gas along the inside of the header is also feasible. In this arrangement the header is exposed to 700K (800°F) acid vapor

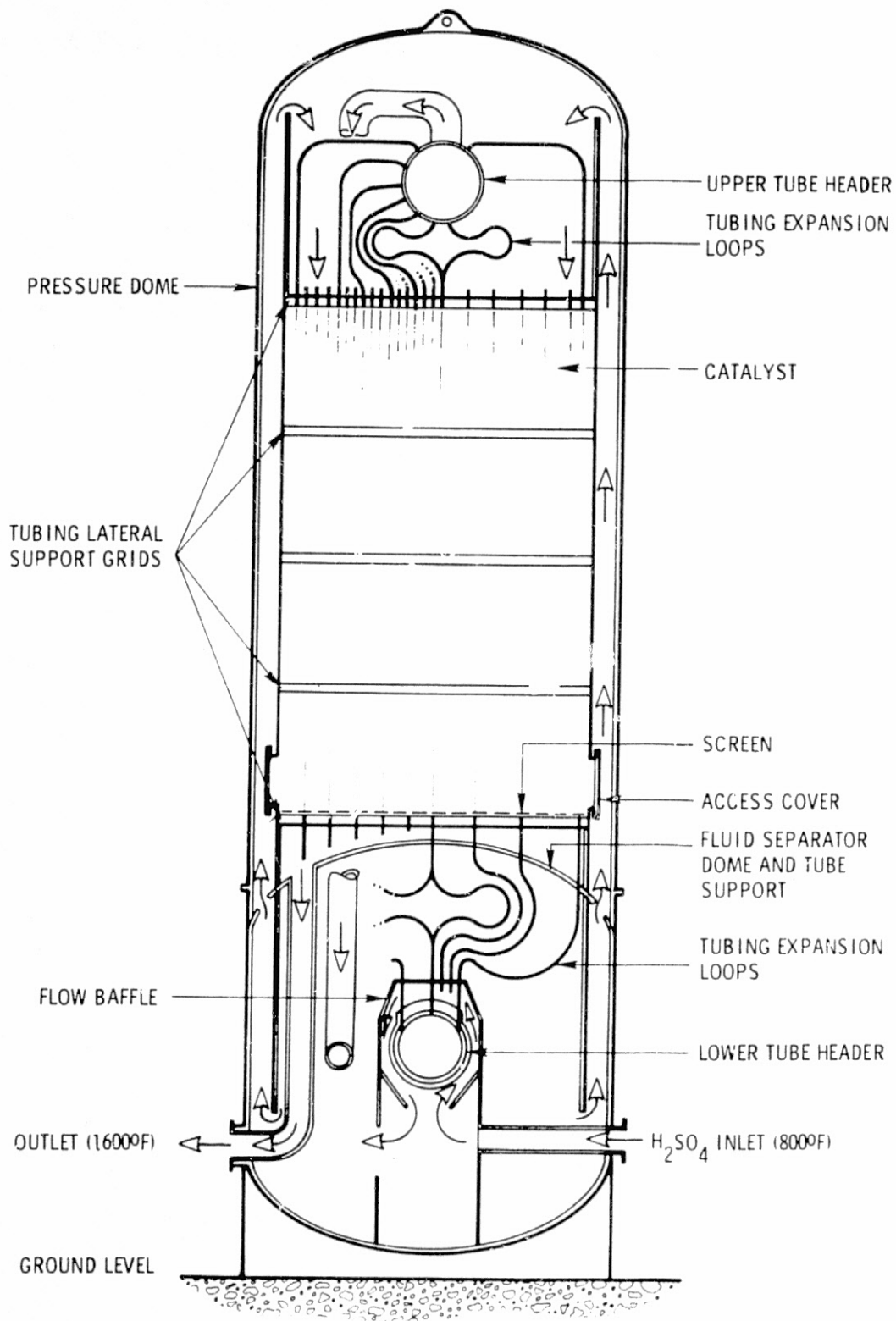


Figure 2.5.4 Decomposition Reactor

TABLE 2.5.3  
DECOMPOSITION REACTOR (DR-1)

Type of Design	Shell and Tube
Number of Units	15
Characteristics Per Unit	
Heat Duty, MW (Btu/hr)	57.4 (196 × 10 <sup>6</sup> )
Surface Area, m <sup>2</sup> (ft <sup>2</sup> )	1566 (16,860)
Outside Diameter, m (ft)	4.27 (14)
Overall Height, m (ft)	18.3 (60)
Tube Diameter, mm (in)	25.4 (1)
Shell Side	
Fluid	SO <sub>3</sub> , H <sub>2</sub> O, SO <sub>2</sub> , and O <sub>2</sub>
Flow Rate, kg/hr (lb/hr)	170,000 (375,000)
Inlet Temperature, K (°F)	700 ( 800)
Outlet Temperature, K (°F)	1144 (1600)
Inlet Pressure, kPa (psia)	379 ( 55)
Outlet Pressure, kPa (psia)	310 ( 45)
Catalyst Bed Volume, m <sup>3</sup> (ft <sup>3</sup> )	102 (3600)
Space Velocity, hr <sup>-1</sup>	800
Tube Side	
Fluid	Helium
Flow Rate kg/hr (lb/hr)	119,500 (263,500)
Inlet Temperature, K (°F)	1200 (1700)
Outlet Temperature, K (°F)	866 (1100)
Inlet Pressure, kPa (psia)	6895 (1000)
Outlet Pressure, kPa (psia)	6760 ( 980)

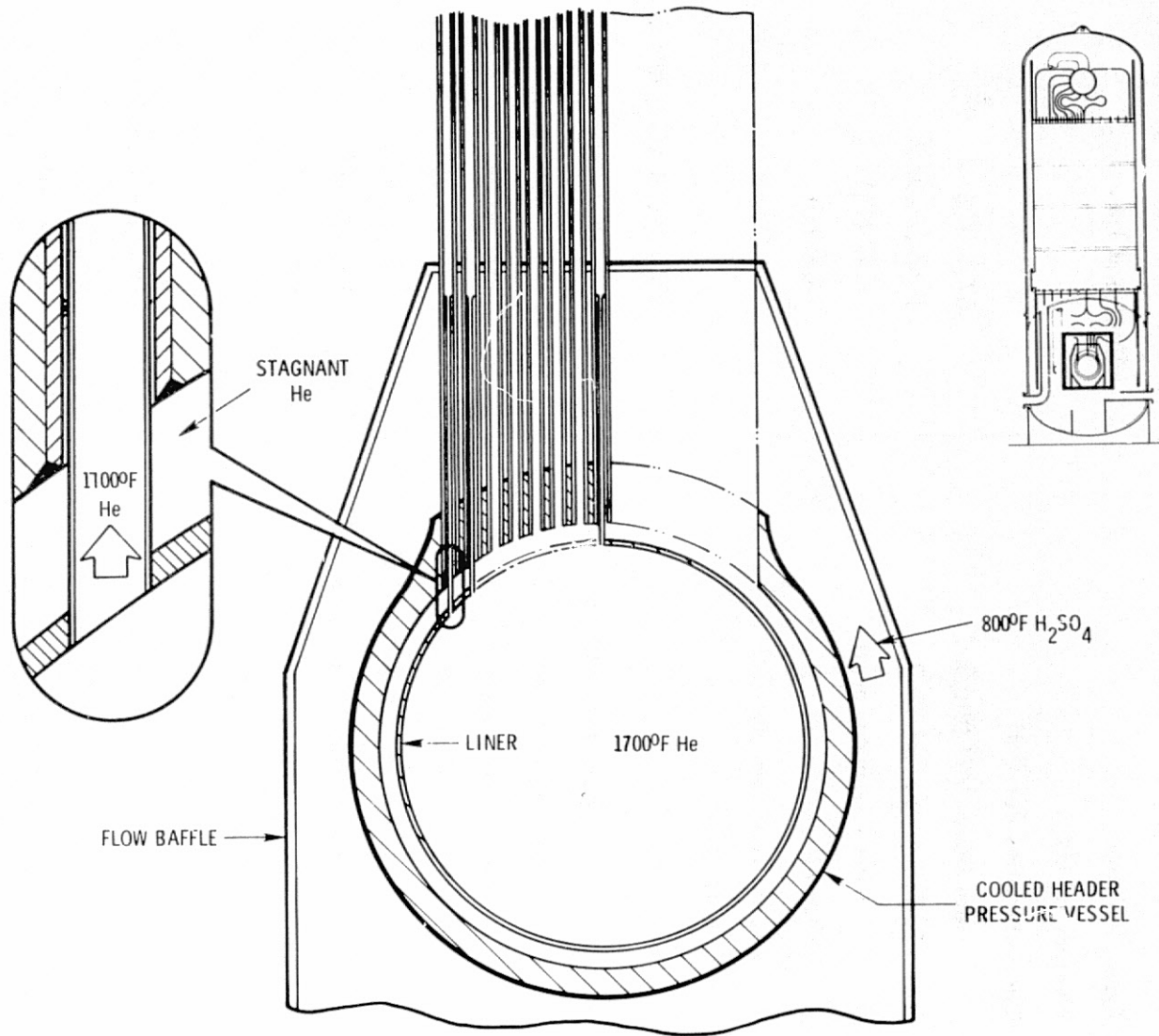


Figure 2.5.5 Detail of Lower Tube Header

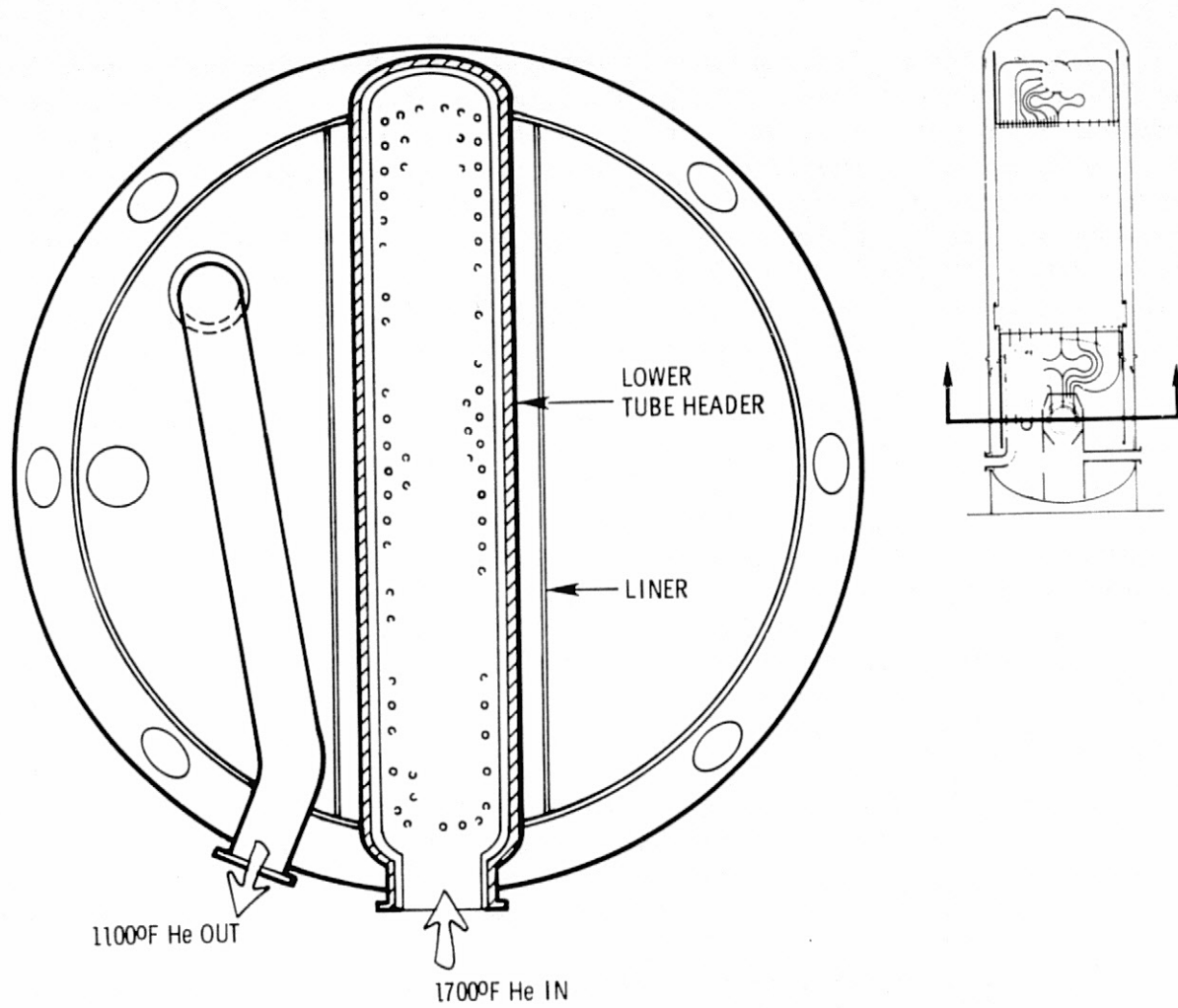


Figure 2.5.6 Lower Header

on the outside and 866K (1100°F) helium on the inside, thus the highly loaded structural vessel is well cooled. The 1200K (1700°F) helium is carried inside an inner vessel which is isolated from the hot gas by a liner and a stagnant helium layer. The inner vessel is loaded only by the pressure difference between the hot and cold helium streams. The hot gas liner is completely unloaded. An arrangement of short tubes, similar to those in the design described in the previous paragraph, transfers the hot helium from the hot gas liner to the heat transfer tubing. This arrangement is shown in Figure 2.5.7.

The question of which particular header arrangement is adopted would depend upon more detailed analysis. Obviously the first and simpler alternative is preferable from the cost standpoint. The second alternative would be used only in the event that the cooling achieved in the first should prove inadequate. In any event, some degree of complication will probably have to be accepted to achieve acceptable metal temperatures in the vessels carrying the high pressure helium gas. The remaining approach of attempting to design a single 6895 (1000 psi) vessel for 1200K (1700°F) results in excessive metal thickness (approximately 242 mm) due to the low creep strength of the best presently available superalloys. The 100,000 hr rupture strength of Inco 617 at 1200K (1700°F) is less than 20,700 kPa (3000 psi). A compromise uncooled header possibility is to divide the header up into a number of smaller diameter pipes which would permit the metal thickness to be reduced. However, in this design a remote tube plugging device would be required to permit repairs of tubing leaks.

The heat exchange tubing is supported in the lateral direction by fabricated grids which are suspended at intervals along the catalyst vessel. The lowermost grid provides support for the screen or grating which retains the catalyst pellets and is itself supported from the fluid separator dome below it by means of short tubular struts. The fluid separator dome also supports the weight of the heat exchange tubing which is welded to it. Expansion loops are provided in the heat exchange tubing at the upper and lower ends to accommodate the differential thermal growth between the tubing and the catalyst vessel.

A 305 mm (12 inch) diameter pipe transfers the 866K (1100°F) helium from the upper header to a point in the side of the lower vessel plenum where it is piped away from the reactor. All piping connections to the decomposition reactor are made in the lower portion of the external vessel. The design therefore provides for easy removal of the upper portion of the external pressure vessel, thus exposing the catalyst vessel. Access covers are provided in the catalyst vessel wall to facilitate the removal of used catalyst. It is envisaged that removal and subsequent replacement by fresh catalyst might be performed by pneumatic transport techniques. Alternatively, manual raking of the catalyst between the heat exchanger tubing, using strategically placed access covers should be possible. The open upper end of the catalyst vessel, exposed on removal of the external pressure vessel, should facilitate placement of fresh catalyst by gravity.

The materials of construction of the decomposition reactor range from carbon steel to superalloys such as Inconel 617. The external pressure vessel is exposed only to the 700K (800°F) acid vapor and is thus able to utilize carbon steel material. The inner surfaces, exposed to the acid vapor, will be treated by Alonizing to minimize corrosion. The hot lower

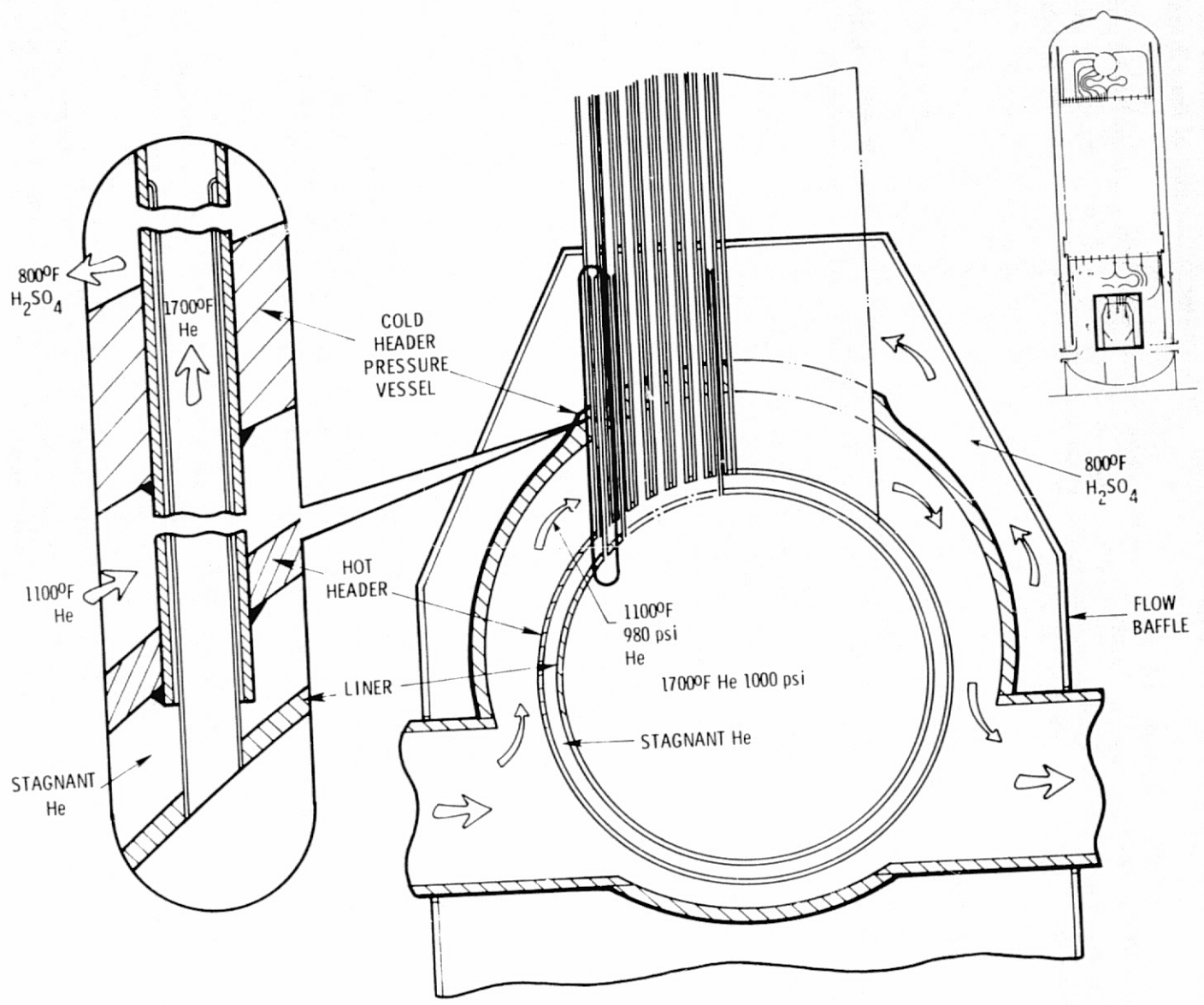


Figure 2.5.7 Alternative Lower Header Arrangement

end of the heat exchange tubing and hot header will require the use of superalloy material such as Inconel 617. Some relaxation in material specification and wall thickness may be made towards the colder ends of the heat exchange tubing, and it is anticipated that Incoloy 800 tubing can be used above the midplane of the catalyst vessel. Protection against corrosion in the hot acid environment will probably be achieved by Alonizing the external surface of the tubing.

Insulation of the external pressure vessel to minimize loss of heat is simplified by the exposure of the vessel to the lowest fluid temperature in the cycle. The low temperature permits the use of economical insulation such as Kaylo (Owens-Corning) or Thermobestos (Johns-Manville) calcium silicate based materials.

#### 2.5.4 Balance of Battery H Equipment

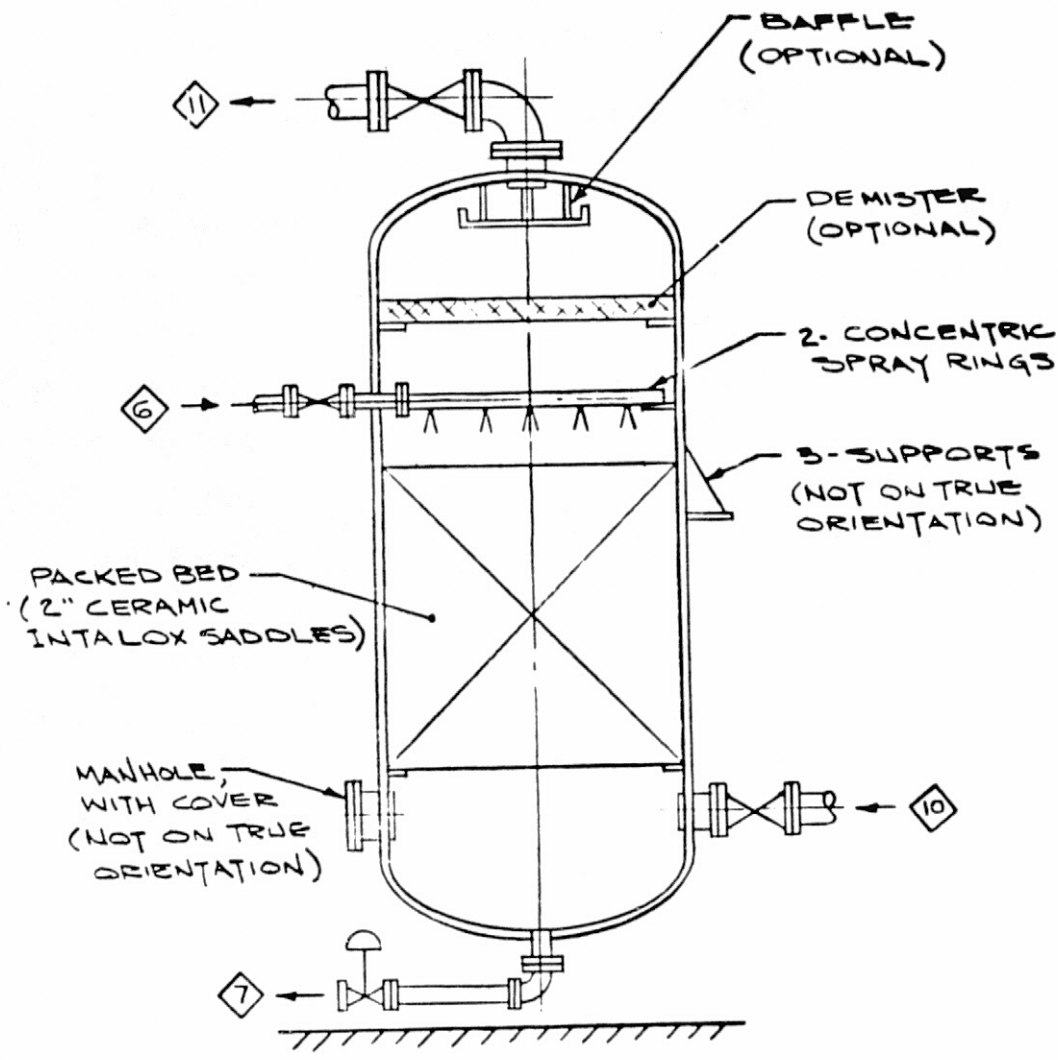
In addition to the acid vaporizers and decomposition reactors, Battery H contains the equipment shown in Figure 2.5.1. The paragraphs below briefly describe this equipment.

The mixing vessel (MV-1) is an in-line static mixer. The static mixer consists of two fixed, helical elements, in series, enclosed in a 610 mm (24 in.) diameter pipe. The total length of the mixer is about 1.9 meters (6.2 feet). The fixed geometric design of the unit produces an unique pattern of simultaneous flow division and radial mixing. The process fluid is divided at the leading edge of each of the two helical elements and follows the channels created by the element shape. Simultaneously, rotational circulation of the process fluid around its own hydraulic center in each channel of the mixer causes radial mixing of the material. All fluids are continuously and completely intermixed, resulting in virtual elimination of radial gradients in temperature, velocity, and materials composition. A total of forty static mixers are employed, in parallel, between the decomposition reactors and the acid contacting packed tower.

The acid contacting packed tower (T-1) is shown in Figure 2.5.8. The tower, of which forty are required, is made of a carbon steel shell lined with acid brick. A 3 meter (10 feet) diameter by 3 meter (10 feet) high packed bed of 50 mm (2 inch) ceramic Intalox saddles provides the extended surface required for the operation of the unit.

The organic heat exchanger (OHX) is a shell and tube exchanger which heats the organic coolant, used as a heat source for the acid vaporizers (AV-1), by high temperature helium from the nuclear intermediate heat transport loop. The characteristics of this heat exchanger are shown in Table 2.5.4.

The boiler feedwater preheater (E-1) is used to recover heat from the overhead stream (process line 11) of the packed tower (T-1) for the purpose of feedwater heating. Table 2.5.5. summarizes the operating parameters of this heat exchanger.



REV. NO.	DATE	DESCRIPTION	ENGR	SUP. ENG
11-5-75		FIRST ISSUE	N.M	DMA

ENGINEER	DATE
STATE REG.	No.
W H <sub>2</sub> PROCESS	
T-1 CONFIGURATION	
6347-L-0044	

Figure 2.5.8

TABLE 2.5.4

## ORGANIC HEAT EXCHANGER (OHX)

Type of Design	Shell and Tube
Number of Units	5
Characteristics Per Unit	
Heat Duty, MW (Btu/hr)	246 ( $840 \times 10^6$ )
Surface Area, $m^2$ ( $ft^2$ )	2397 (25,800)
Shell Diameter, m (ft)	4.24 (13.9)
Overall Length, m (ft)	15.8 (51.8)
Shell Side	
Fluid	Organic
Flow Rate, kg/hr (lb/hr)	$1.75 \times 10^6$ ( $3.85 \times 10^6$ )
Inlet Temperature, K ( $^{\circ}F$ )	617 (650)
Outlet Temperature, K ( $^{\circ}F$ )	755 (900)
Inlet Pressure, kPa (psia)	483 (70)
Outlet Pressure, kPa (psia)	448 (65)
Tube Side	
Fluid	Helium
Flow Rate, kg/hr (lb/hr)	$2.195 \times 10^6$ ( $4.838 \times 10^6$ )
Inlet Temperature, K ( $^{\circ}F$ )	1033 (1400)
Outlet Temperature, K ( $^{\circ}F$ )	644 (700)
Inlet Pressure, kPa (psia)	4520 (655)
Outlet Pressure, kPa (psia)	4480 (650)

TABLE 2.5.5

## BOILER FEEDWATER PREHEATER (E-1)

Type of Design	Shell and Tube
Number of Units	4
Characteristics Per Unit	
Heat Duty, MW (Btu/hr)	34.6 (118 × 10 <sup>6</sup> )
Surface Area, m <sup>2</sup> (ft <sup>2</sup> )	946 (10,180)
Shell Diameter, m (ft)	3.96 (13)
Overall Length, m (ft)	21.3 (70.0)
Shell Side	
Fluid	Boiler Feedwater
Flow Rate, kg/hr (lb/hr)	263,000 (581,000)
Inlet Temperature, K (°F)	322 (120)
Outlet Temperature, K (°F)	435 (323)
Inlet Pressure, KPa (psia)	8690 (1260)
Outlet Pressure, KPa (psia)	8620 (1250)
Tube Side	
Fluid	SO <sub>2</sub> , O <sub>2</sub> , and H <sub>2</sub> O
Flow Rate, kg/hr (lb/hr)	639,000
Inlet Temperature, K (°F)	470 (387)
Outlet Temperature, K (°F)	380 (225)
Inlet Pressure, kPa (psia)	241 (35)
Outlet Pressure, kPa (psia)	207 (30)

There are five vaporizer feed pumps (P-1), each rated at 30 horsepower. These pumps are Duriron to protect against corrosion in high concentration sulfuric acid. There are also five organic heat exchanger feed pumps (P-2). These pumps are each rated at 120 horsepower. Other miscellaneous equipment within Battery H includes surge tanks (ST-1H and ST-2H) to provide both transient storage and net positive suction head (NPSH) requirements of the acid vaporizer and organic heat exchanger feed pumps.

## 2.6 BATTERY I - SULFUR DIOXIDE - OXYGEN SEPARATION SYSTEM

### 2.6.1 General

The Sulfur Dioxide-Oxygen separation system handles the effluent from the Sulfuric Acid Decomposition System (Battery H), as shown in the overall flow diagram (Figure 2.1.1) to produce separate streams of recycle sulfur dioxides, recycle water, and by-product oxygen. The system process flow sheet is shown in Figure 2.6.1, and the mass balance for the system in Table 2.6.1.

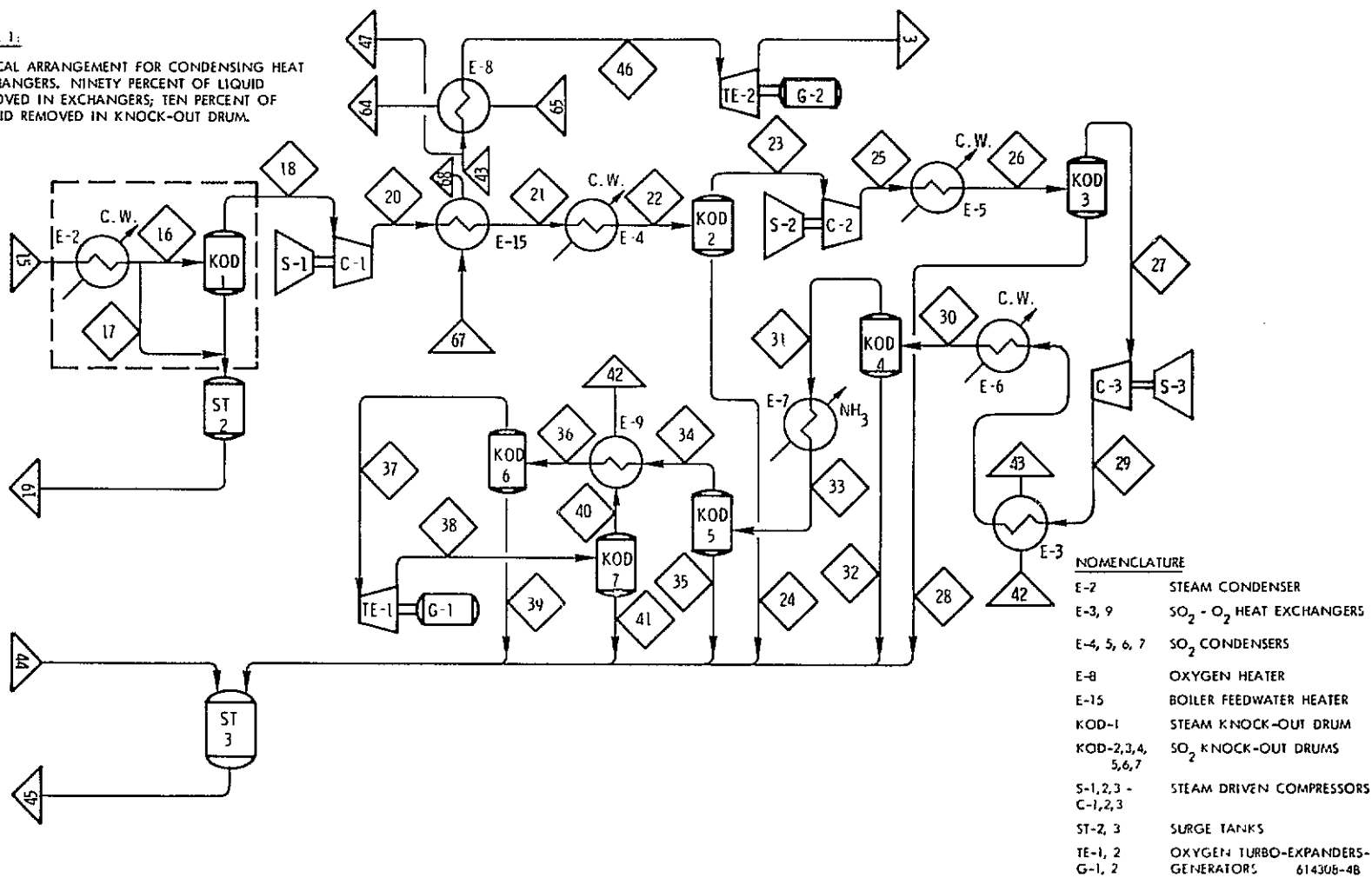
The steam, sulfur dioxide, and oxygen mixtures, leaving the stripping towers in Battery H, are separated in Battery I. These gases are first cooled in the steam condenser (E-2) to condense  $\text{SO}_2$  laden water which is returned to the anolyte mixing drum, MD-1, in Battery G. The remaining gases are compressed to 1034 kPa (150 psia) and cooled in heat exchangers E-15 and E-4 to condense about half of the incoming sulfur dioxide. Further compression, to 1862 kPa (270 psia) with compressor C-2 and to 5171 kPa (750 psia) with compressor C-3, and cooling in heat exchangers E-5 and E-6 succeed in condensing over 90 percent of the incoming sulfur dioxide. Stream (31), which is approximately 80 percent oxygen by weight, is further purified by cooling to 266K ( $20^\circ\text{F}$ ) in E-7, the evaporator of an ammonia refrigeration unit. Following removal of condensed sulfur dioxide in the knock-out drum (KOD-5), the gas (34) is greater than 95 weight percent oxygen. Heat exchange with cold oxygen in heat exchanger E-9 reduces the temperature to 211K ( $-80^\circ\text{F}$ ) and raises the purity (37) to greater than 99.8 weight percent.

Cold oxygen, at a temperature of 176K ( $-142^\circ\text{F}$ ), and electrical power are generated by turboexpander TE-1 which reduces the gas pressure from 4654 to 2482 kPa (675 to 360 psia). After final removal in knock-out drum (KOD-7), residual sulfur dioxide remaining in the oxygen is approximately 1-2 PPM. This gas is warmed to 260K ( $9^\circ\text{F}$ ) in heat exchanger (E-9) and at this point could be made available to a user at 2448 kPa (355 psia). For purposes of this design, the oxygen is assumed to be vented. Exchanger E-3 warms the gas to 376K ( $217^\circ\text{F}$ ), following which oxygen required for the stripping tower, T-1G, is withdrawn (47). The balance is heated by helium in exchanger E-8 to 922K ( $1200^\circ\text{F}$ ) and expanded by the turboexpander TE-2 for auxiliary power generation. Oxygen leaves the process at 441K ( $355^\circ\text{F}$ ) and 103 kPa (15 psia). Sulfur dioxide collected from the knock-out drums is combined with that from condenser E-1G in a surge tank (ST-3). This is pumped, as required, to the anolyte mixing drum (MD-1) in Battery G.

Figure 2.6.1 Battery I Flowsheet

NOTE 1:

TYPICAL ARRANGEMENT FOR CONDENSING HEAT EXCHANGERS. NINETY PERCENT OF LIQUID REMOVED IN EXCHANGERS; TEN PERCENT OF LIQUID REMOVED IN KNOCK-OUT DRUM.



NOMENCLATURE

- E-2 STEAM CONDENSER
- E-3, 9 SO<sub>2</sub> - O<sub>2</sub> HEAT EXCHANGERS
- E-4, 5, 6, 7 SO<sub>2</sub> CONDENSERS
- E-8 OXYGEN HEATER
- E-15 BOILER FEEDWATER HEATER
- KOD-1 STEAM KNOCK-OUT DRUM
- KOD-2,3,4,5,6,7 SO<sub>2</sub> KNOCK-OUT DRUMS
- S-1,2,3 - STEAM DRIVEN COMPRESSORS
- C-1,2,3
- ST-2, 3 SURGE TANKS
- TE-1, 2 OXYGEN TURBO-EXPANDERS-
- G-1, 2 GENERATORS 614308-4B

TABLE 2.6.1  
BATTERY I MASS RATES

Stream Number	3		15		16		17		18		19	
Temperature, K (°F)	441	(335)	380	(225)	311	(100)	311	(100)	311	(100)	311	(100)
Pressure, kPa (psia)	103	(15)	207	(30)	179	(26)	179	(26)	172	(25)	2,930	(425)
Mass Rate, kg/hr (lb/hr)	305,600	(675,000)	2,590,000	(5,710,000)	1,677,000	(3,698,000)	913,000	(2,012,000)	1,597,000	(3,521,000)	993,000	(2,189,000)
Composition, Weight Percent												
H <sub>2</sub>												
O <sub>2</sub>	100.0		12.1		18.7				19.6			
H <sub>2</sub> O			37.4		5.8		95.6		1.3		95.6	
SO <sub>2</sub>	1-2 ppm		50.5		75.5		4.4		79.1		4.4	
SO <sub>3</sub>												
H <sub>2</sub> SO <sub>4</sub>												
Stream Number	20		21		22		23		24		25	
Temperature, K (°F)	473	(392)	341	(155)	311	(100)	311	(100)	311	(100)	350	(170)
Pressure, kPa (psia)	1,034	(150)	1,000	(145)	938	(136)	931	(135)	931	(135)	1,862	(270)
Mass Rate, kg/hr (lb/hr)	1,597,000	(3,521,000)	1,597,000	(3,521,000)	1,597,000	(3,521,000)	793,000	(1,749,000)	804,000	(1,772,000)	793,000	(1,749,000)
Composition, Weight Percent												
H <sub>2</sub>												
O <sub>2</sub>	19.6		19.6		19.6		39.5				39.5	
H <sub>2</sub> O	1.3		1.3		1.3				2.5			
SO <sub>2</sub>	79.1		79.1		79.1		60.5		97.5		60.5	
SO <sub>3</sub>												
H <sub>2</sub> SO <sub>4</sub>												
Stream Number	26		27		28		29		30		31	
Temperature, K (°F)	311	(100)	311	(100)	311	(100)	389	(240)	311	(100)	311	(100)
Pressure, kPa (psia)	1,731	(251)	1,724	(250)	1,724	(250)	5,171	(750)	5,006	(726)	4,999	(725)
Mass Rate, kg/hr (lb/hr)	793,000	(1,749,000)	503,000	(1,109,000)	290,000	(640,000)	503,000	(1,109,000)	503,000	(1,109,000)	393,000	(867,000)
Composition, Weight Percent												
H <sub>2</sub>												
O <sub>2</sub>	39.5		62.3				62.3		62.3		79.6	
H <sub>2</sub> O												
SO <sub>2</sub>	60.5		37.7		100.0		37.7		37.7		20.4	
SO <sub>3</sub>												
H <sub>2</sub> SO <sub>4</sub>												
Stream Number	32		33		34		35		36		37	
Temperature, K (°F)	311	(100)	266	(20)	266	(20)	266	(20)	211	(-80)	211	(-80)
Pressure, kPa (psia)	4,999	(725)	4,827	(700)	4,827	(700)	4,827	(700)	4,661	(676)	4,654	(675)
Mass Rate, kg/hr (lb/hr)	110,000	(242,000)	393,000	(867,000)	328,000	(724,000)	65,000	(143,000)	328,000	(724,000)	313,000	(691,000)
Composition, Weight Percent												
H <sub>2</sub>												
O <sub>2</sub>												
H <sub>2</sub> O												
SO <sub>2</sub>	100.0		20.4		4.7		100.0		4.7		0.2	
SO <sub>3</sub>												
H <sub>2</sub> SO <sub>4</sub>												



## 2.6.2 Components

Performance and sizing calculations have been done for the components of Battery 1 in sufficient detail to establish feasibility and a reasonable basis for cost estimating. The sections below provide a summary of the design characteristics of the equipment within this battery.

### 2.6.2.1 Heat Exchangers

There are nine heat exchange locations shown in Figure 2.6.1 within the Battery 1 boundaries. These are all shell and tube heat exchangers. The characteristics of each of these heat exchangers is shown in Table 2.6.2.

### 2.6.2.2 Knock-Out Drums

Knock-out drums are used to separate liquids from gases or vapors following the various condensation steps in the battery. The knock-out drums are tanks in which the wet gaseous flow is introduced, reduced in velocity, and allowed to impinge on wire mesh demisters. Large moisture droplets will separate from the gas stream in the low velocity area below the demister. Smaller particles will be removed by the multiple impingement of the flow on the wire mesh. Characteristics of the knock-out drums are given in Table 2.6.3.

### 2.6.2.3 Surge Tanks

There are two surge tanks included in the battery to provide collection and temporary storage facilities for liquids drained from the knock-out drums and to provide the NPSH requirements for the pumps taking suction from the tanks. The characteristics of these surge tanks are given in Table 2.6.4.

### 2.6.2.4 Ammonia Chiller

In order to get the required low temperatures in the sulfur dioxide condenser E-7, an ammonia chiller unit is employed. This subsystem provides liquid ammonia, at a temperature of 261K (10°F) to E-7, where it is vaporized and thereby cools the sulfur dioxide - oxygen flow. The total heat absorption requirement, in the E-7 SO<sub>2</sub> condenser, of 10.8 MWt ( $36.9 \times 10^6$  Btu/hr) is met by the vaporization of 29,800 kg/hr (65,700 lb/hr) of ammonia.

The system contains three 1000 ton packaged cooler-condenser units and motor driven geared compressors. Heat rejection for the ammonia chiller system is accomplished by the flow of 37.8 cubic meters per minute (10,000 gpm) of cooling water at an inlet temperature of 305K (90°F).

TABLE 2.6.2

## BATTERY I - HEAT EXCHANGER

Component	E-2	E-3	E-4	E-5	E-6	E-7	E-8	E-9	E-15
Service	Steam Condenser	SO <sub>2</sub> -O <sub>2</sub> HX	SO <sub>2</sub> Condenser	SO <sub>2</sub> Condenser	SO <sub>2</sub> Condenser	SO <sub>2</sub> Condenser	O <sub>2</sub> Heater	SO <sub>2</sub> -O <sub>2</sub> HX	BFW Heater
Number of Units	10	2	4	2	2	3	2	3	2
Characteristics Per Unit									
Heat Duty, MW (Btu/hr)	62.5 (213.3 × 10 <sup>6</sup> )	4.6 (15.7 × 10 <sup>6</sup> )	21.6 (73.6 × 10 <sup>6</sup> )	15.7 (53.5 × 10 <sup>6</sup> )	4.39 (15 × 10 <sup>6</sup> )	3.6 (12.3 × 10 <sup>6</sup> )	21.3 (72.6 × 10 <sup>6</sup> )	2.14 (7.3 × 10 <sup>6</sup> )	25.5 (87.1 × 10 <sup>6</sup> )
Surface Area, m <sup>2</sup> (ft <sup>2</sup> )	7,430 (80,000)	93 (1,000)	2,600 (28,000)	585 (6,300)	570 (6,100)	500 (5,400)	370 (4,000)	430 (4,600)	470 (5,100)
Shell Diameter m (ft)	3.66 (12)	0.91 (3)	2.71 (8.9)	1.37 (4.5)	1.37 (4.5)	1.43 (4.7)	1.52 (5.0)	1.62 (5.3)	1.25 (4.1)
Overall Length, m (ft)	10.97 (36)	3.96 (13)	7.92 (26)	7.92 (26)	7.92 (26)	7.92 (26)	3.96 (13)	3.96 (13)	7.92 (26)
Shell Side									
Fluid	H <sub>2</sub> O	O <sub>2</sub>	H <sub>2</sub> O	H <sub>2</sub> O	H <sub>2</sub> O	NH <sub>3</sub>	O <sub>2</sub>	O <sub>2</sub>	H <sub>2</sub> O, SO <sub>2</sub> , O <sub>2</sub>
Flow Rate, kg/hr (lb/hr)	1,940,000 (4,270,000)	156,000 (345,000)	667,000 (1,470,000)	810,000 (1,790,000)	227,000 (500,000)	9,930 (21,800)	153,000 (338,000)	104,000 (230,000)	798,000 (1,760,000)
Inlet Temperature, K (°F)	305 (90)	260 (91)	305 (90)	305 (90)	305 (90)	261 (110) Liq.	376 (217)	176 (-142)	473 (392)
Outlet Temperature, K (°F)	333 (140)	376 (217)	333 (140)	322 (120)	322 (120)	261 (110) Vap.	922 (1,200)	260 (91)	341 (155)
Operating Pressure, kPa (psia)	345 (50)	2,413 (350)	345 (50)	345 (50)	345 (50)	276 (40)	2,413 (350)	2,475 (359)	1,034 (150)
Tube Side									
Fluid	H <sub>2</sub> O, SO <sub>2</sub> , O <sub>2</sub>	SO <sub>2</sub> , O <sub>2</sub>	H <sub>2</sub> O, SO <sub>2</sub> , O <sub>2</sub>	He	SO <sub>2</sub> , O <sub>2</sub>	H <sub>2</sub> O			
Flow Rate, kg/hr (lb/hr)	259,000 (571,000)	252,000 (555,000)	399,000 (880,000)	397,000 (875,000)	252,000 (555,000)	131,000 (289,000)	29,100 (64,200)	109,000 (241,000)	193,000 (426,000)
Inlet Temperature, K (°F)	380 (225)	389 (240)	341 (155)	350 (170)	339 (150)	311 (100)	1,033 (1,400)	266 (20)	322 (120)
Outlet Temperature, K (°F)	311 (100)	339 (150)	311 (100)	311 (100)	311 (100)	266 (20)	475 (395)	211 (-80)	435 (323)
Operating Pressure, kPa (psia)	207 (30)	5,171 (750)	965 (140)	1,860 (270)	5,030 (730)	4,999 (725)	4,480 (650)	4,830 (700)	8,620 (12,500)

TABLE 2.6.3  
KNOCK-OUT DRUM CHARACTERISTICS

Component	KOD-1		KOD-2		KOD-3		KOD-4		KOD-5		KOD-6		KOD-7	
Number of Units	5		5		3		3		3		3		3	
Characteristics Per Unit														
Diameter, m (ft)	2.29	(7.5)	2.29	(7.5)	2.13	(7)	1.52	(5)	1.07	(3.5)	1.07	(3.5)	0.91	(3)
Length, m (ft)	2.44	(8)	2.44	(8)	1.83	(6)	1.83	(6)	1.83	(6)	1.83	(6)	1.83	(6)
Pressure, kPa (psia)	179	(26)	938	(136)	1731	(251)	5006	(726)	4827	(700)	4661	(676)	2482	(360)
Temperature, K (°F)	311	(100)	311	(100)	311	(100)	311	(100)	266	(20)	211	(-80)	176	(-142)
Demister Thickness, mm (in)	102	(4)	102	(4)	102	(4)	102	(4)	102	(4)	102	(4)	102	(4)
Demister Material	304 SS		304 SS		304 SS									
Drum Material	Carbon Steel		304 SS		304 SS									

TABLE 2.6.4  
SURGE TANK CHARACTERISTICS

Surge Tank	ST-2	ST-3
Number of Units	5	5
Contained Fluid	H <sub>2</sub> O	SO <sub>2</sub>
Diameter, m (ft)	2.44 (8)	2.44 (8)
Length, m (ft)	6.4 (21)	6.4 (21)
Pressure, kPa (psia)	179 (26)	862 (125)
Temperature, K (°F)	311 (100)	311 (100)
Material of Construction	Carbon Steel	Carbon Steel

#### 2.6.2.5 Compressors

There are three compressor stations located in the process stream of Battery I. These compressors progressively increase the pressure of the SO<sub>2</sub>-O<sub>2</sub> flow stream to permit additional sulfur dioxide to be condensed, and thereby removed, from the process by-product oxygen. The compressors are installed in two parallel half capacity trains and are each driven by steam turbines. The steam source for the turbines is shown in Battery J. The characteristics of the compressors are presented in Table 2.6.5.

#### 2.6.2.6 Turbo-Expanders

To maximize the recovery of the energy put into the process in compressing the stream for SO<sub>2</sub> condensation, turbo-expanders are used to reduce the pressure of the oxygen stream and generate useful power while so doing. The turbo-expanders (TE-1 and TE-2) are each coupled to a generator through a speed reducing gearbox and mounted on a rigid steel baseplate. Separately mounted auxiliary systems, consisting of lubrication and instrumentation and control, service the turboexpanders. The major characteristics of the turboexpander-generators are shown in Table 2.6.6.

#### 2.6.2.7 Pumps

Although not shown on the flow sheet, pumps are employed to transfer fluids from the surge tanks ST-2 and ST-3. These pumps have the major characteristics as shown in Table 2.6.7.

TABLE 2.6.5  
PROCESS COMPRESSORS

Component	C-1	C-2	C-3
Number of Units	2	2	2
Characteristics Per Unit			
Fluid	SO <sub>2</sub> , O <sub>2</sub> , H <sub>2</sub> O	SO <sub>2</sub> , O <sub>2</sub>	SO <sub>2</sub> , O <sub>2</sub>
Flow Rate, kg/hr (lb/hr)	799,000 (1.76 × 10 <sup>6</sup> )	397,000 (875,000)	252,000 (555,000)
Inlet Pressure, kPa (psia)	172 ( 25)	931 (135)	1,724 (250)
Outlet Pressure, kPa (psia)	1,034 (150)	1,862 (270)	5,171 (750)
Inlet Temperature, K (°F)	311 (100)	311 (100)	311 (100)
Outlet Temperature, K (°F)	473 (392)	350 (170)	389 (240)
Rating (horsepower)	39,500	7,800	9,100

TABLE 2.6.6  
TURBO-EXPANDERS

Component	TE-1	TE-2
Number of Units	1	5
Total Power Output, MWe	2.84	40.5
Characteristics Per Unit		
Fluid	O <sub>2</sub>	O <sub>2</sub>
Flow Rate, kg/hr (lb/hr)	313,000 (691,000)	61,120 (135,000)
Inlet Pressure, kPa (psia)	4,654 (675)	2,379 (345)
Outlet Pressure, kPa (psia)	2,482 (360)	103 (15)
Inlet Temperature, K (°F)	211 (-80)	922 (1,200)
Outlet Temperature, K (°F)	176 (-142)	441 (335)
Horsepower	3,850	11,000

TABLE 2.6.7  
SURGE TANK DRAIN PUMPS

Component	ST-2 Pump	ST-3 Pump
Number of Units	4	4
Characteristics Per Unit		
Fluid	H <sub>2</sub> O	SO <sub>2</sub>
Flow Rate, kg/hr (lb/hr)	248,000 (547,000)	338,000 (745,000)
Temperature, K (°F)	311 (100)	311 (100)
Inlet Pressure, kPa (psia)	179 (26)	862 (125)
Outlet Pressure, kPa (psia)	2,930 (425)	2,689 (390)
Material of Construction	C.S.	C.S.
Horsepower	300	200

## 2.7 BATTERY J - STEAM TURBINES AND GENERATOR

### 2.7.1 Battery J/Battery A Interface

Battery J and A provide the thermal and electrical energy requirements of the process as shown in Figure 2.7.1. Helium is available at two temperatures, 1200K (1700°F) and 1033K (1400°F). The higher temperature gas (57) is used in the sulfur trioxide thermal reduction reactor, DR-1, to provide process gas temperatures to 1144K (1600°F). This stream upon returning (58) at 866K (1100°F), is used for steam generation (E-12) and superheating (E-13). The lower temperature gas provides the thermal energy consumed in the acid vaporizer (59) and the oxygen preheater (65). Stream (64) returns directly to the HT IHX and stream (60) is used for steam generation (E-11) and feedwater preheating (E-10) before returning to the HT IHX. Table 2.7.1 itemizes the state points for Battery J by stream number.

The bulk of the electrical power is generated by a combined Brayton-Rankine cycle with a generating capacity of approximately 463,800 kw (~ 91 percent of the total power generated). Of this power, 313,700 Kwe is produced by the Battery J steam turbine and 150,100 Kwe by the gas turbines in the VHTR (Battery A). This power is distributed within the plant to provide about 457,800 kw for the hydrogen-producing electrolyzers and the remainder for operation of equipment within both the nuclear heat source (VHTR) and the hydrogen generation plant.

### 2.7.2 Battery J Equipment

Battery J is composed of mechanical equipment which extracts sensible heat from the secondary helium, converts this energy into steam to drive a turbine-generator set (Figure 2.7.1). Steam is extracted from the main turbine (DT-1) to power turbines that drive the secondary helium circulators in Battery A, and that drive the process stream compressors C-1, C-2, and C-3 in Battery I. The principal components are: shell and tube feedwater heater (E-10), two shell and tube vertical steam generators (E-11 and E-12), shell and tube steam superheater (E-13) feed pumps, one turbine-generator set, one condenser (E-14) (a second condenser (E-16) is in Building I), four turbine circulators (that drive the secondary helium loops), and the necessary auxiliaries and controls required for safe operation.

The 314 Mwe steam turbine is a 3600 RPM condensing non-reheat tandem compound 2-flow machine with 0.72 m (28.5 inch) last stage blade length. The generator rating is 348,600 KVA, 0.9 PF. The use of steam extracted from the power turbine to drive the secondary helium circulators and the process stream compressors allows the use of a conventional steam turbine-generator without exceeding the loading limits on the last row of blades.

The feedwater is heated to near saturation temperature in the heat exchanger E-10. The flow is then split, with part of the water being vaporized in exchanger E-11 and the remainder vaporized in exchanger E-12. The flow is then combined and superheated in exchanger E-13. Table 2.7.2 lists the heat duty and physical size of these heat exchangers.

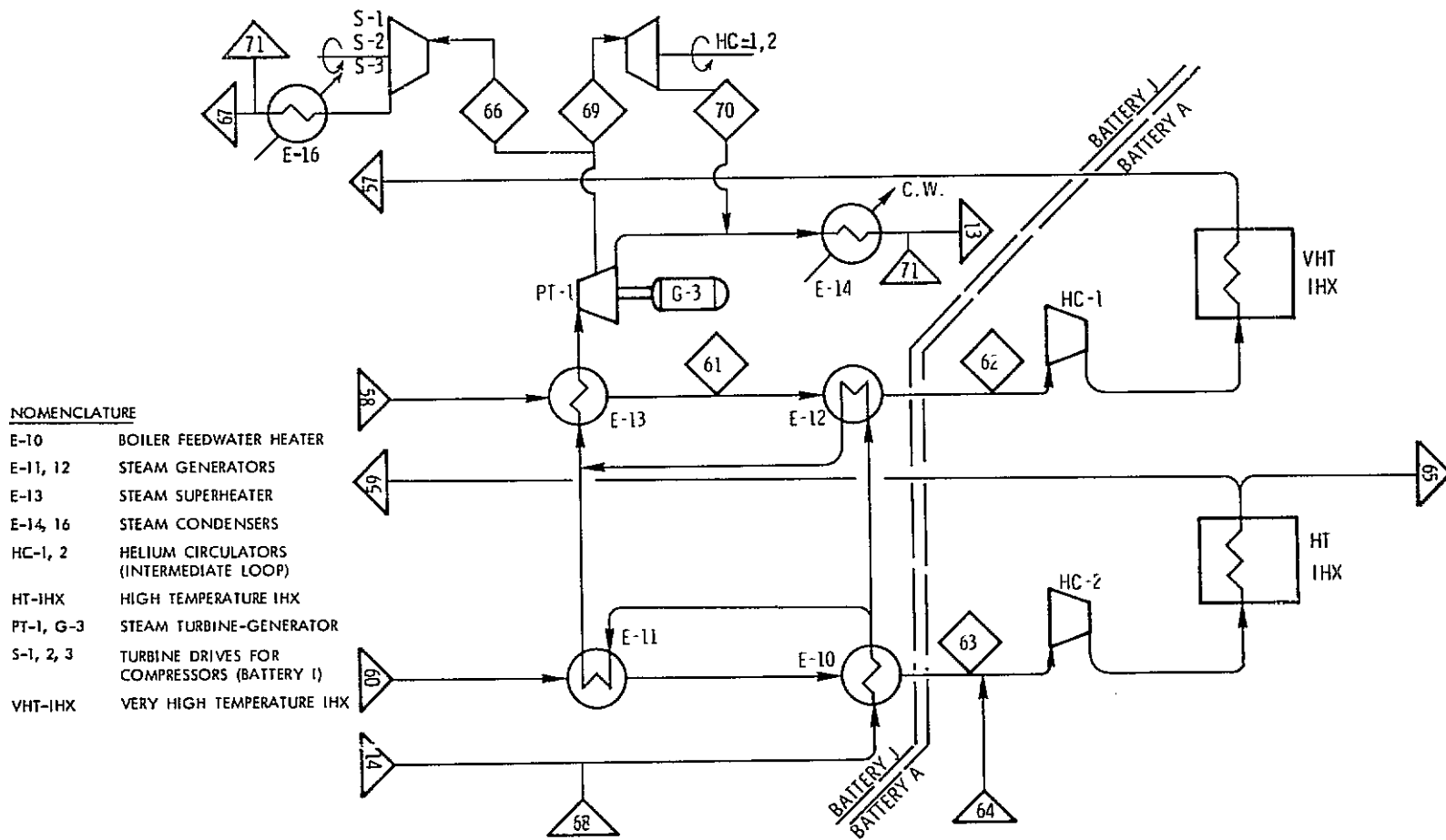


Figure 2.7.1 Batteries J and A. Power Generation and Heat Source Interfaces

TABLE 2.7.1  
BATTERY J MASS RATES

Stream Number	13		14		57		58		59		60	
Temperature, K (°F)	322 (120)		435 (323)		1,200 (1,700)		866 (1,100)		1,033 (1,400)		644 (700)	
Pressure, kPa (psia)	8,688 (1,260)		8,619 (1,250)		6,895 (1,000)		6,757 (980)		4,516 (655)		4,482 (650)	
Mass Rate, kg/hr (lbs/hr)	1,054,000 (2,323,000)		1,054,000 (2,323,000)		1,793,000 (3,953,000)		1,793,000 (3,953,000)		2,195,000 (4,838,000)		2,195,000 (4,838,000)	
Composition	B. F. W.		B. F. W.		He		He		He		He	
Stream Number	61		62		63		64		65		66	
Temperature, K (°F)	755 (953)		608 (635)		500 (441)		475 (395)		1,033 (1,400)		507 (453)	
Pressure, kPa (psia)	6,619 (960)		6,550 (950)		4,413 (640)		4,413 (640)		4,516 (655)		758 (110)	
Mass Rate, kg/hr (lbs/hr)	1,793,000 (3,953,000)		1,793,000 (3,953,000)		2,195,000 (4,838,000)		58,200 (128,400)		58,200 (128,400)		538,000 (1,185,000)	
Composition	He		Steam									
Stream Number	67		68		69		70		71			
Temperature, K (°F)	322 (120)		435 (323)		507 (453)		322 (120)		322 (120)			
Pressure, kPa (psia)	8,688 (1,260)		8,619 (1,250)		758 (110)		11.7 (1.7)		8,688 (1,260)			
Mass Rate, kg/hr (lbs/hr)	386,000 (852,000)		386,000 (852,000)		310,000 (684,000)		310,000 (684,000)		151,000 (333,000)			
Composition	B. F. W.		B. F. W.		Steam		Steam		B. F. W.			

TABLE 2.7.2  
BATTERY J - HEAT EXCHANGERS

<u>Component Function</u>	<u>E-10 Feedwater Heater</u>		<u>E-11 Steam Generator</u>		<u>E-12 Steam Generator</u>		<u>E-13 Steam Generator</u>	
Heat Duty, MWt ( $10^6$ Btu/hr)	262	(894)	193	(660)	456	(1,558)	211	(721)
Heat Transfer Area, Meter <sup>2</sup> (ft <sup>2</sup> )	1839	(19,800)	2388	(25,700)	5834	(62,800)	1245	(13,400)
Height, Meters (ft)	22.0	(72.2)	22.0	(72.2)	22.0	(72.2)	10.3	(33.9)
Diameter, Meters (ft)	3.1	(10.2)	3.7	(12.1)	5.6	(18.4)	3.7	(12.3)

## 2.8 COOLING WATER SYSTEM

The cooling water system for the plant utilizes cooling towers to dissipate the waste heat from the plant. This design decision is made in recognition of environmental concerns with thermal rejection to the river, although the characteristics of the North River, as specified in Reference 2, are such as to permit river cooling to be used. The consequences of the use of cooling towers are increased plant capital costs, decreased plant efficiency (higher "sink" temperature), and increased cost of hydrogen production.

There are two cooling towers employed in the integrated nuclear water decomposition plant. One, designated as L-1 on the plot plan, serves the nuclear heat source. This wet cooling tower is designed as a Class I Structure, in accordance with the requirements of the Nuclear Regulatory Commission in regard to assurance of a heat sink for nuclear facilities. The normal heat load on this tower is approximately 29.3 MWt ( $1 \times 10^8$  Btu/hr). The tower is sized to handle the maximum emergency heat loads for the nuclear system.

The major heat rejection from the plant is accomplished through cooling tower L-2. This tower is a 122 meter (400 ft.) diameter, circular mechanical draft wet cooling tower, as shown in Figure 2.8.1. Circulation through the tower is maintained by twelve fans driven by 200 horsepower motors. A mechanical draft tower was selected to minimize capital investment, at the expense of the thermal efficiency loss associated with the fan power requirements.

Cooling water for the hydrogen production plant is drawn from the cooling tower basin at a temperature of 305K (90°F) by four 2500 horsepower circulating water pumps. These pumps are located adjacent to the tower, as shown in Figure 2.8.2. Traveling screens at the inlet of the pumps prevent the circulation of debris through the cooling water system.

The total heat dissipation from the cooling towers, under normal operating conditions, is shown in Table 2.8.1.

## 2.9 WATER MAKE-UP AND WASTE TREATMENT SYSTEMS

The water requirements for the plant are met by a make-up system taking suction from the river. A pump house, located at the river, contains the raw water pumps as well as the trash rakes and traveling screens needed to keep the make-up water free from debris.

Raw river water is used to make-up the cooling tower water uses associated with evaporative consumption, drift, and blowdown. Raw water is also pretreated by a clarifier (coagulator) and filters to make it suitable as feed to the fire protection system, sanitary system, general plant services, and the make-up demineralization system. The pretreatment system has a nominal capacity of 11.36 m<sup>3</sup>/min (3000 gpm). A block flow sheet of the water make-up system is shown in Figure 2.9.1.

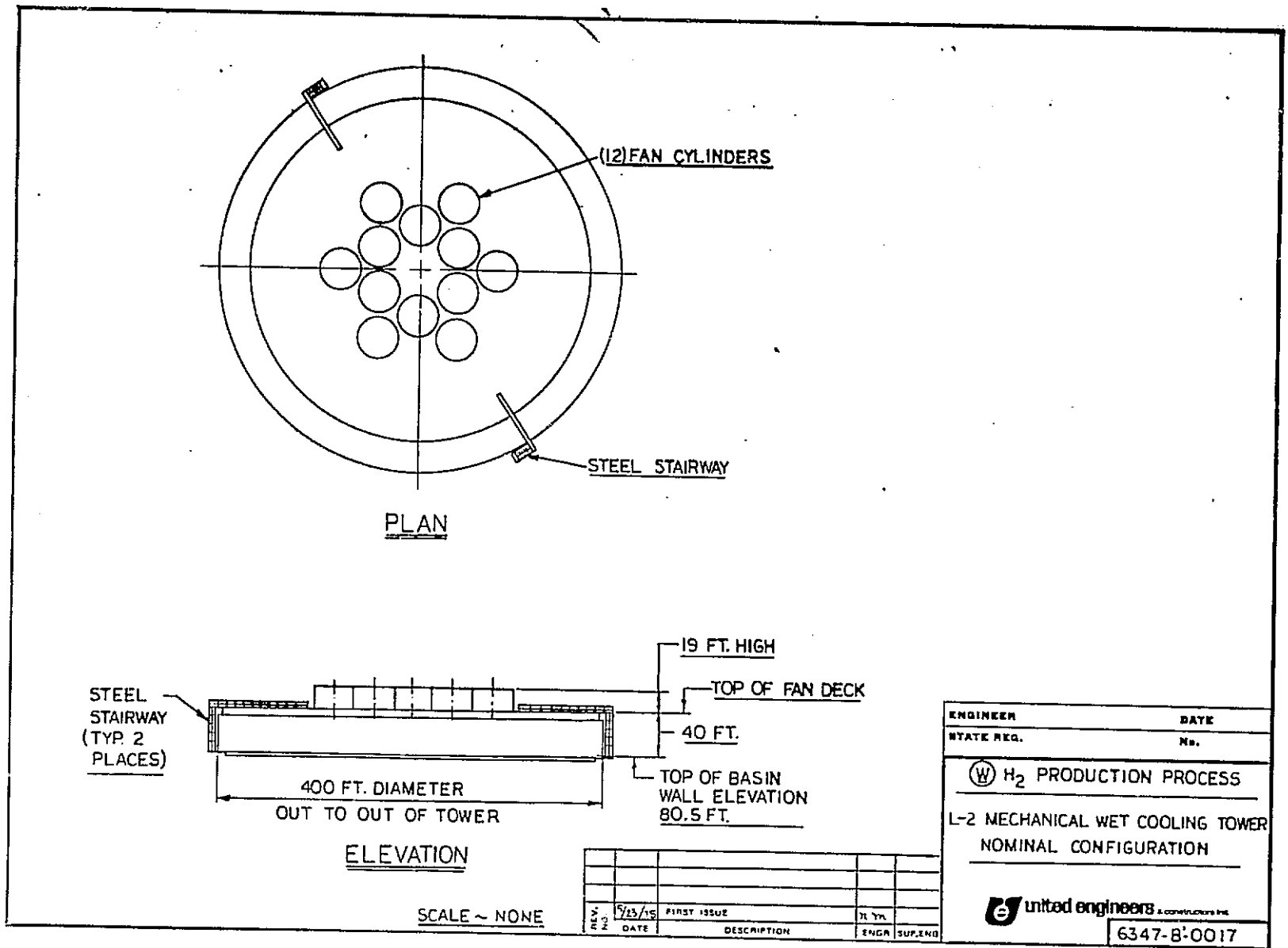


Figure 2.8.1

REPRODUCIBILITY OF THE ORIGINAL PAGE IS POOR

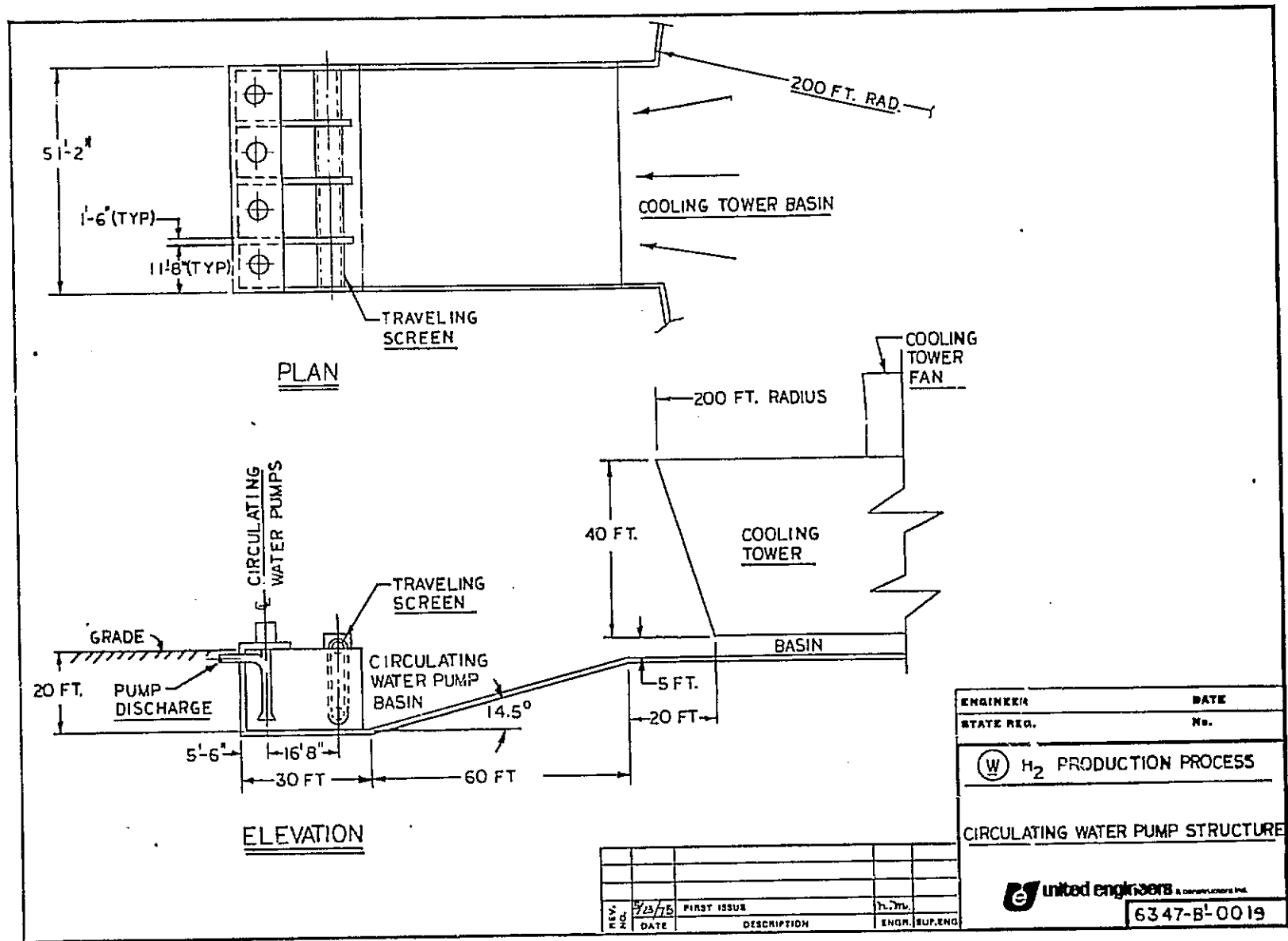


Figure 2.8.2

TABLE 2.8.1  
COOLING TOWER MAJOR HEAT LOADS

<u>Heat Source</u>	<u>Tower</u>	<u>Heat Load</u>	
		<u>MW(t)</u>	<u>Btu/Hr</u>
VHTR	L-1	29.3	$100 \times 10^6$
SO <sub>2</sub> Condenser (E-1G)	L-2	6.6	$22.5 \times 10^6$
Electrolyte Cooler (E-2G)	L-2	159.7	$545 \times 10^6$
Steam Condenser (E-2)	L-2	625.0	$2133 \times 10^6$
SO <sub>2</sub> Condenser (E-4)	L-2	86.3	$294.6 \times 10^6$
SO <sub>2</sub> Condenser (E-5)	L-2	31.4	$107.1 \times 10^6$
SO <sub>2</sub> Condenser (E-6)	L-2	8.8	$30 \times 10^6$
NH <sub>3</sub> Chiller System	L-2	13.2	$45 \times 10^6$
Compressor Coolers	L-2	9.9	$34 \times 10^6$
Main Stream Turbine Condenser (E-14)	L-2	538.8	$1839 \times 10^6$
Compressor Drive Turbine Condenser (E-16)	L-2	320.8	$1095 \times 10^6$
Total		1829.8 MWt	$6245.2 \times 10^6$ Btu/Hr

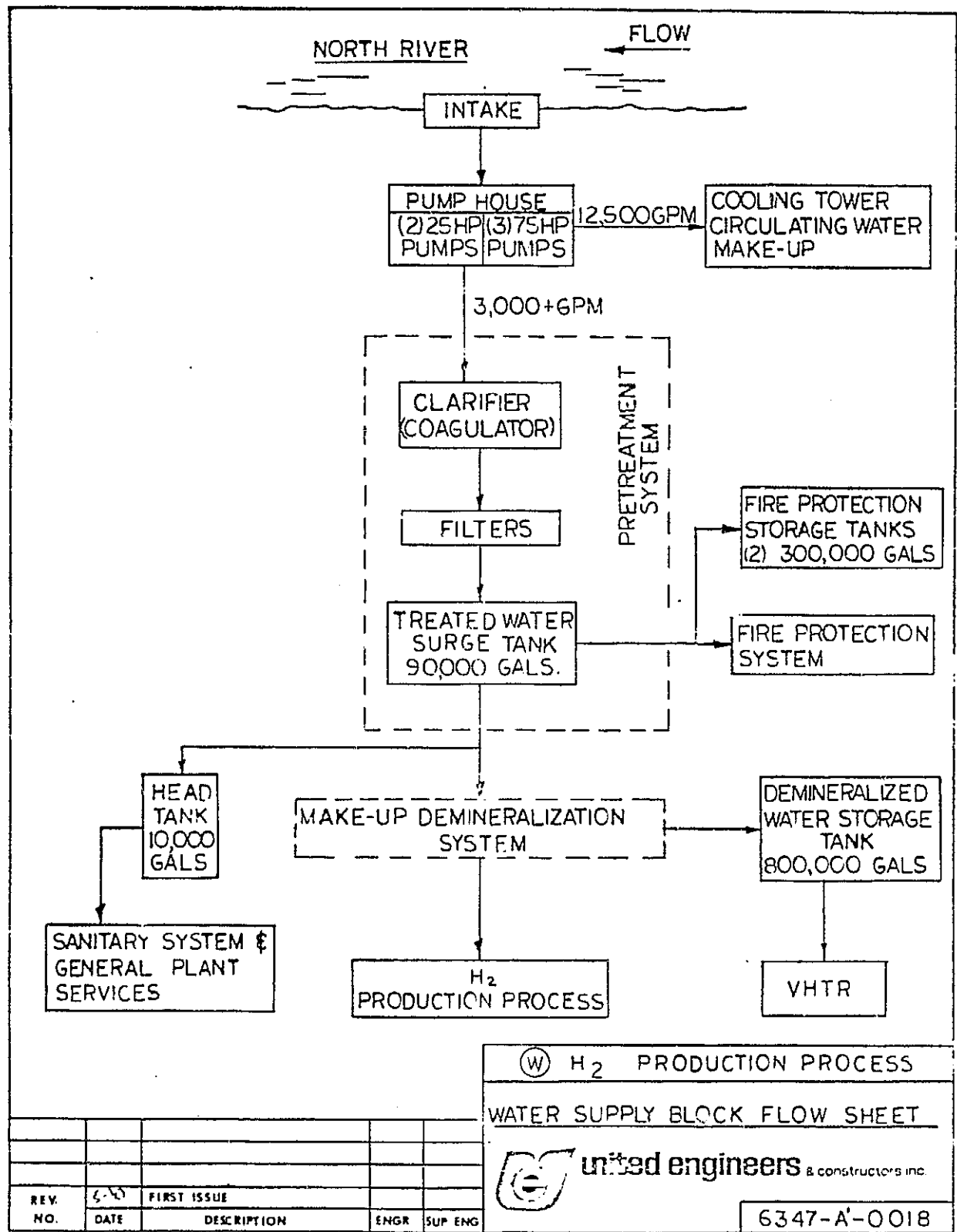


Figure 2.9.1

The clarified and filtered water is used to provide make-up to the fire protection system, sanitary system, and general plant services. For those needs where a higher purity make-up is required, i.e., the VHTR and water feed to the electrolyzer, the water from the pre-treatment system is further purified in a demineralization system.

Water to be demineralized flows initially through a cation exchanger where calcium, magnesium, sodium, and other cations that might be present are exchanged for an equivalent amount of hydrogen ions. The de-cationized water then passes through a forced draft type degasifier where dissolved carbon dioxide is removed to a low level. The degasified effluent then flows through an anion exchanger to remove chloride, sulfate, and other anions. The effluent from the anion exchanger flows through a mixed-bed ion exchanger to insure that the treated water meets the required quality criteria. The  $6.81 \text{ m}^3/\text{min}$  (1800 gpm) deionization plant has the capability of producing deionized water of 2,000,000 ohms/cm. Demineralized water is distributed, as needed, to the hydrogen generation plant and the VHTR nuclear heat source. An  $3030 \text{ m}^3$  (800,000 gal.) stainless steel storage tank provides surge capacity for the demineralized water make-up.

Wastes from the water make-up systems must be treated prior to discharge. These wastes include spent regenerant solutions from the demineralization system, backwash effluent from the filters, and clarifier bottoms.

The waste regenerant solutions will discharge to one of two tanks where it will be neutralized to a pH value of approximately 7 by the addition of an alkali or acid as required. Air sparging is used for mixing purposes. The neutralized solution can then be discharged.

Backwash effluent from the filters will be recycled through the clarifier and will combine with the waste stream from the clarifier bottom.

The clarifier bottoms discharge rate is approximately  $22.7 \text{ m}^3/\text{hr}$  (100 gpm). This stream will consist of a precipitated sludge containing about 3 percent solids by weight. It will be conveyed to a "thickener" where the solids will be further concentrated to about 25-30 percent. The concentrated stream is filtered using a rotary drum type vacuum filter. The resulting sludge - about 18,000 kg/day (20 tons/day) - contains about 50 percent solids by weight and is conveyed by truck to ultimate off-site disposal.

## 2.10 ELECTRICAL AUXILIARY POWER SYSTEM

The electrical auxiliary power system provides the facilities to distribute power to the electrolyzers and process equipment in the plant. Normal power sources are the gas and steam turbines in the plant complex as well as the small power recovery turbines in Battery 1, the  $\text{SO}_2/\text{O}_2$  separation system. Emergency and/or start-up power is supplied by an external 138 kV connection to the electric utility system.

During normal operation, the plant is electrically self-sufficient. All electric power needed for operation of the VHTR and hydrogen production facilities is generated on-site, with no excess power for sale nor need to import power.

Table 2.10.1 shows the electrical loads that are carried by the plant under normal operating conditions. Table 2.10.2 indicates the sources of electric power to meet these loads.

TABLE 2.10.1  
PLANT ELECTRICAL POWER REQUIREMENTS

<u>Battery</u>	<u>Load Name</u>	<u>Normally Running Load (KWe)</u>
A	VHTR Nuclear Island <sup>(1)</sup>	27,950
G	Electrolyzers	457,800
G	Electrolyzer Auxiliary Pumps	1,550
H	Pumps	630
I	Pumps <sup>(2)</sup>	375
I	Ammonia Compressors	4,000
J	Boiler Feed Pumps	4,100
L	Cooling Tower Fans	1,950
L	Cooling Water Pumps	7,300
-	Water Make-Up, Purification, and Feed	365
	Miscellaneous Loads (Undefined)	<u>1,120</u>
		507,140 KWe

(1) Intermediate Loop Circulators are Steam Driven

(2) Battery I Compressors, except for Ammonia Chiller System, are Steam Driven

TABLE 2.10.2

PLANT ELECTRICAL POWER GENERATION

<u>Battery</u>	<u>Generation Source</u>	<u>Generating Capacity (KWe)</u>
A	Turbocompressors	150,100
I	Turboexpander (TE-1)	2,840
I	Turboexpander (TE-2)	40,500
J	Steam Turbine Generator	<u>313,700</u>
	Total	507,140 KWe

2.11 GENERAL FACILITIES

Included within the plant complex are the general facilities that service the entire nuclear water decomposition plant. These fall into the categories of site improvements, auxiliary systems, miscellaneous buildings, and special facilities and equipment.

The site improvements consist of the on-site roads and parking areas, an eight kilometer (5 mile) off-site access railroad line plus on-site trackage, fencing surrounding the plant area, including gates and a guardhouse, and area lighting and landscaping.

The auxiliary systems consist of instrument and plant air systems; interplant communications; a fire protection system consisting of pumps, mains, hydrants, elevated storage tank, hose stations, fire and smoke detection equipment, and portable fire fighting equipment; a steam boiler for space heating, and a sanitary sewage system adequate for a population of 250 people.

The miscellaneous buildings include an administration building, maintenance and service buildings, and a plant warehouse.

Special facilities and equipment consist of chemical laboratory equipment, office furnishings and fixtures, change room equipment, cafeteria equipment, and maintenance tools and equipment.

## 2.12 Overall Plant Performance and Areas for Improvement

The usual way to evaluate the performance of a process plant, in particular a hydrogen production plant, is in terms of its thermal efficiency and cost of product. In this section, an evaluation of the thermal efficiency of the plant is presented, as well as an indication of the process and plant design areas which, in iterations of this present conceptual design, would provide significant improvements in thermal efficiency. The evaluation of the economics of hydrogen production, including the potential effects of the improvements discussed, are discussed in Section 3.0.

### 2.12.1 Plant Thermal Efficiency

The thermal efficiency of the plant is defined as the higher heating value of the product hydrogen divided by the total heat input to the plant complex. Since the plant is self-sufficient from an energy viewpoint, i.e., no net sale or purchase of power or heat is required for the normal operation of the VHTR and the water decomposition plant, the heat input is the full thermal rating of the VHTR.

The overall thermal efficiency of 45.2 percent is calculated as shown in Table 2.12.1. This efficiency results from the process flowsheets, parameters, and design approaches selected for this conceptual design and represents what may be considered to be a base-line efficiency level. Areas for improvement have been identified, and are discussed in Section 2.12.2. These improvements in performance, resulting from optimization and development activities, can result in efficiency levels in excess of 60 percent.

### 2.12.2 Areas for Performance Improvement

The performance of the overall process plant has been evaluated on the basis of a first conceptual design effort. This work has demonstrated that the hydrogen production process can be designed, that it can be integrated into a nuclear heat source and that the efficiency levels and economics are sufficiently attractive to warrant continued work. As an initial evaluation of the process, the conceptual design has not attempted to optimize the overall plant, but has rather made design decisions that were expedient and led to a reasonable, but not an ultimate, design. One of the by-products of a conceptual effort of this sort is the identification of areas where, with modifications of design approach or development, improvement in the overall concept can be achieved. Several such areas have been identified and are briefly discussed below.

- Optimization of VHTR-Water Decomposition Plant interfaces. In particular, the pressures, temperatures, and flow rates in the intermediate helium heat transport system and the amount of electric power produced by the high temperature helium turbogenerators should be re-evaluated to better utilize the high temperature capability of the nuclear plant.

TABLE 2.12.1  
OVERALL PLANT EFFICIENCY

Heat Input

VHTR Thermal Output	12,040 GJ/hr	(11.42 x 10 <sup>9</sup> Btu/hr)
---------------------	--------------	----------------------------------

Heat Output

Hydrogen Production Rate	4.254 x 10 <sup>5</sup> std m <sup>3</sup> /hr	(15.88 x 10 <sup>6</sup> SCF/hr)
Heating Value	12.79 MJ/std m <sup>3</sup>	(325 Btu/SCF)
Total Heat Output	5440 GJ/hr	(5.16 x 10 <sup>9</sup> Btu/hr)

Overall Efficiency

$$\frac{5440 \text{ GJ/hr} \times 100}{12,040 \text{ GJ/hr}} = 45.18\%$$

- Elimination of the present  $\text{SO}_2/\text{O}_2$  separation system. As an alternative, sulfur dioxide can be removed by scrubbing with electrolyzer anolyte, followed by a smaller compression-condensation system for the residual  $\text{SO}_2$  remaining.
- Improvements in the thermal evaporative sulfuric acid vaporization system. Operation of this system at higher pressures and temperatures would result in reduced power requirements for the subsequent compression steps in the  $\text{SO}_2/\text{O}_2$  separation system and the probable elimination of the tertiary organic heat transfer system for the acid vaporizers.
- Satisfactory completion of the high temperature materials development programs, sponsored by ERDA and scheduled to start in fiscal year 1976, would permit higher VHTR gas temperatures and thereby more efficient electric power generation and inherently higher process efficiency.
- Use of acyclic d-c generators to provide electric powers for the electrolyzers. This could eliminate the need for rectification and the power losses associated therewith.
- Re-evaluation and optimization of heat sources and heat sinks, to better utilize the energy for process thermal needs and power generation.
- Re-evaluation of waste heat dissipation techniques. This conceptual design uses a mechanical draft cooling tower. The use of a natural draft tower would eliminate the need for electric power for fan drives.
- Continued success in development activities related to the electrolyzer, which is expected to demonstrate that the cell voltage and power requirements selected for this conceptual design can be substantially improved upon.
- Optimization of equipment and piping sizes and plant layout to reduce pumping power requirements, within the constraints of reasonable costs.
- Perhaps the most significant area of development that could produce substantial improvement in performance is in the acid concentration system. With the thermal evaporative concentration system employed in the current flowsheet, serious compromises must be made in process parameters in order to maintain reasonable performance levels. Since the concentration requires a great deal of thermal energy to evaporate the water diluting the sulfuric acid (this thermal energy is subsequently thrown away when the water vapor is condensed), the concentration of sulfuric acid leaving the electrolyzer is kept high to minimize this loss. The high sulfuric acid concentration requires higher electric power consumption in the electrolyzers for a given quantity of hydrogen production. Trade-offs have to be made to balance the electrical needs of the electrolyzer against the thermal requirements and dissipations of the vaporization step. The

development of a more efficient sulfuric acid concentration system, employing chemical or thermochemical reactions rather than thermal vaporization, would enable the  $\text{SO}_2$  - depolarized electrolyzers to operate with lower acid concentrations while reducing the heat rejection from the concentration step. Such a system would thereby dramatically reduce power consumption. Potential increases in hydrogen output - at a given thermal rating - of twenty percent or greater are possible.

## 3.0 PLANT ECONOMICS

### 3.1 GENERAL AND GROUND RULES

The cost of producing hydrogen is evaluated for the plant design discussed in Section 2.0. In determining the overall costs, estimates were made of the capital, operation and maintenance, and fuel costs for the facility in the general format used in reporting nuclear power-plant costs, as defined in NUS-531 (Reference 2). The costs of the VHTR nuclear heat source were taken from the ERDA sponsored conceptual design study reported in Reference 3. These costs were adjusted to account for the interfacing of the VHTR with the hydrogen production plant. The effects on the production costs of different capacity factors, fuel costs, and type of ownership were also considered. The major economic groundrules for the evaluation of the hydrogen production systems are as follows:

- All capital and operating costs are in July, 1974 dollars.
- No escalation has been included in the cost estimates. The sensitivity analysis of the effect of fuel costs on the system does, of its nature, imply a certain rate of escalation.
- The economic analysis assumes private industry financing and tax rates.
- The annual fixed charge rate for depreciable capital investments is 15 percent for utility-type ownership and 25 percent for industrial-type ownership. The annual charge includes recovery of capital (profit, interest, and depreciation), Federal and State income taxes, local property taxes, interim replacements, and property insurance, as shown in Table 3.1.
- The annual fixed charge rate for non-depreciable and working capital is 10 percent.
- Interest rate during construction is 8 percent.
- The plant availability is 90 percent.
- The plant capacity factor is 80 percent.
- Nuclear fuel cost assumptions (materials, enrichment, reprocessing, etc.) for the very high temperature nuclear heat source are shown in Table 3.2 and are identical to those used in Reference 3.
- Cost estimates are based on the assumption that the plant is not the first of a kind, but is a developed mature type with no special non-recurring engineering or development costs associated with it. The cost of any necessary R&D is treated separately in Section 4.

TABLE 3.1  
ANNUAL CHARGE RATE ON DEPRECIABLE INVESTMENT

	<u>Utility</u>	<u>Industrial</u>
<u>Assumptions:</u>		
Plant Lifetime, Years (for economic write-off)	30.0	15.0
Percentage of Investment in Bonds	55.0	30.0
Interest Rate on Bonds, Percent	10.0	10.0
Return on Equity, Percent	10.0	15.0
Federal Income Tax Rate, Percent	48.0	48.0
State Income Tax Rate, Percent	3.0	3.0
Local Property Tax Rate, Percent	3.0	3.0
Interim Replacements Rate, Percent	0.35	0.35
Property Insurance Rate, Percent	0.25	0.25
 <u>Annual Charge Rate, Percent:</u>		
Recovery of Capital		
Interest on Bonds	5.5	3.0
Return on Equity	4.5	10.5
Sinking Fund Depreciation	0.61	2.38
Federal Income Tax	1.28	4.70
State Income Tax	0.08	0.30
Local Property Tax	2.18	2.05
Interim Replacements	0.35	0.35
Property Insurance	<u>0.25</u>	<u>0.25</u>
	<u>14.8</u>	<u>23.5</u>
Total, Percent		
Total (Rounded Off), Percent	15	25

TABLE 3.2  
NUCLEAR FUEL COST ASSUMPTIONS (VHTR)

<u>Item</u>	<u>Cost</u>
U <sub>3</sub> O <sub>8</sub> (natural uranium)	\$ 22.05/Kg (\$10/lb)
Conversion of U <sub>3</sub> O <sub>8</sub> to UF <sub>6</sub>	\$ 2.2/Kg (\$1/lb)
Separative Work	\$ 40/Kg
Reprocessing	\$ 170/Kg
Plutonium	\$9280/Kg
Thorium	\$ 9/Kg
Uranium-233	\$ 17,000/kg

### 3.2 CAPITAL COSTS

The capital cost estimate is based on preliminary sizing of most of the major plant equipment and determining appropriate costs for that equipment. Factors, based on experience with these types of systems, were used to account for the costs of installation, piping, valves, instrumentation, structures, and miscellaneous equipment. Indirect costs were also estimated by applying factors in the manner described below.

The VHTR costs used in the economic evaluation were taken from Reference 3 and adjusted to account for refinements in the interface conditions, inclusion of the intermediate coolant loop piping and circulators, and upgrading of the reactor rating from 3000 to 3345 MWt. The VHTR direct costs, as reported in Reference 3, and as adjusted in this evaluation, are shown in Table 3.3.

The hydrogen production plant, producing  $10.15 \times 10^6$  standard m<sup>3</sup>/day ( $380 \times 10^6$  SCFD), is estimated to require a direct cost investment, in mid-1974 dollars, of \$382,482,000, as shown in Table 3.4. The direct cost is presented according to a code of accounts that divides systems among on-sites and off-sites, with the former relating to closely related mainline process steps and the latter consisting of support and service systems and facilities. The off-sites accounts reflect the consideration that the VHTR and hydrogen plant are at the same location, resulting in shared services, buildings, and facilities. The off-sites, therefore, consist of the incremental costs, relative to that already included in the VHTR costs to provide the required services.

The total plant investment, shown in Table 3.5, includes the direct costs plus contingencies, indirect costs, and interest during construction. For the purpose of evaluation, land and land rights are shown separately from other direct costs since it is a non-depreciating asset.

TABLE 3.3  
NUCLEAR HEAT SOURCE (VHTR)  
DIRECT CAPITAL COSTS  
(July, 1974 Dollars)

Account <sup>(1)</sup>	Item	Installed Cost (\$ Thousand) <sup>(2)</sup>		Remarks
		Reference	This Study	
20	Land and Land Rights	\$ 800	\$ 800	
21	Structures and Site Facilities			
211	Site Improvements and Facilities	2,515	2,515	
212	Reactor Building	16,196	16,900	Increased Plant Rating
214	Intake and Discharge Structures	798	-----	Cooling Tower Instead of River Cooling
215	Reactor Auxiliary Building	25,009	25,800	Increased Plant Rating
216	Control and Electrical Building	4,065	4,065	
217	Diesel Generator Building	1,932	1,932	
218	Administration/Service Building	851	851	
219	Helium Storage Building	180	275	Storage for Helium in Intermediate Loop
22	Reactor Plant Equipment			
221	Reactor Equipment	63,401	67,680	Increased Rating
222	Main Heat Transfer and Transport System	73,844	83,440	Increased Rating, Inclusion of Intermediate Loop Equipment
223	Safeguards Cooling Systems	4,965	5,300	Increased Rating
224	Radioactive Waste Treatment	2,332	2,400	Increased Rating
225	Nuclear Fuel Handling and Storage	13,213	13,400	Increased Rating
226	Other Reactor Plant Equipment	12,057	12,400	Increased Rating, Intermediate Loop Helium Purification
227	Instrumentation and Control	8,796	8,900	Intermediate Loop Control
24	Electric Plant Equipment			
241	Switchgear	1,373	1,522	Intermediate Loop
242	Station Service Equipment	3,477	4,083	Intermediate Loop
243	Switchboards	695	710	Intermediate Loop
244	Protective Equipment	303	303	
245	Electrical Structures and Wiring Containers	3,309	3,410	Intermediate Loop
246	Power and Control Wiring	8,285	8,780	Intermediate Loop
25	Miscellaneous Plant Equipment			
251	Transportation and Lifting Equipment	1,279	1,279	
252	Air and Water Service Systems	5,131	6,500	Cooling Tower Instead of River Cooling
253	Communications Equipment	171	171	
254	Furnishings and Fixtures	345	345	
	Total Direct Cost	\$255,322	\$273,761	

(1) Account Numbers are those for Nuclear Plants as Determined in NUS-531.

(2) Includes Contingency Within Each Account.

TABLE 3.4  
 WATER DECOMPOSITION PLANT  
 DIRECT CAPITAL COSTS  
 (July, 1974 Dollars)

<u>Account</u>	<u>Item</u>	<u>Installed Cost (\$ Thousands)</u>
<u>2000</u>	<u>On-Sites</u>	
2100	Battery F - Electrolyzer Power Supply	\$ 17,734
2200	Battery G - Electrolyzers	136,775
2300	Battery H - Sulfuric Acid Decomposition	112,620
2400	Battery I - SO <sub>2</sub> /O <sub>2</sub> Separation	43,395
2500	Battery J - Turbine - Generator	<u>36,900</u>
	On-Sites Subtotal	\$ 347,424
 <u>1000</u>	 <u>Off-Sites</u>	
1100	Cooling System and Water Intake	\$ 6,392
1200	Make-Up and Feedwater	6,862
1300	Waste Water Treatment	301
1500	Steam Generation	See Battery J
1600	Electrical Auxiliary Power	14,277
1700	General Off-Sites Investment	
1710	Land and Land Rights	200
1720	Site Improvements and Facilities	954
1730	Administration/Service/Laboratory Buildings	1,269
1740	Instrument and Plant Air	2,350
1750	Maintenance Facilities	1,372
1760	Fire Protection, Communications	846
1770	Furnishings, Fixtures, Laboratory Equipment	<u>235</u>
	Off-Sites Subtotal	\$ 35,058
	Total Direct Capital Cost	\$ 382,482

TABLE 3.5

NUCLEAR WATER DECOMPOSITION  
ESTIMATED CAPITAL COST SUMMARY

(In Thousands of Dollars)

<u>Non-Depreciating Assets</u>	<u>VHTR</u>	<u>Water Decomposition</u>
Land and Land Rights	\$ 800	\$ 200
<u>Depreciating Assets</u>		
Special Materials	\$ 342	\$ 4,065
Physical Plant	\$ <u>273,761</u>	\$ <u>382,482</u>
Subtotal	\$ 274,103	\$ 386,547
Contingency	(Included Above)	\$ <u>57,982</u>
Subtotal	\$ 274,103	\$ 444,529
Indirect Costs		
Construction Facilities, Equipment & Services	\$ 17,707	\$ 9,563
Engineering Services	\$ 43,034	\$ 15,938
Other Costs	\$ 13,650	\$ 4,098
Interest During Construction	\$ <u>95,059</u>	\$ <u>76,114</u>
Subtotal	\$ 169,450	\$ 105,713
Total Depreciating Assets	\$ 443,553	\$ 550,242
Total Plant Investment	\$994,795	

Special materials comprise the initial supply of chemicals, catalysts, lubricants and other materials needed for operation of the plant. A contingency of 15 percent is applied, for the hydrogen generation facilities, to the estimated cost of the special materials and the direct cost of the physical plant. Contingencies are included within the VHTR direct cost estimate.

Indirect costs are expense items of a general nature which apply to the overall project of building an operable plant, rather than to one of the direct costs. These costs, except for interest during construction, have not been estimated in detail, but calculated as a percentage of the direct costs based on the procedure defined in NUS-531 and updated by ERDA in 1974 for use in the study reported in Reference 3. The indirect costs for the water decomposition facilities are calculated as incremental costs to that already included in the VHTR estimate.

Construction facilities, equipment, and services include general costs associated with the plant construction, such as field offices, warehouses, temporary power and utility lines, cost or rental of construction equipment and supplies, purchase of electric power, water, and other utilities, security guards, training programs for the labor force, inspection and testing of construction materials, site cleanup, insurance, and the like.

Engineering services include items such as preliminary investigations; site selection; air and water environmental studies; subsurface investigations; preparation of specifications and evaluation of proposals for major equipment packages, preparation of preliminary and final design documents, design reviews, procurement, inspection, and expediting of materials and equipment; preparation of pre-operational test and plant startup procedures; assistance in securing plant permits; management and direction of construction activities, including selection of subcontractors, scheduling, maintaining cost and quality control; on-site procurement and receiving of materials and equipment; field accounting; supervising and pre-operational testing of systems and components; field engineering inspection of construction work to assure compliance with plans and specifications; and preparation of as-built drawings.

Other costs include the owner's property and all-risk insurance, state and local property taxes on the site and improvements during construction, sales taxes on purchased materials and equipment, staff training, plant startup, and the owner's general and administrative (G&A) costs.

Interest during construction is calculated as simple interest, at an 8 percent annual rate, on the plant investment as it is made. For the purpose of the evaluation, it is assumed that the land is purchased six months prior to the start of the project and that special materials are delivered and paid for nine months prior to plant commercial operation. The remainder of the plant investment is made as design and construction proceeds. Figure 3.1 shows the rate of expenditures as a function of time. The overall project period of eight years is dictated by the design, licensing, and construction time for the VHTR. The water decomposition plant requires a shorter construction time, and therefore the major investments in that part of the facility are delayed so that a common completion of construction can be achieved. Engineering

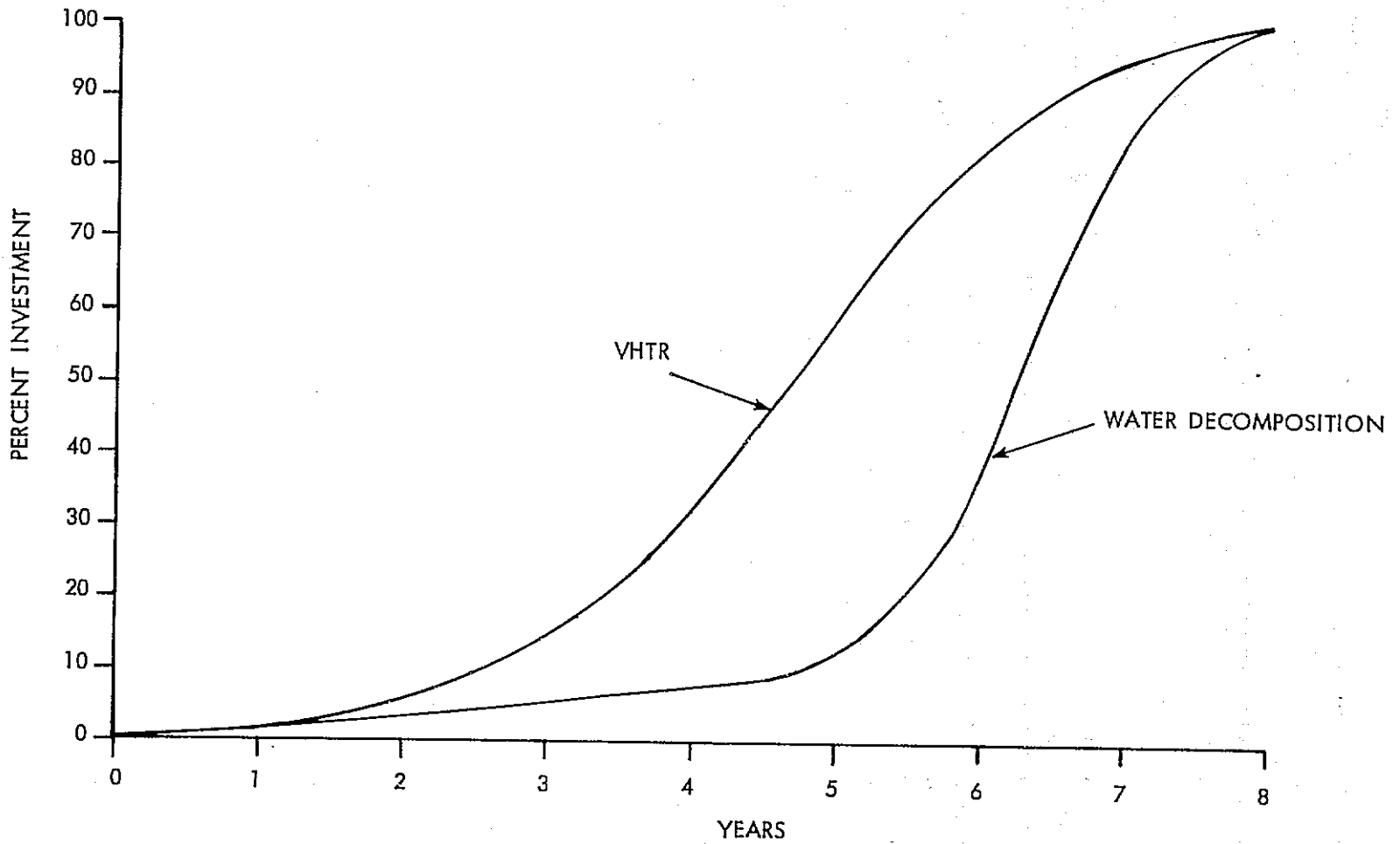


Figure 3.1 Nuclear Water Decomposition - Plant Capital Investment Expenditures Versus Time

and the development of information required for environmental impact statements and construction permits for the water decomposition plant proceeds in parallel with the comparable effort for the VHTR to assure that no schedular delays occur.

The total plant investment, including all direct and indirect costs but excluding escalation, is estimated to be \$994,795,000 for the grass roots facility.

### 3.3 OPERATION AND MAINTENANCE COSTS

The costs of operation and maintenance includes the expense of maintaining a plant staff, consumable supplies and equipment, outside support services, miscellaneous items of cost, and indirect costs of maintaining the plant working capital.

The direct O&M costs are shown in Table 3.6, as the costs estimated for the VHTR (Reference 3), plus the incremental costs for the water decomposition plant. The staff costs are based on a 140 person staffing level for the combined VHTR and water decomposition plant at an average cost of \$19,300 per man-year. The costs of chemicals and catalysts are based on their assumed use rate. An allowance has been included for miscellaneous consumables.

Outside support services are taken to embrace all services obtained other than from the normal plant complement during normal working hours. This includes personnel from other locations, as well as the cost of station personnel working overtime on special tasks such as refueling and equipment maintenance or repair. Other requirements for outside support services include such items as film-badge processing, laundering of contaminated clothing, off-site disposal of wastes, major equipment overhauls, and consultants to provide various forms of operational support. An allowance equal to 50 percent of the VHTR costs is used for these costs attributed to the water decomposition plant.

Miscellaneous O&M costs include such items as:

- Training new staff personnel
- Requalification of operators
- Rent (for property, equipment, or facilities which are used or occupied in connection with plant operation)
- Travel, such as to staff conferences at the main office, or to professional society meetings or other conferences
- Licenses and fees
- Office supplies, postage, and telephone/telegraph bills, and
- Fuel and upkeep of station vehicles

TABLE 3.6

NUCLEAR WATER DECOMPOSITIONANNUAL O & M COSTS

(IN THOUSANDS OF DOLLARS)

<u>STAFF PAYROLL (140)</u>		\$ 2,702
<u>CONSUMABLE SUPPLIES AND EQUIPMENT</u>		\$ 2,045
VHTR	\$ 492	
H <sub>2</sub> PLANT	\$1,553	
<u>OUTSIDE SUPPORT SERVICES</u>		\$ 228
VHTR	\$ 152	
H <sub>2</sub> PLANT	\$ 76	
<u>MISCELLANEOUS</u>		\$ 128
VHTR	\$ 85	
H <sub>2</sub> PLANT	\$ 43	
	SUBTOTAL	\$ 5,103
<u>G &amp; A</u>		\$ 765
<u>NUCLEAR LIABILITY INSURANCE</u>		\$ 406
	TOTAL DIRECT O & M COSTS	\$ 6,274

As before, an allowance of 50 percent of the VHTR costs is used for the water decomposition plant.

An annual premium of \$406,000 is assumed for nuclear liability insurance. This premium is in addition to other insurance premiums included in the annual charge on capital.

The total direct annual operation and maintenance cost of \$6,274,000 includes a 15 percent G&A assessment on all costs, except for nuclear liability insurance.

The indirect O&M costs are shown in Table 3.7. These are the costs of maintaining the working capital required for continued operation of the plant and is evaluated at a 10 percent annual charge rate. The working capital is made up of the cash in hand needed to meet the day to day operating expenses plus the value of materials and supplies in inventory. The average net cash required is calculated at 2.7 percent of the direct O&M costs, less the nuclear insurance premium. A two month supply of consumables is assumed to be kept in inventory. To account for pre-payment of nuclear insurance, 50 percent of the premium is included as working capital.

The total O&M costs, at a plant capacity factor of 80 percent, are shown in Table 3.8.

### 3.4 FUEL COSTS

Fuel costs are all expenses associated with the nuclear fuel cycle of the VHTR. These include items such as procurement of all materials, uranium enrichment, fuel fabrication, fuel reprocessing, credits for materials of value in spent fuel, and carrying charges in all parts of the fuel cycle. The fuel cycle costs, as reported in Reference 3, in accordance with the economic groundrules of Section 3.1, is 24.75¢/GJ (26.1¢/10<sup>6</sup> Btu).

The plant, operating at an 80 percent capacity factor and a thermal output of 3345 mw, will accumulate a total annual fuel cost of \$20,850,000.

### 3.5 HYDROGEN PRODUCTION COSTS

The hydrogen production cost is made up of the contributions of capital, operation and maintenance, and fuel costs. These are normally calculated on an annual basis. The percentage of the plant investment that is charged against production each year is a function of the type of plant ownership, i.e., utility or industrial, and the manner in which the owner can do business. As discussed in Section 3.1, the annual charge on non-depreciating assets, e.g., land, is 10 percent for either type of ownership while the annual charge on depreciating assets is 15 percent for utility ownership and 25 percent for industrial ownership. Although production costs are calculated on both a utility and industrial basis, it is not realistic to consider that the production of hydrogen, on the scale contemplated and with distribution to remote "users", would be an "industrial" enterprise. It is considered that this sort of production plant would much more readily fit a "regulated utility" type of enterprise - much like today's natural gas and electric utility operations.

TABLE 3.7  
 NUCLEAR WATER DECOMPOSITION  
 INDIRECT OPERATION AND MAINTENANCE COSTS

	Cost (Thousands)
Average Net Cash Required	\$ 158
Materials and Supplies In Inventory	
Consumable Supplies and Equipment	\$ 341
50% of Nuclear Liability Insurance Premium	\$ 203
Total Working Capital	\$ 702
Annual Charge Rate	10%
Annual Indirect O&M Cost	\$ 70

TABLE 3.8  
 NUCLEAR WATER DECOMPOSITION  
 TOTAL ANNUAL O&M COST  
 (80% Capacity Factor)

	Cost
Direct O&M Costs	\$ 6,274
Indirect O&M Costs	\$ <u>70</u>
Total	\$ 6,344

The cost of hydrogen production, on both bases, is shown in Table 3.9. As can be seen, the cost, which is equivalent to a "gate selling price", is 5.96¢ standard m<sup>3</sup> (\$1.59/MSCF), or \$4.65/GJ (\$4.90/10<sup>6</sup> Btu) on a utility basis. The cost to the ultimate consumer would be this production cost plus the allocated capital and operating costs of transmission and distribution.

### 3.6 SENSITIVITY ANALYSIS

The cost of hydrogen production from the plant will vary with the cost of fuel, the type of ownership, and the utilization, i.e., capacity factor, of the facility. For the base case calculation, it was assumed that fuel costs were 24.75¢/GJ (26.1¢/10<sup>6</sup> Btu), the capacity factor was 80 percent, and utility ownership prevailed.

Figure 3.2 shows the effect on hydrogen production cost of variations in the cost of fuel for both utility and industrial ownership, with the capacity factor remaining at 80 percent as in the base case. The effect on the production cost of hydrogen, if the oxygen was sold instead of vented, is shown for one assumed selling price of oxygen.

Table 3.10 indicates the manner in which the capacity factor affects the production cost. In this table, all of the cost assumptions are the same as the base case with only the capacity factor allowed to vary within a range of 40 to 90 percent. As can be seen, the cost of capital remains constant regardless of how the plant is operated. Operation and maintenance costs are divided into two parts, i.e., fixed and variable. The fixed costs are independent of the plant performance and accrue whether or not the plant is operated. The variable costs are a direct function of the plant operation. Nuclear fuel costs also have fixed and variable components.

### 3.7 COMPARATIVE HYDROGEN PRODUCTION COST

The economic value of a hydrogen production system can only be assessed by comparing the cost of production of a system to competitive systems. As part of the study performed under this contract, and reported in NASA-CR-134918 (Reference 1), the hydrogen production cost for water electrolysis and coal gasification systems were determined using the same economic groundrules. These costs can therefore be used for realistic comparative cost evaluations to assess the attractiveness of any of the systems.

The hydrogen production plants selected for economic comparison with the Sulfur Cycle Water Decomposition System were a near-term technology water electrolysis plant using Tele-dyne electrolyzers, a Koppers-Totzek coal gasification plant and a coal gasification plant using the developing Bi-Gas technology. The results of the production cost assessment, plotted as a function of the cost of coal, are shown in Figure 3.3.

The water electrolysis plant, using near term technology, is assumed to be powered by a dedicated light water nuclear power plant to provide the least expensive energy cost for the process. The electrolysis plant, including water treatment and all auxiliaries and service loads, is estimated to operate at an efficiency of 81 percent. The electrical generation efficiency, for the LWR, is estimated to be 34 percent, resulting in a net overall process efficiency of 28 percent. Nuclear fuel costs for the light water reactor were assumed to be 19.9¢/GJ (21¢/million

TABLE 3.9  
 NUCLEAR WATER DECOMPOSITION  
 HYDROGEN PRODUCTION COST COMPARISON  
 (80% Capacity Factor)

<u>Annual Costs</u>	<u>Utility</u>	<u>Ownership</u>	<u>Industrial</u>
Non-Depreciating Capital	\$ 100,000		\$ 100,000
Depreciating Capital	149,069,000		248,449,000
Operation and Maintenance	6,344,000		6,344,000
"Fuel"	<u>20,850,000</u>		<u>20,850,000</u>
Total Annual Cost	\$176,363,000		\$275,643,000
 <u>Annual Gas Production</u>	 2.96 x 10 <sup>9</sup> std m <sup>3</sup> (1.11 x 10 <sup>11</sup> SCF)		 2.96 x 10 <sup>9</sup> std m <sup>3</sup> (1.11 x 10 <sup>11</sup> SCF)
 <u>Production Cost</u>	 5.96¢/std m <sup>3</sup> (\$1.59/MSCF) \$4.65/GJ (\$4.90/10 <sup>6</sup> Btu)		 9.31¢/std m <sup>3</sup> (\$2.48/MSCF) \$7.26/GJ (\$7.66/10 <sup>6</sup> Btu)

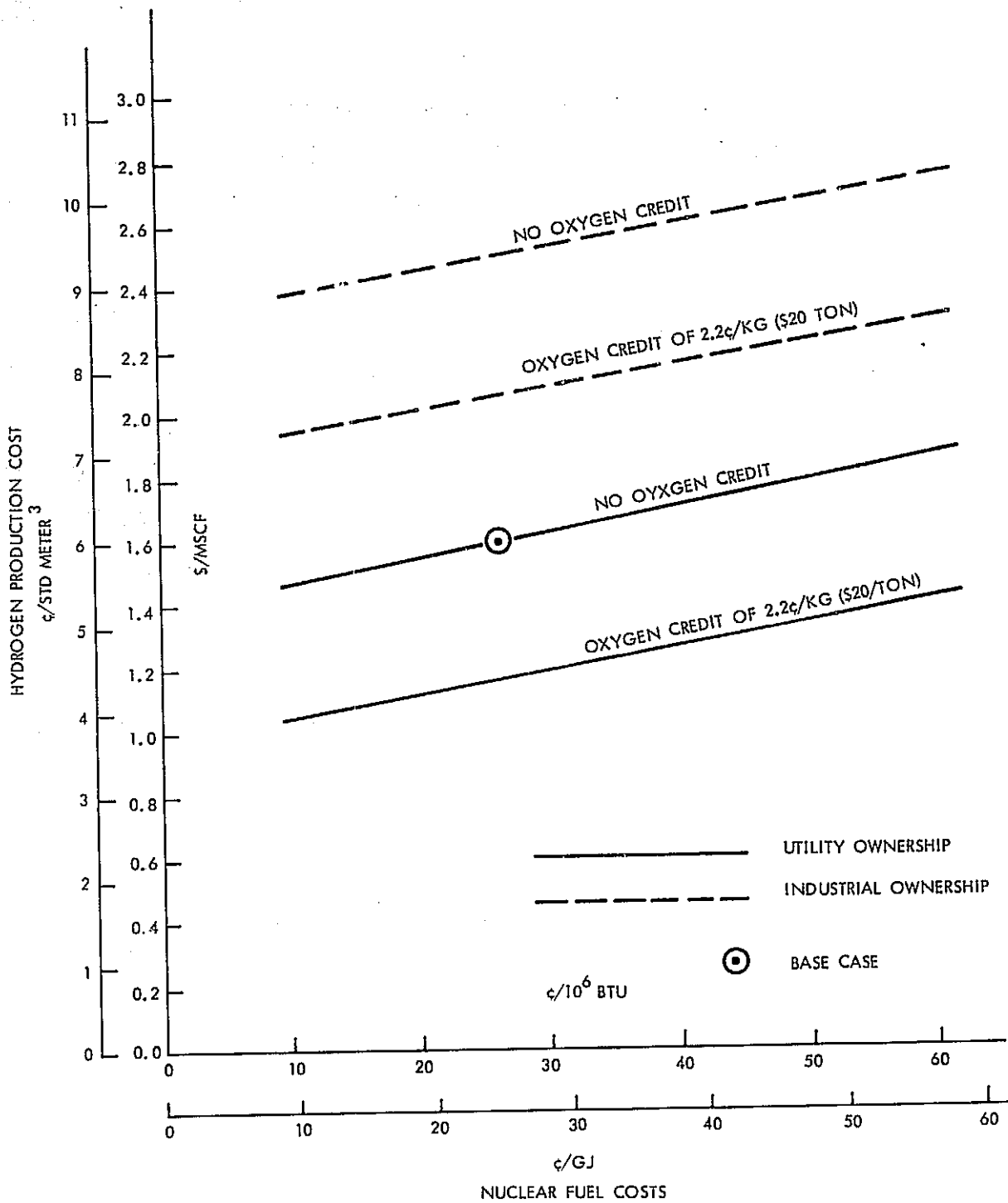


Figure 3.2 Nuclear Water Decomposition Hydrogen Cost Versus Nuclear Fuel Cost (80% Capacity Factor)

TABLE 3.10

NUCLEAR WATER DECOMPOSITION  
 SENSITIVITY OF H<sub>2</sub> PRODUCTION COST TO CAPACITY FACTOR  
 (Base Case Cost Assumption)  
 (Thousands of Dollars)

Item	Capacity Factor			
	40%	60%	80%	90%
Capital Cost	\$149,169,000	\$149,169,000	\$149,169,000	\$149,169,000
Fixed O&M	5,053,000	5,053,000	5,053,000	5,053,000
Variable O&M	646,000	968,000	1,291,000	1,452,000
Fixed Fuel Costs	6,610,000	6,610,000	6,610,000	6,610,000
Variable Fuel Costs	<u>7,120,000</u>	<u>10,680,000</u>	<u>14,240,000</u>	<u>16,020,000</u>
Total Annual Cost	\$168,598,000	\$172,480,000	\$176,363,000	\$178,304,000
Annual Gas Production	1.48 x 10 <sup>9</sup> std m <sup>3</sup> (5.55 x 10 <sup>10</sup> SCF)	2.22 x 10 <sup>9</sup> std m <sup>3</sup> (8.32 x 10 <sup>10</sup> SCF)	2.96 x 10 <sup>9</sup> std m <sup>3</sup> (1.11 x 10 <sup>11</sup> SCF)	3.33 x 10 <sup>9</sup> std m <sup>3</sup> (1.25 x 10 <sup>11</sup> SCF)
Production Cost	11.39¢/std m <sup>3</sup> (\$3.11/MSCF)	7.77¢/std m <sup>3</sup> (\$2.07/MSCF)	5.96¢/std m <sup>3</sup> (\$1.59/MSCF)	5.35¢/std m <sup>3</sup> (\$1.43/MSCF)

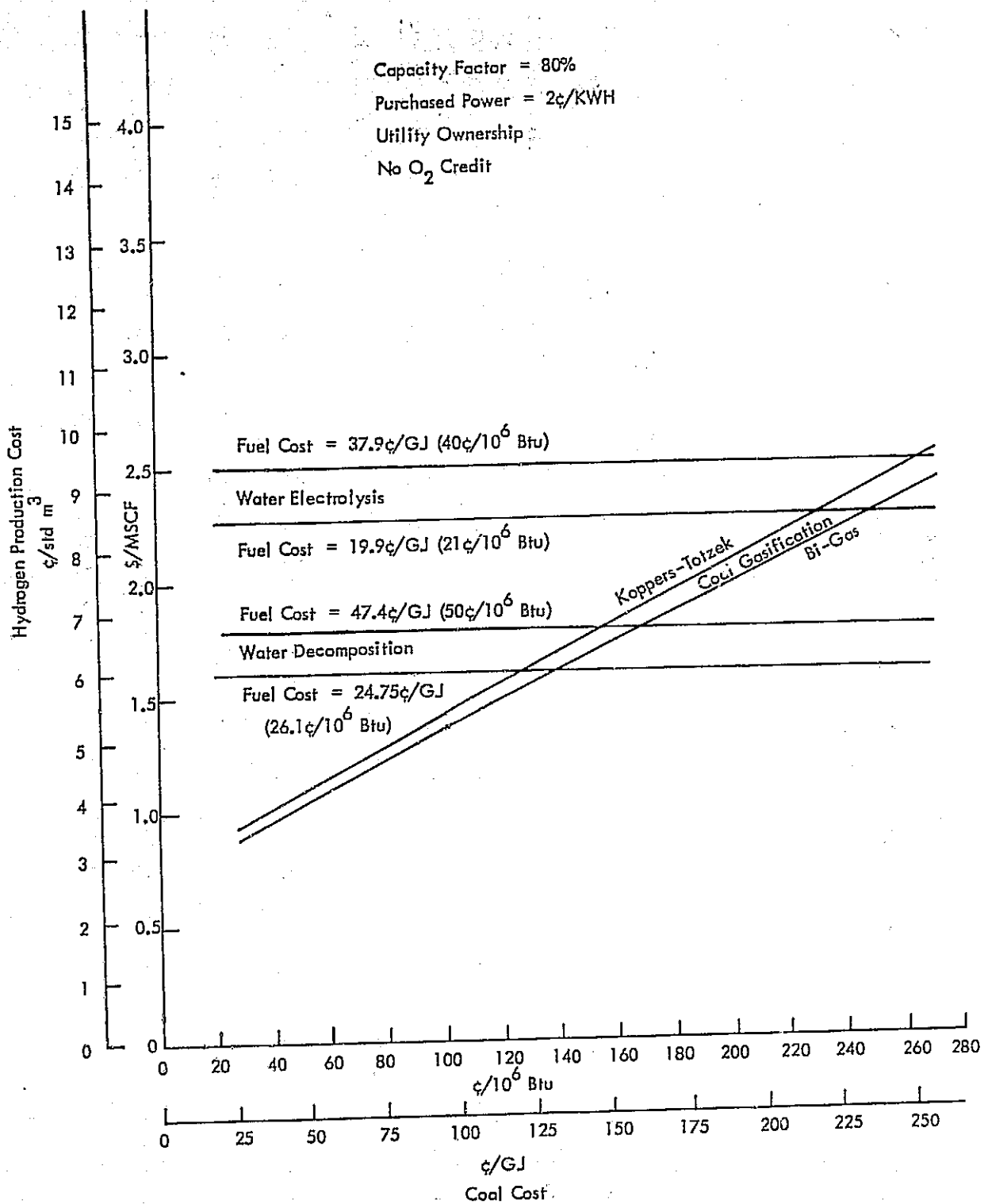


Figure 3.3 Comparative Hydrogen Production Costs

Btu), leading to a power cost, on the economic groundrules selected, e.g., no escalation, 1974 costs, etc, of 12.3 mills/kwh. Doubling the nuclear fuel cost would increase the power cost to 14.9 mills/kwh and raise the hydrogen production cost by about 10.9 percent.

A water electrolysis plant is, of course, subject to improvements in performance dependent upon continued development effort. A recent study (Reference 4) has looked at an advanced nuclear electrolytic hydrogen production facility which, if the requisite research and development is carried out, could be available at the same time that the VHTR-Sulfur Cycle Water Decomposition System can be commercialized, i.e., the 1990's. The advanced water electrolysis plant utilizes the technology of the VHTR to operate in a direct combined cycle electrical generation mode to produce electricity at an overall thermal efficiency of 50 percent. The combined cycle uses helium gas turbines and a bottoming ammonia Rankine cycle. The electricity is generated as d.c. power in acyclic generators, thereby avoiding the inefficiency of power conditioning and rectification. Hydrogen is produced in high pressure, high current density electrolyzers based on solid polymer electrolyte (SPE) technology. The overall efficiency of the water electrolysis plant is estimated to be 86.3 percent. Including the effects of energy losses in power generation (efficiency of 50 percent) and power distribution (efficiency of 99.5 percent), the net overall efficiency of the advanced system is estimated to be 42.9 percent. The cost of hydrogen produced by the advanced water electrolysis plant is estimated in Reference 4 to be higher than the base line cost predicted for the VHTR-Sulfur Cycle Water Decomposition plant estimated herein. Differences in estimating ground rules and technologies, however, preclude a final judgment on the magnitude of production cost differences between the two systems.

The two coal gasification processes result in reasonably comparable hydrogen costs which vary, naturally, as a function of the cost of coal fed to the process. The thermal efficiency for these units, based on all of the energy consumed in the process, e.g., oxygen production for the gasifiers, compressor work, etc., is in the order of 50 percent when hydrogen, at pressures suitable for pipeline delivery, is the only plant product.

The hydrogen cost for the water decomposition plant represents the capital, O&M, and fuel costs of the integrated, self-sufficient production plant defined in the conceptual design. The cost is evaluated at a nuclear fuel cost of 24.75 ¢/GJ (26.1¢/million Btu), which, although higher than the fuel cost of a LWR, represents that which can be achieved in a VHTR using comparable economic groundrules. The hydrogen production cost is relatively insensitive to nuclear fuel cost, showing an increase of about 11.8 percent for a doubling of the nuclear fuel cost. The hydrogen production costs for the water decomposition plant and the water electrolysis plant do not include any credits for the sale of by-product oxygen. If the oxygen were to be sold, instead of vented, as assumed in the design study, the cost of hydrogen would be reduced by the value of the oxygen revenue. If, for example, one were able to sell the oxygen for 2.2¢/kg (\$20/ton), the cost of hydrogen would be reduced by 1.7¢/m<sup>3</sup> (42¢/MSCF).

The comparative economic evaluation shows that the cost of hydrogen produced by the Sulfur Cycle Water Decomposition System is substantially lower than the cost of hydrogen produced by water electrolysis. Further, nuclear water decomposition holds great promise of lower hydrogen production costs as reasonable extrapolations of future nuclear and coal costs are made.

## 4.0 DEVELOPMENT PLAN FOR COMMERCIAL PLANT

### 4.1 GENERAL

Since the conception of the Sulfur Cycle Water Decomposition System in 1973, laboratory work, funded by the Westinghouse Electric Corporation, has established the technical feasibility of the two major steps of the process, i.e., the sulfur trioxide thermal reduction step and the electrochemical hydrogen generation. Results of that development effort are summarized in Sections 5.3.6 and 5.3.7. The development effort required to build upon the early laboratory work and bring the water decomposition system to commercial viability is described in the paragraphs below.

The conceptual design effort reported herein has shown the attractiveness of integrating the hydrogen generation facilities with a VHTR nuclear heat source. Development efforts in the joint AEC/NASA nuclear rocket (NERVA) program and the gas cooled reactor programs in the United States and Europe have provided a base of technology upon which the VHTR is built. To achieve, both safely and economically, the high temperatures required for process needs requires additional development beyond that already accomplished. These needs have been evaluated as part of ERDA Contract AT(11-1)-2445, reported in Reference 3, and summarized below.

### 4.2 DEVELOPMENT OF THE VHTR

The research and development program required to bring the VHTR to first large-scale demonstration was determined as part of the ERDA study on high temperature nuclear heat sources (Reference 3), and is summarized below. The program as currently envisaged reflects the conceptual design of the VHTR as presented in this report. Depending upon the results of further design studies, optimization and trade-off studies, and the results of the research and development as the program proceeds, the details of the program may require adjustment.

Some of the assumptions used in developing the research and development program, its schedule and costs, were:

1. All costs are in July, 1974 dollars.
2. The costs reflect "contractor" costs only. Nothing has been added, for example, for costs accrued by ERDA in administering the program.
3. No major facility costs are included. It is assumed, for example, that a Helium Turbine Test Facility is funded elsewhere and the facility is available to and adequate for the VHTR program.

4. A large scale demonstration plant is built on a schedule consistent with that shown in the Research and Development program schedule. The funding for the plant engineering and design, but not the equipment, components, and construction, is included as part of the VHTR program described here.
5. Irradiation testing is done in government facilities. Therefore, no costs have been included for irradiation time, in-pile loops, or high level hot cell facilities.
6. No costs are included for labor or services provided in government furnished facilities, nor any costs included for modifications to existing facilities or construction of new facilities.

Figure 4.2.1 summarizes the research and development program foreseen. This program, with a duration of about twelve years, culminates in the commercial operation of a large scale demonstration plant. This plant should be of a sufficient size to be commercially viable and would desirably be industrially sponsored.

There are seventeen major tasks indicated in the R&D program, scheduled so that information is generated in a timely fashion to meet the needs of the other tasks and the overall demonstration schedule. Programs that start at the inception of the VHTR development program are those of either a critical nature or of long duration - programs where an early start is required to meet the overall objective of having a demonstration plant operating in the late 1980's and commercial stations operating in the 1990's.

The total cost of the VHTR program, shown in Figure 4.2.1, is estimated to be  $\$350 \times 10^6$ . This includes a 25 percent contingency to account for omissions, errors, and as an allowance for changes in direction of the program as the work proceeds. If the demonstration plant design, and its share of contingency, is eliminated from the basic R&D program, the costs are then estimated to be \$240.6 million.

Details of the VHTR program, consisting of descriptions of the tasks and subtasks and costs, as a function of both task and year, are given in Reference 3.

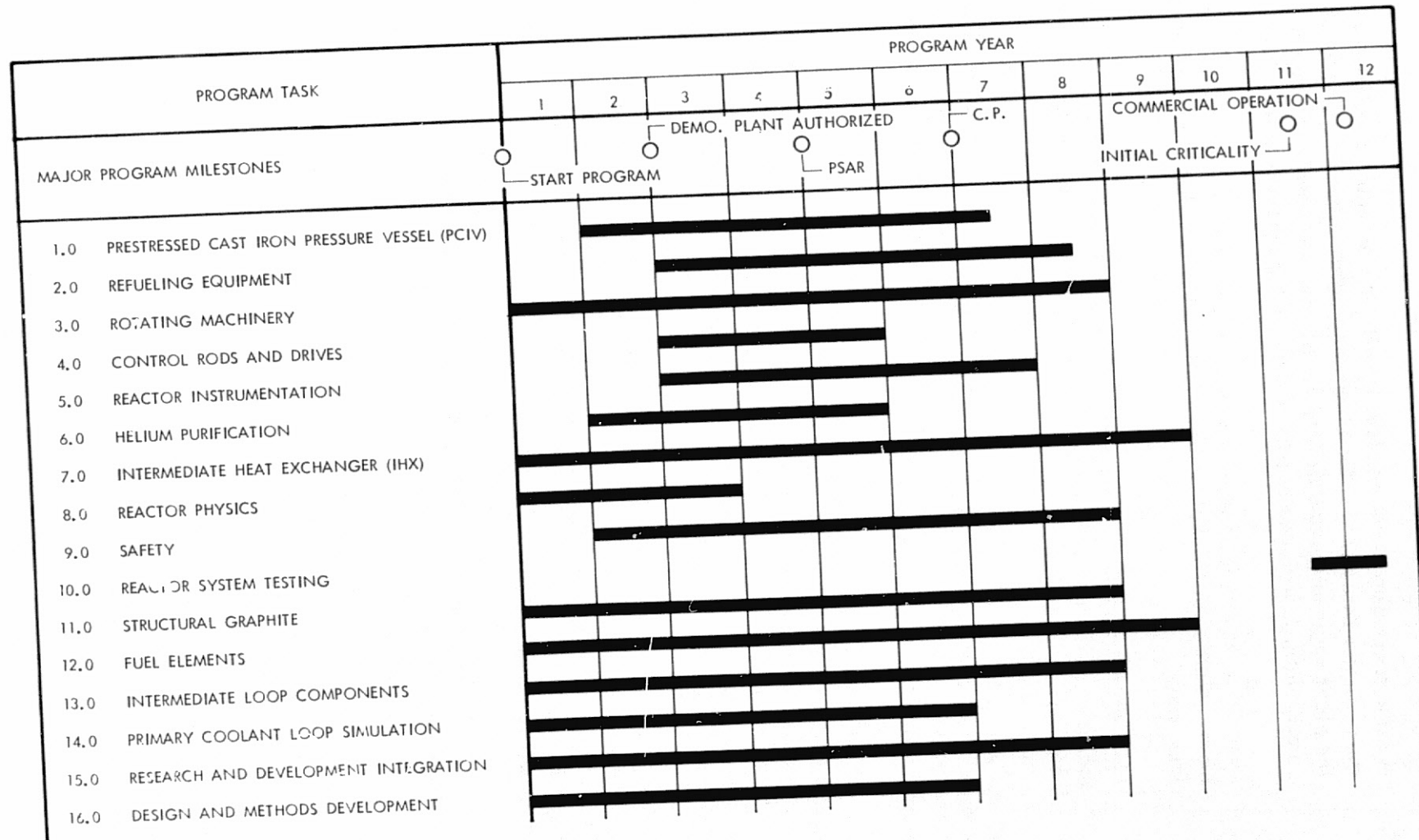


Figure 4.2.1 VHTR Research and Development Program Summary

## 4.3 DEVELOPMENT OF THE SULFUR CYCLE WATER DECOMPOSITION SYSTEM

The development of the hydrogen generation process is expected to proceed in the six phases below:

- 1.0 Supporting Research
- 2.0 Laboratory Demonstration
- 3.0 Process Evaluation
- 4.0 Pilot Scale Development
- 5.0 Pilot Plant
- 6.0 Demonstration or Commercial Plant

Table 4.3.1 summarizes the approximate size and scope of equipment employed in each phase, while Figure 4.3.1 illustrates the schedule and sequence of development leading to pilot plant operation. This schedule, and the costs of the program as discussed later, is predicated on the diligent prosecution of the development leading to a large scale demonstration or commercially sized plant operational by 1990. In this manner, the development of both the VHTR and the hydrogen production process can proceed, in logical fashion, along parallel paths with the integration of the two facilities being made at the large scale demonstration stage.

### 4.3.1 Phase 1.0 - Supporting Research

The Phase I program is divided into three major tasks, i.e., 1.0 Acquisition of Materials and Design Data; 2.0 Evaluate Alternate Systems; and 3.0 Revise Commercial Economics.

The efforts in this phase are concentrated in two general areas. The first is concerned with identifying improved materials and catalysts for use in the key process components. This effort is contained in Task 1.0 and deals specifically with the electrolyzer and the sulfur trioxide reduction reactor.

Small scale laboratory studies will be conducted to evaluate the performance of candidate sulfuric acid electrolyzer cell configurations. Energy efficiencies and hydrogen over-voltages will be determined as a function of temperatures, pressure, current density and time. To prevent sulfuric acid migration from the anolyte into the catholyte, with consequent deposition of sulfur at the cathode and loss of faradaic efficiency for hydrogen generation, a membrane must be placed between the two electrode compartments, while simultaneously, the catholyte must be overpressured. The consequences of these operational constraints are: (a) the internal resistance of the cell is increased, and (b) there is net sulfuric acid transport through the membrane from the catholyte into the anolyte. An ideal membrane, apart from satisfying the requirements of mechanical integrity and chemical stability, will minimize the effects of

TABLE 4.3.1

## SULFUR CYCLE WATER DECOMPOSITION SYSTEM DEVELOPMENT PROGRAM SUMMARY

DEVELOPMENT PHASE	SUPPORTING RESEARCH	LABORATORY DEMONSTRATION	PROCESS EVALUATION	PILOT SCALE DEVELOPMENT	PILOT PLANT
PURPOSE	PROOF-OF-PRINCIPLE. ACQUISITION OF KINETIC AND FUNDAMENTAL DESIGN DATA.	PROCESS VERIFICATION. ACQUISITION OF PRESSURIZED DESIGN DATA.	PRELIMINARY DEMONSTRATION OF KEY COMPONENTS.	SCALE-UP KEY PROCESS EQUIPMENT.	EVALUATE INTEGRATED PLANT OPERATION.
EQUIPMENT SCOPE	AS REQUIRED TO OBTAIN FUNDAMENTAL INFORMATION.	INTEGRATED OPERATION OF MAJOR PROCESS SECTIONS.	INTEGRATED PROCESS AND SUPPORTING AUXILIARIES.	INTEGRATION OF ALL PLANT FUNCTIONS.	OPERATION OF ALL PROCESS AND UTILITY FUNCTIONS IN COMMERCIAL SIZE MODULES.
EQUIPMENT SIZES					
ELECTROLYZER (TOTAL CAPACITY)	1 WATT	10-50 WATTS	1 KWE	30-100 KWE	1-5 MWE
SO <sub>3</sub> DECOMPOSITION	1/8" x 10" GLASS TUBE	1" x 12" METAL TUBE	SEVERAL 1" x 24" METAL TUBES	SMALL SCALE PROTOTYPE	1/4 TO FULL SCALE REACTOR
PLANT AREA	TABLE TOP	HOOD	20' x 20'	25' x 50'	120' x 200'

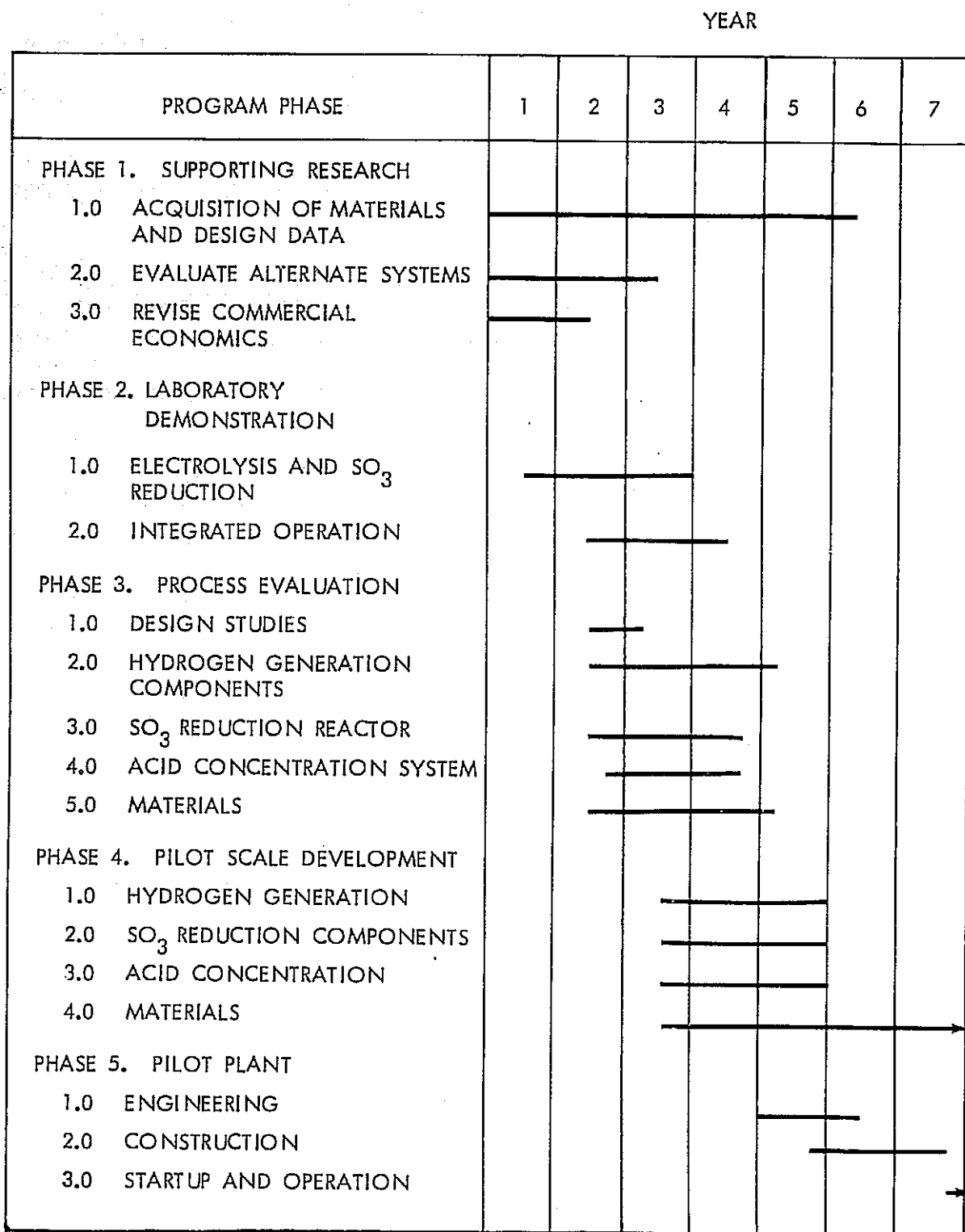


Figure 4.3.1 Overall Program Schedule

(a) and (b). Three membrane properties - through-porosity, pore-volume distribution as a function of pore radius, and thickness - determine the magnitudes of effects (a) and (b). Several classes of membranes will be investigated in order to identify that membrane with the optimum mix of desirable characteristics. Testing would include permeability and resistivity determinations as a function of time in a range of concentrated acid solutions at different temperatures. Electrode materials and types and electrocatalysts will be investigated and tested in the laboratory electrolyzer cells. Data will be acquired to select a low cost, stable, and active electrocatalyst for use in the electrolyzer.

The thermal decomposition of sulfur trioxide into sulfur dioxide and oxygen proceeds very slowly unless catalyzed. Tests performed by Westinghouse indicate that at temperatures to 1283K (1850°F) and with reactor residence times of four minutes, no perceptible sulfur dioxide formation occurs in the absence of catalysts. This is fortuitous in that the separation of SO<sub>2</sub> and O<sub>2</sub> can be accomplished without concern for a reaction reversal occurring. It does, however, require that suitable catalysts for the decomposition reaction be identified.

The selection of a catalyst for use in the sulfur trioxide thermal reduction reactor and the design optimization for the vessel necessitates that specific information be obtained. Catalyst activity is important. The ability to achieve equilibrium conversions at high space velocities leads to compact reactors. Similarly, the ability of a catalyst to maintain high activities for extended periods of time lowers maintenance and catalyst replacement costs. Ideally, a catalyst will possess both high activity and long life. Most often trade-offs between activity and life are required and these are reflected in an optimization of the capital and operating costs associated with the chemical reactor. The basic information necessary to conduct a sulfur trioxide thermal reduction reactor design and optimization will be acquired. Candidate catalysts will be tested to determine their activity and to estimate service life under process conditions. The specific reaction rate constants determined in this task are then used later to provide the detailed system models which enable design optimization and cost estimation to be performed.

Tasks 2.0 and 3.0 address the technology and economics of alternate process configurations. These include the optimization of the sulfur dioxide-oxygen separation system and the identification and evaluation of an efficient sulfuric acid concentration method. The development of an efficient thermal or thermochemical sulfuric acid concentration system enables the SO<sub>2</sub>-depolarized electrolyzers to operate with lower acid concentrations. Lowering the sulfuric acid concentration lowers the electrolyzer power requirements, expands the materials which can be considered in its construction, and increases the sulfuric dioxide solubility in the cell anolyte. Evaporation of excess water from sulfuric acid solutions is an expensive and thermally inefficient method of concentration. It is, however, technically proven, and little impetus has existed heretofore to examine potentially less costly and more efficient methods. The identification of an efficient concentration technique can significantly improve the economics of sulfur-based water splitting cycles by leading to potential increases in hydrogen output (at a given thermal rating) of 20 percent or greater and reducing the cost, complexity, and inefficiencies associated with the evaporation system used in this conceptual design. During this task, such alternative methods will be examined and their suitability for this application assessed.

Task 3.0 also provides iterations upon the conceptual design prepared in this present study to evaluate the potential of systems optimization and modifications, determine the worth of development results, and provide guidance and goals for the ensuing program.

#### 4.3.2 Phase 2.0 - Laboratory Demonstration

Westinghouse-funded research on the two major components of the process - the sulfur trioxide thermal reduction step and the electrochemical hydrogen generator - has established the technical feasibility of these two steps. Similarly, this study has provided a process conceptual design which serves to delineate the important process features and operating conditions. As a result of this past effort, Phase 2.0 development on the electrolyzer and sulfur trioxide decomposition reactor can generally proceed in parallel with Phase 1.0, as shown in Figure 4.3.1.

The purpose of the program may be simply stated - to demonstrate, with an integrated bench scale unit, closed cycle operation of the process. With overall process feasibility thus established, developmental effort to assure engineering and economic feasibility then can proceed with full confidence in the fundamental soundness of the process. The demonstration unit, when fully integrated, will have the characteristics shown in Table 4.3.1 and will be sized to produce a few liters of hydrogen per day.

The demonstration will include an  $\text{SO}_2$ -depolarized electrolyzer which converts sulfurous acid and water into hydrogen and sulfuric acid, an acid vaporizer for converting aqueous sulfuric acid into steam and sulfur trioxide, a thermal reduction reactor for catalytically reducing sulfur trioxide into sulfur dioxide and oxygen, and a recovery system for recycling water, sulfur dioxide, and unreacted sulfuric acid to the electrolyzer. This equipment will be capable of operating continuously for hundreds of hours in a fully closed cycle.

A small make-up of sulfur dioxide to the electrolyzer will be required to replace the small quantities of sulfur dioxide leaving with the oxygen stream. For this demonstration unit, larger quantities of sulfur dioxide will be vented than would occur in commercial systems. A commercial sulfur dioxide recovery system would operate at pressures of 5170 kPa (750 psia) or greater. The demonstration unit will operate at lower pressures due to the unavailability of compressors for handling gas flows this low. The degree of sulfur dioxide recovery is directly affected by operating pressure, becoming greater as pressure is increased.

The equipment, catalysts, and materials employed in the demonstration unit may, in some instances, differ from those which would be used in commercial systems. The sulfur dioxide recovery system mentioned above is one example. Similarly, operation of the electrolyzer will be demonstrated using platinized platinum electrodes. The use of this electrocatalyst enables the electrochemical reaction to be conveniently demonstrated. Platinized platinum electrodes, due to their cost, probably would not be used in commercial systems, and supporting programs in Phase I would identify suitable substitutes. Also, the catalyst used for conducting the sulfur trioxide reduction reaction would be the most promising of those evaluated to that time. Further testing and analysis will be required to identify the optimum catalyst, from cost and performance viewpoints, for use in a commercial system.

Included in the Phase 2.0 program, and continuing as a task in all subsequent phases, is a structural materials program designed to determine materials of construction for all process components. Although most of the systems use fluids at pressures and temperatures for which much component experience exists, there are several unique conditions within the process which will require structural materials investigation and development.

The ultimate success of the process is strongly dependent on finding suitable materials for two critical components, the acid vaporizer and the high temperature decomposition reactor. In the acid vaporizer, concentrated sulfuric acid is converted to the gaseous state at high temperatures. In the gaseous state the sulfuric acid exists primarily as  $H_2O$  and  $SO_3$ . This gaseous mixture leaves the acid vaporizer and enters the decomposition reactor. In this portion of the process cycle, the temperature of the  $SO_3$  and superheated water is increased to 1144K (1600°F). The  $SO_3$ , in the presence of a catalyst, is reduced to  $SO_2$  and  $O_2$ . The decomposition reactor construction materials must be compatible with the reactants, products, catalyst, and superheated steam.

Conditions employed in this process depart from those normally used in the sulfuric acid industry. As a result, little or no quantitative data exist for acid resistant materials at high temperatures and concentrations. However, recent advances in materials technology have produced materials and processes which have potential for high temperature sulfuric acid service. Identifying suitable structural materials that can provide an economical life for each of the critical components must be accomplished as early as possible to demonstrate the process operation at design temperature and pressure conditions. Sufficient test and evaluation must be done to characterize the materials sufficiently for Code acceptance.

#### 4.3.3 Phase 3.0 - Process Evaluation

Phase 3.0 concerns the design, construction, and semi-integrated operation of prototypes representing key process components. Materials of construction and vessel geometries expected in the full scale reactors would be employed. Integrated operation of as many system components as is practical would be demonstrated.

The program, as shown in Figure 4.3.1, is expected to take approximately 33 months and is a technological bridge between the laboratory scale work in the earlier phases and the larger, more expensive undertaking of the subsequent phases. Table 4.3.1 shows the characteristics of the equipment sizes for the Process Evaluation in comparison with those for other parts of the overall development.

Included in this phase, in addition to the scale-up and operation of the key components, is a Design Study Task, for the purpose of continuing the iterations of the conceptual design for evaluation of development results and guidance of future work, and a continuation of the Materials work started in the previous phase. The acid concentration system used in this phase would reflect the results of the work on alternate systems started in Phase 1.0.

#### 4.3.4 Phase 4.0 - Pilot Scale Development

Phase 4.0 verifies the scale-up procedures established in Phase 3.0, employing now more sophisticated reactors which duplicate in design, but not in size, those expected in actual operation. Extensive process integration would be demonstrated, with all major chemical intermediates recycling in closed cycle operation.

Phase 4.0 continues the philosophy of minimizing risk by taking small, but significant, steps in scaling up to commercially sized units. This is shown in Table 4.3.1. The materials program is continued during this phase.

#### 4.3.5 Phase 5.0 - Pilot Plant

Phase 5.0 provides a pilot plant demonstration of the process. As such, all major aspects of the system are demonstrated in closed cycle operation and in reactors either commercially sized or sufficiently close that further scale-up can be accomplished with certainty. Emphasis shifts to a verification of long duration process operation during which time the process control models and computer software are developed. Safe start-up, shut-down, and emergency procedures are developed and the effects of longer time operating transients are determined.

For the pilot plant, the energy source for the process would be non-nuclear. Fired helium heaters would be used to simulate the interface between the hydrogen process and the VHTR. The hydrogen generation would use 1-2 full scale electrolyzer modules, while the  $\text{SO}_3$  decomposition reactor would be at least one-quarter of a full scale module.

It is expected that the pilot plant would be operated for at least two years to gather sufficient information and experience for confident design, construction, and operation of commercial units.

#### 4.3.6 Phase 6.0 - Demonstration or Commercial Plant

Phase 6.0, depending upon the size and scope of the pilot plant effort, would be either a commercially sized plant or a semi-commercially sized demonstration plant. The thermal rating of the process would be between 1000 to 4000 MWt.

#### 4.3.7 Development Cost

The cost of the development program for the Sulfur Cycle Water Decomposition process, described above, has been estimated. Depending upon the results of further design studies, optimization and trade-off studies, and the results of the research and development as the program proceeds, the details of the program may require adjustment.

Some of the assumptions used in developing the cost of the development program were:

1. All costs are in July, 1974 dollars. This provides consistency in cost basis between the development costs, the development costs for the VHTR, and the cost estimate for the conceptual design.
2. The costs reflect "contractor" costs only. Nothing has been added, for example, for costs accrued by government agencies in administering the program.
3. The cost of design and construction of a pilot plant is included, but no costs are estimated for the operation of the pilot plant.
4. No costs are included for a large demonstration or commercial unit (Phase 6.0).
5. A 25 percent contingency is applied to all development cost estimates to account for omissions, errors, and as an allowance for changes in direction of the program as the work proceeds.

The total program cost is estimated to be \$63,300,000. Figure 4.3.2 shows the estimated cost of the development program as a function of both phase and year.

PROGRAM PHASE	PROGRAM YEAR							PROGRAM COST
	1	2	3	4	5	6	7	
1. SUPPORTING RESEARCH	—————							\$ 2,600
2. LABORATORY DEMONSTRATION	—————							\$ 1,500
3. PROCESS EVALUATION		—————						\$ 6,500
4. PILOT SCALE DEVELOPMENT			—————					\$ 8,000
5. PILOT PLANT				—————▶				\$32,000
CONTINGENCY (25%)								\$12,700
TOTAL COST	\$ 900	\$ 3,200	\$ 5,000	\$ 7,100	\$15,600	\$20,200	\$11,300	\$63,300

Figure 4.3.2 Development Program Costs  
(Dollars In Thousands)

111

## 5.0 SUPPORTING ENGINEERING STUDIES AND CONSIDERATIONS

### 5.1 GENERAL

To support the hydrogen production plant design presented in Section 2, this section provides additional technical considerations. A preliminary analysis of the plant's environmental impact was performed during the study and the results of this work are presented in Section 5.2. The general state-of-the-art of the Sulfur Cycle Water Decomposition Process is discussed in detail in Section 5.3 including its basis of selection, technology status of the main subsystem of the process, sensitivity analysis, materials technology and potential alternative fuels.

### 5.2 ENVIRONMENTAL IMPACTS

The evaluation of the environmental impact of the VHTR-hydrogen production plant is based on the need to (1) identify those special or unique impacts that are associated with this facility and (2) present the overall environmental impacts. This will enable the identification of particular environmental concerns that need to be included in the further evaluation and development of this hydrogen production concept. Because environmental impact is specific to the location and specific design of the facility, the design features identified in Section 2.0 and the standard hypothetical "Middletown", Reference 2, site are used as the basis for evaluation. The specific evaluation of the environmental impacts as related to the Middletown site are presented in this section.

#### 5.2.1 Resource Consumption

The construction and operation of the plant will require the use of basic resources in finite quantities. These resources include uranium, thorium and graphite fuel materials, water and chemicals for plant operation and materials of construction. Because the fuel materials do not have to be acquired from a particular localized or limited resource, the impact of consuming the fuel materials required for operation of this plant ( $\sim 10^6$  lb per year) out of the total national resource would not be significant for this single plant. Similarly, the chemical and catalyst requirements can be easily supplied from available resources. Therefore, the meeting of resource requirements is not anticipated to have a detrimental impact on the available supplies of fuel, chemicals and catalysts. It further follows that the resource requirements of this plant would not necessitate increased mining or materials supply activities with consequent environmental impacts.

The other major resource requirement for this plant is water as needed for both the decomposition cycle and the plant service and cooling requirements. The water supply must be obtained from local water resources and thus the potential for impact on resources does exist. However, at the Middletown site, the North River, which flows adjacent to the site, is about 1/2 mile wide and provides an ample supply of water without measureable impact on the resource.

### 5.2.2 Non-Radiological Air Impacts

Two major waste discharge streams are emitted to the atmosphere from the hydrogen production plant. These are the oxygen vent stream and the air stream effluent from the cooling tower containing water vapor. Neither the oxygen nor the water vapor are considered to be noxious, toxic or regulated. However, if not adequately dispersed, these two releases could have some localized impact. For example, an excess concentration of oxygen could enhance oxidation processes or more readily support combustion. The water vapor in the cooling tower effluent could produce a persistent visible plume of condensed water and local fogging.

The oxygen vent stream would not be expected to have any significant impact as rapid dispersion would be expected. Only under conditions of a severe downwash from a low-level release point could even a potential for impact exist, and then only at very short distances from the release point, which would be limited to on-site locations.

The potential for impact of cooling tower operation is not different than that incurred in the operation of cooling towers for conventional electric generating power stations. Thus, potential localized impact of visible plumes, ground fogging and drift from the cooling tower can be evaluated and alleviated by normal means. Being situated in a valley bounded by ridges on both sides, having a major river flowing down that valley and having a dominant wind direction along the valley axis, a potential problem of plume persistence might be anticipated. Visible plume lengths in excess of 6000 m (about 3-1/2 miles) might be expected during periods of high ambient humidity and low ambient temperatures. While humidity - temperature frequency data are not presently available for the Middletown site, it can be estimated that the periods of extended plumes from the cooling towers would be limited to a few hours annually. Through the use of the circular cooling tower configuration with the consequent higher plume rise, ground fogging along local access roads, railroad spurs and over the North River would not be anticipated. A limited frequency of plume impingement on the higher elevations of the ridges and hills bounding the valley might be anticipated. However, this would not produce a negative impact on the ecology or on population concentrations. While the longest visible plumes would not be expected to come close to the Middletown Municipal Airport located about ten miles north of the site, it may be possible to have some minor disruption of flight patterns for local small aircraft in the vicinity of the airport. Drift from the operation of the cooling tower would not be expected to extend beyond the site boundaries.

While the above discussion suggests that potential impact from cooling tower operation might exist at the Middletown site, the following two factors should be strongly considered. Firstly, the potential cooling tower impacts are not unique to this plant and thus in no way deter or influence the development of hydrogen production processes and facilities. Secondly, the specific potential for impact is both site-specific and subject to conventional cooling tower design and operation modifications. Should cooling tower operation be evaluated to pose a significant impact potential in any case, the cooling system can be redesigned for a different tower selected to avert the problem as is done conventionally with all power plants.

### 5.2.3 Water Impacts

Potential impacts on water resources and aquatic ecology can be associated with the intake, consumption and discharge of water to support plant requirements. Since the volumetric intake flow requirement is small relative to the total flow in the North River, the effects of consumption and depletion of water resources would not be anticipated to be adverse. Specific potential for impact of the intake and discharge systems as related to this site should be evaluated, but these do not constitute unique or unsolvable impact problems.

The specific flow characterization of the North River at the plant site is not available. For a broad river such as this one, there could be expected to be shallow areas in the river along the banks. The design of the plant would be expected to include consideration of these areas and the intake and discharge would be located to avoid such areas. The intake system could have a potential problem with the impingement and entrainment of fish and lower forms of aquatic biological life. The shallow areas could readily be spawning areas or areas conducive to congregation of fish. Withdrawal of water on these shallow areas through the plant intake could have a significant impact. However, this can be easily averted through the location and design of the intake system. Thus, an impact at the intake would not be anticipated.

Similarly, the discharge from the plant could potentially result in an environmental impact if not properly designed or located. The chemical composition of the discharge stream would not be significantly different from the intake composition as there are no major chemical liquid effluents being discharged from the plant. The major component of the discharge would be the blowdown from the cooling system and this would have both a greater concentration of the river water constituents and a small thermal component. For a typical cold-side blowdown from a tower designed to a  $15^{\circ}\text{F}$  approach to wet-bulb temperature, the discharge would be expected to be about  $15^{\circ}\text{F}$  over the ambient river water temperature. If a submerged, high momentum discharge is used, the low flow from this discharge would be readily dissipated in the high flow volume of the North River. However, a surface discharge into a shallow area along the river could lead to a thermal plume spreading over a significant area of the river surface with a consequent effect on the biological life in that area of the river. However, as before, this potential for impact is not unique to a hydrogen-production facility and can be readily alleviated by appropriate design consideration.

### 5.2.4 Solid Wastes

Three types of solid wastes from the plant can be expected. They include the discharged nuclear fuel, the replaced chemicals and catalysts, and the sludge from the water and waste treatment system. The discharged fuel will be transported off-site for reprocessing, recovery and disposal as appropriate and consistent with NRC requirements. Similarly, the replacement of chemicals (sulfur) and catalysts will be handled by off-site disposal. The sludge resulting from the water and waste treatment system clarifier and filters will be conveyed by truck to alternate off-site disposal in quantities of about 18,000 kg/day (20 tons/day). These wastes would not be expected to contain any unique or particularly toxic chemicals that could generate environmental problems either at the site or at the off-site disposal location.

## 5.2.5 Radiological Impacts on Humans

Liquid and gaseous effluents containing very small quantities of radionuclides will be released to the environment during operation of the VHTR. The radiological impact of these releases on humans is evaluated in the following sections.

### 5.2.5.1 Exposure Pathways

For this evaluation, potential pathways for radiation exposure to persons living at or beyond the site boundary are restricted to only the gaseous effluent release routes, since for a similar HTGR, the doses due to liquid pathway releases were found to be very small (Reference 5). The gaseous effluent pathways considered in this evaluation included: (1) external gamma exposure due to releases of the noble gases, (2) inhalation doses from tritium and radioactive iodine, (3) direct radiation from radioactive components within the Reactor Containment and Auxiliary buildings, (4) ingestion of contaminated food products (milk, meat and leafy vegetables) and (5) external exposure from the transport of radioactive fuel and wastes.

### 5.2.5.2 Evaluation Methods

The analytical models utilized in this analysis are generally the same as utilized for the Clinch River Breeder Reactor Plant (CRBRP) (Reference 6), except for the dose components were analyzed by use of the latest AEC guide, Docket RM-50-2 (Reference 7), which provides a more realistic (less conservative) approach than that given in the CRBRP report.

The gaseous effluent release rates for the VHTR were assumed to be the same as for the Fulton Generating Station (Reference 5), an HTGR of 3000 MWt. Although the VHTR design differs in several respects from that of the HGTR, the gaseous radwaste systems have not yet been designed and these systems will effectively control the gaseous release. Thus, for this analysis, it has been assumed that the Fulton Station gaseous release rates are directly applicable to the VHTR.

The site meteorology dispersion factors ( $X/Q$ ) were calculated as a function of radial distance from the VHTR using the Gaussian diffusion model and wind speed and Pasquill stability class data as obtained from "The Guide for Economic Evaluations of Nuclear Reactor Plant Designs" (Reference 2). The data utilized in this analysis represent the conditions for an "average: reactor site designated "Middletown, U. S. A." (Reference 2). Population distribution data as a function of radial distance were also taken from Reference 2. Since no values were available for the exact azimuthal and radial distribution of population, it was assumed that the population in the radial increment 0.5 to 1.0 mile was all located at the inner radius of the radial increment, i.e., at 0.5 mile. This assumption would result in a conservative estimate of the population dose as compared to the more reasonable assumption of an evenly distributed resident population.

### 5.2.5.3 Results of the Dose Evaluations

Results of the population dose assessment for the VHTR out to a radial distance of 30 miles are given in Table 5.2.1. These values are also compared with similar values obtained for the Fulton Station HGTR. A comparison of the VHTR values with the comparable Fulton Plant values shows that for some of the pathways (e.g., air immersion, ingestion of leafy vegetables) the VHTR values are significantly lower than the Fulton Plant. This is most likely due to differences in the dose models and population distributions. (The Fulton Plant has a higher population density in the near vicinity of the site than for the assumed VHTR site.)

The estimated population dose component due to transportation of spent fuel and packaged radioactive waste was assumed to be exactly the same for the VHTR as for the Fulton Plant on the basis that the irradiated fuel and waste shipments would be comparable. The assumed shipping distance for spent fuel of 1000 miles may be somewhat of an overestimate but it is consistent with other assumptions made for the standard hypothetical site utilized in the analysis of the VHTR.

Other dose pathways for the VHTR are significantly higher than for the Fulton Plant. These include: (1) the direct radiation component, (2) the inhalation pathway and (3) the food (milk and meat) ingestion pathways.

To meet the requirement of 2.0 mrem/yr at site boundary for the direct radiation component, the leakage dose rate at the Reactor Auxiliary Building cannot exceed 0.35 mrem/hr based on the dose model previously described. Thus the Reactor Auxiliary Building, which will contain spent fuel storage, will be designed to meet the above criteria.

Based on these conditions, the direct radiation component population dose for the VHTR was calculated to be very similar to that for the Fulton Plant HGTR (Table 5.2.1).

The dose components from inhalation, and ingestion via eating meat or drinking milk are not presented for the Fulton Plant. Thus no comparisons are possible for these pathways. Very conservative assumptions were utilized to estimate these components for the VHTR. For example, it is assumed that all meat and milk ingested by the population within 30 miles of the site is obtained from local sources.

A comparison of the dose component due to ingestion of leafy vegetable food crops containing tritium resulting from VHTR releases with those from the Fulton Plant shows the latter to be much higher. The higher estimate for the Fulton Plant is due to the very conservative assumptions made concerning the tritium dispersion and uptake through this pathway.

TABLE 5.2.1

COMPARISON OF ESTIMATED POPULATION DOSE FOR VHTR  
WITH POPULATION DOSE FOR FULTON PLANT HGTR

<u>Pathway</u>	<u>Population Dose, person-rem/yr</u>	
	<u>VHTR</u>	<u>Fulton Plant HGTR</u>
Air Immersion	0.036	0.31
Inhalation	2.9	-
Direct Radiation	0.66	0.7
Eating Vegetation	2.9	18.0
Drinking Milk	1.0	-
Transportation	1.8	1.8
Meat Ingestion	<u>1.3</u>	<u>-</u>
Total	10.6	21.8

Total Population Dose From Background

Radiation = 131,000 person-rem/yr

The direct dose component was calculated by the same method as utilized for the CRBRP (Reference 6) using a source term of 0.35 mrem/yr at the surface of the Reactor Auxiliary Building.\*

A comparison of the total population dose for the VHTR with the Fulton Plant shows the VHTR to be about a factor of 2 lower in spite of the addition of several significant components (e.g., inhalation, meat ingestion, drinking milk) apparently not included in the analysis of the Fulton Plant. Thus the 10.6 person-rem/yr population dose estimated for the VHTR would result in a very minor and acceptable radiation impact on persons living in the vicinity of the plant from normal operation of the plant.

The total population dose resulting from the VHTR can also be compared with the population dose due to background radiation exposure within the 30-mile radius area. Based on an average whole body exposure of an individual in the USA of 130 mrem/yr (Reference 9), the 1,010,000 persons in this area receive a total background population exposure of 131,000 person-REM. Thus, the slight increase from the VHTR is less than 0.01 percent of background.

#### 5.2.6 Land Use, Terrestrial Effects and Aesthetics

The use of 380 acres of land adjacent to the North River at the Middletown site would not be expected to result in adverse land use practices. The flood plain along the river has sufficient land area to accommodate the plant and its exclusion area. The use would not be expected to adversely alter land-use patterns in the area or result in significant loss in cultivated or forested acreage. The industrial use of the site is compatible with the area in that five industrial manufacturing plants are located within 15 miles of the site.

The site is accessible to local highways, a railroad, barge traffic, and all necessary services and utilities. Therefore, impact associated with the installation of access roads, transmission lines, pipelines and other service requirements would not be anticipated.

Since the plant site is located about five miles from the state highway and the population within five miles is only about 5,000, the plant would not be expected to be viewed as an aesthetic intrusion. In addition, the plant would have clean lines, no tall protruding stacks or coal or chemical storage areas. Therefore, the aesthetic impact would be not significant. While some noise from the cooling tower will be noticeable on-site, it will not be significant off-site.

It is not expected that the plant site will involve the destruction of any unique or particularly valuable habitat or ecological areas. None of the plant effluent streams would have an adverse effect on the terrestrial ecosystems.

\* This value is consistent with the dose limits at the site boundary to meet "as low as practicable" criteria as defined by 10CFR50, Appendix I (Reference 8).

### 5.2.7 Social and Economic Impacts

The construction and operation of a major facility can have a number of impacts on the social and economic environment of the local community. These impacts are evidenced in terms of taxes, jobs, housing, education, traffic and other local goods and services. In some cases, a major influx of workers and industrial activity can cause a basic change in the local social structure and local economic growth. The nature and magnitude of these impacts will be highly project specific depending on:

- the magnitude of the project requirements
- the specific location
- the time frame of project activities.

The selection of a site location near Middletown enables the construction and operation of the plant without the imposition of any serious social or economic impacts. While the city of Middletown has a large population (250,000), the site itself is located in an area of low population density. The labor force required for the construction of the plant would be anticipated to be similar to that required for a typical moderate size nuclear power station or about 3,000 workers at the peak and an average of 2,000 workers over the 4-year construction period. Because the city of Middletown is within 25 miles of the site, and the cumulative population within a 30-mile radius is over 1 million, it is anticipated that over 95 percent of the construction labor force can be supplied by the local indigenous population. The influx of construction workers for periods not usually in excess of a year would be expected to be less than 150 at any one time during the construction period. The existing community infrastructure would be able to accommodate this influx without the need for major capital expenditure and without significant adverse impact.

The permanent operating labor force of 40 for the water decomposition plant and 80 for the nuclear reactor will add 120 direct jobs to the permanent labor market. These positions should be readily filled by persons living in the vicinity of the plant so that potential impact that could result from an influx of personnel can be averted. The additional jobs in the area will increase the personal income in the area and reduce the local unemployment, even if only to a minor extent. The additional jobs and personal income will stimulate a secondary growth in local economic factors through an economic multiplier (Reference 10).

The projected capital cost of this plant is about \$1 billion. This investment will provide an economic stimulus to the design, engineering, hardware and fuels industries. In addition, a major part of this capital requirement will consist of local vendor supplies, building materials and services. Annual expenditures of about \$6 million for the operation and maintenance of the facility will add some economic benefit to the community in terms of personal income and support of small business activity. The estimated annual tax payments of this facility include about \$22 million in local property tax and about \$14 million in federal and state income taxes. The local property tax income is a significant benefit to the community.

Because of the low anticipation of an influx of workers and families to the area for the construction and operation of the plant, there are no major adverse social, cultural, or economic impacts that are anticipated. However, the local property tax will significantly enhance the local economy.

## 5.2.8 Summary Benefit-Cost Analysis

In this section, the benefits and costs (environmental, social, economic) that have been presented in other sections are summarized. These benefits and costs are evaluated to determine that a favorable balance exists for the proposed plant, with the benefits outweighing the costs. This evaluation includes the benefits and costs as applicable to both the local and national levels.

### 5.2.8.1 Benefits

#### Primary Benefits

The most significant benefit of the proposed facility lies in the value of the hydrogen generated at the plant. While the end use and location of use has not been specified, the hydrogen product provides an energy form that is both useful and versatile for a number of potential purposes. Potential uses of hydrogen include use as a feedstock in the production of synthetic natural gas, ammonia production for subsequent fertilizer applications, direct reduction of iron ore, and use as a direct fuel. Market projections have indicated that, by the year 2000, total demand for hydrogen in the United States be about 48 TCF<sup>(1)</sup> per year compared to a 1973 value of about 3.2 TCF (Reference 1).

#### Secondary Benefits

The construction and operation of the facility will lead to local benefits which consist of the creation of jobs (3,000 peak construction, and 120 operating force), local personal income and small business growth and taxes (\$20 million annual local property taxes).

### 5.2.8.2 Costs

In the section on environmental impact, the environmental and social impact of the construction and operation of the facility have been presented and discussed. No major adverse impacts are anticipated. The Middletown site is particularly suitable for a project of this nature and adverse impacts on air, water, land, ecosystems, resources, and local social

---

(1) TCF, or Trillion Cubic Feet, is defined as  $1 \times 10^{12}$  standard cubic feet. This is equivalent to  $2.68 \times 10^{10}$  standard cubic meters.

structure will not be anticipated. Even though the source of radiological releases for this facility is different from conventional nuclear plants, the magnitude and type of radiological impacts resulting from the operation of the VHTR are not unique or special. These can be accommodated by the design so that there will be no adverse environmental impacts.

#### 5.2.8.3 Balance of Benefits and Costs

The proposed hydrogen production facility will produce hydrogen as a useful product to the nation. In addition, it will generate jobs, local economic growth and tax income that will benefit the local community. The environmental, social and economic costs to the nation and the community are not significant as a result of the selection of the Middletown site and the adaptability of the design of plant systems to avert adverse impact. Therefore, in balance, the benefits outweigh the costs at both the national and local levels.

## 5.3 TECHNOLOGY OF THE SULFUR CYCLE WATER DECOMPOSITION SYSTEM

### 5.3.1 General

Water decomposition hydrogen production processes, as used here, are those processes in which water is used as a feedstock and, through thermochemical or combined thermochemical-electrolysis reactions, is dissociated to form hydrogen and oxygen. A characteristic of this class of hydrogen production processes is that the thermochemical reactions are cyclic in nature, i.e., the chemical intermediates are recovered and reused. Water decomposition processes employing only electrolysis and are excluded from this category of hydrogen production systems and considered as a separate class of processes.

In principle, water can be decomposed thermally in a single step. Extremely high temperatures are necessary to achieve significant degrees of dissociation and effective separation of the hydrogen/oxygen mixture is required. By employing a series of reactions involving cyclic intermediates, the maximum temperature necessary for decomposing water can be significantly reduced. Several such "water splitting" processes have been proposed and many are under active investigation in laboratories around the world. Inherent in all of these systems is the desire to maximize thermal efficiency, minimize overall (including power generation) capital investment, and utilize chemical reactions which can be demonstrated to occur.

All water splitting processes, due to their cyclic nature, are Carnot-limited. As a result, the overall process thermal efficiency depends upon both the maximum temperature one can obtain from the thermal source driving the process and the particular series of chemical reactions employed in the water decomposition sequence. The maximum thermodynamic process thermal efficiency is represented by the equation (Reference 4).

$$\eta_M = \min \left\{ \frac{\Delta H^\circ}{\Delta G^\circ} \cdot \frac{T_H - T_C}{T_H} \right\}, \text{ where}$$

$\eta_M$  = Maximum thermal efficiency

$\Delta H^\circ$  = Heat of formation of water at 298K

$\Delta G^\circ$  = Free energy of water at 298K

$T_H$  = Heat source temperature

$T_C$  = Heat sink temperature

REPRODUCIBILITY OF THE  
ORIGINAL PAGE IS POOR

Table 5.3.1 shows the maximum thermal efficiency as a function of heat source temperature. As indicated, with heat sources above 1089K (1500°F) available, water splitting process efficiencies theoretically equivalent to those for fossil-based processes are possible.

TABLE 5.3.1  
MAXIMUM THERMAL EFFICIENCY OF WATER DECOMPOSITION PROCESSES

<u>Heat Source Temperature</u>		<u>Maximum Thermal Efficiency, %</u>
<u>K</u>	<u>°F</u>	
800	980	75.3
900	1160	80.3
1000	1340	84.4
1100	1520	87.7
1200	1700	90.4
1300	1880	92.7
1400	2060	94.7

Water splitting processes assume particular importance when methods are sought for generating hydrogen from indirect sources of heat, particularly that available from either high temperature gas-cooled nuclear reactors or from solar collectors. Hydrogen is more easily stored and transported than thermal energy. Significant markets for hydrogen and oxygen will be created as plants for converting coal into synthetic oil and gas go onstream. If this hydrogen can be obtained from other than fossil-based processes, our ultimate reserves of fossil fuels can be prolonged.

Hydrogen obtained from water splitting processes can similarly be expected to be important in nuclear process heat applications, especially those involved with substituting nuclear heat for coal in coal conversion systems. The substitution of nuclear for fossil energy in a fossil-based hydrogen production system is limited by the chemical characteristics of the process. A certain portion of the hydrocarbon feedstock is consumed in chemical reactions; the balance in meeting the process heat requirements. Only the latter may be substituted. Water splitting processes enable complete substitution and enable a single hydrogen production process to be employed, regardless of energy source.

### 5.3.2 Water Splitting Processes as a Class of Hydrogen Generation Methods

A variety of methods exist for producing hydrogen. As hydrogen is not a primary energy form, its synthesis, in all instances, requires the addition of more primary energy than

is subsequently recovered during hydrogen combustion. Depending upon the form of the primary (or secondary energy), the method of hydrogen production may vary. Steam-hydrocarbon reforming designates processes which employ a gaseous feedstock such as methane, ethane, naphtha, or similar light hydrocarbons. Partial oxidation processes are those which use a liquid feedstock such as heavy or residual oil, and gasification refers to processes operating with a solid feedstock such as coal, coke, char, and perhaps municipal or process waste. In general, chemical reactors designed for one primary feedstock are not readily converted to another. For example, a steam-methane reformer cannot be used to conduct coal gasification reactions, nor can a coal gasifier be used effectively as a methane reformer. Similarly, within each group, the chemical reactor and its operation will depend upon the physical and chemical properties of the feedstock. Not all coal gasifiers, for example, can accommodate caking or agglomerating coals, and all gasifiers require some degree of coal preparation and sizing prior to gasification. For all steam-hydrocarbon processes, steam and fuel requirements vary with feedstock, as does the nature and the duty of downstream processing. Electrolysis characterizes those processes employing electrical energy, as DC power, to electrolytically decompose water into hydrogen and oxygen. Water splitting processes similarly decompose water, but employ a series of chemical reactions involving cyclic chemical intermediates to decompose water at temperatures well below its thermal decomposition temperature.

While electrolysis and water splitting are clearly water decomposition processes - each using a form of energy to produce hydrogen and oxygen from water - it is important to note that the conventional steam - hydrocarbon processes for hydrogen production are in reality water decomposition systems as well.

Consider, as an example, the gasification of carbon with steam to produce a synthesis gas for hydrogen production. The gasification reaction is



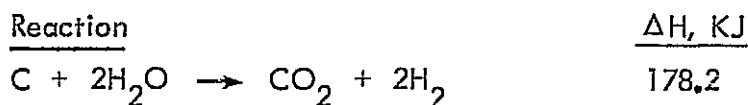
This is followed by the water gas-shift reaction



so that the total process is represented as



Overall, Reaction 3 is endothermic by 178.2 KJ, thus for an ideal process, the energy balance shown below applies



Thermal Inputs

Carbon Heating Value	393.5
Endothermic Reaction Heat	178.2
Total	571.7

Comparing this with the thermal requirements of an ideal water decomposition process illustrates the similarities and differences in the two methods of hydrogen production.

Coal Gasification

<u>Reaction</u>	<u><math>\Delta H</math>, KJ</u>
$C + 2H_2O \rightarrow CO_2 + 2H_2$	178.2

Thermal Inputs

Coal Heating Value	393.5
Endothermic Reaction Heat	178.2
Total	571.7

Water Decomposition

<u>Reaction</u>	<u><math>\Delta H</math>, KJ</u>
$2H_2O \rightarrow 2H_2 + O_2$	571.7

Thermal Inputs

Water Heating Value	0
Endothermic Reaction Heat	571.7
Total	571.7

A similar situation exists with regard to steam methane reforming. In this case, the energy balances shown below apply.

Steam Methane Reforming

<u>Reaction</u>	<u><math>\Delta H</math>, KJ</u>
$0.5CH_4 + H_2O \rightarrow 0.5CO_2 + 2H_2$	126.5

Thermal Inputs

0.5 mole $CH_4$	445.2
Process Heat	126.5
Total	571.7

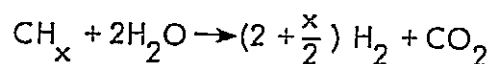
Water Decomposition

<u>Reaction</u>	<u><math>\Delta H</math>, KJ</u>
$2H_2O \rightarrow 2H_2 + O_2$	571.7

Thermal Inputs

$2H_2O$	0
Process Heat	571.7
Total	571.7

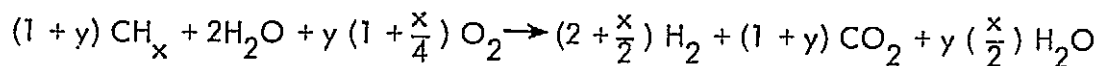
The mass and energy balances illustrated earlier show that coal gasification and steam methane reforming are specific methods by which hydrocarbons may be used to decompose water in order to obtain hydrogen. The results are general, since in all cases the overall process reaction is given by



The heat of reaction is  $\Delta H_{\text{rxn}} = \Delta H_{\text{CO}_2} - 2 \Delta H_{\text{H}_2\text{O}} - \Delta H_{\text{CH}_x}$  where  $\Delta H_i$  is the heat of formation of compound  $i$  from the elements at the reference temperature. The process thermal inputs are:

Heating Value of $\text{CH}_x$	$\Delta H_{\text{CH}_x} - \Delta H_{\text{CO}_2} - (\frac{x}{2}) \Delta H_{\text{H}_2\text{O}}$
Reaction Enthalpy	$\Delta H_{\text{CO}_2} - 2 \Delta H_{\text{H}_2\text{O}} - \Delta H_{\text{CH}_x}$
Total	$-(2 + \frac{x}{2}) \Delta H_{\text{H}_2\text{O}}$

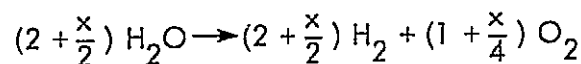
As the total balance shows, the process energy inputs as reactants and fuel will always be identical to those which would have been required had water been decomposed directly. When hydrocarbon fuels are burned to meet the process energy needs, the overall mass balance becomes



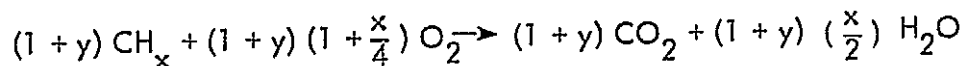
where

$$y \cong \frac{\Delta H_{\text{CO}_2} - 2 \Delta H_{\text{H}_2\text{O}} - \Delta H_{\text{CH}_x}}{\Delta H_{\text{CH}_x} - \Delta H_{\text{CO}_2} - (\frac{x}{2}) \Delta H_{\text{H}_2\text{O}}}$$

A water decomposition process operating on the same fuel at the same thermal efficiency would accomplish the reaction



by combusting the fuel in air to drive the process. From combustion one has



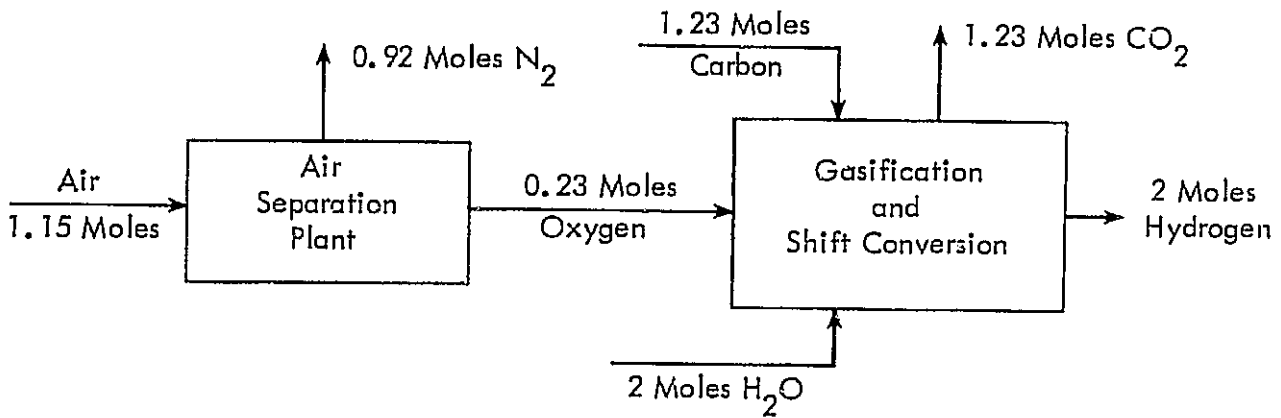
As the net mass balances for the process indicate, overall fuel and water consumption remain unchanged. The water decomposition process, however, has the advantage of being able to provide oxygen as well as hydrogen.

Two major differences exist between water decomposition and steam-hydrocarbon processes for hydrogen generation. The first relates to the amount of process energy which can be supplied by non-fossil means. For the steam-hydrocarbon processes, less than 25 percent of the theoretical energy requirements can be substituted with non-fossil energy sources. The balance of the hydrocarbon is consumed as a chemical reactant, not as a process fuel. In practice, due to process inefficiencies, much larger fractions of the hydrocarbon feedstock are devoted to fuel usage and thus larger portions are potentially available for substitution.

Reductions in the quantities of hydrocarbons required to produce hydrogen can be achieved in any of three ways. Non-fossil energy can be substituted for that portion of the fossil feedstock which is consumed as fuel, efforts can be taken to improve the efficiency of the hydrogen generation process; or efficient processes independent of hydrocarbon feedstocks can be developed. While fuel substitution within existing processes and improvements in overall thermal efficiency are worthwhile, it is important to note that all three methods of reduction can be achieved with the water-splitting processes.

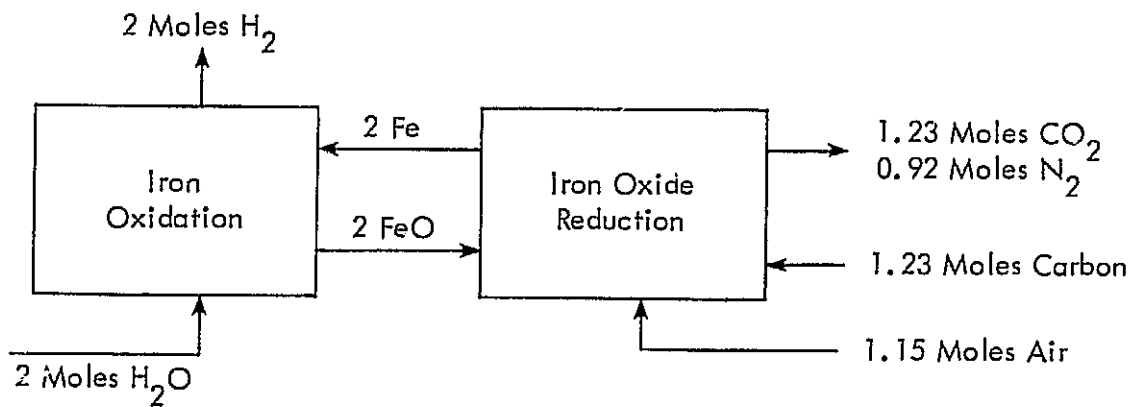
The second major difference between water splitting and steam-hydrocarbon is the by-product formed during hydrogen generation. Both processes operate with the same total thermal inputs yet one produces a useful by-product, oxygen, while the other does not. The primary reason for this difference rests with the partitioning of reactants and fuels within the process. Considering the case of coal gasification, it is theoretically possible (at one hundred percent thermal efficiency) to obtain 2 moles of hydrogen by reacting 1.23 moles of carbon with 2 moles of water and at least 1.15 moles of air. Depending upon the equipment configuration, either the process will require an oxygen plant, or it will avoid the need for an oxygen plant, or it will act as though it is simultaneously an oxygen plant.

It is instructive to consider three processes by which hydrogen may theoretically be obtained from carbon and water. The first involves the use of oxygen-blown gasification followed by shift conversion. Assuming an ideal process, the mass balances shown below will apply.

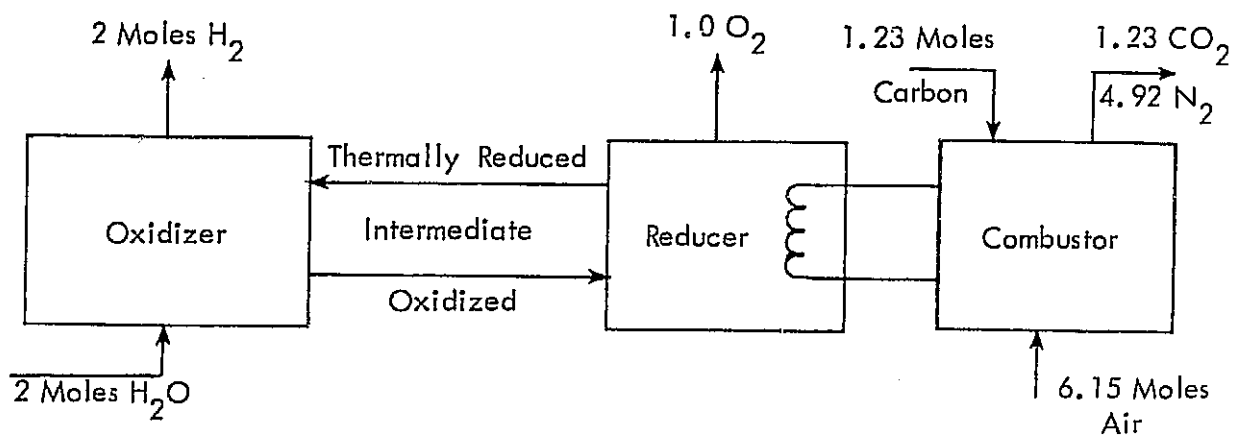


The fact that carbon is being oxidized in the same vessel that is being used to conduct the hydrogen generation reaction requires an oxygen plant to prevent dilution of the product gas with nitrogen. If the hydrogen generating reaction can be separated from the major endothermic process reaction, then air rather than oxygen can be used in fueling the process.

This is the approach used when hydrogen is generated using a steam-iron process. In this instance, again assuming an ideal process, the mass balances shown below apply.



In its simplest form, a thermochemical process for decomposing water is similar to an indirectly heated steam-iron process. For an ideal process, the mass balances shown below apply.



Compared with the steam iron process, 1.15 moles of air are required to combust 0.23 moles of carbon for process heat. The remaining five moles are effectively separated into four moles of nitrogen which are vented and a mole of oxygen which is recovered.

Notice also, by adding carbon to the reduction step of the thermochemical process for decomposing water, that it theoretically becomes equivalent to the steam-iron process. Similarly, indirect heating of iron oxide to liberate oxygen would make this equivalent to a thermochemical process. As the energy balances show, 109.6 MJ (103,827 BTU) must be expended to decompose a mole of water vapor into hydrogen and oxygen. Mass and energy balances for a carbon-fueled process indicate that at least 1.23 moles of carbon and 1.15 moles of air are necessary. Processes can be devised to meet these mass and energy requirements in different ways.

The use of a single reaction vessel requires an oxygen plant to prevent dilution of the product gas with nitrogen and fails to recover the oxygen for subsequent utilization. The use of two primary reaction vessels is sufficient to avoid the use of oxygen and enables the process to employ air instead. Firing one process vessel directly with carbon and air potentially leads to higher thermal efficiencies, but also fails to recover the oxygen byproduct. Indirectly firing the second vessel, while perhaps lowering the thermal efficiency, enables both decomposition products to be recovered for utilization.

Additional advantages are obtained by using the water decomposition process. The most important of these is the fact that hydrogen can be generated from any convenient fuel, e.g., coal, oil, gas, nuclear, or solar. For each of the hydrocarbon processes, an unique fossil fuel/feedstock requirement is evident. The potential of substitution of one energy form for another is limited.

In the case of steam-methane reforming, methane equivalent to 200 MJ/kg-mole (86,080 Btu/lb-mole) hydrogen must be provided as a chemical reactant. In principle, only an additional .085 moles  $\text{CH}_4$ /mole  $\text{H}_2$  is required for the process heat requirement. Even allowing the possibility of substitution, a sizeable methane requirement remains. For the

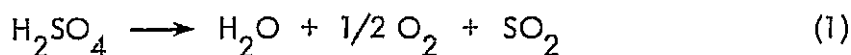
water decomposition process, however, the most economic energy source - whatever it may be - can be used by modifying that equipment through which the energy is transmitted to the process. This energy can be provided as either methane, oil, coal, nuclear, solar, or any combination of sources to result in the most economical hydrogen production. This feature will be of ever increasing importance in the decades to come, as the cost and availability of various fuels and feedstocks vary with economic conditions and energy reserves.

### 5.3.3 The Westinghouse Sulfur Cycle Water Decomposition Process

The Westinghouse hydrogen production process is a two-step thermochemical cycle for decomposing water into hydrogen and oxygen. Oxides of sulfur serve as recycling intermediates within the process. The use of sulfur compounds results in several process advantages:

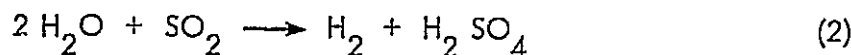
- Sulfur is abundant, inexpensive, and substantially non-toxic.
- An assured supply of make-up sulfur is available from coal conversion and stack gas scrubbing processes.
- Sulfur is an item of commerce and processes, equipment, catalysts, literature, and distribution systems for it and its compounds abound.
- Sulfur assumes a variety of valence states, thereby facilitating its use in oxidation-reduction reactions.
- The properties of sulfur and its compounds are well documented, thereby reducing the amount of basic information needed in a process development effort.
- Environmental regulations for the use of sulfur exist today, reducing uncertainties in the design of process equipment.

The process, in its most general form, consists only of two chemical reactions - one for producing oxygen and the other for producing hydrogen. The production of oxygen occurs via the thermal reduction of sulfur trioxide obtained from sulfuric acid.

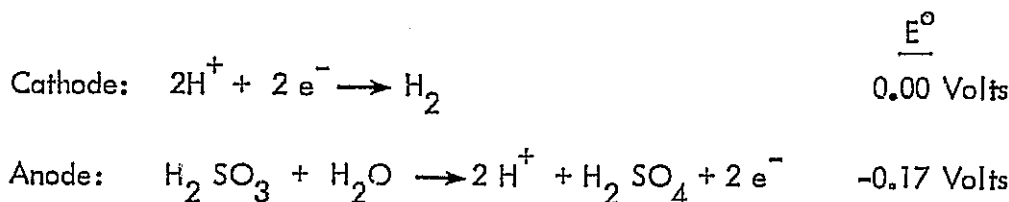


The equilibrium for Reaction 1 lies to the right at temperatures above 1000K. Catalysts are available for accelerating the rate of sulfur trioxide reduction to sulfur dioxide and oxygen. The results of Westinghouse's evaluation of two of these catalysts is reported elsewhere in this document.

The process is completed by using the sulfur dioxide from the thermal reduction step to depolarize the anode of a water electrolyzer. The overall reaction occurring electrochemically is



This is comprised of the individual reactions



As is apparent by summing Reactions 1 and 2, the overall process decomposes water into hydrogen and oxygen and involves only sulfur oxides as recycling intermediates. Although electrical power is required in the electrolyzer, much smaller quantities than those necessary in conventional electrolysis are needed. The theoretical voltage to decompose water is 1.23 V, with many commercial electrolyzers requiring over 2.0 V. The power requirements for Reaction 2 (0.17 volts at unit activity for reactants and products) are thus seen to be less than 15 percent of those required in conventional electrolysis. This changes dramatically the theoretical heat and work required to decompose water and leads to high thermal efficiencies.

The process is shown schematically in Figure 5.3.1. Hydrogen is generated electrolytically in an electrolysis cell which anodically oxidizes sulfurous acid to sulfuric acid while simultaneously generating hydrogen at the cathode. Sulfuric acid formed in the electrolyzer is sent to a surge tank from where it is fed to two vaporizers in series. The first of these is a recuperative heat exchanger heated by the effluent from the high temperature sulfur trioxide reduction reactor. The second is heated by helium from the VHTR. The sulfur trioxide - steam mixture from the second vaporizer flows to the helium heated reduction reactor where sulfur dioxide and oxygen are formed. These gases are subsequently cooled against the incoming acid and unreacted sulfur trioxide is recovered as sulfuric acid in a knock-out system. Wet sulfur dioxide and oxygen flow to the separation system. Steam is first condensed, following which the  $\text{SO}_2/\text{O}_2$  mixture is compressed and sulfur dioxide recovery effected.

Bulk sulfur dioxide removal is accomplished by condensation against cooling water. Final removal is achieved by condensation against low-temperature oxygen. This refrigeration and some auxiliary power production is generated by expansion of the oxygen stream prior to its venting.

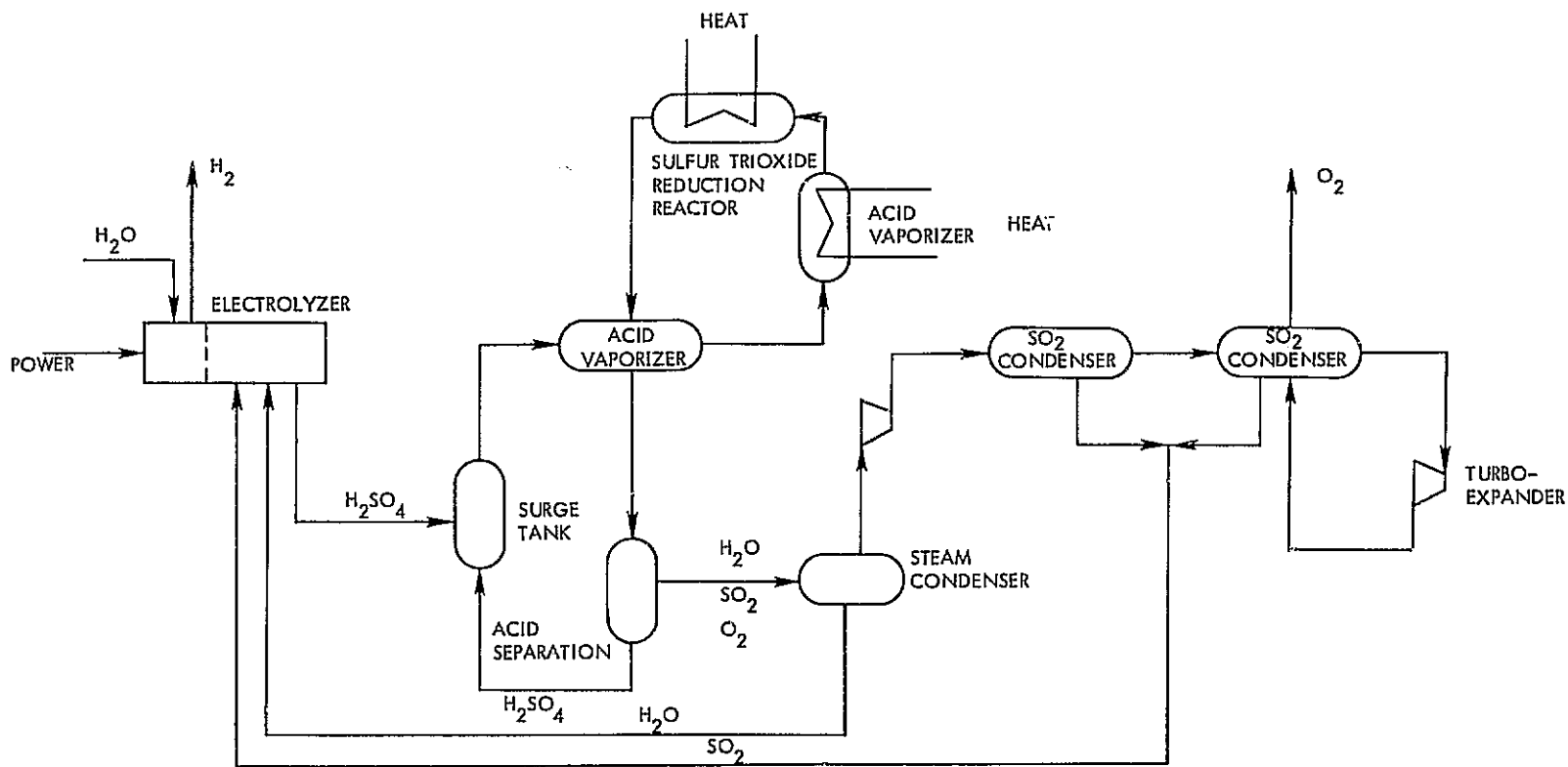


Figure 5.3.1 Sulfur Cycle Schematic Flowsheet

Two important trade-offs exist in specifying process conditions for the flowsheet shown. The first relates to the concentration of the sulfuric acid leaving the electrolyzer. Operation at very high acid concentrations raises the power requirements in the electrolyzer while simultaneously reducing the mass rates and thermal energy demand in the acid vaporization, decomposition, and recovery loop. Similarly, operation at very low acid concentrations lowers the electrolyzer power requirements, but leads to high mass rates and thermal demands in the acid decomposition loop. An optimal acid concentration exists.

Pressure is important due to the pressurized  $\text{SO}_2/\text{O}_2$  recovery system employed in the process as well as the pressure dependence of the sulfur trioxide reduction reaction (the equilibrium conversion at a given temperature declines with increasing system pressure). Operation at low pressures leads to high conversions, low recycle rates, and large compression requirements. Operation at higher pressures reduces the compressor duties, but at the expense of the sulfuric acid recycle rate. Thus, an optimal pressure similarly exists.

Both the optimum acid concentration and the optimum pressure vary with the heat source temperature. Similarly, overall thermal efficiency rises with increasing heat source temperature. Raising the heat source temperature increases power cycle efficiencies and shifts the optimal acid concentration to more concentrated solutions. This in turn reduces the thermal requirements in the acid decomposition system. Similarly, higher heat source temperatures enable higher system pressures to be employed without sacrificing the conversion per pass achieved in the sulfur trioxide reduction reactor. This reduces compression requirements and improves the process efficiency.

For the purpose of the evaluation, the hydrogen generation system was considered to have the process flowsheet presented schematically in Figure 5.3.1 and in more detail in subsequent sections. The principal operating and performance characteristics of the process are given in Table 5.3.2.

The process, as currently defined, is arranged for its primary energy inputs to be made as electricity in the electrolyzer and heat, from the intermediate heat transport loop of the nuclear heat source, to the acid vaporizer and the  $\text{SO}_3$  reduction reactor. Other heat sources, including combustion, solar, or geothermal, can provide the heat energy for the  $\text{SO}_3$  reduction reactor and the generation of electric power.

This alternate fueling capability provides the flexibility to consider operation of the hydrogen production facility with any economic source of heat and electric power. Alternate energy sources for the water decomposition process are discussed in more detail in Section 5.3.5.

#### 5.3.4 Process Performance Sensitivity Analysis

Sensitivity studies were conducted using the University of Kentucky HYDRGN computer program suitably modified to simulate the major features of the Westinghouse Hydrogen Generation Process. An optimum set of process conditions was determined by maximizing the thermal efficiency over a range of process variables. A schematic of the process flowsheet

TABLE 5.3.2

PRINCIPAL OPERATING AND PERFORMANCE CHARACTERISTICS OF THE  
WESTINGHOUSE SULFUR CYCLE WATER DECOMPOSITION SYSTEM

General

Hydrogen Production Rate	$10.12 \times 10^6$ standard m <sup>3</sup> /day	( $380 \times 10^6$ SCFD)
Hydrogen Purity	99.9 volume percent	
Oxygen Production Rate	306,100 kg/hr	(675,000 lb/hr)
Nuclear Heat Source Rating	3345 MWt	
Net Process Thermal Efficiency	45.2 percent	

Electrolysis

Acid Concentration	75 wt percent	
Pressure	2586 kPa	(375 psia)
Temperature	361 K	(190°F)
Electrolyzer Power Req't	458 MWe	
Cell Voltage, Nominal	0.45 volts <sub>s<sub>2</sub></sub>	
Cell Current Density, Nominal	2000 A/m <sup>2</sup>	(186 A/ft <sup>2</sup> )

Sulfur Trioxide Reduction System

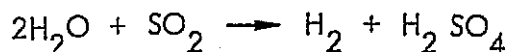
Peak Temperature	1144 K	(1600°F)
Operating Pressure	310 kPa	(45 psia)

Sulfur Dioxide - Oxygen Separator System

SO <sub>2</sub> Liquefaction Pressure	5171 kPa	(750 psia)
Oxygen Discharge Pressure	103 kPa	(15 psia)

used in the sensitivity study is shown in Figure 5.3.2, with the major process steps identified in Table 5.3.3.

Hydrogen is provided electrolytically according to the following reaction:



The sulfuric acid formed is sent to a surge tank, ST, from which it is fed to two vaporizers, one recuperatively heated - AV-1, and the other externally heated - AV-2.

The resultant sulfur trioxide - steam mixture is sent to the thermal reduction reactor, where sulfur dioxide and oxygen are formed. This gas mixture ( $\text{SO}_3$ ,  $\text{SO}_2$ ,  $\text{O}_2$ ,  $\text{H}_2\text{O}$ ) is subsequently cooled and the unreacted sulfur trioxide is condensed as sulfuric acid. The sulfuric acid is recovered and recycled to the surge tank. The remaining wet sulfur dioxide and oxygen flow to the separation system. Steam is first condensed and recycled. The sulfur dioxide - oxygen mixture is compressed to 5171 kPa (750 psia) and separated with the recovery of sulfur dioxide for recycle to the electrolyzer. Oxygen is available as a by-product.

For each of the above steps there is an associated enthalpy change - dependent upon such process conditions as pressure, temperature, and acid concentration - which influences the overall thermal requirements of the process. The determination of those process conditions which lead to the lowest total heat input requires an analysis of each step of the process.

Several important tradeoffs exist in specifying process conditions. One relates to the concentration of the sulfuric acid leaving the electrolyzer. The electrolyzer power requirement increases with increasing acid concentration, as shown in Figure 5.3.3. As Figure 5.3.4 indicates, the energy required to heat, vaporize, and decompose the electrolyzer acid (Steps 4, 5, 6 and 7 in Figure 5.3.2) diminishes with increasing acid concentration. Figure 5.3.5 shows that mass rates also decline with an increase in acid concentration. Analogously, operation at very low acid concentrations lowers the electrolyzer power requirements, but leads to high mass rates and thermal demands in the acid decomposition loop. An optimal acid concentration exists.

This optimum acid concentration can be expected to be a function of the temperature of heat source driving the process. The electrolyzer power, for example, can be generated more efficiently with thermal energy at higher temperatures. Similarly, higher temperatures enable higher conversions per pass to be obtained in the  $\text{SO}_3$  decomposition reactor, thereby reducing the recycle rates in this part of the system.

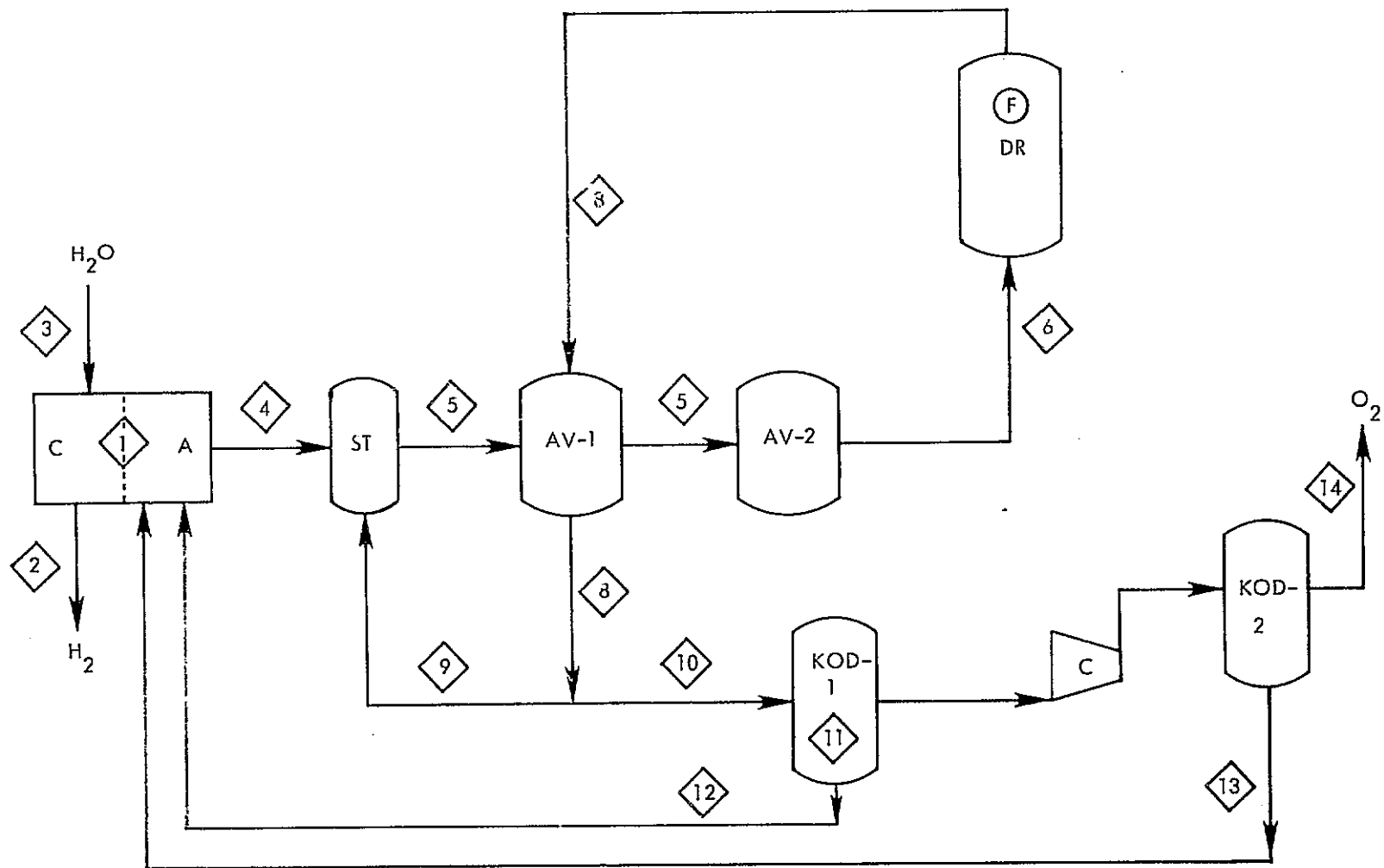


Figure 5.3.2 Flowsheet for H<sub>2</sub> Generation Process  
(Based on Sensitivity Study Simulation)

TABLE 5.3.3  
PROCESS STEPS

- 1 Electrolysis:  

$$2\text{H}_2\text{O} + \text{SO}_2 \longrightarrow \text{H}_2 + \text{H}_2\text{SO}_4$$
- 2 Cooling of  $\text{H}_2$  from electrolyzer temperature (360K) to 298 K, collection of  $\text{H}_2$
- 3 Heating make-up water to 360K for electrolyzer
- 4 Heating dilute sulfuric acid (from electrolyzer) from 360K to its boiling point
- 5 Vaporization of the dilute  $\text{H}_2\text{SO}_4$
- 6 Heating  $\text{H}_2\text{SO}_4(\text{g})$  and  $\text{H}_2\text{O}(\text{g})$  to the temperature of decomposition reactor
- 7 Decomposing  $\text{H}_2\text{SO}_4$  into  $\text{H}_2\text{O}$  and  $\text{SO}_3$ , then decomposing  $\text{SO}_3$  to  $\text{SO}_2$  and  $1/2 \text{O}_2$
- 8 Cooling gas mixture from DR to the temperature at which unreacted  $\text{SO}_3$  condenses as dilute  $\text{H}_2\text{SO}_4$
- 9 Condensation of unreacted  $\text{SO}_3$  as dilute acid; recycling this acid to the surge tank
- 10 Cooling  $\text{H}_2\text{O}$ ,  $\text{SO}_2$ ,  $\text{O}_2$  gas mixture to the temperature at which  $\text{H}_2\text{O}$  condenses
- 11 Condensation of  $\text{H}_2\text{O}$ ; Separation of  $\text{SO}_2 - \text{O}_2$  mixture
- 12 Cooling water to 360 K for recycle to electrolyzer
- 13 Cooling  $\text{SO}_2$  to 360 K for recycle to electrolyzer
- 14 Cooling  $\text{O}_2$  to 298 K for venting

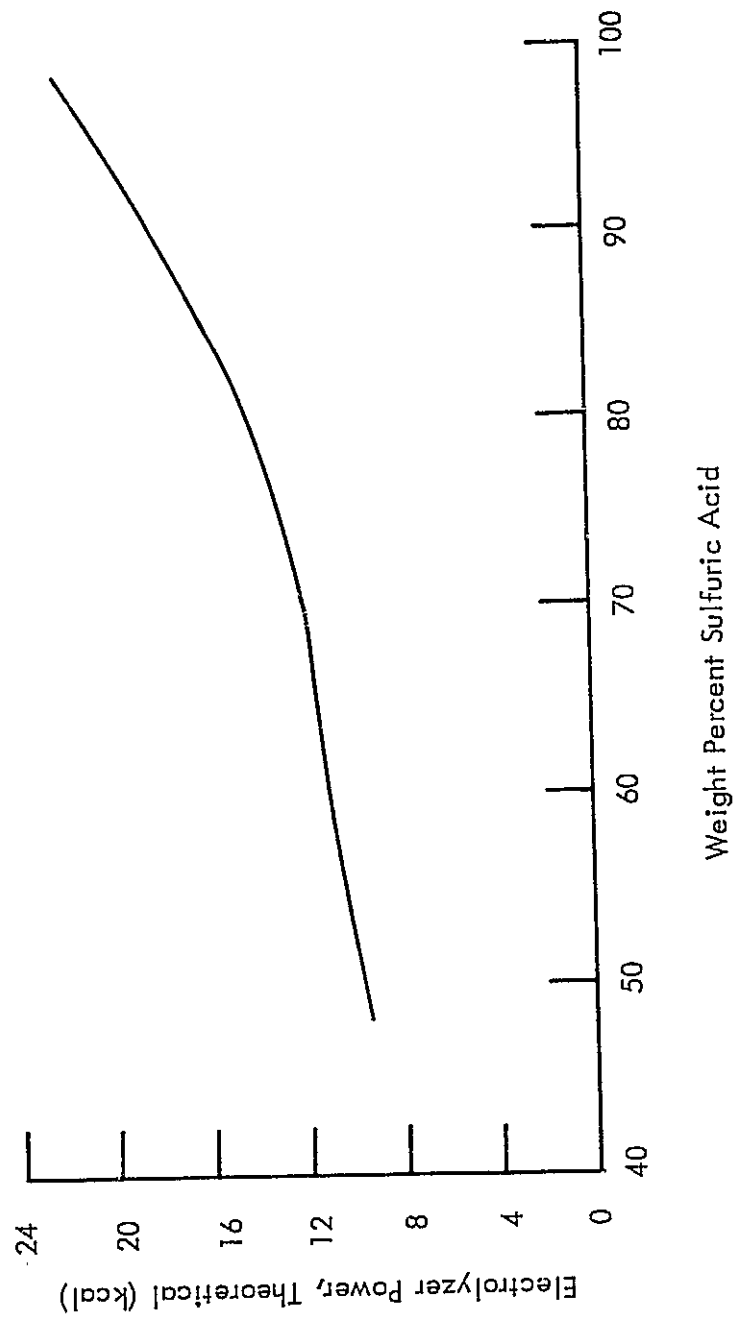


Figure 5.3.3 Variation in Theoretical Electrolyzer Power with Acid Concentration

REPRODUCIBILITY OF THE ORIGINAL PAGE IS POOR

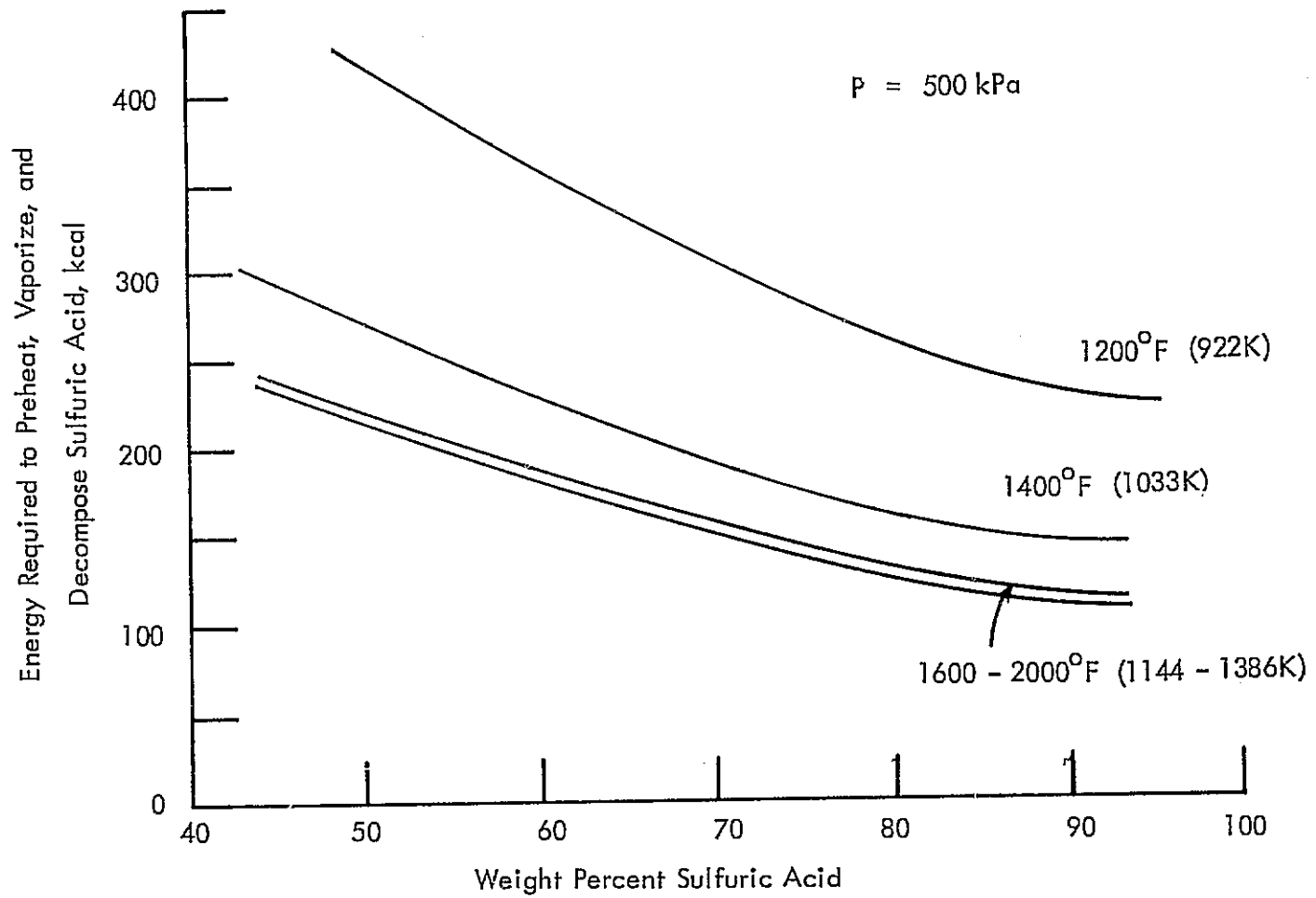


Figure 5.3.4 Variation in Acid Decomposition Energy with Acid Concentration

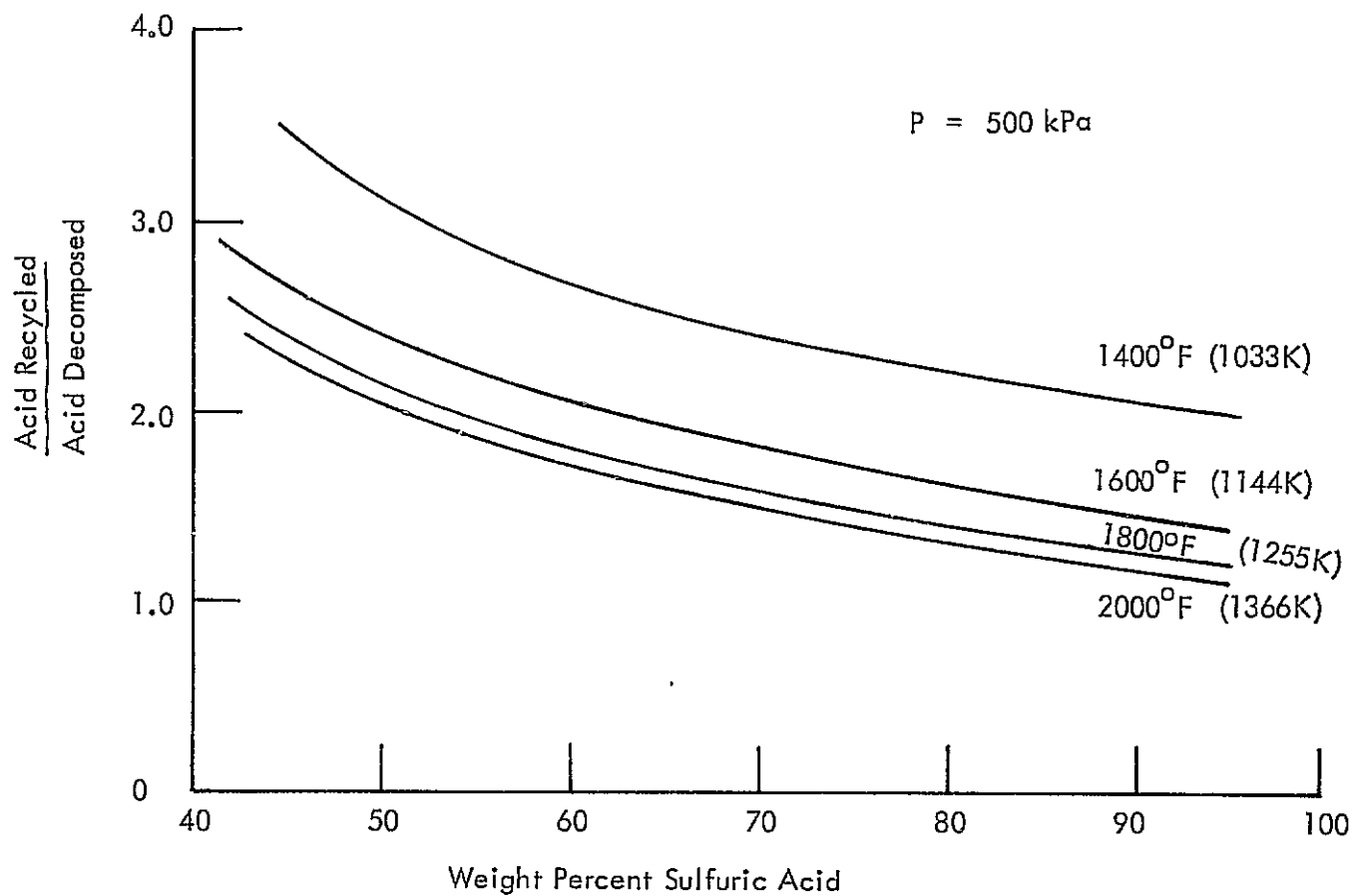


Figure 5.3.5 Variation of Recycle Rate with Acid Concentration

Pressure is important due to the pressurized sulfur dioxide - oxygen recovery system employed in the process as well as the pressure dependence of the sulfur trioxide reduction reactors (the equilibrium conversion at a given temperature declines with increasing system pressure). As Figure 5.3.6 shows, recycle rates increase with increasing pressure. Similarly, operation at low pressures leads to high conversions, low recycle rates, and large compression requirements. Thus, an optimal pressure also exists.

The optimum pressure is also a function of temperature. For a given conversion per pass, an increase in temperature permits the use of a higher decomposition system pressure. Referring to Figure 5.3.7, where details of the compression system are shown, this reduces the number of compression stages required in the  $\text{SO}_2 - \text{O}_2$  separation system. As Figure 5.3.7 shows, operation of the decomposition system at pressures above 1010 kPa (10 atm) can achieve significant reductions in compression energy.

The preceding section indicates trends in thermal requirements produced by varying the process conditions over selected ranges. Knowledge of the total heat requirement,  $Q_T$ , is necessary to determine process efficiency. The smaller  $Q_T$ , the higher the efficiency.  $Q_T$  is a function of process conditions and can be reduced by using recuperative heat exchange, whereby heat released in exothermic steps is used to supply those steps requiring heat. The major recuperative heat exchange occurs in AV-1 (see Figure 5.3.2) where the energy in streams 8 and 9 is used to preheat the vaporize acid entering the  $\text{SO}_3$  decomposition system.

Estimates of the process thermal efficiency were made for a range of process conditions. These were generated by choosing five values for each of three critical process variables, pressure, temperature, and acid concentration, as shown in Table 5.3.4. Based on these variables, 125 processes were generated, each one uniquely determined by its combination of values for the process conditions.

TABLE 5.3.4  
VARIATIONS IN PROCESS CONDITIONS

<u>Pressure (kPa)</u>	<u>DR Temperature (K)</u>	<u>Acid Concentration (wt percent)</u>
101	922	50
507	1033	60
1013	1144	70
2026	1255	80
5065	1366	90

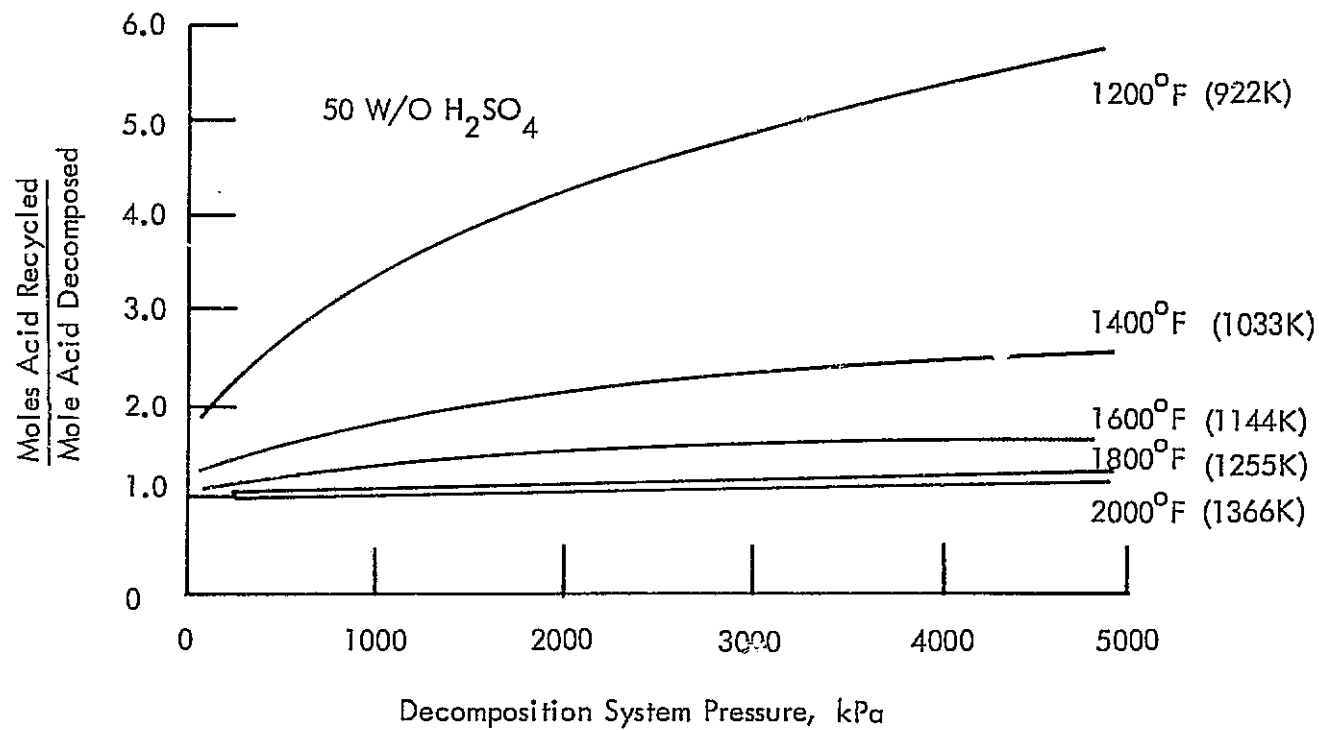


Figure 5.3.6 Variation of Recycle Rate with Pressure

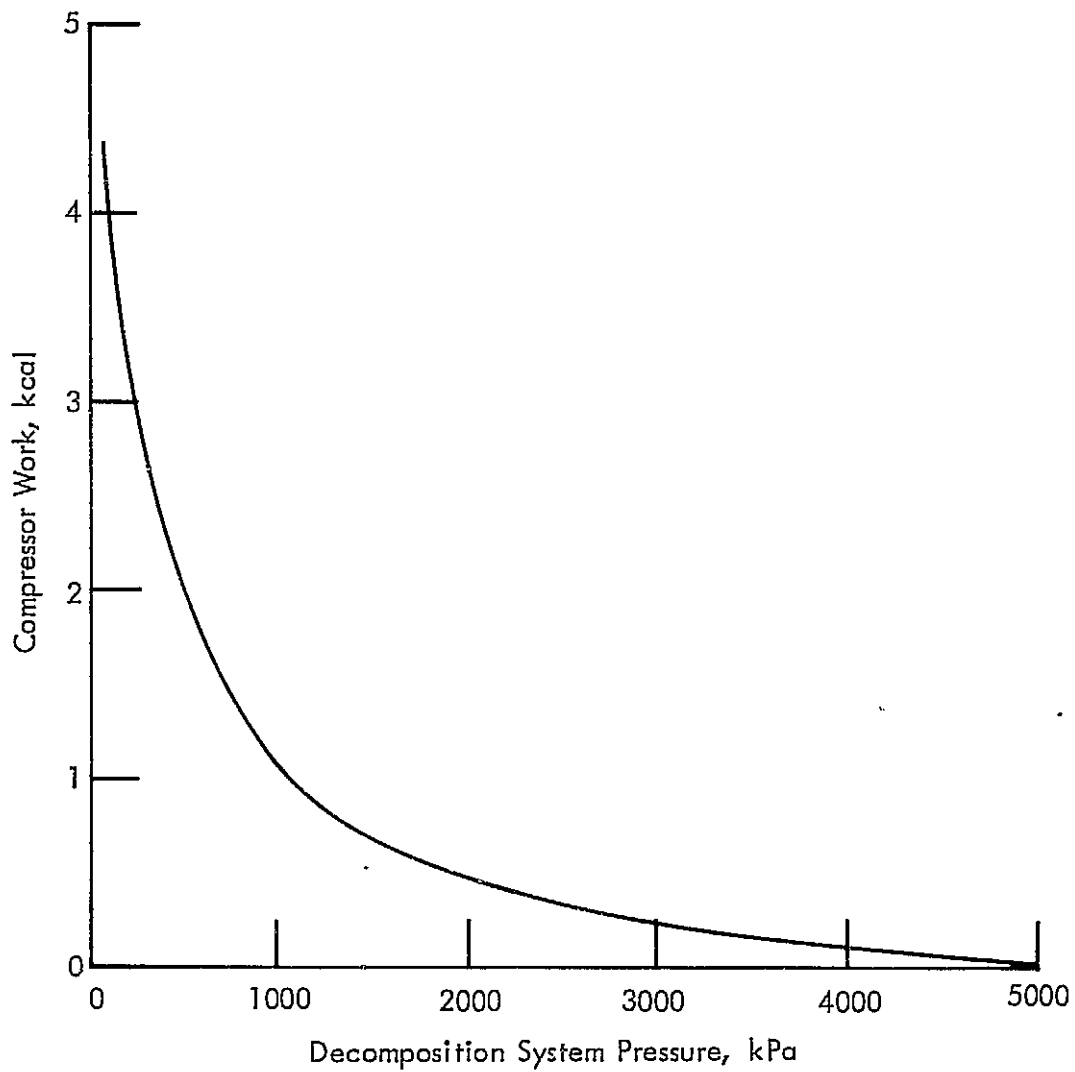


Figure 5.3.7 Variation of  $\text{SO}_2/\text{O}_2$  Separation System Compressor Requirements with Decomposition System Pressure

The total energy required by each of these processes was considered to be composed of three parts. The first of these, designated  $Q_1$ , represents the heat required to generate the electrolyzer power. Both an electrolyzer efficiency and a power generation efficiency were assumed in calculating  $Q_1$ . Specifically, the electrolyzer efficiency was assumed to be 50 percent. The power generation efficiencies were typical of those achievable using a combined gas and steam turbine cycle operating at a temperature 139K (250°F) above that of the process temperature. The second heat input,  $Q_2$ , represents the net heat required to heat, vaporize, and decompose the electrolyzer acid (4 + 5 + 6 + 7 - 8 - 9). The third input is  $Q_3$ , the heat requirement for the  $SO_2 - O_2$  separation process, which was calculated as described above in Figure 5.3.7.

Figures 5.3.8 and 5.3.9 are plots of efficiency as a function of pressure and acid concentration, respectively. The optimum combination of conditions, as determined within the limits of this study, is the following: pressure between 1013 and 2026 kPa (10 and 20 atm) and acid concentration between 70 and 85 w/o.

Not unexpectedly, the analysis shows (Figure 5.3.10) overall thermal efficiency to increase monotonically with temperature. Similarly (Figure 5.3.11), the thermal energy exchanged in the recuperative vaporizer (a measure of the recycle rate in the acid decomposition loop) decreases hyperbolically with temperature. At low temperatures, 922 to 1033K (1200 - 1400°F), system pressure strongly influences the size of the recycle system. At high temperatures, 1255 to 1266K (1800 - 2000°F), pressure is important, with the lower range, 103 to 517 kPa (15 to 75 psia), being preferred.

It should be noted that the sensitivity analysis often predicts lower thermal efficiencies than those obtained by analysis of the engineering flowsheets. This may be understood by recognizing that the sensitivity study uses a simplified flowsheet that does not utilize "waste" heat in the way that the engineering flowsheet does, e.g., producing power via the pressure letdown of the oxygen stream through a power turbo-expander.

### 5.3.5 Energy Sources for the Westinghouse Sulfur Cycle Water Decomposition System

The Sulfur Cycle water decomposition process, in its reference configuration, has its primary energy inputs made as electricity in the electrolyzer and heat, from the intermediate heat transport loop of a nuclear heat source, to the  $SO_3$  reduction reactor and the acid vaporizer. Other heat sources, including fossil fuel combustion, solar, or geothermal, can provide the thermal energy for the process steps and the generation of electric power. The thermal energy would be introduced into the process in a manner dependent upon the characteristic of the heat source. The electric energy needed for the electrolyzers would be produced in the manner most appropriate for each of the alternate fuels.

For the process flowsheet used in the conceptual design, heat from alternate energy sources could be introduced to the process in the same manner as for the nuclear powered system. The process heat exchanger ( $SO_3$  reduction reactor) and acid vaporizer design could,

REPRODUCIBILITY OF THE  
ORIGINAL PAGE IS POOR

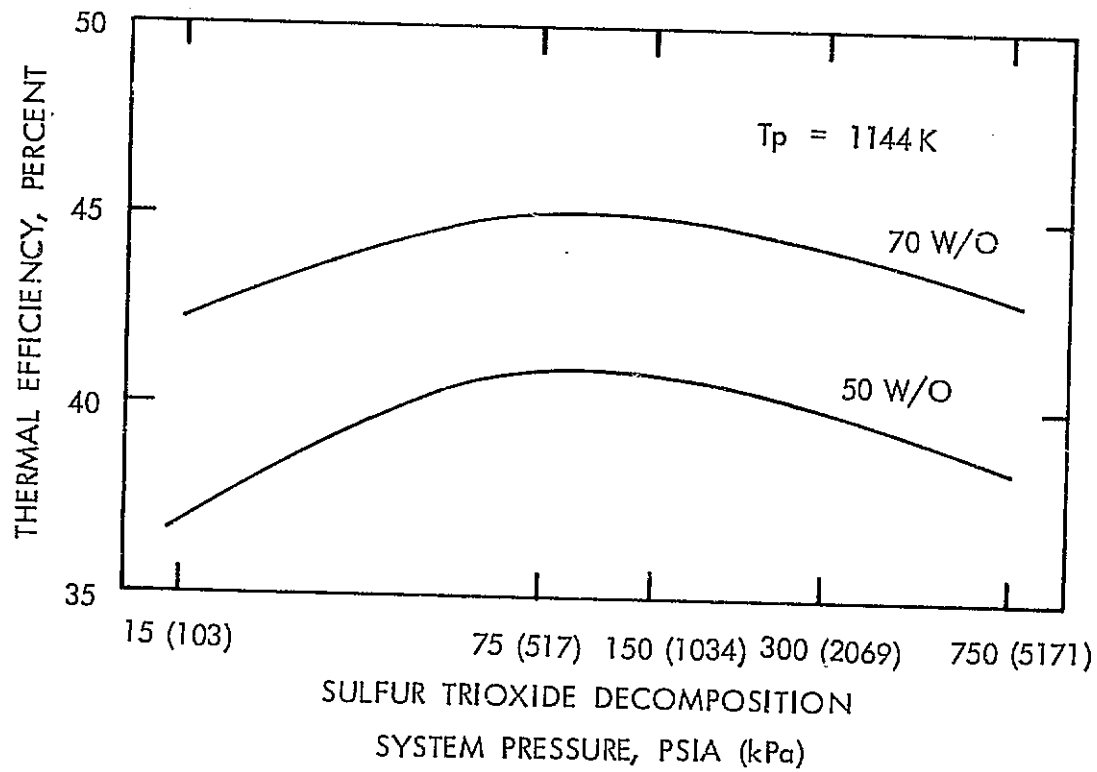


Figure 5.3.8 Variation of Process Thermal Efficiency with Pressure

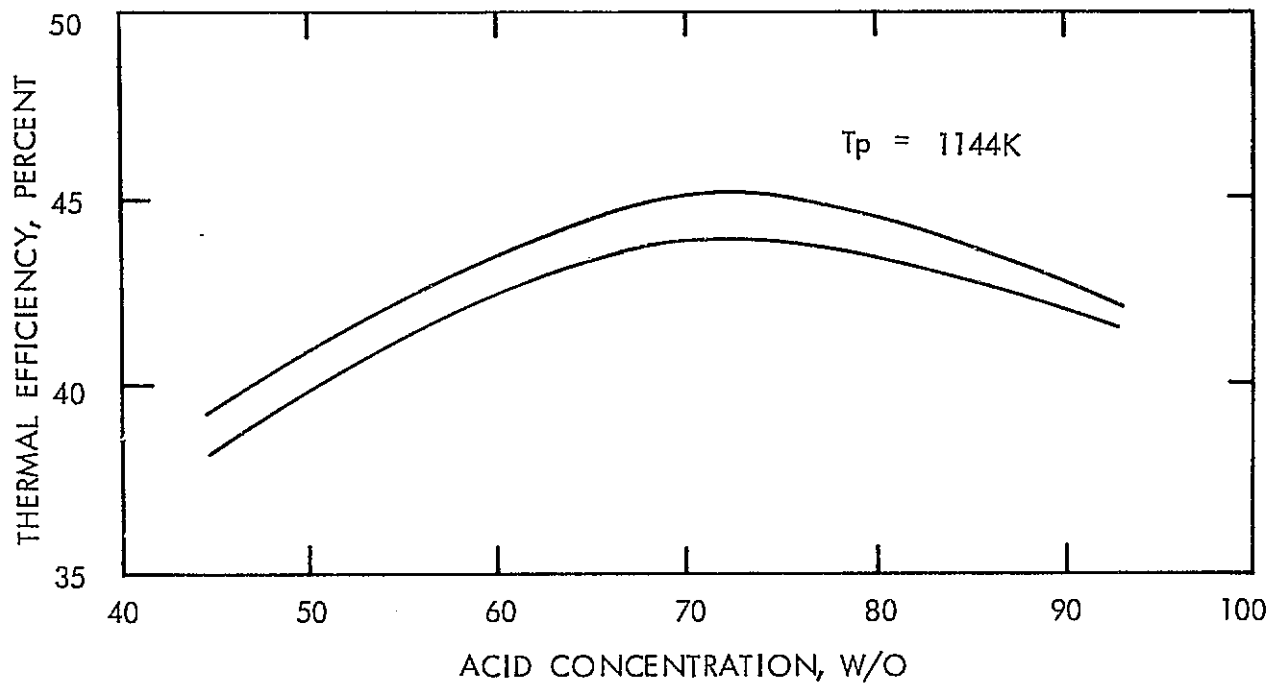


Figure 5.3.9 Variation of Process Thermal Efficiency with Acid Concentration

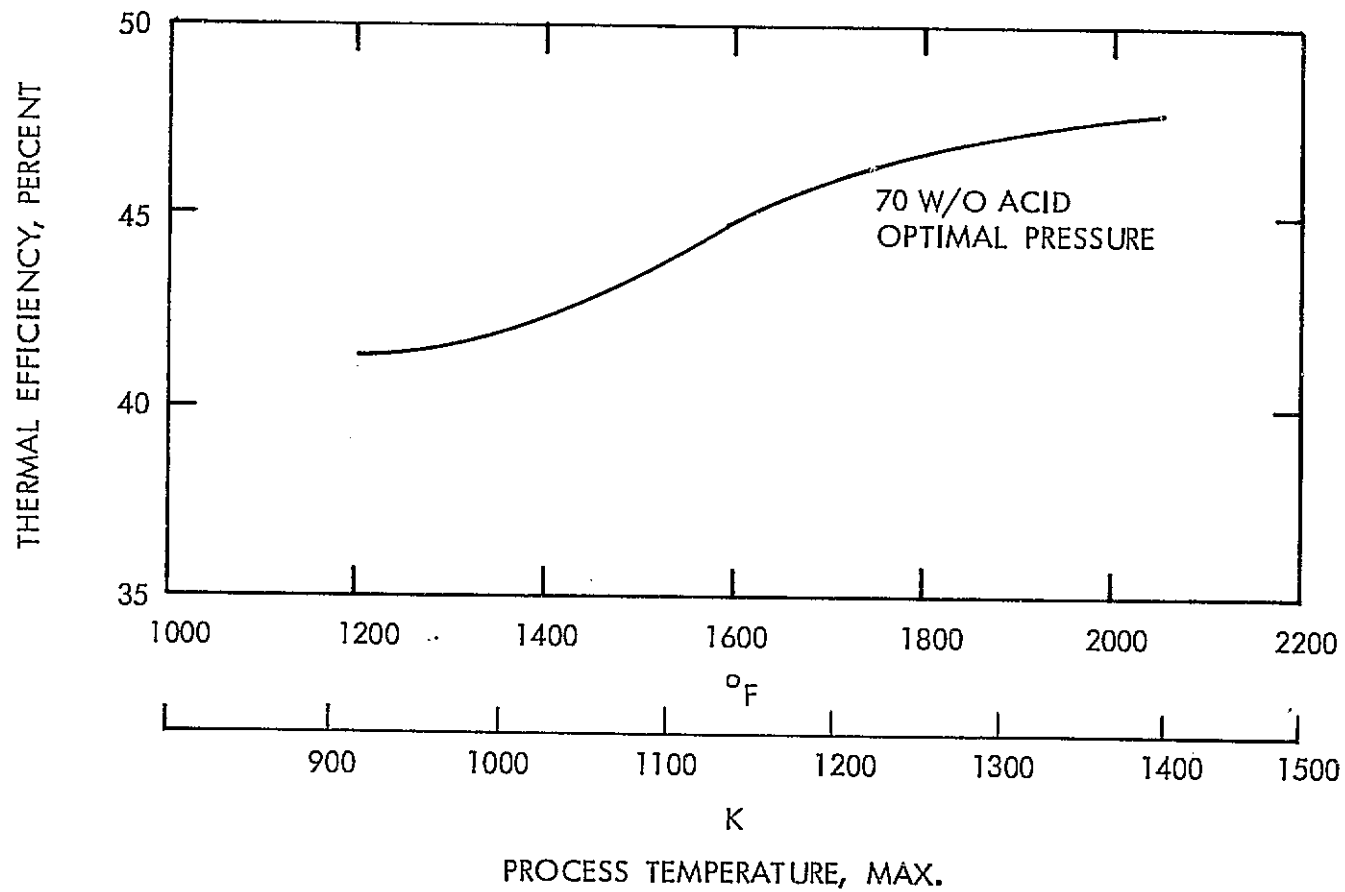


Figure 5.3.10 Variation of Process Thermal Efficiency with Process Gas Temperature

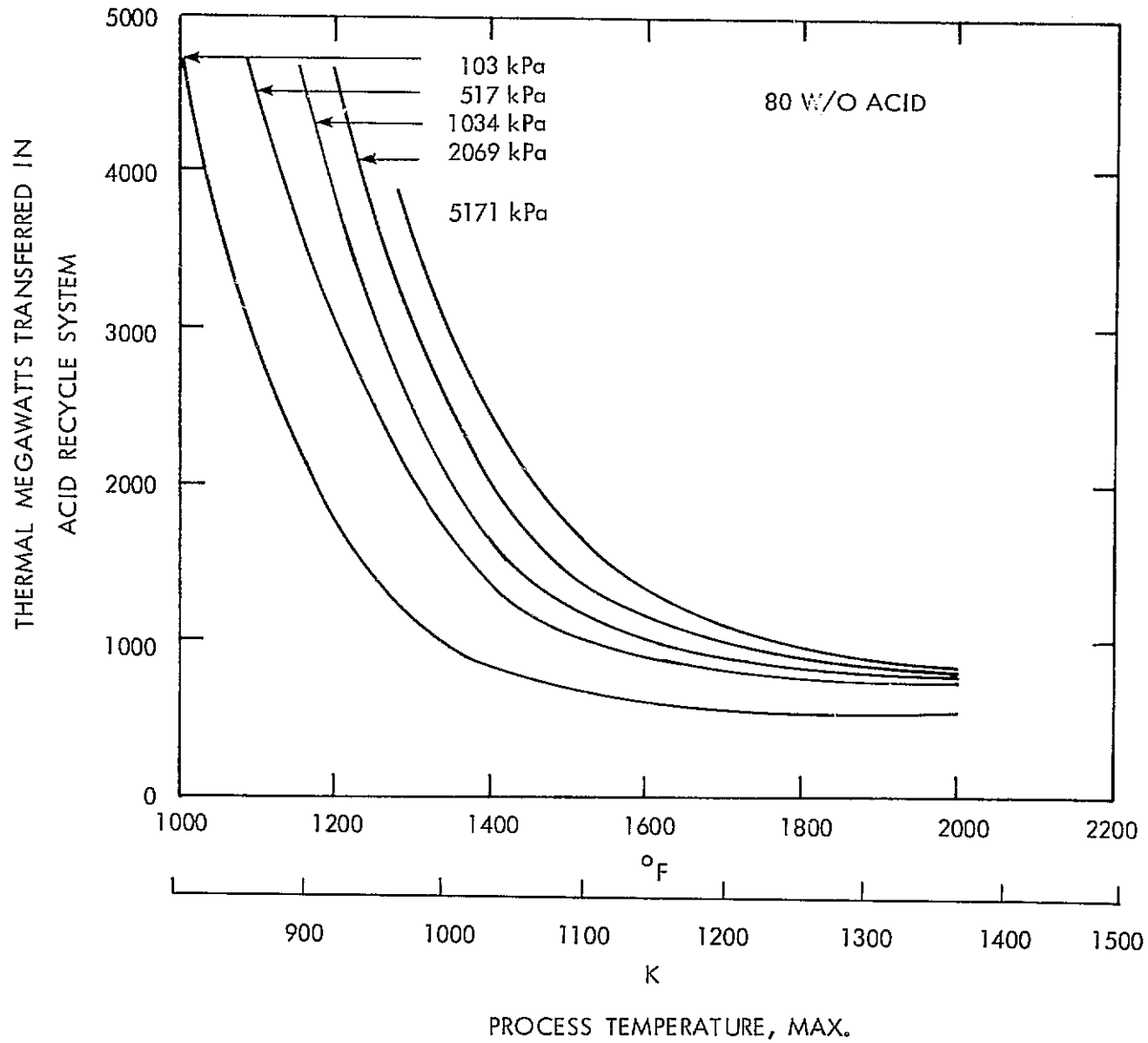


Figure 5.3.11 Energy Recycle as a Function of Process Temperature

for example, be modified for heat inputs from an intermediate fluid which in turn is heated by the energy source. Alternately, the process heat exchanger and acid vaporizer could be designed for direct "firing", much like conventional reformers or boilers. The specific approach to be used would depend upon design optimization for each of the potential energy sources.

Other process variations of the cycle can be developed which can utilize any convenient or economical source of process energy. One such process alternate that has been investigated can accept the process energy either directly as a fuel gas or indirectly as thermal energy entering the system through a heat exchanger. This process alternative uses a different acid concentration system and a different approach to the sulfur trioxide reduction than the reference process.

When the alternate process configuration is operating in the directly fueled mode, any gaseous fuel may be employed. This includes not only light hydrocarbon gases, but also the product gases obtained from air-blown coal or oil gasifiers, as well as any process or plant fuel gases which may be available. The sulfur content of the feed gas is unimportant as the hydrogen process contains provisions for sulfur removal. No oxygen plants or acid gas removal facilities are required and the hydrogen purity is independent of the feed gas composition.

When operated in the indirectly fueled mode, with the indirect addition of thermal energy, oxygen as well as hydrogen production is achieved. Under these circumstances, fuel or flue gas desulfurization may be necessary to meet environmental regulations (as it would be if the gas were to be burned elsewhere), but, as before, low Btu fuels can be employed

The two operating modes of the process are illustrated in Figures 5.3.12 and 5.3.13. As in the reference configuration, hydrogen is generated electrolytically in an electrolysis cell which anodically oxidizes sulfurous acid to sulfuric acid while simultaneously generating hydrogen at the cathode.

The regeneration of  $\text{SO}_2$  from the electrolyzer sulfuric acid effluent is accomplished by chemically extracting, as ferric sulfate, the sulfur trioxide formed in the electrolyzer, followed by the subsequent thermal decomposition of the sulfate into iron oxide, oxygen, and  $\text{SO}_2$ . The extraction of the sulfur trioxide takes place in two stages as shown in Figure 5.3.12. The electrolyzer effluent is assumed to contain about 40 W/O  $\text{H}_2\text{SO}_4$  (Point B). Iron oxide is dissolved into this to the limits of its solubility at 333K (Point C). This solution, when heated to 473K produces a liquid phase containing about 15 W/O  $\text{H}_2\text{SO}_4$  (Point A). This solution is cooled and recycled to the electrolyzer where its concentration is once again increased by the reactions given earlier to 40 W/O  $\text{H}_2\text{SO}_4$ . Leaving the crystallizer is a hydrated ferric sulfate having the composition  $\text{Fe}_2\text{O}_3 \cdot 2\text{SO}_3 \cdot \text{H}_2\text{O}$  and consisting of a mixture of  $\text{Fe}_2\text{O}_3 \cdot 3\text{SO}_3$  and  $\text{Fe}_2\text{O}_3 \cdot 3\text{H}_2\text{O}$ . Steam requirements in the crystallizer are met by evaporating boiler feed water injected into the oxide coolers contained in the dryer and decomposition reactors.

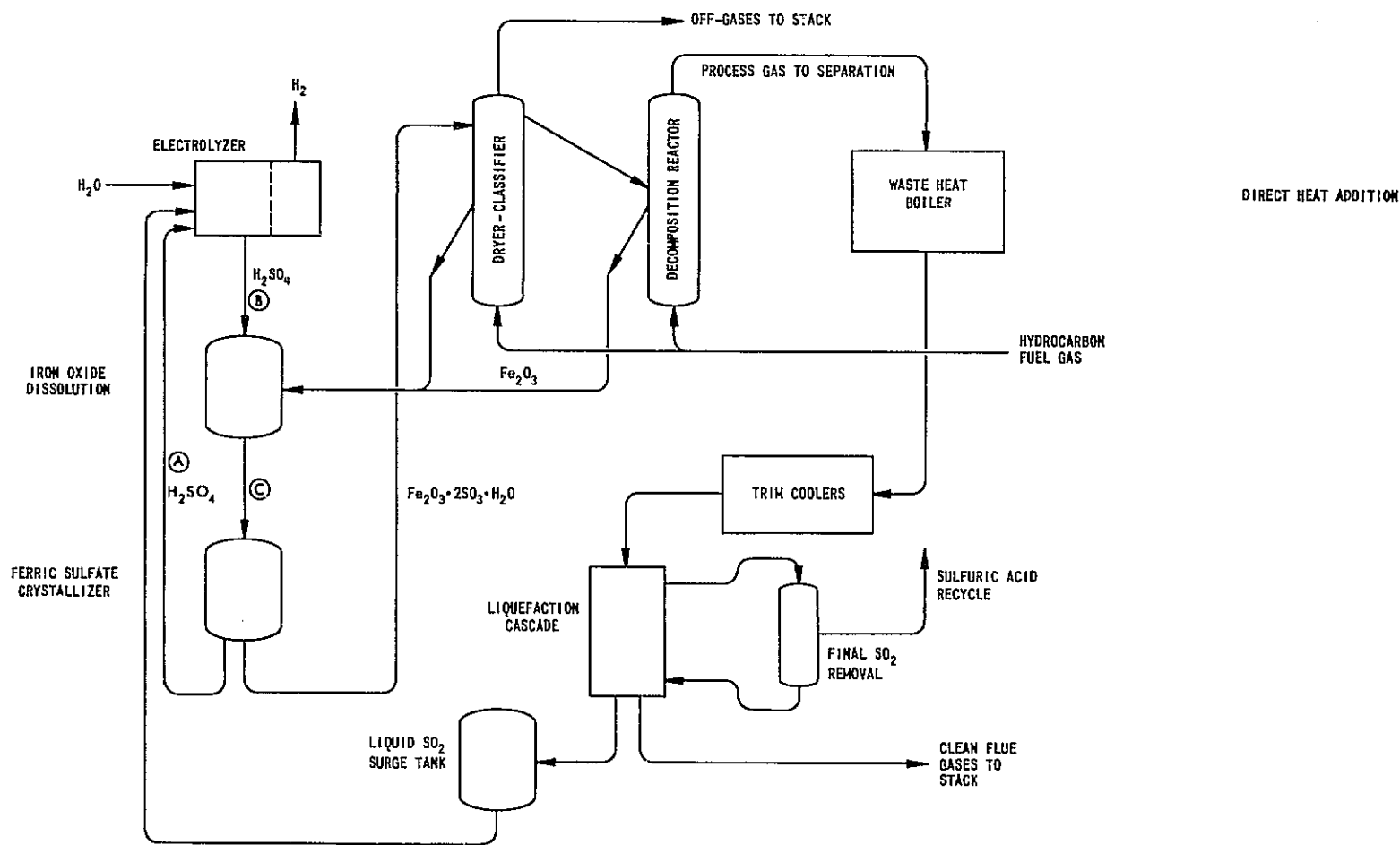


Figure 5.3.12 Direct Heat Mode of Operation for the Westinghouse Hydrogen Production System

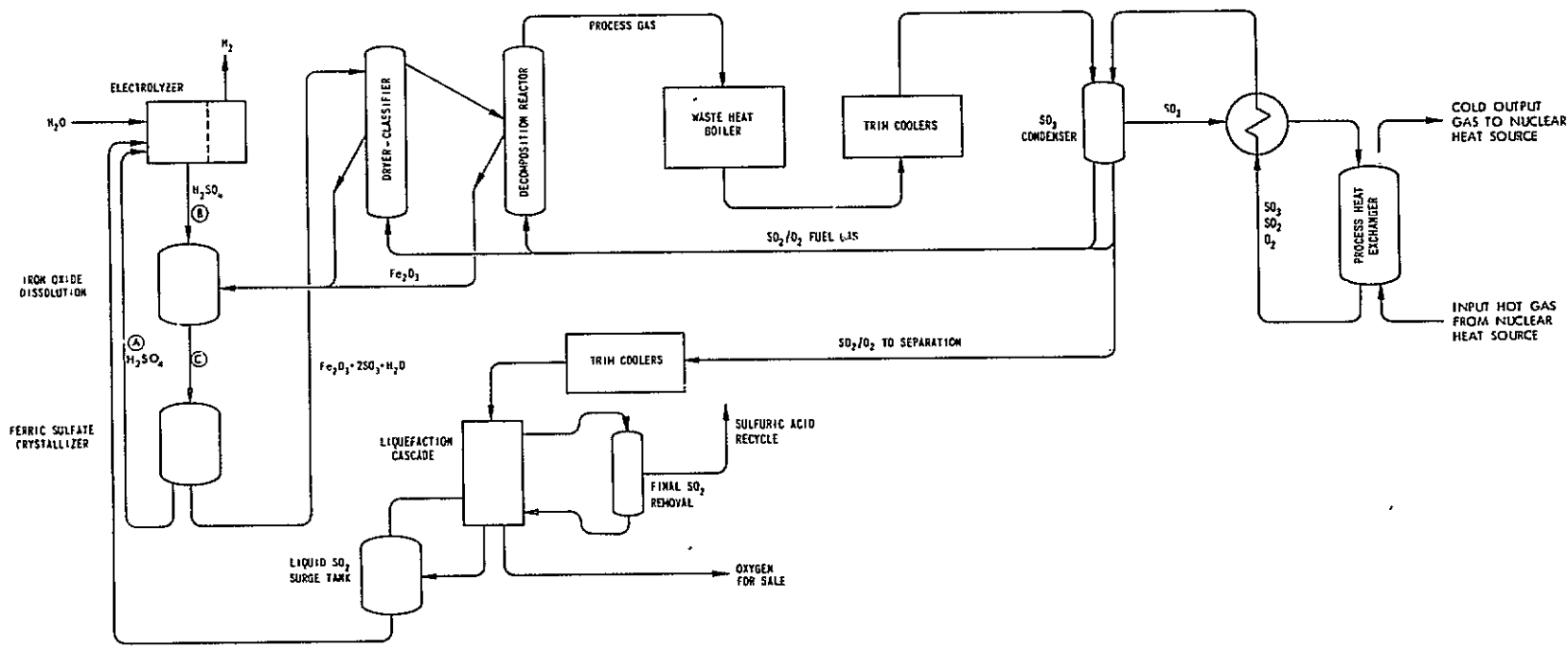
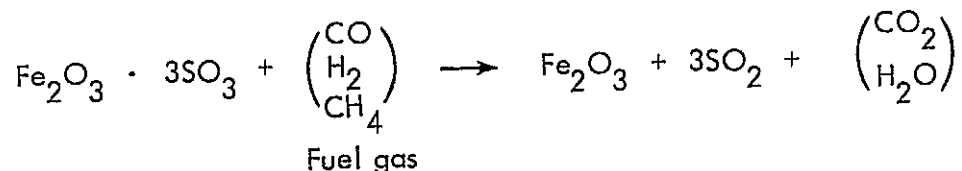


Figure 5.3.13 Indirect Heat Mode of Operation for the Westinghouse Hydrogen Production System

The mixture of  $\text{Fe}_2\text{O}_3 \cdot 3\text{SO}_3$  and  $\text{Fe}_2\text{O}_3$  obtained from the crystallizer yields, after decomposition,  $\text{SO}_3/\text{H}_2\text{O}$  ratios comparable to those obtained in fuming sulfuric acid. This concentration is achieved from a 40 percent feed acid without evaporating large quantities of water as is required in thermal concentrators. The inclusion of this system into the process enables the electrolyzer to operate with low activities of sulfuric acid, thereby with low power requirements, while simultaneously avoiding the need to recycle large quantities of water into the  $\text{SO}_3$  reduction system. The need to employ a thermal concentrator with the subsequent generation of large quantities of low pressure steam is similarly avoided. The use of ferric sulfate within the process offers additional advantages which become apparent in examining the operation of the sulfate decomposition system. The hydrated ferric sulfate leaving the crystallizer is fed next into a dryer-classifier and then into a decomposition reactor. These vessels are fluidized beds operating at pressures between 2000 and 5000 kPa (20 to 50 atm). Both contain three stages. The upper portion of the bed is an expanded section for lighter  $\text{Fe}_2\text{O}_3$  particles, the central section is narrower and contains  $\text{Fe}_2\text{O}_3 \cdot 3\text{SO}_3$  and  $\text{Fe}_2\text{O}_3$ , while the bottom section is the oxide cooler which accepts overflow from the upper section of each bed.

Considering first the system operation with low Btu gas, the hydrated ferric sulfate is fed through lock hoppers and into the central section of the dryer-classifier. Combustion of low-Btu gas provides the thermal energy necessary to decompose  $\text{Fe}_2\text{O}_3 \cdot 3\text{H}_2\text{O}$  into iron oxide and steam. The lighter  $\text{Fe}_2\text{O}_3$ , after decomposition, is blown into the upper section of the bed. Overall temperature is maintained above that required to decompose  $\text{Fe}_2\text{O}_3 \cdot 3\text{H}_2\text{O}$  but below that at which  $\text{Fe}_2\text{O}_3 \cdot 3\text{SO}_3$  decomposes. In spite of this, local hot spots near the distributor will liberate some  $\text{SO}_3$  which will be recaptured in the upper bed section. Iron oxide overflow from the upper section flows to the cooler. This portion of the vessel is fluidized with steam and contains nozzles for injecting boiler feed water into the bed. The cooling of the  $\text{Fe}_2\text{O}_3$  prior to letdown is accomplished while generating process steam for use in the crystallizer. Ferric sulfate contained in the central section of the bed flows to the decomposition reactor.

The decomposition reactor operates at the same nominal pressure as the dryer, but at higher temperatures. The fact that the bed contains  $\text{Fe}_2\text{O}_3$  - a contact catalyst for sulfuric acid manufacture - aids in establishing the equilibrium  $\text{SO}_3 \rightarrow \text{SO}_2 + 1/2 \text{O}_2$ . The oxygen liberated by the  $\text{SO}_3$  thermal reduction as well as that present in excess air added to the system serves to combust the fuel gas and to thereby provide the thermal energy necessary to decompose the ferric sulfate. Overall the following reaction occurs:



Precise air and fuel requirements in the decomposition reactor will depend upon the fuel gas employed.  $\text{SO}_2$  concentrations in excess of 20 percent are obtained with most common fuel gases. Representative outlet compositions corresponding to a low-Btu fuel gas are shown in Table 5.3.5. In this instance 8.65 moles of fuel gas and 1.312 moles of air are required to decompose one mole of  $\text{Fe}_2\text{O}_3 \cdot 3\text{SO}_3$ . The effluent from the decomposition reactor passes through a waste heat boiler which raises steam to drive the turbine generators which power the electrolyzer. The process gases are subsequently cooled and the water vapor condensed, and are then dried before entering the  $\text{SO}_2$  liquefaction cascade.

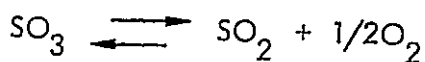
The  $\text{SO}_2$  liquefaction cascade starts with a higher temperature bulk  $\text{SO}_2$  removal step at 266K (20°F) or above, depending upon process pressure. Final  $\text{SO}_2$  removal is obtained using refrigeration generated by the process gases as they are expanded to 101 kPa (one atmosphere). Before the final gas expansion to atmospheric pressure, the remaining  $\text{SO}_2$  is removed by oxidation to  $\text{SO}_3$  and scrubbing. The resultant sulfuric acid is recycled to the iron oxidation dissolution stage or is available for sale.

In the indirectly - heated operating mode, Figure 5.3.13, the energy required for the drying and thermal decomposition of ferric sulfate is obtained by the catalytic oxidation of  $\text{SO}_2$  to  $\text{SO}_3$  within the process vessel. In the dryer, which operates at lower temperatures and elevated pressures,  $\text{SO}_3$  formation and subsequent reaction with  $\text{Fe}_2\text{O}_3$  is favored and provides the exothermic reaction heat necessary to decompose  $\text{Fe}_2\text{O}_3 \cdot 3\text{H}_2\text{O}$ .

In the sulfate decomposition reactor, two equilibria over the catalyst  $\text{Fe}_2\text{O}_3$  are established.



$$K_1 = P_{\text{SO}_3}^3$$



$$K_2 = \frac{P_{\text{SO}_2}}{P_{\text{SO}_3}} P_{\text{O}_2}^{1/2}$$

The proper operating pressure for the vessel as well as the  $\text{SO}_2/\text{O}_2$  recycle required for the decomposition energy will depend upon the system operating temperature. For process temperatures between 1200 and 1300 K, operating pressures above 4050 kPa (40 atm) can be employed (See Table 5.3.6). The effluent from the decomposition reactor contains about 31 percent  $\text{SO}_3$ , 46 percent  $\text{SO}_2$ , and 23 percent  $\text{O}_2$  for all operating temperatures and pressures shown.

TABLE 5.3.5  
 REPRESENTATIVE DECOMPOSITION REACTOR EFFLUENT  
 WHEN OPERATING ON LOW-BTU FUEL GAS

<u>Fuel Gas Composition</u>		<u>Decomposition Reactor Effluent</u>	
<u>Component</u>	<u>Volume %</u>	<u>Component</u>	<u>Volume %</u>
N <sub>2</sub>	54.5	N <sub>2</sub>	43.7
CO	18.6	SO <sub>2</sub>	22.7
H <sub>2</sub>	12.1	CO <sub>2</sub>	18.7
CH <sub>4</sub>	2.4	H <sub>2</sub> O	14.7
CO <sub>2</sub>	6.9	O <sub>2</sub>	0.2
H <sub>2</sub> O	5.5		
TOTAL	100.0	TOTAL	100.0

TABLE 5.3.6  
 OPERATING PRESSURE OF THE SULFATE DECOMPOSITION  
 REACTOR AS A FUNCTION OF REACTOR TEMPERATURE

<u>Temperature</u>		<u>Pressure</u>	
<u>K</u>	<u>°F</u>	<u>kPa</u>	<u>atm</u>
1000	1340	91.5	0.903
1100	1520	730.0	7.200
1200	1700	3,962.0	39.100
1300	1880	16,620.0	164.000

The gases leaving the decomposition reactor may be cooled either by recuperative heat exchange with the incoming  $SO_2/O_2$  mixture or, as shown, by passage through a waste heat boiler prior to condensation of the sulfur trioxide. The sulfur dioxide and oxygen in the mixture are recycled to the decomposition reactor while the sulfur trioxide is vaporized and sent to the  $SO_3$  thermal reduction reactor. This reactor contains both high and low temperature contact catalysts and is indirectly heated by whatever energy source is driving the process.

The process energy required to regenerate  $SO_2$  from the sulfur trioxide formed in the electrolyzer is input here, as well as that which was input to the dryer and the ferric sulfate decomposition reactors as a result of the  $SO_2$  oxidation which occurred in those vessels. An alternate process variation would be to reduce the duty of the  $SO_3$  thermal reduction reactor by adding indirect heat to the dryer and the ferric sulfate decomposition reactor.

To do this would require heat exchange surface in a high temperature ( $>1144K$ ) environment and would substantially increase the size and complexity of both the dryer and the ferric sulfate decomposition reactor. This not only complicates the operation of the system when indirectly heated, but in addition renders more difficult the use of hydrocarbon or low-Btu fuel gases within the process if oxygen recovery is not desired. Finally, the energy demands of these vessels is for process energy above, say  $1144K$  ( $1600^\circ F$ ), which if provided in an indirectly heated fashion makes available a high temperature gas stream whose effective utilization elsewhere may be difficult.

In evaluating these requirements, it is felt that the vessel energy demand is best met by conducting an exothermic reaction within the unit. This then enables fuel gases to be used directly if oxygen is not desired, while enabling  $SO_2$  and  $O_2$  to serve as a "fuel gas" in the indirectly-heated mode of operation. The subsequent thermal decomposition of  $SO_3$  is a reaction more amenable to indirectly heated reactors than is the decomposition of ferric sulfate. Sulfur trioxide will decompose over a broad temperature range, thereby providing for more compact heat exchangers operating at lower overall mean temperatures.

Further advantages accrue when one considers overall system reliability. If the ferric sulfate decomposition reactor were to be indirectly heated, inspection and maintenance of the heat exchange would require shutting down the entire process. Using a separate  $SO_3$  reduction reactor enables repair and maintenance to be conducted while the process continues to operate in the fuel gas mode.

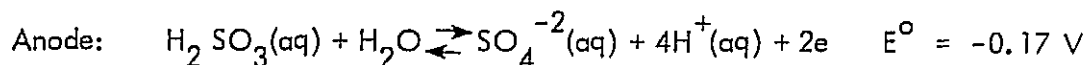
The gases leaving the  $SO_3$  reduction reactor are cooled against the incoming stream and unreacted  $SO_3$  is condensed for recycle. Sulfur dioxide and oxygen sufficient to meet the thermal demands of the dryer and the ferric sulfate decomposition reactor are separated and rejoin the recycle to those vessels. The electrolyzer sulfur dioxide, with the process oxygen product, proceeds to the liquefaction cascade for separation. Sulfur dioxide recovered here is returned to the electrolyzer while the oxygen is a process by-product available for sale or disposal.

### 5.3.6 Status of Electrochemical Hydrogen Generation Technology

The Westinghouse Sulfur Cycle water-splitting process, based on the oxidation of  $\text{SO}_2$  to  $\text{SO}_3$  with subsequent thermal reduction of  $\text{SO}_3$ , requires that a means be found to carry out the following reactions:

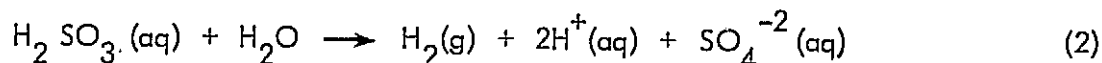


Although this reaction is not spontaneous and cannot be thermally driven, it may be accomplished electrochemically in an acid electrolyte by coupling the following half-cell reactions:



It should be noted that sulfur dioxide,  $\text{SO}_2$  dissolves in an aqueous strong acid to yield sulfurous acid,  $\text{H}_2\text{SO}_3$ .

From the above, it may be concluded that, under standard conditions, the minimum driving voltage for the reaction



is 0.17 volts, which compares very favorably with the corresponding value of 1.23 volts for the electrolysis of water, i.e.,



Earlier work at Westinghouse confirmed that Reaction 2 proceeds substantially as written by operation of an electrolytic cell with platinized platinum electrodes in 50 w/o sulfuric acid at room temperature. However, with the anode and cathode compartments separated only by a sintered glass frit, the formation of a white solid simultaneous with the evolution of hydrogen was observed. This white powder was later identified as sulfur.

Examination of Table 5.3.7, which lists the standard reduction potentials of sulfur-containing species in acid solutions, reveals that sulfurous acid will depolarize the cathode reaction (see half-cell Reaction 2). If enough  $\text{H}_2\text{SO}_3$  is supplied to the cathode, no hydrogen will be evolved. Furthermore, sulfur formed by this reaction can also act as a cathode depolarizer, also inhibiting hydrogen evolution (see half-cell Reaction 4). Sulfur deposition is therefore to be expected if sulfurous acid is not excluded from the catholyte.

Juda and Moulton (Reference 12) did not report sulfur deposition when they used sulfur dioxide as an anodic depolarizer in an electrolysis cell operating at 368K in 30 w/o sulfuric acid. The important difference between their work and the preliminary Westinghouse work was that Juda and Moulton employed a flow-through electrode, i.e., the sulfurous acid solution was forced through a platinum-catalyzed porous carbon electrode under current, so that the solution was depleted of  $\text{H}_2\text{SO}_3$  by the time it reached the interelectrode electrolyte. Under these circumstances, sulfur deposition at the cathode could not occur.

Two other papers (References 13, 14) which discuss the electrocatalytic oxidation of sulfurous acid make no comment on the processes occurring at the cathodes of their systems. Das and Roy (Reference 13), who used an experimental apparatus similar to that used by Westinghouse, must have observed sulfur deposition but reported only on the anode polarizations. Wiesener (Reference 14) did similarly.

Sulfurous acid migration from the catholyte to the anolyte was fully inhibited by the simple and elegant experimental procedure devised by Bowman and Onstott (Reference 15). The use of a membrane and slight overpressuring of the catholyte resulted in the total avoidance of sulfur deposition at the cathode, and thus 100 percent current efficiency for hydrogen production.

In contrast to the complex situation existing at the cathode, only one reaction, i.e., the electro-oxidation of sulfurous acid, occurs at the anode. The extent to which sulfurous acid depolarizes the anode (oxygen-evolution electrode) in an electrolysis cell is shown in Figure 5.3.14, which is taken from the work of Juda and Moulton (Reference 12). The depolarized cell operates at 0.8 V below the voltages required for water electrolysis.

The effect of temperature on the polarization characteristics of platinized platinum electrodes in the anodic oxidation of sulfurous acid in about 25 percent  $\text{H}_2\text{SO}_4$  is shown in Figure 5.3.15. Das and Roy (Reference 13) employed a saturated calomel electrode (SCE) in their experimentation. Using a value of 0.263 V for the SCE versus the hydrogen electrode in normal sulfuric acid (Reference 16), an approximate scale for the electrode polarization versus the normal hydrogen electrode is provided for purposes of comparison. Increasing temperature results in a lowering of the electrode polarization - the effect amounting to 125 mV at  $100 \text{ mAcm}^{-2}$  on going from 303K to 353K ( $30^\circ\text{C}$  to  $80^\circ\text{C}$ ).

Wiesener's (Reference 14) data for 27 w/o  $\text{H}_2\text{SO}_4$  at 333K ( $60^\circ\text{C}$ ) are shown in Figure 5.3.16. The best performing electrode consisted of air-, steam-, or carbon dioxide-activated carbon, catalyzed by platinum and a mixed oxide,  $\text{V}_2\text{O}_5 \cdot 3 \text{Al}_2\text{O}_3$ . An

TABLE 5.3.7  
STANDARD REDUCTION POTENTIALS OF SULFUR-CONTAINING  
SPECIES AT 298K IN ACID SOLUTION

	<u>Reaction</u>	<u>Potential, Volts</u>
1.	$S_2O_6^{-2} + 4H^+ + 2e \rightleftharpoons 2H_2SO_3$	0.57
2.	$H_2SO_3 + 4H^+ + 4e \rightleftharpoons S + 3H_2O$	0.45
3.	$SO_4^{-2} + 4H^+ + 2e \rightleftharpoons H_2SO_3 + H_2O$	0.17
4.	$S + 2H^+ + 2e \rightleftharpoons H_2S$	0.141
5.	$S_4O_6^{-2} + 2e \rightleftharpoons 2S_2O_3^{-2}$	0.09
6.	$2H^+ + 2e \rightleftharpoons H_2(g)$	0.00
7.	$2H_2SO_3 + H^+ + 2e \rightleftharpoons HS_2O_4^- + 2H_2O$	-0.08
8.	$2SO_4^{-2} + 4H^+ + 2e \rightleftharpoons S_2O_6^{-2} + H_2O$	-0.22

REPRODUCIBILITY OF THE  
ORIGINAL PAGE IS POOR

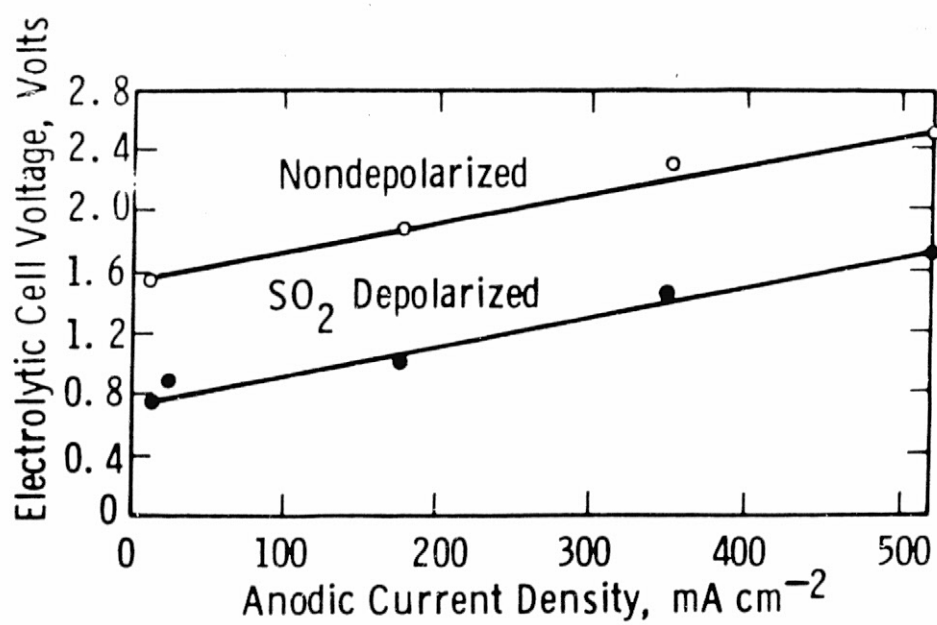


Figure 5.3.14 Effect of SO<sub>2</sub> on Electrolysis (After Juda and Moulton)

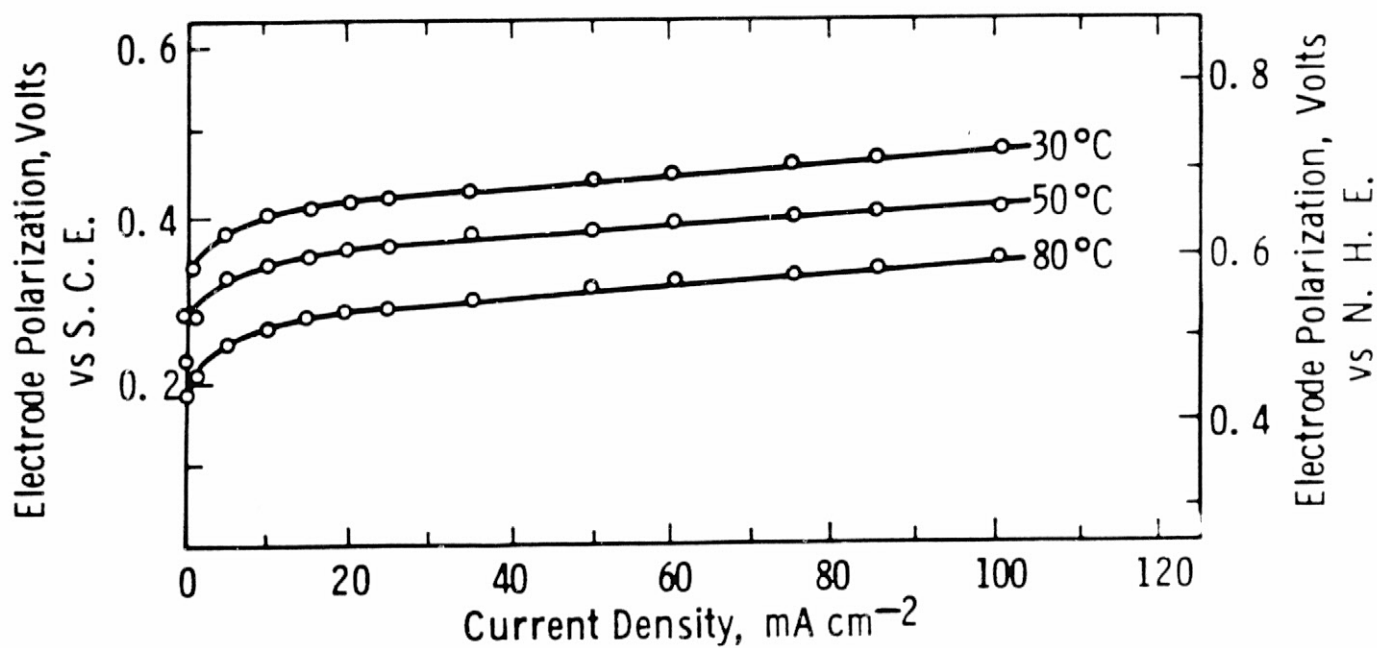
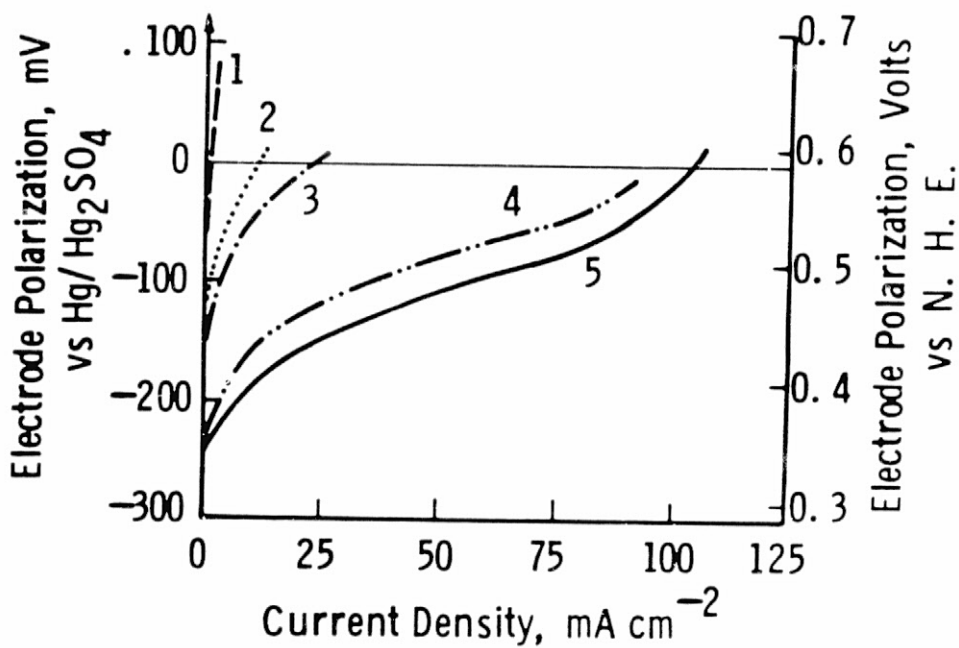


Figure 5.3.15 Polarization Characteristics of SO<sub>2</sub> Oxidation on Platinized Platinum Electrodes in 6N H<sub>2</sub>SO<sub>4</sub> at Different Temperatures (After Das and Roy)



NOTE:

- 1 - Carbon
- 2 - Activated Carbon
- 3 - Activated Carbon +  $V_2O_5 \cdot 3Al_2O_3$
- 4 - Activated Carbon + Pt
- 5 - Activated Carbon + Pt +  $V_2O_5 \cdot 3Al_2O_3$

Figure 5.3.16 Effect of Activation and Catalysts on the Current Density-Potential Characteristics of a Carbon Electrode in the Oxidation of Sulfurous Acid - Temperature;  $60^\circ C$ : Electrolyte 27 w/o  $H_2SO_4$  (Reference 14)

TABLE 5.3.8

SUMMARY OF DATA OF WIESENER, AND DAS AND ROY,  
FOR THE ANODIC OXIDATION OF SULFUROUS ACID

<u>Anode Material</u>	<u>H<sub>2</sub>SO<sub>4</sub> Conc. (w/o)</u>	<u>Temp. (K)</u>	<u>Polarization at 100 mA cm<sup>-2</sup> (mV vs. N. H. E.)</u>	<u>Reference</u>
Platinum black	25	303	640	46
		323	585	46
		353	550	46
Platinized platinum	25	303	735	46
		323	670	46
		353	610	46
Gas-activated carbon + Pt catalyst	27	333	610	47
Carbon + Pt + 3 Al <sub>2</sub> O <sub>3</sub> · V <sub>2</sub> O <sub>5</sub>	27	333	575	47

approximate scale, to allow polarization values to be read in mV versus the normal hydrogen electrode, was constructed by the use of data (Reference 17) for the cell,  $H_2/H_2SO_4/Hg_2SO_4/Hg$ , at  $60^\circ C$ , and is included in Figure 5.3.16.

A summary of the relevant results of Das and Roy and Wiesener is presented in Table 2. Platinized platinum is not as effective an anodic electrocatalyst as platinum black. Wiesener's best performing electrode compares very favorably with the platinum black electrodes of Das and Roy. Electrolytic cell voltages of 0.7 V or less at  $100 \text{ mAcm}^{-2}$  should be achievable with this electrode, if the cell is operated at temperatures of 333K ( $60^\circ C$ ) or greater with a platinized platinum hydrogen-evolution electrode ( $\eta \sim 0.07 \text{ V}$  at  $100 \text{ mAcm}^{-2}$ ) and an interelectrode spacing of 5 mm or less ( $\rho(H_2SO_4) \sim 1 \Omega\text{-cm}$  at 333K).

The results of Bowman and Onstott (Reference 15) for cells operating in  $SO_2$ -saturated  $2M H_2SO_4$  is shown in Figure 5.3.17. The pronounced effect of temperature on the cell voltage is obvious. The cell voltage at  $100 \text{ mA/cm}^2$  decreased from 900 mV to 750 mV when the temperature of operation is increased from 295K ( $22^\circ C$ ) to 353K ( $80^\circ C$ ). The data of Das and Roy (Reference 13), presented above, indicate that the voltage decrease is mainly due to a reduction of the activation polarization at the anode.

The main thrust of the experimental work funded and performed by Westinghouse to date has been to demonstrate technical feasibility, i.e., cell operation for extended periods with little or no sulfur deposition (current efficiencies in excess of 99 percent) and with acceptable voltage efficiencies at practical current densities (cell voltage  $< 0.6 \text{ V}$  at  $200 \text{ mA/cm}^2$ ). The suggestions of Bowman and Onstott (Reference 15) regarding the use of a membrane to separate the catholyte and anolyte, as well as catholyte overpressure, were incorporated into the experimental apparatus.

Figure 5.3.18 summarizes and puts into perspective the current density-voltage relationships observed in the Westinghouse work to date. The upper dotted line represents typical room temperature ( $22$  to  $30^\circ C$ ) observations of other investigators in 17-27 w/o  $H_2SO_4$ , while the lower dotted line indicates the best of the high temperature data in other work. The two upper solid lines represent early data observed in 50 w/o  $H_2SO_4$  at 303K ( $30^\circ C$ ) with the Westinghouse cell design. The break at approximately  $100 \text{ mA/cm}^2$  indicates the onset of a limiting current density phenomena due to the failure to maintain adequate activity of sulfurous acid at the anode. When due attention was paid to anode placement and the method of anolyte saturation with  $SO_2$ , the lowest solid line data set was observed at about 303K ( $30^\circ C$ ) in 50 w/o  $H_2SO_4$ . With the assurance of an approximately 150 mV drop in cell voltage on raising the temperature to 363K ( $90^\circ C$ ), cell voltages of  $< 0.65 \text{ V}$  at current densities of  $200 \text{ mA/cm}^2$  are seen to be achievable.

In summary, electrolytic cell operation, without sulfur deposition at the cathode and with about 100 percent current efficiency for hydrogen production has been successfully conducted over extended periods. Thus, the technical feasibility of  $SO_2$  depolarized electrolyzers has been demonstrated.

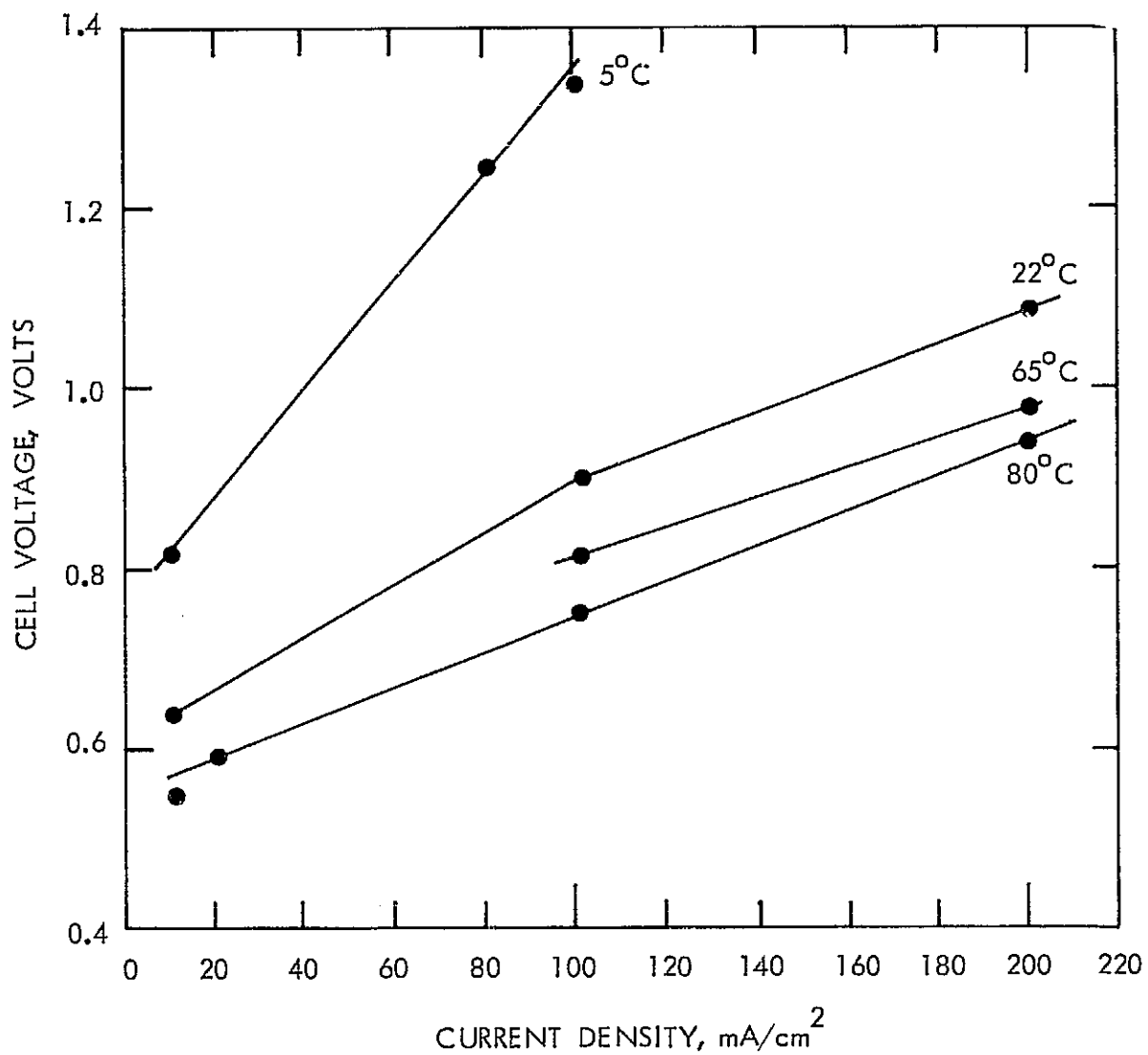


Figure 5.3.17 Electrolyzer Performance with Platinum Black Electrodes in 2M H<sub>2</sub> SO<sub>4</sub> Solutions at Different Temperatures (After Bowman and Onstott, LASL)

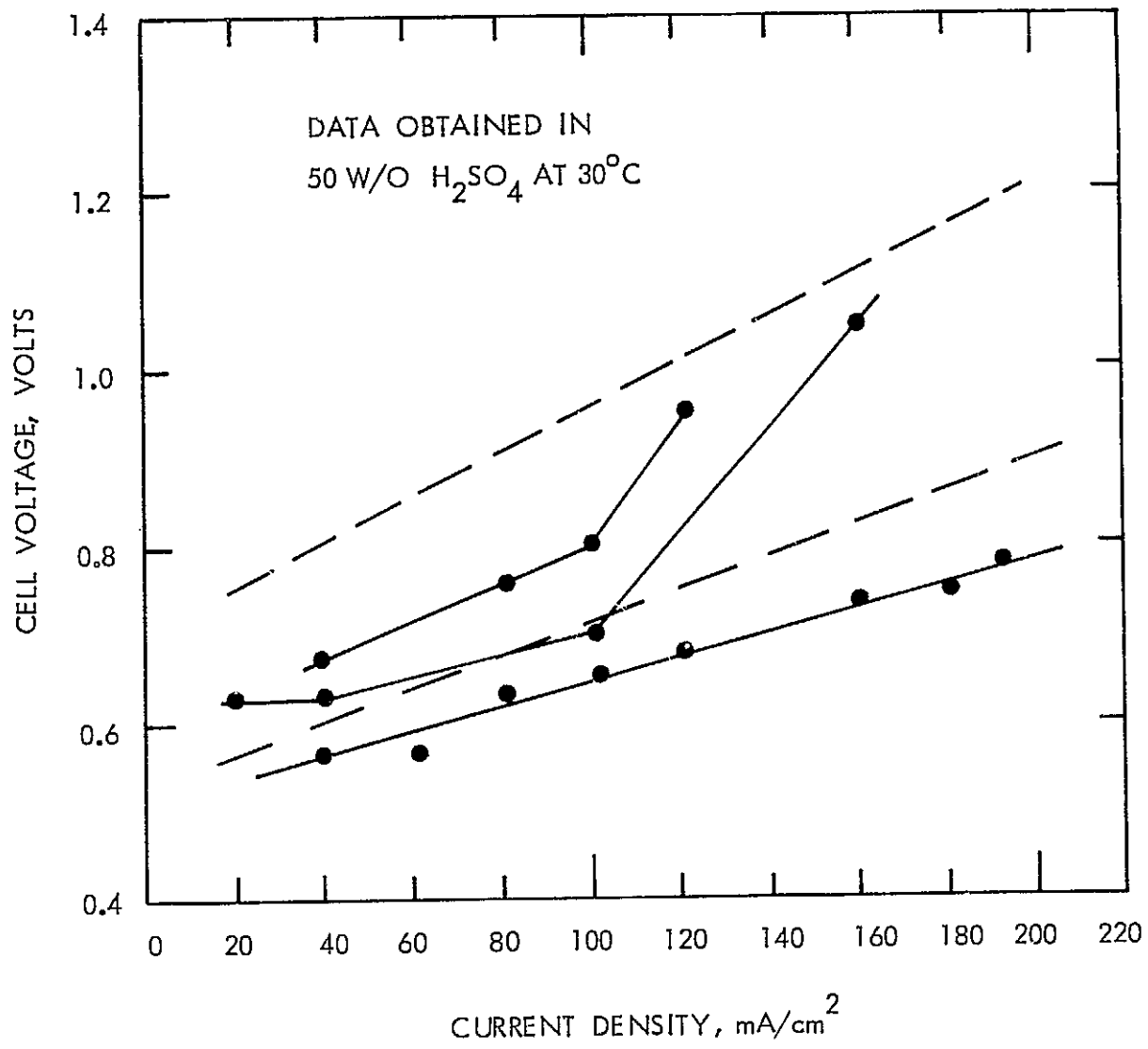


Figure 5.3.18 Recent Electrolyzer Performance Results

### 5.3.7 Status of Sulfur Trioxide Reduction Technology

A substantial portion of the thermal energy entering the hydrogen generation process is introduced in the sulfur trioxide thermal reduction reactor. Consequently, the thermal reduction reactor is simultaneously a chemical reactor as well as a process heat exchanger. The design of such a piece of equipment is sensitive to both the heat and mass transfer characteristics of the system. The employment of large tubes and low overall temperature differences leads to a situation where the rate at which the endothermic chemical reaction proceeds is limited by the heat transfer rate. Similarly, the use of very small tubes and large temperature differences produces a design in which the mass transfer and chemical reaction rates, rather than the rate of heat transfer, influences the vessel size. Designing under heat transfer limited conditions leads to larger, more bulky equipment, whereas design under mass transfer limited conditions leads to poorer heat economy and more fragile equipment. The proper design involves an optimization with regard to both the heat and mass transfer characteristics of the system.

In order to define the range of gas residence time of technical interest, as well as to provide a basis for initiating design of the heat exchanger, preliminary concentration and axial temperature profiles along the exchanger/reactor were calculated for a near optimal design. These computations assumed a tube and shell exchanger using the same heat transfer coefficient calculated for the helium to helium intermediate heat exchanger in the nuclear heat source (VHTR) system. The chemical reaction was taken to be in equilibrium and the maximum allowable space velocity (or minimum residence time) consistent with equilibrium conversions at various temperatures was determined.

The design showed that for minimum catalyst activity, the catalyst must be capable of achieving equilibrium conversions along the entire length of the thermal reduction reactor at space velocities between 3500 and 6000  $\text{hr}^{-1}$  and at temperatures between 773 and 1173K (500 and 900°C). For more compact reactors, the catalyst must be capable of achieving equilibrium conversions by the time the process gas has reached the end of the reactor (temperatures about 1173K for space velocities between 30,000 and 60,000  $\text{hr}^{-1}$ ).

The purpose of the sulfur trioxide decomposition program is to identify a catalyst with sufficient activity and life for use in the  $\text{SO}_3$  thermal reduction reactor. Accordingly, Westinghouse constructed an experimental apparatus for investigating the kinetics of the thermal reduction of sulfur trioxide.

The first experiments run on this apparatus have been to determine the degree of reaction reversal to be expected upon quenching the high temperature gas mixture expected from the thermal reducer. This information is vital to an interpretation of the thermal reduction rate data taken later. Even more important, however, is the fact that if significant re-oxidation of  $\text{SO}_2$  would occur following the thermal reduction reactor, the entire process concept would be rendered either useless or highly inefficient.

The degree of reaction reversal to be expected was estimated by passing  $\text{SO}_2$  at a constant rate through the reactor with  $\text{N}_2$  and air carrier gases at various rates. Both hot and cold tests were performed. Under hot conditions, the mixture spent approximately two minutes flowing through the furnace ( $500 - 1000^\circ\text{C}$ ) and an additional two minutes in flowing from the  $500^\circ\text{C}$  furnace end to the analytical train. Under cold conditions, the gas mixtures traversed the system at room temperature. Residence times lower than four minutes were obtained by increasing the carrier flow while maintaining constant the  $\text{SO}_2$  rate.

A statistical analysis of the resultant data indicated identical  $\text{SO}_2$  rates into the analytic train for the  $\text{SO}_2/\text{N}_2$  hot runs and the  $\text{SO}_2/\text{air}$  cold runs. No effect upon residence time - up to four minutes - was observed in the  $\text{SO}_2/\text{air}$  hot runs. Additionally, the  $\text{SO}_2$  rate into the analytic train for the hot runs with air at all residence times was identical with that for the cold runs and the inert runs. Since over 100 determinations of  $\text{SO}_2$  rate were made during this period - none of which showed any significant statistical departure from the delivery rate - it is certain that  $\text{SO}_2$  reoxidation during quench will not be a problem so long as contact catalysts are not present.

The kinetics of two catalysts have also been investigated in the experimental apparatus. These catalysts, by reason of their proprietary nature, are designated as WX-1 and WX-2. For each catalyst, the reaction order was determined by testing integrated mass balance and reaction rate equations against the integral reactor data obtained in the system. Once the reaction order is known, the rate constant can be expressed as a function of a reaction group. This group contains a complex function of initial and final sulfur trioxide concentrations and varies with reaction order.

Plots of the reaction group versus  $1/T$  correspond to plotting the rate constant versus  $1/T$ . Figure 5.3.19 shows the curves obtained by plotting the data for catalyst WX-1. The agreement between predicted and experimental results is shown in Figure 5.3.20.

Figure 5.3.21 illustrates the expected conversions to be obtained with this catalyst at various temperatures and space velocities. The region of interest for the process heat exchanger is encompassed by space velocities between  $3000$  and  $8000 \text{ hr}^{-1}$ . As this clearly shows, WX-1 is a poor catalyst in this range at temperatures below  $1233\text{K}$  ( $950^\circ\text{C}$ ). Similarly, based upon the data to date there is no reason to expect it to be an effective catalyst below  $1073\text{K}$  ( $800^\circ\text{C}$ ), even at very low space velocities.

Data for the WX-2 catalyst is summarized in Figures 5.3.22 through 5.3.26. This catalyst was studied at space velocities of  $1000$ ;  $10,000$ ;  $30,000$ ; and  $60,000 \text{ hr}^{-1}$ . Figure 5.3.22 plots the data obtained at  $60,000 \text{ hr}^{-1}$  according to the proposed rate equation. As predicted, the data yields a straight line. Figure 5.3.23, for  $30,000 \text{ hr}^{-1}$ , also shows a straight line which is parallel to that obtained at  $60,000 \text{ hr}^{-1}$ . The graphs at  $1000$  and  $10,000 \text{ hr}^{-1}$ , Figure 5.3.24, are different. Data plotted according to the model for these space velocities yield two superimposed curves. The fact that identical data was obtained at two different space velocities suggested that the reaction was at equilibrium over the entire temperature range of interest for the

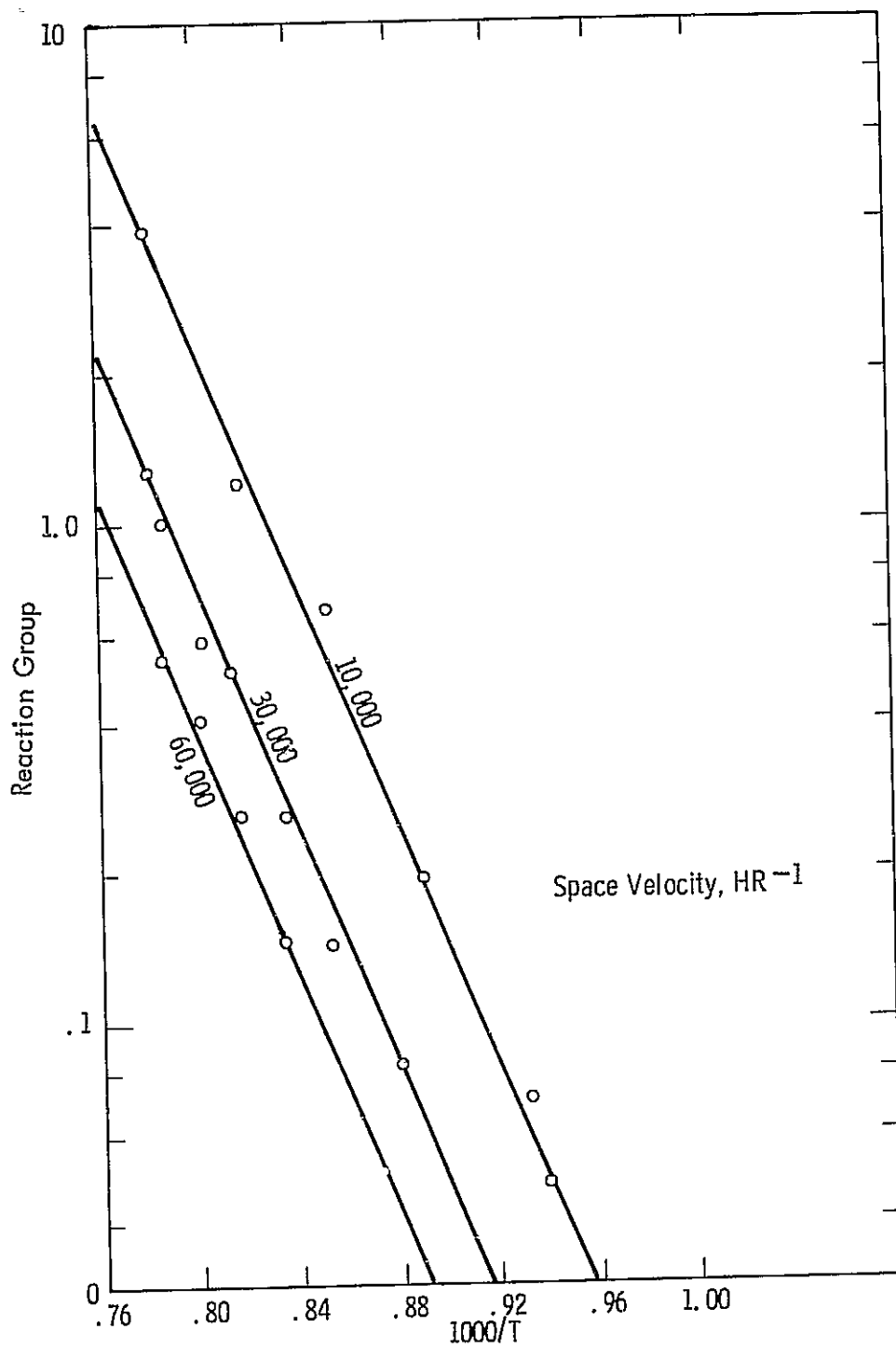


Figure 5.3.19 Arrhenius Plot of Sulfur Trioxide Reduction Data Obtained using WX-1 Catalyst

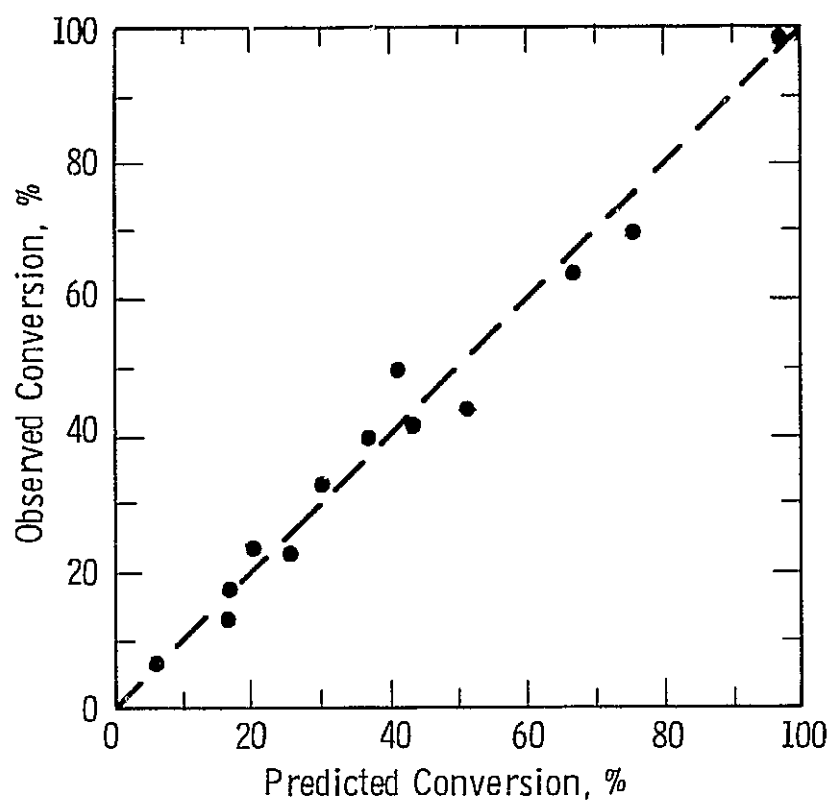


Figure 5.3.20 Agreement Between Observed Conversions and Those Predicted by Equation 5 for WX-1 Catalyst

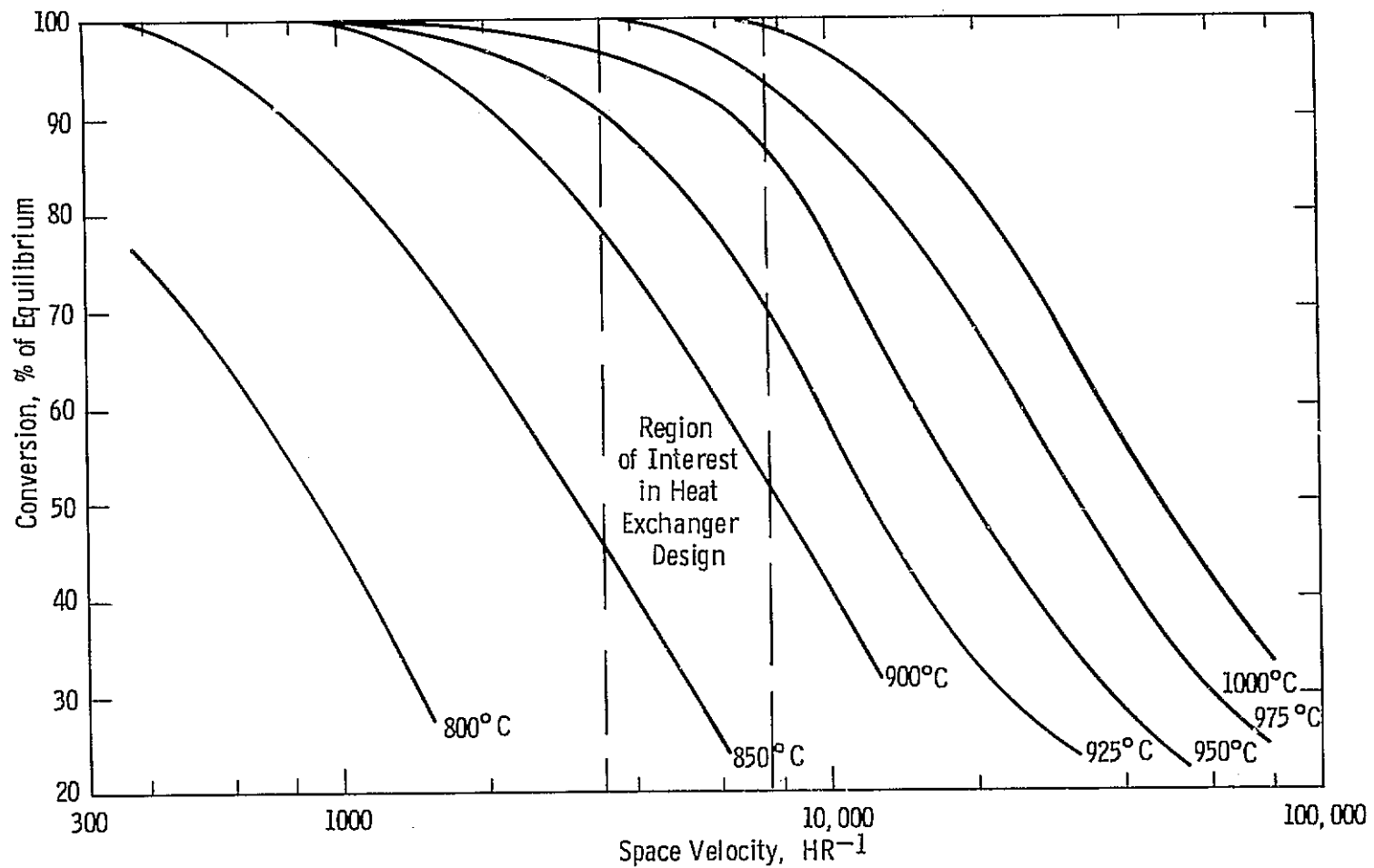


Figure 5.3.21 Predicted Sulfur Trioxide Conversions Over WX-1 Catalyst At Atmospheric Pressure

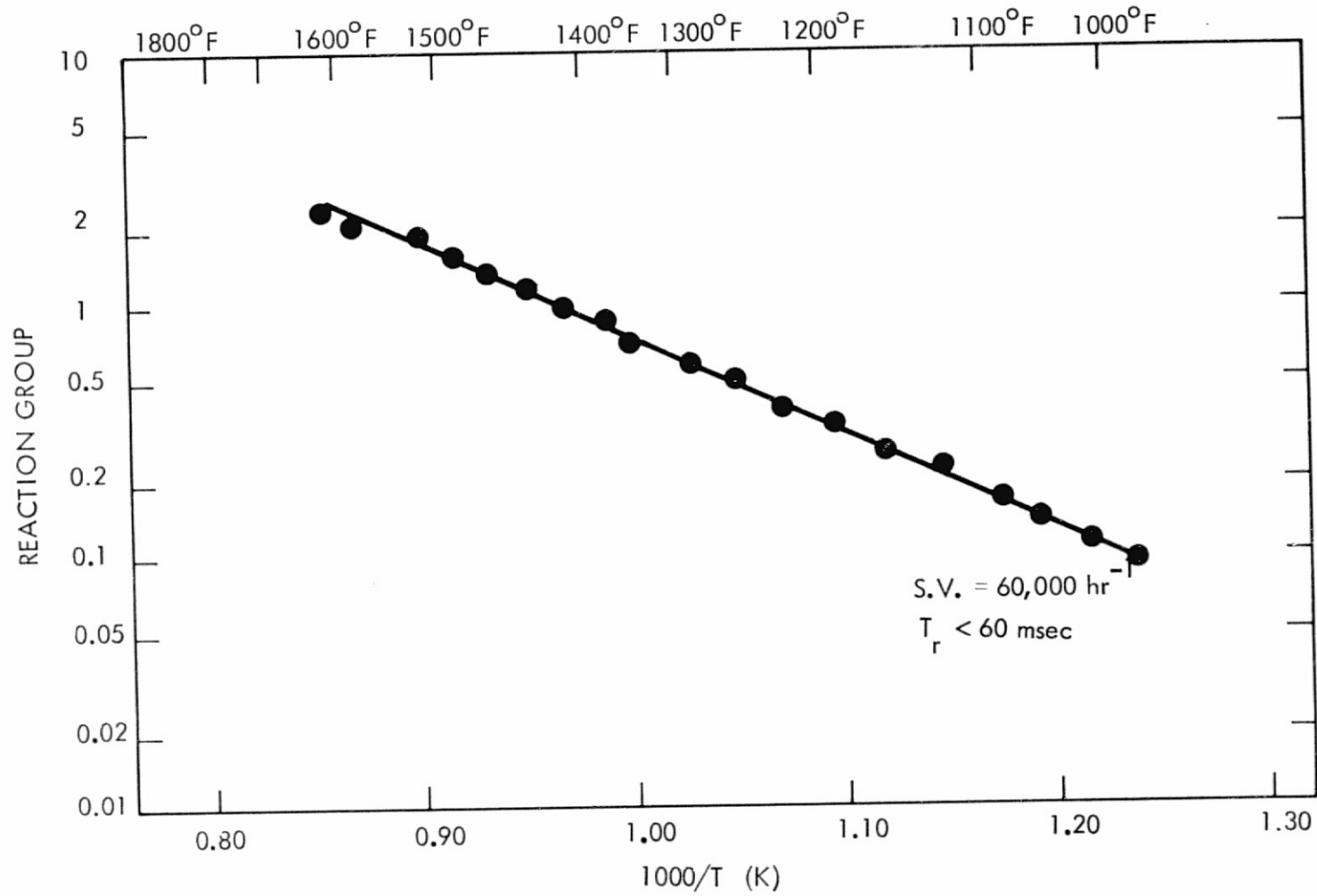


Figure 5.3.22 Sulfur Trioxide Thermal Reduction Reactor Catalyst Evaluation Results

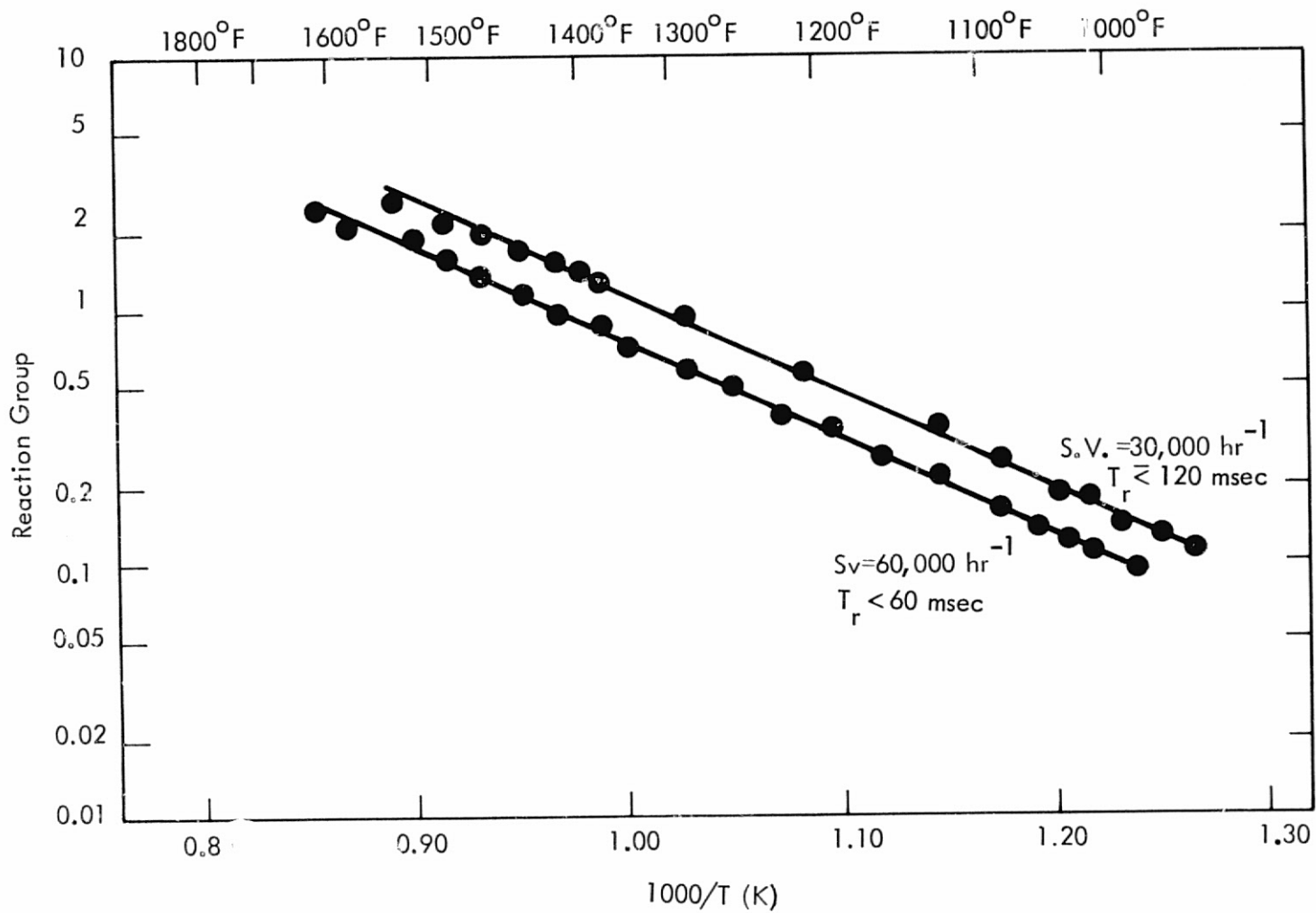


Figure 5.3.23 Sulfur Trioxide Thermal Reduction Reactor Catalyst Evaluation Results

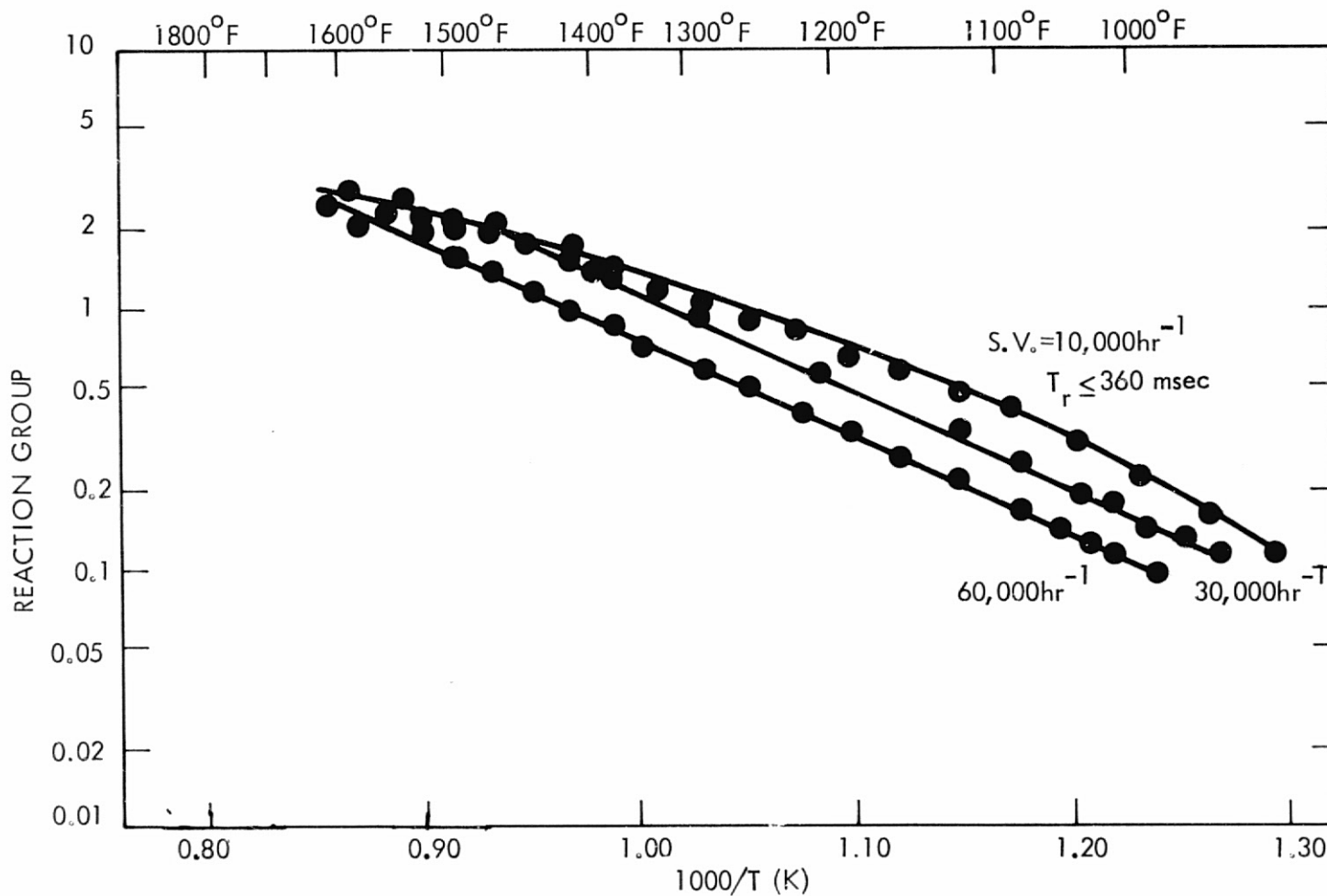


Figure 5.3.24 Sulfur Trioxide Thermal Reduction Reactor Catalyst Evaluation Results

given space velocities. A calculated equilibrium curve superimposes over the curves in Figure 5.3.25, supporting this hypothesis. A 1000 hour life test was conducted using the WX-2 catalyst. As Figure 5.3.26 indicates, the catalyst maintained its initial activity throughout the life test.

The data from both catalysts support the kinetic model. So far, only the WX-2 catalyst shows sufficient activity and life for use in the  $\text{SO}_3$  thermal reduction reactor. Accordingly, these catalyst results are being employed in the decomposition reactor design.

### 5.3.8 Status of Materials Technology

A materials investigation has been performed to determine unique or unusual materials requirements for the Sulfur Cycle Water Decomposition System. It has been determined that the critical problem areas involve the high temperature sulfuric acid loop. The remainder of the system operates at relatively low temperatures,  $>476\text{K}$  ( $>400^\circ\text{F}$ ) and thus can utilize commercially available components. The high temperature acid decomposition loop, because of the temperatures and pressures involved, departs significantly from standard sulfuric acid handling practice.

The acid decomposition process is carried out in three successive steps involving two heat exchangers and a packed acid contacting tower. Each of the major components of the acid vaporization loop represented in Battery "H" impose a unique and severe burden on structural materials, as will be indicated in the following review of materials considerations.

#### Material Considerations

The compatibility of the most common structural materials for sulfuric acid service is summarized in Table 5.3.9. The data are given for various acid concentrations with upper temperature limits noted. In those cases where the boiling point is indicated, it is assumed to be one atmosphere. Of the materials which appear in the table, only a few are suitable for use with acid at concentrations above 80 percent. Temperature limitations reduce the number of candidate materials even further. The materials with the highest probability of surviving the conditions encountered in the sulfur cycle water decomposition cycle are listed below, along with comments concerning suitability with respect to requirements listed previously.

#### Precious Metals

Gold, platinum and their alloys are noted for their resistance to acid attack to very high temperatures (Reference 19). Their cost restricts their use to thin clads on less expensive substrates. The use of precious metals in the water decomposition system is not considered because of the associated economic burden.

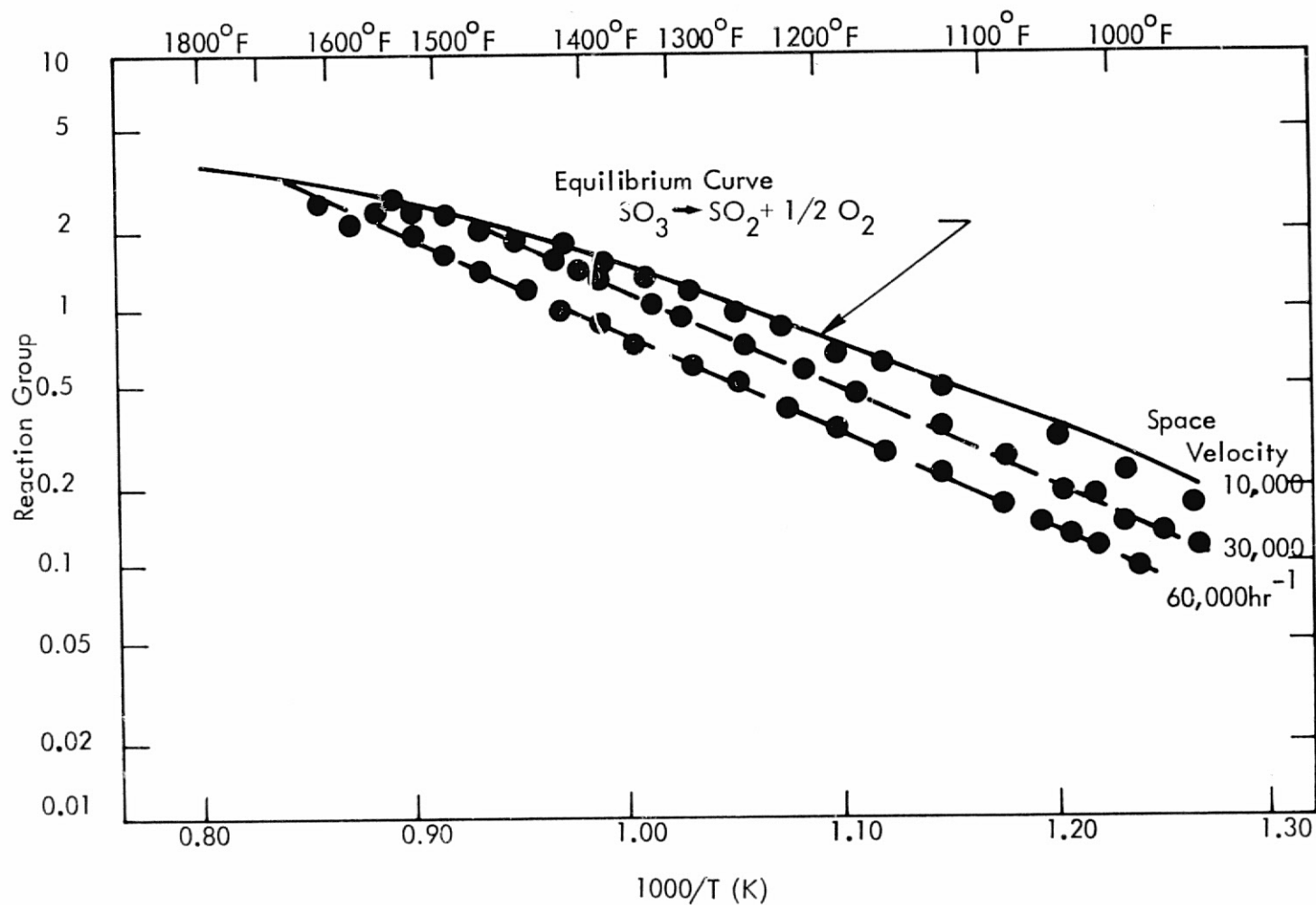


Figure 5.3.25 Sulfur Trioxide Thermal Reduction Reactor Catalyst Evaluation Results

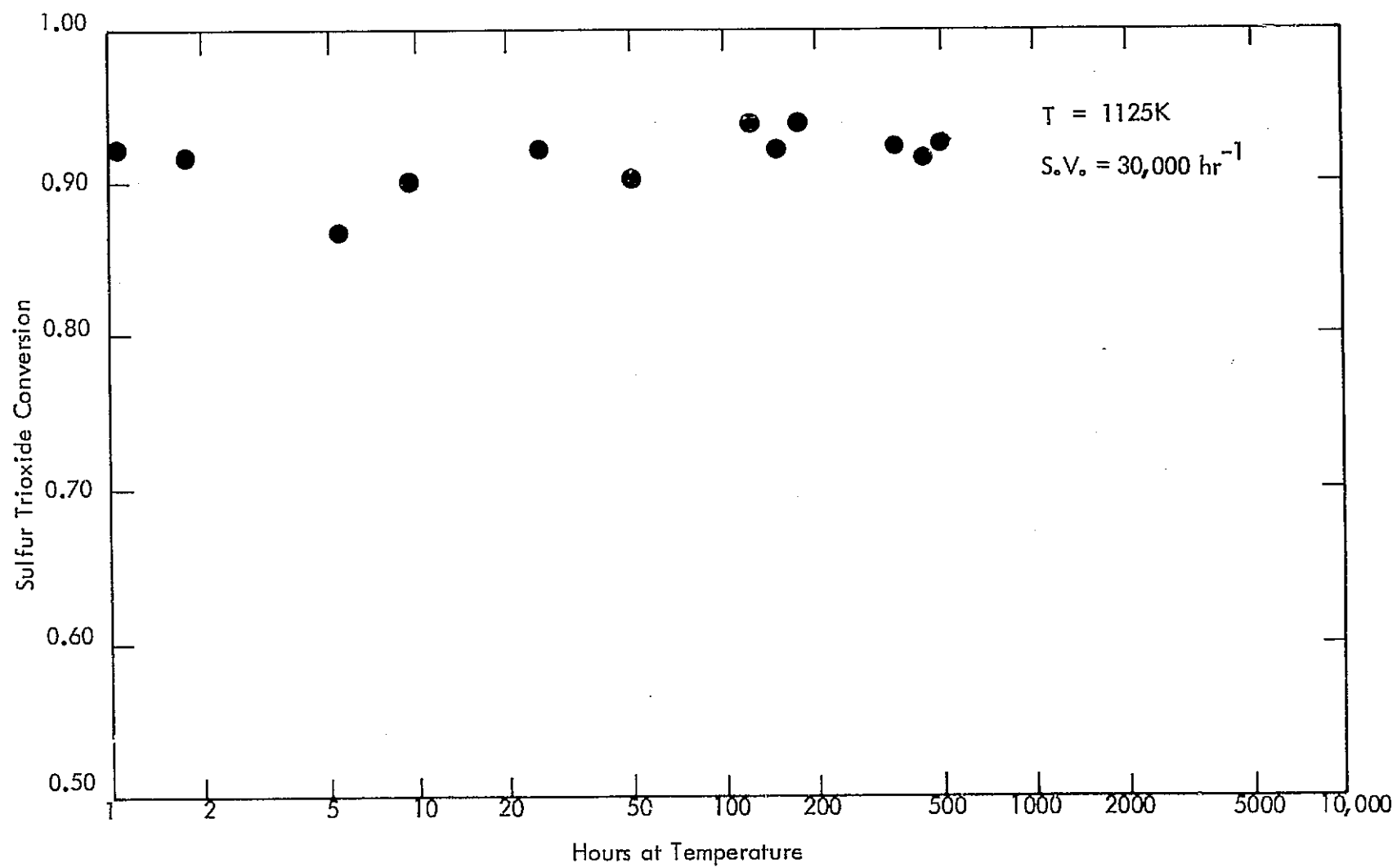


Figure 5.3.26 Sulfur Trioxide Thermal Reduction Reactor Catalyst Life Test Results

TABLE 5.3.9

MATERIALS OF CONSTRUCTION FOR SULFURIC ACID  
AND OLEUM HANDLING (REFERENCE 18)

MATERIALS	0-10% H <sub>2</sub> SO <sub>4</sub>	10-50% H <sub>2</sub> SO <sub>4</sub>	50-60% H <sub>2</sub> SO <sub>4</sub>	60-75% H <sub>2</sub> SO <sub>4</sub>	75-90% H <sub>2</sub> SO <sub>4</sub> (includes 60° acid)	90-98% H <sub>2</sub> SO <sub>4</sub> (includes 66° acid)	98-100% H <sub>2</sub> SO <sub>4</sub>
Cast iron					to 175°F	to 225°F	
Platinum, gold or gold-platinum alloys	to b.p.	to b.p.	to b.p.	to b.p.	to b.p.	to b.p.	to b.p.
Lead or lead lining	to b.p.	to 400°F	to 400°F	to 400°F	to 85%, 350°F; to 90%, 250°F	to 96%, 140°F	
High silicon cast iron (Duriron)	to b.p.	to b.p.	to b.p.	to b.p.	to b.p.	to b.p.	to b.p.
DURIMET 20	to b.p.	to 176°F	to 176°F	to 150°F	to 150°F	to 176°F	to 176°F
CHLORIMET 2 or 3	2 to b.p. 3 to b.p.	2 to b.p.; 3 to 200°F	2 to b.p.; 3 to 200°F	2 to 250°F 3 to 175°F	2 to 250°F 3 to 175°F	2 to 250°F 3 to 225°F	2 to 250°F 3 to 250°F
Glass lined steel (avoid thermal shock)	to 500°F	to 500°F	to 500°F	to 500°F	to 500°F	to 176°F	to 500°F
HASTELLOY ALLOYS B-C-D-F	B to b.p. C to b.p. D to b.p. F to 150°F	B to b.p. C to 200°F D to b.p. F to 150°F	B to b.p. C to 200°F D to b.p. F to 150°F	B to 250°F C to 175°F D to b.p. F not recommended	B to 250°F C to 175°F D to b.p. F not recommended	B to 300°F C to 200°F D to b.p. F not recommended	B to 300°F C to 200°F D to b.p. F not recommended
WORTHITE	to b.p.	to 175°F	to 150°F	to 140°F	to 140°F	93% to 150°F 98% to 175°F	to 175°F
Stainless steel type 316 and 317	to 5% below 150°F						
Carpenter Stainless 20Cb-3	to 5% below 250°F						
Ceramics SiN <sub>4</sub> SiC Cermets	to b.p.	to b.p.	to b.p.	to b.p.	to b.p.	to b.p.	to b.p.

REPRODUCIBILITY OF THE  
ORIGINAL PAGE IS POOR

TABLE 5.3.9

MATERIALS OF CONSTRUCTION FOR SULFURIC ACID  
AND OLEUM HANDLING (REFERENCE 18)  
(Continued)

MATERIALS	0-10% H <sub>2</sub> SO <sub>4</sub>	10-50% H <sub>2</sub> SO <sub>4</sub>	50-60% H <sub>2</sub> SO <sub>4</sub>	60-75% H <sub>2</sub> SO <sub>4</sub>	75-90% H <sub>2</sub> SO <sub>4</sub> (includes 60° acid)	90-98% H <sub>2</sub> SO <sub>4</sub> (includes 66° acid)	98-100% H <sub>2</sub> SO <sub>4</sub>
Rubber or neoprene lined steel	to 150°F	to 150°F					
Special hard rubber lined steel	to 200°F	to 200°F					
Butyl rubber lined steel	to 200°F	to 200°F	to 150°F				
Carbon and graphite	to 340°F	to 340°F	to 340°F	to 340°F	to 340°F	to 96%, 340°F	
MONEL, copper, 10% alum. bronze	to 200°F in absence of oxygen	to 200°F in absence of oxygen	to 200°F in absence of oxygen				
Tantalum (avoid fluoride contaminated acid)	to b.p.	to b.p.	to b.p.	to b.p.	to 375°F	to 375°F	to 375°F
HERESITE	to b.p.	to b.p. up to 35% to 150°F over 35%	to 150°F	to 150°F	to 150°F	to 150°F	to 150°F
Fluoropolymers (Teflon, Kynar)	to 400°F	to 400°F	to 400°F	to 400°F	to 400°F	to 400°F	to 400°F
KOROSEAL	to 140°F	to 140°F					
Cypress or redwood	to 190°F						
HAVEG 41	to 300°F	to 300°F	to 240°F	to 205°F	to 150°F		
ILLIUM G, 98 and R	G to b.p. 98 to b.p. R to b.p.	G to 195°F above 40%, to b.p. below 40%; 98 to b.p.; R to b.p.	G to 195°F 98 to b.p. R to b.p.	G to 140°F 98 to 195°F R to 180°F	G for 75-80% to 140°F, for 80-85%, to 195°F; 98 to 195°F; R to 180°F	G to 195°F 98 to 225°F R to 180°F	G to 195°F 98 to 225°F R to 180°F
Acid Proof Brick	to 600°F	to 600°F	to 600°F	to 600°F	to 600°F	to 600°F	to 600°F

REPRODUCIBILITY OF THE  
ORIGINAL PAGE IS POOR

## Tantalum and Its Alloys

The use of this refractory metal in acid service is increasing. At acid concentrations below 80 percent and temperatures below 464K (375°F), the excellent corrosion resistances more than offset the relatively high cost of this material. However, at acid concentrations above 80 percent tantalum has a tendency to become embrittled due to hydrogen pickup. Tantalum also reacts with  $\text{SO}_3$  and  $\text{O}_2$  at temperatures above 472K (400°F), limiting its use to lower temperatures.

## Alloys with High Silicon Content

Metallic alloys with high silicon content, such as Hastelloy D, Duriron, Durimet, and Chlorimet, are the standard structural materials used in the sulfuric acid industry today (References 18, 20). These materials are primarily casting alloys which are brittle, not readily joined by welding and are also notch sensitive. Consequently these materials are not normally utilized in a structural load-bearing capacity.

The effect of silicon content on the corrosion resistance of iron and steel is illustrated in Figures 5.3.27 and 5.3.28. In Figure 5.3.27 the corrosion rate of steel is shown as a function of acid concentration for a number of temperatures. In Figure 5.3.28 the corrosion behavior of Duriron, a cast iron with approximately 15 percent silicon, is shown at the boiling temperature as a function of acid concentration. A corrosion rate of 0.127 mm (5 mils) per year is indicated at the boiling point for concentrations above 80 percent. This corrosion rate is lowest for any non-precious metal. The effect of higher temperatures due to higher system pressure and the resulting increase in boiling point of the acid must be investigated.

## Glass and Glass Lined Steel

Glass or glass lined steel is commonly used for handling acid in the chemical industry. The behavior of glass in contact with sulfuric acid at various concentrations is shown in Figure 5.3.29 as a function of temperature (Reference 22). Above 80 percent concentration, glass is not resistant to attack at the acid boiling point. The reason for this behavior is shown in Figure 5.3.30 which shows the effect of superheated water on the corrosion of Pyrex glass. As the temperature increases above 422 K (400°F), the silica in the glass becomes hydrated forming,  $\text{H}_2\text{SiO}_3$ , which is soluble in superheated water. Thus, the incompatibility is not with sulfuric acid, but with water, a decomposition product. Pyrex, according to Corning, is their most corrosion resistant glass. As indicated by the curve in Figure 5.3.4, the corrosion rate approaches 0.76 cm per year (0.3 inch per year) as the temperature nears 478K (400°F) and presumably continues to increase above 478K (400°F). This corrosion rate is unacceptable for long time applications.

## Fluoropolymers (Teflon, Kynar)

Polymers such as Teflon exhibit excellent resistance to acid attack at all concentrations up to 478K (400°F) where thermal decomposition begins to occur. Polymers are used as liners on structural materials where loads are encountered, Reference 21.

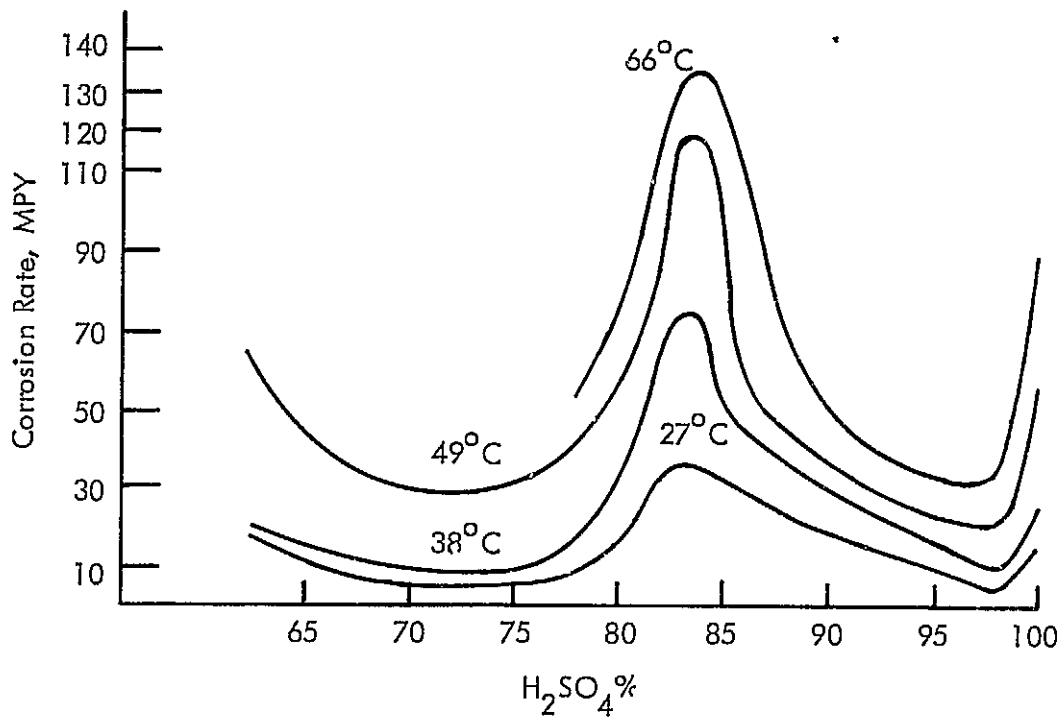


Figure 5.3.27 Corrosion of Steel by Sulfuric Acid, General Chemical Data (Reference 21)

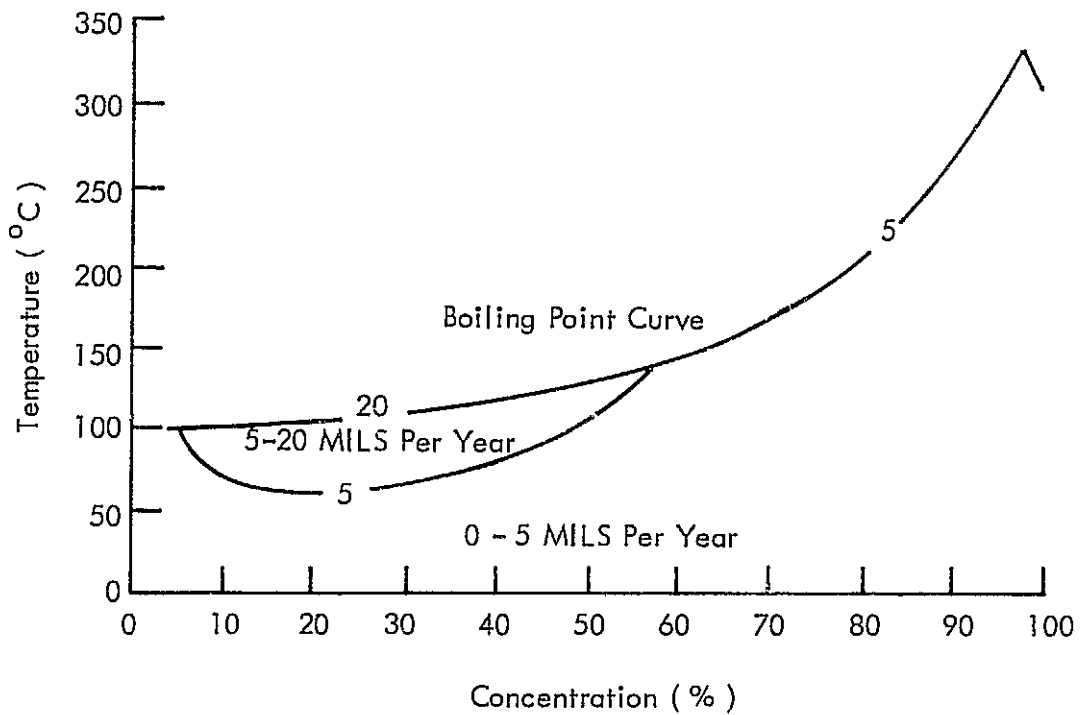


Figure 5.3.28 Corrosion Rate of Duriron in Sulfuric Acid (Reference 21)

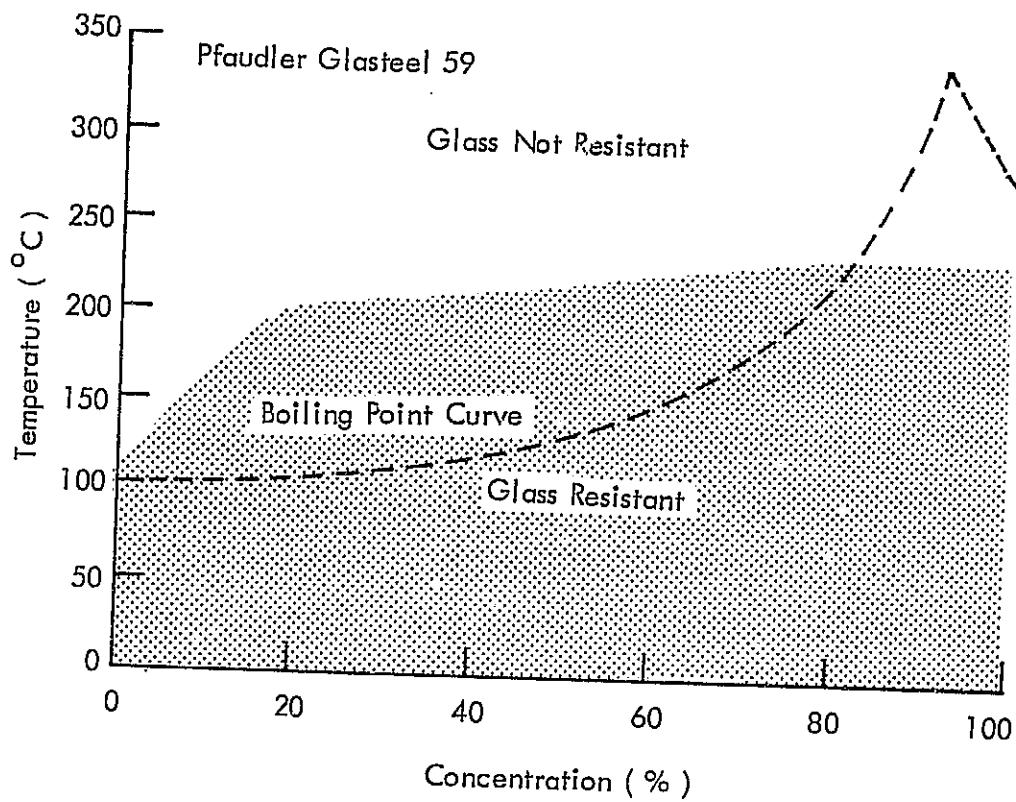


Figure 5.3.29 Corrosion Rate of Glass-Lined Steel in Sulfuric Acid

(Reference 21)

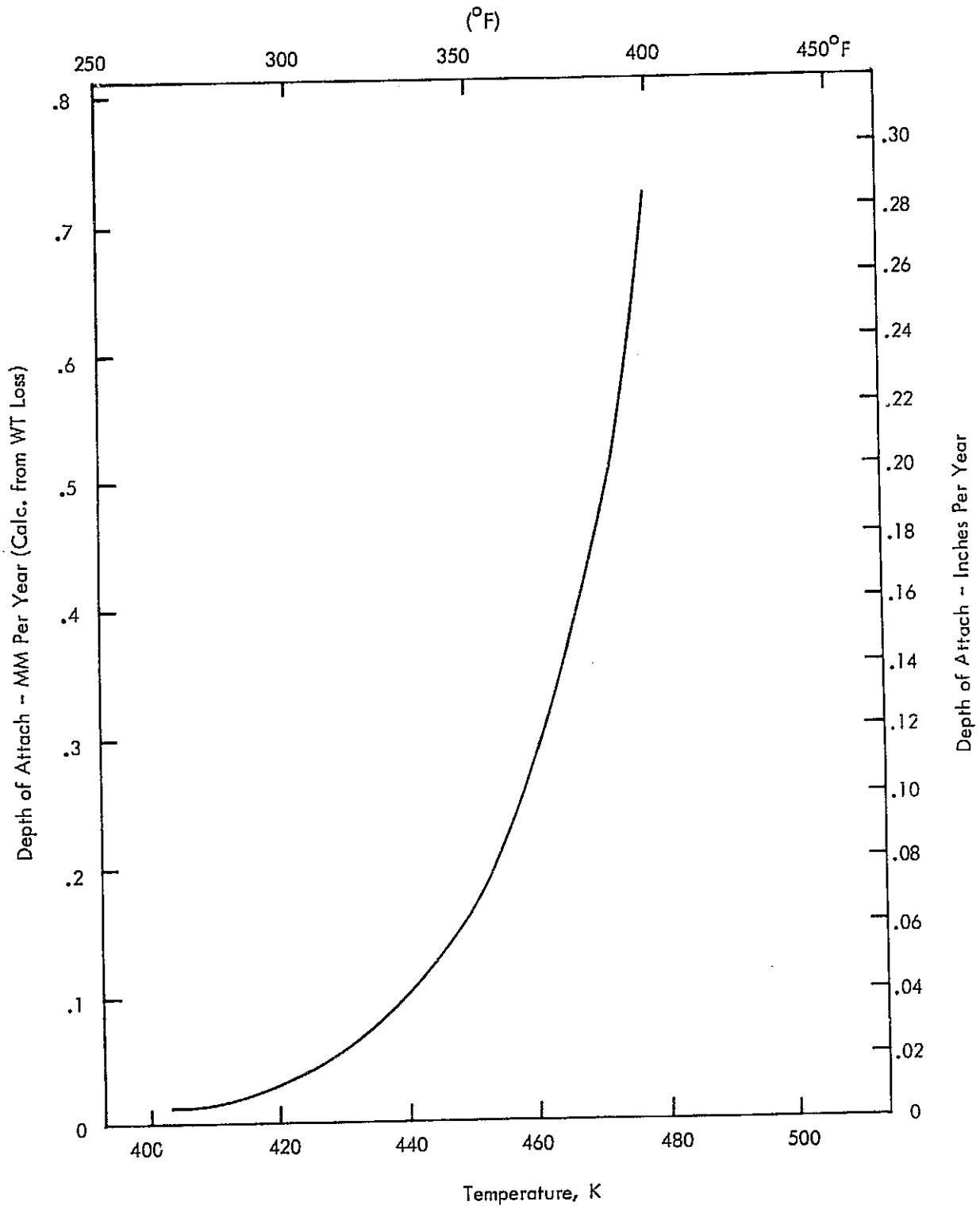


Figure 5.3.30 Affect of Superheated Water on Corrosion of Pyrex Glass (Corning No. 7740) (Reference 22)

### Acid Proof Brick

Acid proof brick is the most widely used non-metallic material for construction of sulfuric acid plants (Reference 21). The bricks are used to line carbon steel shells. The lining serve to reduce temperatures at the surface of the metallic vessel. The brick linings are usually backed-up by a polymer or asphaltic mastic to protect the metallic liner from acid seepage through the brick-work. Recent advances in mortars have helped in overcoming swelling, a problem encountered in mist acid conditions or where frequent filling and emptying occurs. Special construction techniques have been used to overcome the swelling problem. Acid proof bricks have been used at temperatures as high as 589K (600°F). With proper construction techniques, higher temperatures are possible.

### Ceramics and Cermets

Ceramics such as silicon carbide and silicon nitride are highly inert in oxidizing environments at elevated temperatures. Silicon carbide has been reported to withstand exposure to 95 percent concentrated sulfuric acid at 200°C (392°F) producing a weight gain after 288 hours equivalent to 5 μm (0.2 mils) per year (Reference 23). Exposure for greater than 1000 hours to 80 percent concentrated sulfuric acid at the boiling point yielded a weight gain equivalent to 2.5 μm (0.1 mil) per year. Silicon nitride, which exhibits similar elevated temperature oxidation resistance, will most likely behave in a similar manner. Cermets consisting of a mixture of elemental chromium or chromium alloy powder and alumina consolidated to a high density has been shown to have excellent resistance to concentrated sulfuric acid at low temperatures (Reference 24). Quantitative data for elevated temperature exposure at high acid concentrations are lacking.

### Summary of Materials Technology

The pertinent characteristics of available materials with known compatibility with sulfuric acid is summarized in Table 5.3.10. Precious metals meet all the prerequisites, however, their very high cost for this application is prohibitive. High silicon containing alloys, such as Duriron, have acceptable corrosion rates up to the boiling point under normal atmospheric pressures. Corrosion rates at higher pressures must be determined. Methods for joining the cast material to provide leak tight joints must be developed. Glass, because of its poor compatibility with superheated water, must be restricted to use at temperatures below 422K (300°F). Polymers are restricted because of their thermal instability at temperatures above 478K (400°F). Acid proof brick, because of its insulating properties, make an excellent liner or barrier material for reducing temperatures between the process stream and the pressure vessel wall.

### Materials for Use in the High Temperature - Superheated Steam Environment

In the reduction reactor, DR-1, the process stream which consists primarily of gaseous water and SO<sub>3</sub> is heated from 725 to 1144K (845 to 1600°F) and the SO<sub>3</sub> is reduced to SO<sub>2</sub> and O<sub>2</sub> by catalytic action. Compatibility data for structural materials exposed under these

TABLE 5.3.10

## SUMMARY OF CHARACTERISTICS OF AVAILABLE MATERIAL FOR USE IN SULFURIC ACID LOOP

Material	Compatibility With H <sub>2</sub> SO <sub>4</sub>	Compatibility With Superheated Water, SO <sub>3</sub> & SO <sub>2</sub>	Strength	Fabricability	Joinability	Thermal Conductivity	Relative Cost
Precious Metals (Gold, Platinum)	Excellent	Excellent	Fair	Must be used as clad on substrate	Good	Excellent	Very High
Metals High in Silicon (Duriron)	Excellent	Poor	Fair	Available as castings	Poor	Fair	Moderate
Glasses (Pyrex)	Excellent below 422K	Poor	Poor	Must be used on metal substrate	Poor	Poor	Low
Polymers (Teflon)	Excellent below 473K	Poor	Poor	Must be used on metal substrate	Good	Poor	Low
Acid Proof Bricks	Excellent	Excellent	Fair	Available as bricks and simple shapes	--	Poor	Low
Ceramics SiC, SiN Cermets	Excellent	Excellent	Fair	Available as bricks and tubes	Poor	Excellent	High

conditions are nonexistent. Some work however, has been done to investigate the behavior of a number of alloys in superheated steam at comparable temperatures. The most extensive research into the performance of materials in high temperature steam has been conducted by the ASME Research Committee on High Temperature Steam Generation (Reference 25). Test results indicated that highly alloyed superalloys, such as Inconel 600, Incoloy 800, Hastelloy X, etc., promise a high degree of probability of meeting the requirements imposed by the operating conditions in DR-1. Alloys high in chromium which exhibit excellent oxidation resistance in air, also hold up well in superheated steam. The introduction of  $\text{SO}_3$ ,  $\text{SO}_2$ , and  $\text{O}_2$  into the superheated steam introduce another degree of complexity. Thermodynamic analysis indicates that under the expected oxidizing conditions, sulfidization corrosion of nickel will not be a problem. Experimental data under DR-1 operating conditions will be required to verify material corrosion behavior.

#### Recommended Programs

- The corrosion behavior of Duriron, cast iron containing 15 percent silicon, in contact with boiling sulfuric acid over the concentration range of 80 to 100 percent under pressures up to 2069 kPa (300 psi) must be determined for an extended period of time; e.g., >10,000 hours.
- Investigate the sulfuric acid corrosion resistance of steel substrates coated with chemical-vapor-deposited silicon. Recent advances in coating technology have made it possible to produce complex geometrical shapes with a uniform adherent coating. Steel which has been fabricated to a final shape can be siliconized by deposition of a layer of silicon of an appropriate thickness followed by a heat treatment to diffuse the silicon into the substrate. The resulting structure has a surface with a high silicon content which is highly resistant to sulfuric acid corrosion. The corrosion behavior of such a structure under boiling acid conditions must be determined.
- Ceramics such as silicon carbide, silicon nitride, and cermets (77 Cr-23  $\text{Al}_2\text{O}_3$ ) possess excellent resistance to sulfuric acid corrosion at ambient temperature and at low acid concentration. These materials have excellent thermal conductivity, can be fabricated into tubing of limited lengths, and can be joined by brazing. They possess sufficient potential to warrant further characterization.
- Compatibility of the organic heat transfer fluid with sulfuric acid under conditions which exist in the acid vaporizer must be investigated to determine compatibility of the process steam with the heat transfer media.

C-3

## 6.0 SUMMARY OF RESULTS

The scope of work called for in Task III of the "Studies of the Use of Heat from High Temperature Nuclear Sources for Hydrogen Production Processes," reported herein, requires that a conceptual design of an integrated nuclear-hydrogen production plant be prepared using the Westinghouse Sulfur Cycle hydrogen production process. An evaluation of the economics, environmental effects, benefits, and the program, in respect to technical areas, costs, and schedules, needed to develop the hydrogen production system to the demonstration stage is to be included. The major results of the Task III efforts are briefly summarized in this section.

### 6.1 CONCEPTUAL DESIGN OF THE NUCLEAR DRIVEN WATER DECOMPOSITION PLANT

In the Westinghouse Sulfur Cycle process, hydrogen and sulfuric acid are produced electrolytically by the reaction of sulfur dioxide and water. The process is completed by vaporizing the sulfuric acid and thermally reducing, at higher temperatures, the resultant sulfur trioxide into sulfur dioxide and oxygen. Following separation, sulfur dioxide is recycled to the electrolyzer. As in conventional water electrolysis, hydrogen is produced at the electrolyzer cathode. Unlike conventional electrolysis, sulfuric acid rather than oxygen, is produced at the anode. Operation in this fashion reduces the theoretical power required per unit of hydrogen production by more than 85 percent over that required in water electrolysis. This is partially offset, however, by the need to add thermal energy to the process in the acid vaporizer and the sulfur trioxide reduction reactor. By avoiding the high overvoltages at the oxygen electrode of a conventional electrolyzer, as well as the inefficiencies associated with power generation, this hydrogen generation process provides overall thermal efficiencies approximately double those attainable by conventional electrolytic hydrogen and oxygen production technology.

The overall process flowsheet for the water decomposition system is shown in Figure 6.1. The energy source for the water decomposition system is a very high temperature nuclear reactor (VHTR) producing both electric power and a high temperature helium stream to the process. Within Battery G, electrical power, water, and recycled sulfur dioxide are consumed to produce hydrogen and sulfuric acid. The hydrogen, of electrolytic purity, is withdrawn as product while the sulfuric acid is sent to Battery H. Using thermal energy from the VHTR, the acid in Battery H is vaporized to produce a mixture of steam and sulfur trioxide. The sulfur trioxide is thermally reduced at higher temperatures to produce sulfur dioxide and oxygen. These gases are separated within Battery I. The sulfur dioxide is recycled to Battery G and the oxygen is available as a by-product for sale. The only major consumable for the process is water. Small quantities of make-up are naturally required to compensate for sulfur leakage and losses, catalyst deactivation, and similar things. The sulfur oxides are recycled and all process and plant energy needs are provided by the VHTR.

The plant is presumed to be located at the hypothetical Middletown site. A preliminary plot plan was prepared, showing the general location and space requirements for all plant facilities, including the nuclear heat source. The plot plan has indicated that the hydrogen

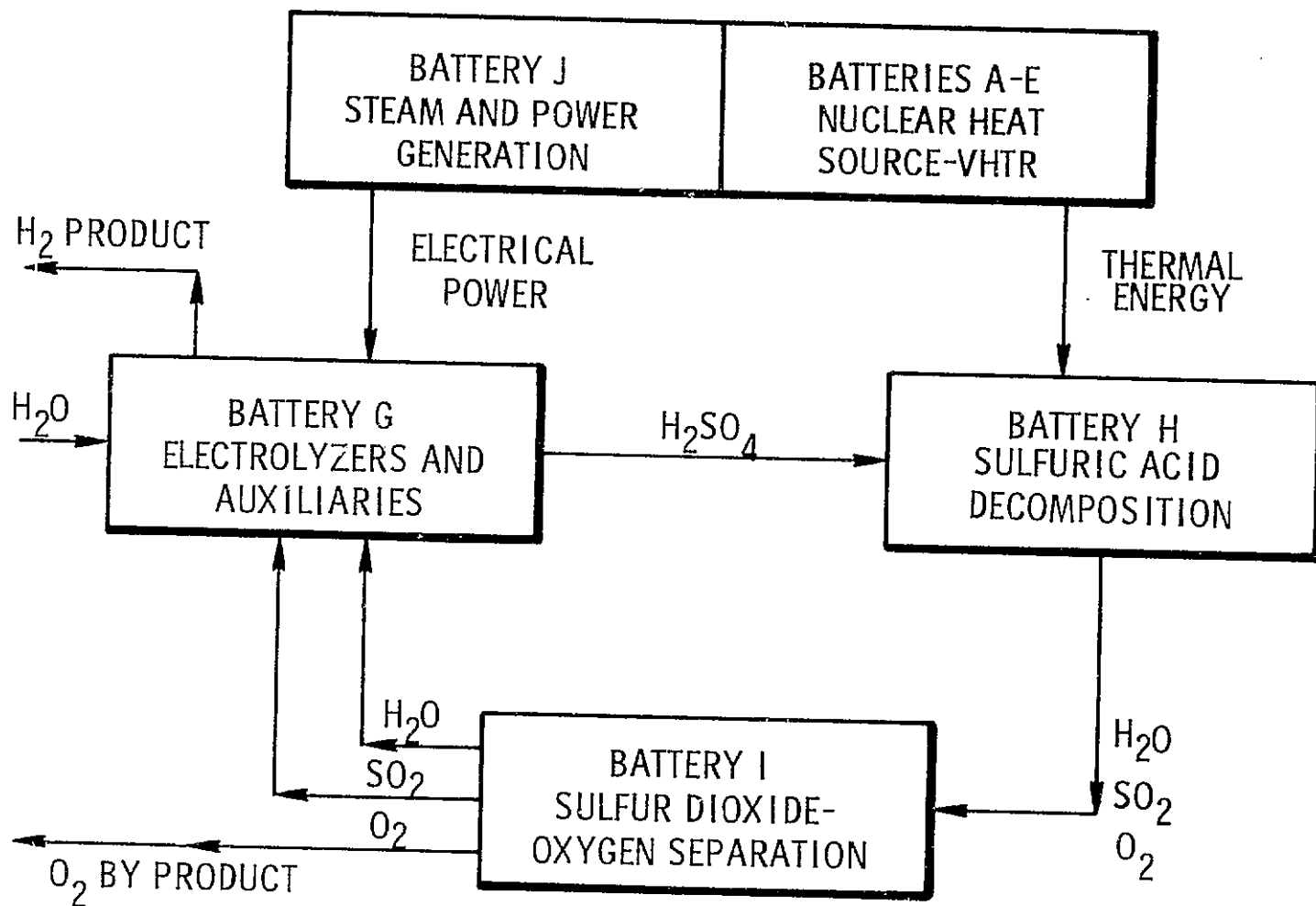


Figure 6.1 Overall Process Schematic

production facilities can be arranged so that piping and other interconnections are kept to a minimum while sufficient space is provided to allow for constructability and maintainability of the unit.

The VHTR provides 1283K (1850°) helium working gas for electric power and process heat. The plant sized to produce approximately ten million standard cubic meters per day (or 380 million standard cubic feet per day (SCFD)) of electrolytically pure hydrogen and has an overall thermal efficiency of 45.2 percent.

## 6.2 PLANT ECONOMICS

The cost of producing hydrogen has been evaluated for the plant conceptual design with estimates made for the capital, operation and maintenance and fuel costs. The effects on hydrogen production costs of various capacity factors fuel costs and type of ownership also were considered.

### 6.2.1 Capital Costs

The capital costs estimate is based on preliminary sizing of most of the major plant equipment and determining appropriate costs for that equipment. Factors, based on experience with these types of systems, were used to account for the costs of installation, piping, valves, instrumentation, structures, and miscellaneous equipment. Indirect costs were also estimated by applying appropriate factors.

The total plant investment, including the direct costs plus contingencies, indirect costs, and interest during construction, but excluding escalation, has been estimated to be \$994,795,000.

### 6.2.2 Operation and Maintenance Costs

The costs of operation and maintenance includes the expense of maintaining a plant staff, consumable supplies and equipment, outside support services, miscellaneous items of cost, and indirect costs of maintaining the plant working capital. The total operating and maintenance costs at an 80% plant capacity factor have been estimated at \$6,344,000 including direct and indirect costs.

### 6.2.3 Fuel Costs

Fuel costs are all expenses associated with the nuclear fuel cycle of the VHTR. These include items such as procurement of all materials, uranium enrichment, fuel fabrication, fuel reprocessing, credits for materials of value in spent fuel, and carrying charges in all parts of the fuel cycle. The fuel cycle costs have been calculated to be 24.75¢/RJ (26.1¢/10<sup>6</sup> Btu) based on a specified set of ground rules. The plant, operating at an 80 percent capacity factor and a thermal output of 3345 mw, accumulates a total annual fuel cost of \$20,850,000.

#### 6.2.4 Hydrogen Production Costs

The hydrogen production cost is made up of the contributions of capital, operation and maintenance, and fuel costs. These are normally calculated on an annual basis. The percentage of the plant investment that is charged against production each year is a function of the type of plant ownership; i.e., utility or industrial, and the manner in which the owner can do business. The annual charge on non-depreciating assets; e.g., land, is 10 percent for either type of ownership while the annual charge on depreciating assets is 15 percent for utility ownership and 25 percent for industrial ownership. The cost of hydrogen production is shown in Table 6.1 for both bases.

TABLE 6.1

#### HYDROGEN PRODUCTION COST COMPARISON (80% Capacity Factor)

Ownership	
Utility	Industrial
5.96¢/std m <sup>3</sup>	9.31 ¢/std m <sup>3</sup>
(\$1.59/MSCF)	(\$2.48/MSCF)
\$4.65/GJ	\$7.26/GJ
(\$4.90/10 <sup>6</sup> Btu)	(\$7.66/10 <sup>6</sup> Btu)

These costs are equivalent to a "gate selling price." The cost to the ultimate consumer would be one of these production costs plus the allocated capital and operating costs of transmission and distribution.

#### 6.2.5 Sensitivity Analysis

The cost of hydrogen production from the plant will vary with the cost of fuel, the type of ownership, and the utilization; i.e., capacity factor, of the facility. For the base case calculation, it was assumed that fuel costs were 24.75¢/GJ (26.1¢/10<sup>6</sup> Btu), the capacity factor was 80 percent, and utility ownership prevailed. The hydrogen production cost was shown to be relatively insensitive to increases in nuclear fuel cost. For example a 92 percent increase in nuclear fuel cost (from 26.1 to 50¢/10<sup>6</sup> Btu) would increase the hydrogen production cost by only 12 percent.

The manner in which the capacity factor affects the production cost has been estimated with all of the cost assumptions the same as the base case. With the capacity factor allowed to vary within a range of 40 to 90 percent, the production costs range from a high of 11.39¢/std m<sup>3</sup> (\$3.11/MSCF) at 40 percent capacity to a low of 5.35¢/std m<sup>3</sup> (\$1.43/MSCF) at 90 percent capacity.

### 6.2.6 Comparative Hydrogen Production Cost

The economic value of a hydrogen production system can only be assessed by comparing the cost of production of a system to competitive systems. As part of the study performed under Task II under this contract, the hydrogen production cost for water electrolysis and coal gasification systems were determined using the same economic groundrules. These costs can therefore be used for realistic comparative cost evaluations to assess the attractiveness of any of the systems.

The hydrogen production plants selected for economic comparison with the Sulfur Cycle Water Decomposition System were a near-term technology water electrolysis plant using Tele-dyne electrolyzers, a Koppers-Totzek coal gasification plant and a coal gasification plant using the developing Bi-Gas technology. The results of the production cost assessment, plotted as a function of the cost of coal, are shown in Figure 6.2.

The water electrolysis plant, using near term technology, is assumed to be powered by a dedicated light water nuclear power plant to provide the least expensive energy cost for the process. The electrolysis plant, including water treatment and all auxiliaries and service loads, is estimated to operate at an efficiency of 81 percent. The electrical generation efficiency, for the LWR, is estimated to be 34 percent, resulting in a net overall process efficiency of 28 percent. Nuclear fuel costs for the light water reactor were assumed to be 19.9¢/GJ (21¢/million Btu), leading to a power cost, on the economic groundrules selected; e.g., no escalation, 1974 costs, etc., of 12.8 mills/kwh. An advanced water electrolysis plant, using a VHTR to produce electricity in a combined cycle at an efficiency of 50 percent and high pressure, high current density solid polymer electrolyte (SPE) electrolyzers, has been estimated, in Reference 4, to have a net overall process efficiency of 42.9 percent and production costs somewhat higher than the base line costs for the VHTR-Sulfur Cycle Water Decomposition plant.

The two coal gasification processes result in reasonably comparable hydrogen costs which vary, naturally, as a function of the cost of coal fed to the process. The thermal efficiency for these units, based on all of the energy consumed in the process; e.g., oxygen production for the gasifiers, compressor work, etc., is in the order of 50 percent when hydrogen, at pressures suitable for pipeline delivery, is the only plant product.

The hydrogen cost for the water decomposition plant represents the capital, O&M, and fuel costs of the integrated, self-sufficient production plant defined in the conceptual design. The cost is evaluated at a nuclear fuel cost of 24.75¢/GJ (26.1¢/million Btu), which, although higher than the fuel cost of a LWR, represents that which can be achieved in a VHTR using comparable economic groundrules.

The comparative economic evaluation shows that the cost of hydrogen produced by the Sulfur Cycle Water Decomposition System is substantially lower than the cost of hydrogen produced by water electrolysis. Further, nuclear water decomposition holds great promise of lower hydrogen production costs as reasonable extrapolations of future nuclear and coal costs are made.

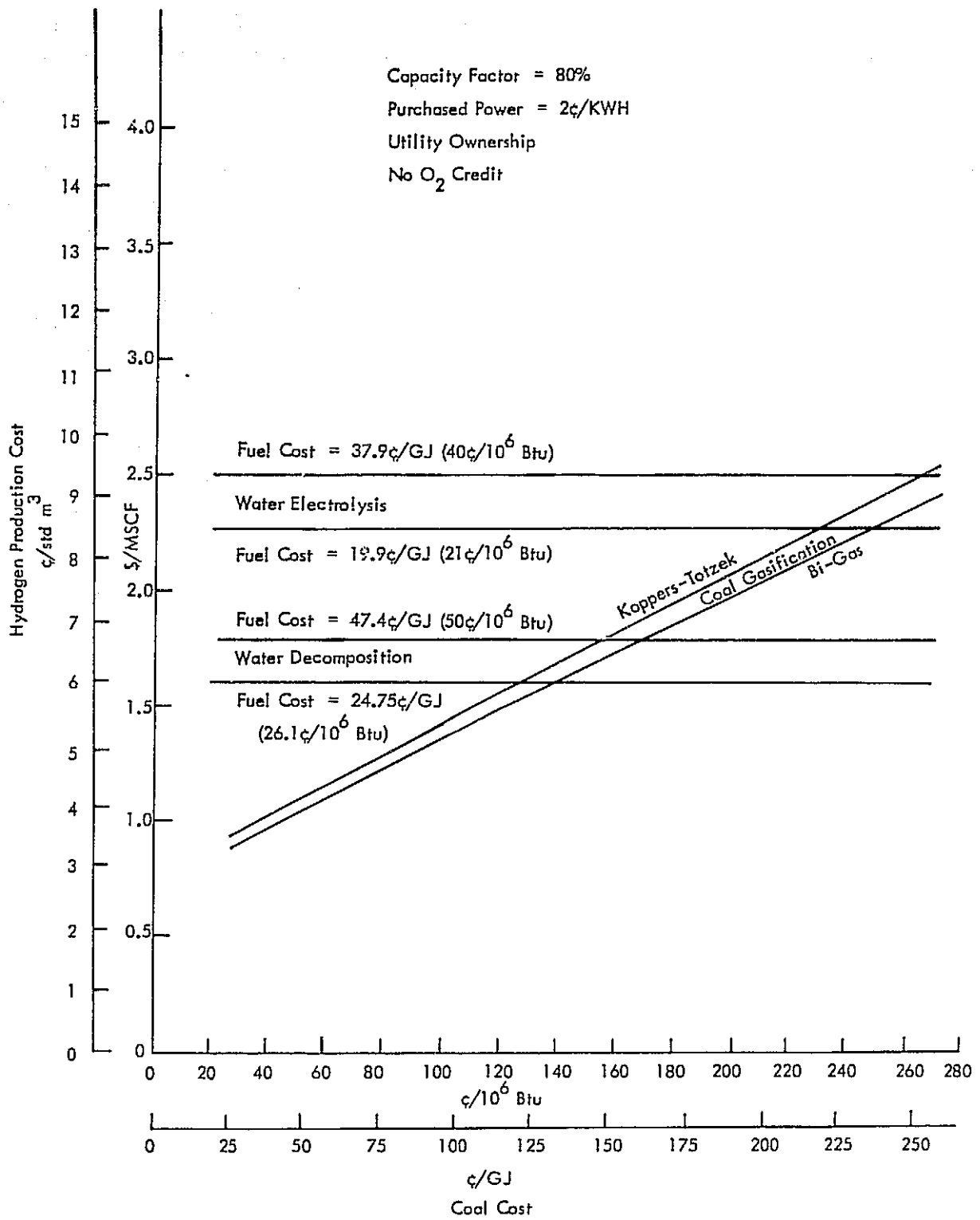


Figure 6.2 Comparative Hydrogen Production Costs

### 6.3 ENVIRONMENTAL IMPACT

The evaluation of the environmental and social impacts of the construction and operation of the hydrogen plant has indicated that no major adverse impacts are anticipated. The Middletown site is particularly suitable for a project of this nature and adverse impacts on air, water, land, ecosystems, resources, and local social structure will not be anticipated. Even though the source of radiological releases for this facility is different from conventional nuclear plants, the magnitude and type of radiological impacts resulting from the operation of the VHTR are not unique or special. These can be accommodated by the design so that there will be no adverse environmental impacts.

A comparison of the benefits and costs (environmental, social economic) has indicated that a favorable balance exists for the proposed plant, with the benefits outweighing the costs. This evaluation includes the benefits and costs as applicable to both the local and national levels.

The most significant benefit of the proposed facility lies in the value of the hydrogen generated at the plant. While the end use and location of use has not been specified, the hydrogen product provides an energy form that is both useful and versatile for a number of potential purposes. Potential uses of hydrogen include use as a feedstock in the production of synthetic natural gas, ammonia production for subsequent fertilizer applications, direct reduction of iron ore, and use as a clean, storable, and transportable fuel.

The construction and operation of the facility will lead to local benefits which consist of the creation of jobs (3,000 peak construction, and 120 operating force), local personal income and small business growth and taxes (\$20 million annual local property taxes).

The proposed hydrogen production facility will produce hydrogen as a useful product to the nation. In addition, it will generate jobs, local economic growth and tax income that will benefit the local community. The environmental, social and economic costs to the nation and the community are not significant as a result of the selection of the Middletown site and the benefits outweigh the costs at both the national and local levels.

## 6.4 DEVELOPMENT PLAN FOR COMMERCIAL PLANT

Since the conception of the Sulfur Cycle Water Decomposition System in 1973, laboratory work, funded by the Westinghouse Electric Corporation, has established the technical feasibility of the two major steps of the process, i.e., the sulfur trioxide thermal reduction step and the electrochemical hydrogen generation. The development effort required to build upon the early laboratory work and bring the water decomposition system to commercial viability is summarized below.

The conceptual design effort has shown the attractiveness of integrating the hydrogen generation facilities with a VHTR nuclear heat source. Development efforts in the joint AEC/NASA nuclear rocket (NERVA) program and the gas cooled reactor programs in the United States and Europe have provided a base of technology upon which the VHTR is built. To achieve, both safely and economically, the high temperatures required for process needs requires additional development beyond that already accomplished. These needs have been evaluated as part of ERDA Contract AT(11-1)-2445, and are summarized as follows.

### 6.4.1 Development of the VHTR

The research and development program required to bring the VHTR to first large-scale demonstration reflects the conceptual design of the VHTR as presented in this report. Depending upon the results of further design studies, optimization and trade-off studies, and the results of the research and development as the program proceeds, the details of the program may require adjustment.

Some of the assumptions used in developing the research and development program, its schedule and costs, were:

1. All costs are in July, 1974 dollars.
2. The costs reflect "contractor" costs only. Nothing has been added, for example, for costs accrued by ERDA in administering the program.
3. No major facility costs are included. It is assumed, for example, that a Helium Turbine Test Facility is funded elsewhere and the facility is available to and adequate for the VHTR program.
4. Irradiation testing is done in government facilities. Therefore, no costs have been included for irradiation time, in-pile loops, or high level hot cell facilities.
5. No costs are included for labor or services provided in government furnished facilities, nor any costs included for modifications to existing facilities or construction of new facilities.

The research and development program, with a duration of about twelve years, culminates in the commercial operation of a large scale demonstration plant. This plant should be of a sufficient size to be commercially viable and would desirably be industrially sponsored.

The total cost of the VHTR program is estimated to be \$240.6 million, not including costs of a demonstration plant. This includes a 25 percent contingency to account for omissions, errors, and as an allowance for changes in direction of the program as the work proceeds.

#### 6.4.2 Development of the Sulfur Cycle Water Decomposition System

The development of the hydrogen generation process is expected to proceed in the six phases: supporting research, scientific demonstration, process evaluation, pilot plant development, pilot plant, and demonstration or commercial plant. Table 6.2 summarized the approximate size and scope of equipment employed in each phase up to and including the pilot plant. The costs of the program are predicated on the diligent prosecution of the development leading to a large scale demonstration or commercially sized plant operational by 1990. In this manner, the development of both the VHTR and the hydrogen production process can proceed, in logical fashion, along parallel paths with the integration of the two facilities being made at the large scale demonstration stage.

The cost of the development program for the Sulfur Cycle Water Decomposition process, has been estimated, and some of the assumptions used in developing the cost of the development program were as follows:

- All costs are in July, 1974 dollars. This provides consistency in cost basis between the development costs, the development costs for the VHTR, and the cost estimate for the conceptual design.
- The costs reflect "contractor" costs only. Nothing has been added, for example, for costs accrued by government agencies in administering the program.
- The cost of design and construction of a pilot plant is included, but no costs are estimated for the operation of the pilot plant.
- No costs are included for a large demonstration or commercial unit (Phase 6.0).
- A 25 percent contingency is applied to all development cost estimates to account for omissions, errors, and as an allowance for changes in direction of the program as the work proceeds.

The total program cost is estimated to be \$63,300,000. Figure 6.3 shows the estimated cost of the development program as a function of both phase and year.

TABLE 6.2

## SULFUR CYCLE WATER DECOMPOSITION SYSTEM DEVELOPMENT PROGRAM SUMMARY

DEVELOPMENT PHASE	SUPPORTING RESEARCH	LABORATORY DEMONSTRATION	PROCESS EVALUATION	PILOT SCALE DEVELOPMENT	PILOT PLANT
PURPOSE	PROOF-OF-PRINCIPLE. ACQUISITION OF KINETIC AND FUNDAMENTAL DESIGN DATA.	PROCESS VERIFICATION. ACQUISITION OF PRESSURIZED DESIGN DATA.	PRELIMINARY DEMONSTRATION OF KEY COMPONENTS.	SCALE-UP KEY PROCESS EQUIPMENT.	EVALUATE INTEGRATED PLANT OPERATION.
EQUIPMENT SCOPE	AS REQUIRED TO OBTAIN FUNDAMENTAL INFORMATION.	INTEGRATED OPERATION OF MAJOR PROCESS SECTIONS.	INTEGRATED PROCESS AND SUPPORTING AUXILIARIES.	INTEGRATION OF ALL PLANT FUNCTIONS.	OPERATION OF ALL PROCESS AND UTILITY FUNCTIONS IN COMMERCIAL SIZE MODULES.
EQUIPMENT SIZES					
ELECTROLYZER (TOTAL CAPACITY)	1 WATT	10-50 WATTS	1 KWE	30-100 KWE	1-5 MWE
SO <sub>2</sub> DECOMPOSITION	1/8" x 10" GLASS TUBE	1" x 12" METAL TUBE	SEVERAL 1" x 24" METAL TUBES	SMALL SCALE PROTOTYPE	1/4 TO FULL SCALE REACTOR
PLANT AREA	TABLE TOP	HOOD	20' x 20'	25' x 50'	120' x 200'

PROGRAM PHASE	PROGRAM YEAR							PROGRAM COST
	1	2	3	4	5	6	7	
1. SUPPORTING RESEARCH	—————							\$ 2,600
2. LABORATORY DEMONSTRATION	—————							\$ 1,500
3. PROCESS EVALUATION		—————						\$ 6,500
4. PILOT SCALE DEVELOPMENT				—————				\$ 8,000
5. PILOT PLANT					—————			\$32,000
CONTINGENCY (25%)								\$12,700
TOTAL COST	\$ 900	\$ 3,200	\$ 5,000	\$ 7,100	\$15,600	\$20,200	\$11,300	\$63,300

Figure 6.3 Development Program Costs  
(Dollars In Thousands)

## 6.5 CONCLUSIONS

The conceptual design of a  $10 \times 10^6$  std m<sup>3</sup>/day hydrogen production plant has been prepared based on a hybrid electrolytic-thermochemical process for decomposing water. The process, called the Sulfur Cycle Water Decomposition System, is driven by a VHTR that provides 1283K (1850°F) helium working gas for electric power and process heat. The plant produces approximately ten million standard cubic meters per day of electrolytically pure hydrogen and has an overall thermal efficiency of 45.2 percent. As development goals are achieved, projected improvements indicate that efficiencies greater than 60 percent should be attainable.

The economics of the plant have been evaluated - predicated on a consistent set of groundrules. Total capital investment has been estimated at \$994,795,000. Taking into account operation, maintenance and nuclear fuel cycle costs, the cost of product hydrogen has been calculated at 5.9¢/std m<sup>3</sup> (\$1.59/SCFD) for utility financing. With no credit taken for by-product oxygen production, these values are significantly lower than hydrogen costs from conventional water electrolysis plants. Further more, they are competitive with hydrogen from coal gasification plants when coal costs are in the order of \$1.35 per GJ (\$1.42 per million Btu). As projected improvements in the Sulfur Cycle plant are attained, hydrogen costs from the plant can break even with hydrogen from coal gasification plants when coal costs are as little as \$0.55 per GJ (\$0.58 per million Btu).

Supporting analyses of the plant design have included a preliminary evaluation of environmental impacts based on a standard plant site definition. Areas of impact assessment include resource consumption; air, water and radiological impacts; waste products, land use and aesthetics; socio-economic impacts and environmental cost/benefit factors. A comparison of the environmental, social and economic benefits and costs has indicated that a favorable balance exists for the proposed plants, with the benefits outweighing the costs.

A development plan to take the Sulfur Cycle Water Decomposition System to commercial viability has been defined. The plan involves several phases and can lead to an operating pilot plant in seven to eight years. The development plan builds on previous laboratory scale programs that have verified the scientific feasibility of two major steps in the Sulfur Cycle; electrochemical hydrogen generation and the sulfur trioxide reduction step. A seven year development plan for the Sulfur Cycle, leading to a pilot plant, has been estimated to cost approximately \$63,000,000; the estimated cost of a twelve year development program for the VHTR "nuclear island."

## 7.0 REFERENCES

1. Studies of the Use of Heat from High Temperature Nuclear Sources for Hydrogen Production Processes. Westinghouse Electric Corporation, NASA-CR-134918, January, 1976.
2. Guide for Economic Evaluation of Nuclear Reactor Plant Designs. NUS-531, January, 1969.
3. The Very High Temperature Reactor for Process Heat - A Technical and Economic Assessment. Westinghouse Electric Corporation, WANL-2445-1, December, 1974.
4. A Preliminary Systems Engineering Study of an Advanced Nuclear-Electrolytic Hydrogen Production Facility, W. J. D. Escher, et. al., Institute of Gas Technology, Contract NAS 8-30757, December, 1975.
5. Applicant's Environmental Report - Construction Permit Stage, Fulton Generating Station, Units 1 and 2, Philadelphia Electric Company, Docket 50463-3 and 50464-3.
6. Clinch River Breeder Reactor Plant Environmental Report, Volumes I Through IV, Docket 50-537, April, 1975, Project Management Corporation.
7. Attachment to Concluding Statement of Position of the Regulatory Staff, Public Hearing on: "Numerical Guides for Design Objectives and Limiting Conditions for Operation to Meet the Criterion 'As Low As Practicable' for Radioactive Material in Light-Water-Cooled Nuclear Power Reactors." Draft Regulatory Guides for Implementation, February 20, 1974, Docket No. RM-50-2, U. S. AEC Washington, D. C. 20545, p. A51.
8. Federal Register, Volume 40, No. 172, Thursday, September 4, 1975, pp. 4016-40818.
9. "Estimates of Ionizing Radiation Doses in the United States, 1960-2000", ORP.CSD 72-1, U. S. Environmental Protection Agency, Office of Radiation Programs, Division of Criteria and Standards, Alfred W. Klement, Jr. et al, August, 1972.
10. "What New Jobs Mean to a Community", Chamber of Commerce of the United States, Washington, D. C., 1973.
11. I&C Process Design and Development. Funk, J. E. and Reinstrom, R. M., Vol. 5, No. 3, July, 1966, p. 337.
12. Cheap Hydrogen from Basic Chemicals. Juda, W. and Moulton, D. M., Chemical Engineering Progress, Vol. 63, No. 4, 1967.
13. Electrocatalytic Oxidation of Sulfur Dioxide. Das, S. C. and Roy, C. B., Indian Journal of Chemistry, Vol. 9, No. 9, 1971.

14. Anodic Oxidation of Sulfur Dioxide on Porous Carbon Electrodes in Acid Electrolyzers. Wiesener, K., Wissenschaft Zeitschrift Tec. University Dresden, 1972.
15. Hydrogen Production by Low Voltage Electrolysis in Combined Thermochemical and Electrochemical Cycles. Bowman, M. G. and Onstott, E. I., The Electrochemical Society Fall Meeting, Abstract No. 232, 1974.
16. Experimental Electrode Kinetics. Greene, N. D. Rensselaer Polytechnic Institute, Troy, New York, 1965.
17. Electrolyte Solutions, Robinson, R. A. and Stokes, R. H., 2nd Edition, Butterworths, London, 1959.
18. Sulfuric Acid Users Handbook. U. S. Industrial Chemical Company, 1961.
19. Corrosion Handbook. Uhrig.
20. Metals Handbook. American Society for Metals.
21. Sulfuric Acid Plants - Materials of Construction. McDowell, D. W., Jr., Chemical Engineering Progress, Vol. 71, No. 3, March, 1975.
22. Properties of Selected Commercial Glasses. Corning Brochure B-83, Corning Glass Works, Corning, New York, 1961.
23. Carborundum Sales Brochure Form No. A1716- July, 1963.
24. Haynes Metal Ceramics; Brochure F-30, 115 D; July, 1963.
25. Behavior of Superheated Alloys in High Temperature High Pressure Steam. Lien, G. E., ASME, 1968.